ZooKeys 974: 1–21 (2020)
doi: 10.3897/zookeys.974.54536
https://zookeys.pensoft.net

RESEARCH ARTICLE

A peer-reviewed open-access journal
ZooKeys
Launched to accelerate biodiversity research

Contribution to the taxonomy of Mexican Tersilochinae (Hymenoptera, Ichneumonidae), with descriptions of five new species

Andrey I. Khalaim[1,2], Enrique Ruíz-Cancino[1]

1 *Facultad de Ingeniería y Ciencias, Universidad Autónoma de Tamaulipas, Cd. Victoria, Mexico* **2** *Zoological Institute, Russian Academy of Sciences, St. Petersburg, Russia*

Corresponding author: Andrey I. Khalaim (akhalaim@gmail.com)

Academic editor: J. Fernandez-Triana | Received 22 May 2020 | Accepted 7 August 2020 | Published 7 October 2020

http://zoobank.org/6D2221A8-8CBD-4694-8591-4D1362BF8C81

Citation: Khalaim AI, Ruíz-Cancino E (2020) Contribution to the taxonomy of Mexican Tersilochinae (Hymenoptera, Ichneumonidae), with descriptions of five new species. ZooKeys 974: 1–21. https://doi.org/10.3897/zookeys.974.54536

Abstract

Five new species of Tersilochinae (Ichneumonidae) are described from Mexico: *Meggoleus hidalgoensis* **sp. nov.**, *M. whartoni* Khalaim, **sp. nov.**, *Phradis belovi* Khalaim, **sp. nov.**, *Stethantyx covida* **sp. nov.,** and *St. oaxacana* **sp. nov.** *Meggoleus whartoni* Khalaim, **sp. nov.** is also recorded from Panama, and *St. covida* **sp. nov.** from Guatemala. The species recently described from Mexico *Probles contrerasi* Khalaim & Ruíz-Cancino is transferred to the genus *Gelanes* Horstmann, **comb. nov.** A partial key to the species of *Meggoleus* with small propodeal spiracles and a key to Mexican species of *Phradis* are provided.

Resumen

Se describen cinco especies nuevas de Tersilochinae (Ichneumonidae) para México: *Meggoleus hidalgoensis* **sp. nov.**, *M. whartoni* Khalaim, **sp. nov.**, *Phradis belovi* Khalaim, **sp. nov.**, *Stethantyx covida* **sp. nov.** y *St. oaxacana* **sp. nov.** *Meggoleus whartoni* Khalaim, **sp. nov.** se registra también para Panamá y *St. covida* **sp. nov.** para Guatemala. *Probles contrerasi*, una especie recientemente descrita para México, se transfiere al género *Gelanes* Horstmann, **comb. nov.** Se elaboró una clave parcial de las especies de *Meggoleus* con espiráculos propodeales pequeños y una clave para las especies mexicanas de *Phradis*.

Keywords

Central America, keys, Mexico, new combination, new species, North America, Panama, parasitoids, taxonomy

Introduction

The Tersilochinae is a moderately large, cosmopolitan subfamily of parasitoid wasps comprising more than 560 described species in 27 genera (Yu et al. 2016; Khalaim pers. obs.). The primary hosts of tersilochine parasitoids are larvae of various Coleoptera, but lepidopteran (Lepidoptera: Eriocraniidae) and symphytan (Hymenoptera: Tenthredinidae, Xyelidae) larvae also serve as hosts of some tersilochine taxa (Yu et al. 2016).

The Mexican fauna of Tersilochinae was virtually unknown until the 21st century, being represented by only one species, *Stethantyx nearctica* Townes, 1971 recorded from northern Mexico. Due to our and several other researchers work, many Tersilochinae taxa have been described or recorded from Mexico since 2002 (see Yu et al. 2016; Khalaim and Ruíz-Cancino 2017, 2018, 2019), and currently ten genera with 29 species are known from Mexico: *Allophrys* Förster (1 species), *Aneuclis* Förster (2 species), *Barycnemis* Förster (2 species), *Diaparsis* Förster (1 species), *Gelanes* Horstmann (1 species), *Labilochus* Khalaim (1 species), *Meggoleus* Townes (1 species), *Phradis* (2 species), *Probles* Förster (12 species), and *Stethantyx* Townes (6 species). Despite the extensive study of Mexican Tersilochinae in the past two decades, many Mexican species still remain undescribed, and some genera require further investigation.

The aim of this work is to describe five new species in the genera *Meggoleus*, *Phradis*, and *Stethantyx* from Mexico, revise the generic positions of recently described species of *Probles*, and provide identification keys to the species of *Meggoleus* and *Phradis*.

Materials and methods

A large number of tersilochine specimens was examined from the Universidad Autónoma de Tamaulipas, Cd. Victoria, Mexico (**UAT**); Instituto de Biología, Universidad Nacional Autónoma de México, D.F., Mexico (**UNAM**); and Texas A&M University, College Station, Texas, USA (**TAMU**). Additional paratype of *Stethantyx covida* sp. nov. was loaned from the University of California, Riverside, California, USA (**UCR**), and several paratypes are preserved in the Natural History Museum, London, UK (**BMNH**), Florida State Collection of Arthropods, Gainesville, Florida, USA (**FSCA**) and Zoological Institute of the Russian Academy of Sciences, St. Petersburg, Russia (**ZISP**).

Morphological terminology follows that of Townes (1969) with changes according to Khalaim (2011). Photographs were taken in the Zoological Institute RAS (St. Petersburg, Russia), with a Canon EOS 70D digital camera attached to an Olympus SZX10 stereomicroscope. Images were assembled with Helicon Focus 6 Pro software. General data on the distribution and biology of the genera follow the catalogue TaxaPad (Yu et al. 2016).

Taxonomy

Genus *Gelanes* Horstmann, 1981

Type species. *Thersilochus fusculus* Holmgren, 1860.

A moderately large Holarctic genus with 15 species in the Nearctic region (including two species from Mexico) and 20 species in the Palaearctic region. Parasitoids of xyelid sawflies (Hymenoptera: Xyelidae: *Xyela* spp.) feeding in staminate cones on pines (Pinaceae: *Pinus* spp.) (Khalaim and Blank 2011).

Two species of *Gelanes* are known to occur in Mexico: *G. horstmanni* Khalaim from the State of Tlaxcala in Central Mexico (Khalaim and Ruíz-Cancino 2017) and *G. contrerasi* (Khalaim & Ruíz-Cancino), comb. nov. The latter species was recently described as a species of *Probles* Förster from the State of Hidalgo in Central Mexico (Khalaim and Ruíz-Cancino 2019).

Gelanes contrerasi (Khalaim & Ruíz-Cancino, 2019), comb. nov.

Probles (*Euporizon*) *contrerasi* Khalaim & Ruíz-Cancino, 2019: 210 [holotype female (UNAM), Mexico, Hidalgo, Huasca de Ocampo, Rancho Santa Elena, 20°06'N, 98°31'W, 2330–2535 m, Hueyapan River, 13.VI.2010, coll. A. Contreras R. et al.].

Remarks. This species was recently described in the genus *Probles* based on a single female from the State of Hidalgo in Central Mexico. The species has a slender first metasomal tergite with glymma situated slightly behind the middle, thin and long foveate groove of mesopleuron and long thyridial depression (see figs 20–25 in Khalaim and Ruíz-Cancino 2019: 211), and therefore formally it runs to *Probles*. However, we consider that its unusually broad clypeus with a flat area centrally and highly polished genae and mesopleuron better correspond with the genus *Gelanes* (comb. nov.).

Gelanes contrerasi may easily be distinguished from another Mexican species, *G. horstmanni* Khalaim, by its genae constricted behind eyes in dorsal view (swollen in *G. horstmanni*), slender antennal flagellum with 16 flagellomeres (robust, with 25 flagellomeres in *G. horstmanni*), and longer basal area of propodeum and second metasomal tergite. In the key to the Nearctic species of *Gelanes* (Horstmann 2013b: 238), *G. contrerasi* runs to *G. incisus* Horstmann and *G. punctipleuris* Horstmann in couplet 3, but differs from the both by having longer genae, propodeum with basal area very narrow and longer than the apical area, and longer second metasomal tergite.

Genus *Meggoleus* Townes, 1971

Type species. *Meggoleus spirator* Townes, 1971.

It is a small Neotropical genus with five species; one Afrotropical species with large propodeal spiracles described in the genus *Meggoleus* (Khalaim 2007) was recently found to belong to the genus *Allophrys* Förster (Khalaim 2017). Nothing is known about host range of any *Meggoleus* species.

Three species of *Meggoleus* occurring in South America were revised by Alvarado (2012). Two of them, *M. spirator* Townes and *M. pampahermosensis* Alvarado, are known from Costa Rica (Khalaim and Broad 2012, Khalaim et al. 2018), and the latter species was recorded also from Mexico (Khalaim et al. 2018). In this paper, we describe two new species of *Meggoleus* from Mexico and Panama. Both new species possess small propodeal spiracles, clearly differing from three previously known taxa which are characterized by strongly enlarged propodeal spiracles. Record of *M. hidalgoensis* sp. nov. from Tamaulipas is a northernmost known locality for the genus *Meggoleus*. A partial key to the species of *Meggoleus* with small propodeal spiracles is provided.

Key to species of *Meggoleus* (partial)

1 Propodeal spiracle small, not or very weakly enlarged (Figs 6, 12)............... **2**

– Propodeal spiracle strongly enlarged.................. **see key by Alvarado (2012)**

2 Antennal flagellum black but with two or three distal flagellomeres white (Fig. 10). Scutellum with lateral longitudinal carinae present at basal 0.1–0.2. Intercubitus (2rs-m) short and very thick, much shorter (0.5 × or less) than abscissa of M between 2rs-m and 2m-cu..................... ***M. whartoni* sp. nov.**

– Antennal flagellum entirely black (Fig. 3). Scutellum with lateral longitudinal carinae present at basal 0.3–0.5. Intercubitus (2rs-m) slightly thickened, ca. as long as abscissa of M between 2rs-m and 2m-cu ..... ***M. hidalgoensis* sp. nov.**

***Meggoleus hidalgoensis* Khalaim & Ruíz-Cancino, sp. nov.**

http://zoobank.org/1C8E9237-B9EC-47D4-9897-774F77C429B6
Figures 1–8

Differential diagnosis. The new species differs from other species of *Meggoleus* by the combination of its relatively small, not enlarged propodeal spiracles (Figs 5, 6) and black antenna (Fig. 3).

Description. Female. Body length 4.4 mm. Fore wing length 3.4 mm.

Head, in dorsal view, strongly constricted, almost straight (holotype) or rounded posterior to eyes; gena 0.65–0.75 × as long as eye width. Eyes glabrous. Clypeus relatively large, lenticular, ca. 2.6 × as broad as long (Fig. 4), weakly convex in lateral view, separated from face by sharp furrow; smooth, with scattered punctures in upper part, sometimes slightly scabrous near upper and lower margins. Mandible not constricted, with upper and lower margins mostly subparallel, distinctly widened at level of teeth; teeth somewhat divergent, upper tooth ca. 1.5 × longer than the lower. Malar space 0.9–1.2 × as long as basal mandibular width. Antennal flagellum (Fig. 3) with 15 or 16 flagellomeres, basally very slender; basal flagellomeres more than 2.5 × as long as broad, subapical flagellomeres distinctly elongate; flagellomeres 4–7 bearing long and thin subapical finger-shaped structures on outer surface (hardly discernible in light microscope). Face weakly convex. Face, frons, and vertex subpolished, weakly shining, with very fine, mostly indistinct punctures. Gena polished, with fine and sparse punctures. Occipital carina complete, somewhat dipped mediodorsally, evenly arcuate in dorsal view. Hypostomal carina absent at least in lower part.

Mesoscutum very finely and shallowly granulate, sometimes almost smooth on lateral lobes, impunctate or with very fine inconspicuous punctures, weakly shining to dull. Notaulus impressed, with distinct wrinkle on anterolateral side of mesoscutum (Fig. 3). Scutellum with lateral longitudinal carinae at basal 0.3–0.5. Epicnemial carina not reaching front margin of mesopleuron, continuing above along front margin of mesopleuron towards subtegular ridge, and vanishing there (Fig. 6). Foveate groove long, narrow, sharp, anteriorly upcurved, with distinct transverse wrinkles (Figs 3, 6). Mesopleuron smooth, very finely punctate (sometimes punctures indistinct), with impunctate area centrally. Propodeal spiracle round, not enlarged, separated from pleural carina by 1.0–2.0 × diameter of spiracle (Figs 3, 5). Propodeum with narrow median longitudinal furrow which is 0.7–1.1 × as long as apical area (Fig. 5). Dorsolateral area polished, impunctate (Figs 5, 6). Apical area flat, rounded or pointed anteriorly (Fig. 5); apical longitudinal carinae usually complete and reaching transverse carina anteriorly, sometimes partly obliterated.

Fore wing with second recurrent vein (2m-cu) postfurcal, weakly pigmented in anterior part and distinct posteriorly. First abscissa of radius (Rs+2r) straight, somewhat longer than width of pterostigma. First and second abscissae of radius (Rs+2r and Rs) meeting at slightly acute angle. Intercubitus (2rs-m) slightly thickened, approximately as long as abscissa of cubitus between intercubitus and second recurrent vein (abscissa of M between 2rs-m and 2m-cu). Metacarpus (R1) almost reaching apex of fore wing. Second abscissa of postnervulus (Cu&2cu-a) present, thus brachial cell is closed posteriorly. Hind wing with nervellus (cu1&cu-a) weakly reclivous. Legs slender. Tarsal claws long and slender, not pectinate.

First tergite ca. 3.8 × as long as posteriorly broad, smooth, sometimes with very weak striae laterally just before glymma; petiole more or less trapeziform in cross-section centrally; in dorsal view, postpetiole distinctly widened at base, wider than petiole and clearly separated from it (Fig. 7); in lateral view, upper margin of tergite weakly arcuate in basal 0.6 and somewhat stronger arcuate in apical 0.4 (Fig. 6). Glymma distinct, situated in apical 0.6 of tergite, joining by weak groove with lower part of postpetiole (Fig. 6), but sometimes this groove is vestigial and glymma is virtually isolated. Second tergite ca. 1.85 × as long as anteriorly broad (Fig. 7). Thyridial depression shallow to deep, 2.0–3.0 × as long as broad, with posterior end rounded. Ovipositor weakly and nearly evenly bent upwards over its total length, with weak dorsal subapical depression (Fig. 8); sheath 1.0–1.4 × as long as first tergite (1.4 × in holotype).

Head and mesosoma black. Palpi, mandible (teeth dark red), lower 0.4–0.5 of clypeus and tegula brownish yellow. Scape and pedicel of antenna yellow-brown ventrally and brown dorsally; flagellum brownish black, sometimes pale at base.

Figures 1–8. *Meggoleus hidalgoensis* sp. nov., holotype female (all except 2) and paratype male (2) **1, 2** habitus, lateral view **3** head with antennae and mesosoma, lateral view **4** head, front view **5** propodeum dorso-postero-lateral view **6** posterior part of mesosoma and base of metasoma, lateral view **7** postpetiole and second tergite, dorsal view **8** apex of metasoma with ovipositor, lateral view.

Pterostigma brown. Legs brownish yellow; hind coxa darkened with brown at base; apex of hind tibia and hind tarsus infuscate. First tergite brown to dark brown. Metasoma posterior to first tergite brown or dark brown dorsally to brownish yellow ventrally.

Male. Similar to female; flagellum slender, more or less tapered towards apex, with 16 flagellomeres (Fig. 2).

Variation. Pale specimens have head and mesosoma mostly reddish brown rather than black, and metasoma pale brown to yellow. Two females from the State of Oaxaca possess foveate groove of mesopleuron very thin, represented by a line of sharp and deep pits.

Etymology. The species is named after the type locality, [State of] Hidalgo.

Material examined. ***Holotype*** female (UNAM), Mexico, Hidalgo, Huasca de Ocampo, Rancho Santa Elena, 20°06'N, 98°31'W, 2330–2535 m, Hueyapan River, 25.I–23.II.2006, coll. A. Contreras R. et al.

***Paratypes*.** **Mexico:** 1 female (UAT, apices of antennae absent), **Tamaulipas**, Gómez Farías, La Gloria, 11.III.1995, coll. D. Zuñiga. 1 female (UAT, head absent), 1 male (UNAM), **Hidalgo**, same data as holotype, but 29.XI–26.XII.2005. 1 female, 1 male (ZISP), **Morelos**, N of Tepoztlán, path to El Tepozteco, 1800–2000 m, 11.X.2014, coll. A.I. Khalaim. 1 female (TAMU), **Veracruz**, 7 mi. W of Jalapa [Xalapa], 24–25.III.1974, coll. J.C. Schaffner. 1 female (TAMU), **Oaxaca**, 10.8 mi. (= 17.4 km) S of El Punto, 6100 ft (= 1860 m), 19.VII.1987, coll. R. Wharton. 1 female (TAMU), Oaxaca, 15 mi. (= 24 km) NE of Ixtlán de Juárez, Llano de las Flores, 21.VII.1985, coll. J.B. Woolley & G. Zolnerovich.

Distribution. Mexico (Tamaulipas, Hidalgo, Morelos, Veracruz, Oaxaca).

Meggoleus whartoni **Khalaim, sp. nov.**

http://zoobank.org/489674A1-97D4-47FB-95D7-98CD4C7601F9

Figures 9–14

Differential diagnosis. The new species is easily distinguished from all other species of *Meggoleus* by the flagellum with distal end white (Fig. 10). It is very similar to *M. hidalgoensis* sp. nov. as both have small propodeal spiracles but differs from this species, in addition to color pattern of the flagellum, by scutellum with shorter lateral longitudinal carinae and fore wing with short and thick intercubitus (2rs-m).

Description. Female. Body length 3.7 mm. Fore wing length 2.8 mm.

Head, in dorsal view, strongly constricted, weakly rounded posterior to eyes; gena 0.6–0.65 × as long as eye width. Eyes glabrous. Clypeus relatively large, almost lenticular (slightly truncated ventrally), ca. 2.5 × as broad as long (Fig. 11), very weakly convex in lateral view, separated from face by fine furrow; smooth, with very fine punctures in upper 0.3–0.5. Mandible slender, not constricted, with upper and lower margins mostly subparallel; upper tooth almost twice longer than the lower. Malar space approximately as long as basal mandibular width. Antennal flagellum (Fig. 10) with 15 flagellomeres, basally very slender; basal flagellomeres almost 2.5 × as long as broad, subapical flagellomeres distinctly elongate; flagellomeres 4 to 6 bearing long and thin subapical finger-shaped structures on outer surface. Face weakly convex. Face and frons subpolished, weakly shining, with very fine punctures. Vertex polished, with very fine and sparse punctures. Gena polished, impunctate. Occipital carina complete, somewhat dipped mediodorsally, evenly arcuate in dorsal view. Hypostomal carina present in upper part, weak or completely obliterated in lower part.

Mesoscutum granulate, impunctate, dull. Notaulus with distinct wrinkle on anterolateral side of mesoscutum (Fig. 10). Scutellum with lateral longitudinal carinae at basal 0.1–0.2. Epicnemial carina not reaching front margin of mesopleuron, continuing above along front margin of mesopleuron towards subtegular ridge, and vanishing there (Fig. 12). Foveate groove long, narrow and sharp, anteriorly upcurved, with dis-

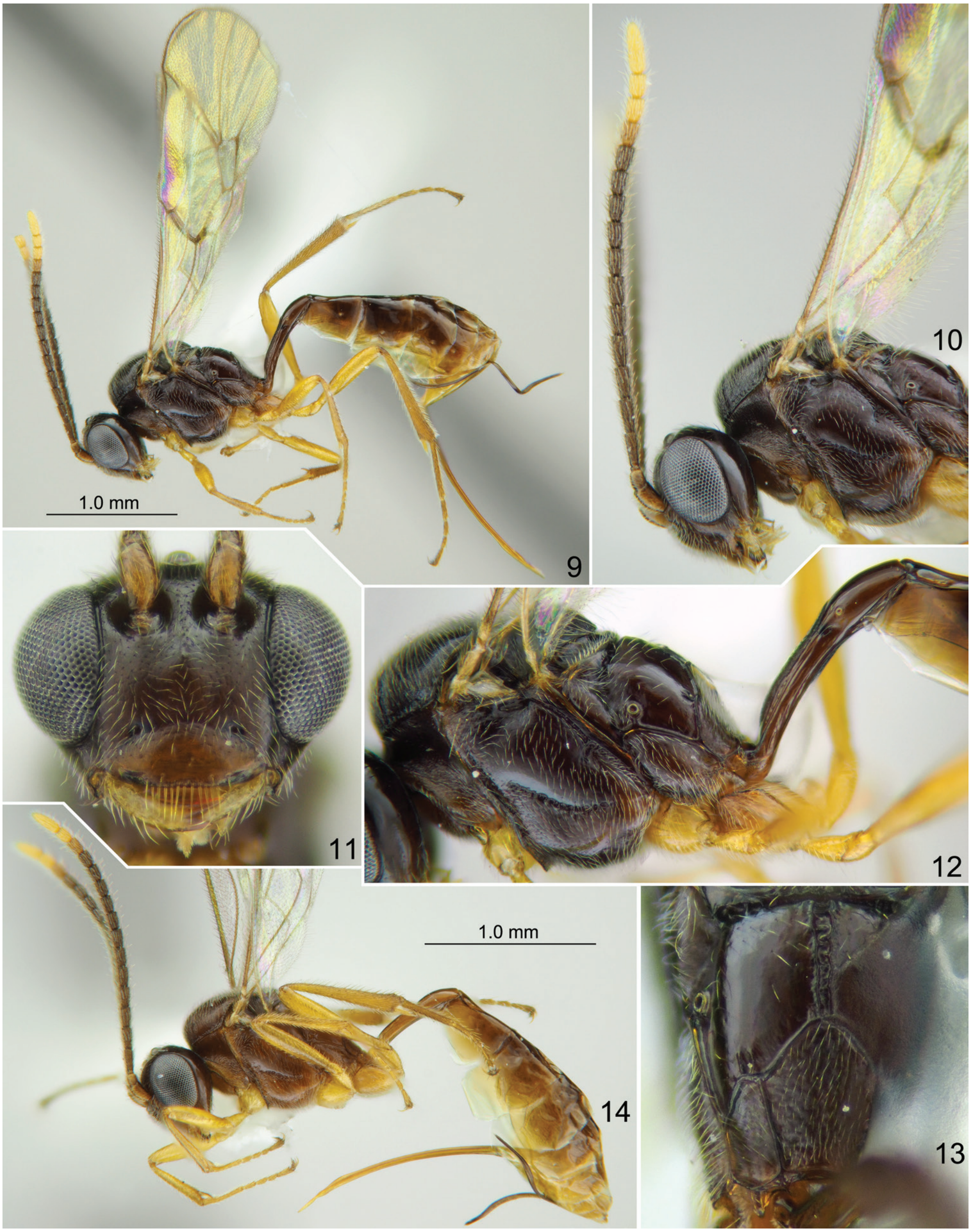

Figures 9–14. *Meggoleus whartoni* sp. nov., holotype (9–13) and paratype (14) females **9, 14** habitus lateral view **10** head with antennae and mesosoma, lateral view **11** head, front view **12** mesosoma and base of metasoma, lateral view **13** propodeum, dorsal view.

tinct transverse wrinkles (Fig. 12). Mesopleuron smooth, with very fine inconspicuous punctures. Propodeal spiracle round, slightly enlarged, separated from pleural carina by 1.0–1.5 × diameter of spiracle (Fig. 12). Propodeum with narrow median longitudinal furrow which is more or less enclosed laterally by a pair of longitudinal carinae, and ca. 0.8 × as long as apical area (Fig. 13). Dorsolateral area polished, impunctate (Fig. 13). Apical area flat, anteriorly rounded (Fig. 13); apical longitudinal carinae complete, reaching transverse carina anteriorly.

Fore wing with second recurrent vein (2m-cu) postfurcal, weakly pigmented in anterior part and distinct posteriorly. First abscissa of radius (Rs+2r) straight, longer than width of pterostigma. First and second abscissae of radius (Rs+2r and Rs) meeting at slightly acute angle. Intercubitus (2rs-m) short and very thick, much shorter (0.5 × or less) than abscissa of cubitus between intercubitus and second recurrent vein (abscissa of M between 2rs-m and 2m-cu). Metacarpus (R1) almost reaching apex of fore wing. Second abscissa of postnervulus (Cu&2cu-a) present, thus brachial cell is closed posteriorly. Hind wing with nervellus (cu1&cu-a) weakly reclivous. Legs slender. Tarsal claws long and slender, not pectinate.

First tergite ca. 4.4 × as long as posteriorly broad, predominantly smooth, with weak striae laterally before glymma; petiole trapeziform in cross-section centrally; in dorsal view, postpetiole widened at base, distinctly broader than petiole and clearly separated from it; in lateral view, upper margin of tergite weakly arcuate in basal 0.6 and somewhat stronger arcuate in apical 0.4. Glymma distinct, situated in apical 0.6 of tergite, joining by weak (sometimes vestigial) groove with lower part of postpetiole (Fig. 12). Second tergite approximately twice as long as anteriorly broad. Thyridial depression deep, ca. 2.5 × as long as broad, with posterior end rounded. Ovipositor weakly and nearly evenly bent upwards over its total length, with weak dorsal subapical depression; sheath approximately as long as first tergite.

Head, mesosoma and first tergite of metasoma orange-brown to dark reddish brown. Palpi and mandible (teeth red) yellow. Clypeus yellow-brown or reddish brown, unicolorous or slightly darkened in upper part. Tegula brownish yellow. Scape and pedicel of antenna yellow-brown ventrally and brown dorsally; flagellum brownish black with two or three distal flagellomeres white (Fig. 10). Pterostigma brown. Legs brownish yellow, hind coxa slightly brownish at base. Metasoma posterior to first tergite predominantly brown, yellow ventrally.

Male. Unknown.

Etymology. The species is named in honor of the American entomologist, expert in Braconidae and Ichneumonidae, Robert Wharton.

Material examined. Holotype female (TAMU), Mexico, “Chiapas”.

Paratypes. **Panama:** 2 females (TAMU), Chiriquí Prov., National Park Volcan Baru, 3 km E of Cerro Punta, 08°50'55"N, 82°32'36"W, 7060 ft. (= 2155 m), 31.VII–4.VIII.1999, coll. A. Gillogly & J. Woolley, Malaise trap, 99/072.

Distribution. South Mexico (Chiapas), Panama.

Genus *Phradis* Förster, 1869

Type species. *Thersilochus* (*Phradis*) *brevis* Brischke, 1880.

A moderately large predominantly Holarctic genus with 20 species in the Nearctic region (including two species from Mexico), ca. 40 species in the Palaearctic region, and several species known from Peru, South Africa, and Australia. In Europe, species of *Phradis* have been reared from sap beetle larvae (Coleoptera: Nitidulidae: *Meligethes* spp.) feeding on rape, but no host record is known for any Nearctic species (Horstmann 2013a).

Two species of *Phradis* were known from Mexico until now (Khalaim and Ruíz-Cancino 2018), and the third species, *P. belovi* sp. nov., is described from North Mexico in this paper. The genus is extremely rare in Mexico as all known Mexican species are represented by a single holotype. Horstmann (2013a) in his revision of the Nearctic fauna, also noted that many Nearctic species are rarely collected, and six of 18 revised species (33%) are known from only one specimen. A key to three Mexican species of *Phradis* is provided below.

Key to species of *Phradis* occurring in Mexico

1 Flagellum with 17 flagellomeres (Fig. 16). Fore wing with vein 2m-cu postfurcal. Notaulus very shallow, with short wrinkle or tubercle distant from anterolateral margin of mesoscutum. Propodeum mediodorsally with narrow longitudinal furrow, without delimited basal area; dorsolateral areas polished. Hind femur brownish yellow, not darkened (Fig. 15). Ovipositor sheath twice as long as first tergite. Hind femur brownish yellow .... ***P. belovi* sp. nov.**

– Flagellum with 14 flagellomeres. Fore wing with vein 2m-cu interstitial. Notaulus with strong wrinkle on anterolateral side of mesoscutum. Propodeum mediodorsally with clearly delimited broad basal area; dorsolateral areas granulate. Ovipositor sheath 1.1–1.4 × as long as first tergite. Hind femur dark brown to black.. **2**

2 Second flagellomere 2.5 × as long as broad. Apical area of propodeum flat. Second metasomal tergite 2.8 × as long as anteriorly broad. Ovipositor with apex needle-shaped, without dorsal notch; sheath 1.1 × as long as first tergite .... ***P. bufalosus* Khalaim & Ruíz-Cancino**

– Second flagellomere 3.5 × as long as broad. Apical area of propodeum impressed along midline. Second metasomal tergite 3.6 × as long as anteriorly broad. Ovipositor evenly tapered apically, with weak but distinct dorsal subapical notch; sheath 1.4 × as long as first tergite.. .... ***P. nanacamilpus* Khalaim & Ruíz-Cancino**

Phradis belovi Khalaim, sp. nov.

http://zoobank.org/08038E88-9796-418C-9758-111496BA7E0A
Figures 15–20

Differential diagnosis. *Phradis belovi* sp. nov. may easily be recognized by the postfurcal second recurrent vein (2m-cu) in the fore wing, narrow and sharp foveate groove on the mesopleuron (Fig. 19), and propodeum with longitudinal furrow mediodorsally and polished dorsolateral areas. It differs from two other Mexican species of *Phradis* by features given in the key above. In the key to Nearctic species of *Phradis* (Horstmann 2013a: 68), *P. belovi* sp. nov. runs to *P. nitidipleuris* Horstmann in couplet 17, but differs from this species by the propodeum mediodorsally with longitudinal furrow (short and broad, irregularly wrinkled basal area in *P. nitidipleuris*, see fig. 77 in Horstmann 2013a: 82), longer metacarpus in the fore wing (Fig. 15 and Khalaim 2019: 413, fig. 52), and its narrow and sharp foveate groove on the mesopleuron (Fig. 19) (broad, with irregular wrinkles in *P. nitidipleuris*, see Khalaim 2019: 413, fig. 5).

Description. Female. Body length 4.3 mm. Fore wing length 3.3 mm.

Head, in dorsal view, rounded posterior to eyes (Fig. 18); gena 0.65 × as long as eye width. Eyes glabrous. Clypeus relatively large, lenticular, 2.6 × as broad as long (Fig. 17), weakly convex in lateral view, separated from face by thin and sharp furrow, with flattened area in lower part centrally; smooth, with fine punctures on slightly scabrous background in upper 0.4. Mandible robust, not constricted (i.e. with upper and lower margins subparallel in front view); upper tooth somewhat longer than the lower. Malar space approximately as long as basal mandibular width. Antennal flagellum filiform, with 17 flagellomeres (Fig. 16); flagellomeres 2 and 3 ca. 2.5 × as long as broad, subapical flagellomeres slightly elongate; flagellomeres 4–7 bearing long and thin subapical finger-shaped structures on outer surface (hardly discernible in light microscope). Face with slightly elongated convexity centrally. Face, frons, and vertex with very fine and dense punctures; gena impunctate anteriorly, with fine and sparse punctures in posterior half. Face and frons subpolished, weakly shining. Vertex and gena polished. Occipital carina complete, weakly and evenly arcuate in dorsal view (Fig. 18), somewhat flattened mediodorsally.

Mesoscutum very finely and densely punctate on very finely and shallowly granulate background, weakly shining, except for central lobe which is dull, with somewhat denser granulation and mostly without distinct punctures. Notaulus very shallow, with short wrinkle or tubercle distant from anterolateral margin of mesoscutum. Scutellum with lateral longitudinal carinae at basal 0.1. Epicnemial carina with upper end at level of centre of pronotum, not reaching front margin of mesopleuron (Fig. 19). Foveate groove situated in center of mesopleuron, very narrow and sharp, anteriorly upcurved (Fig. 19). Mesopleuron smooth and shining, finely punctate. Propodeal spiracle small, round, separated from pleural carina by 1.5 × diameter of spiracle. Propodeum with dorsal part convex in lateral view (Fig. 19), with narrow median longitudinal furrow which is ca. 0.7 × as long as apical area. Dorsolateral area polished, impunctate. Apical area flat, widely rounded anteriorly; apical longitudinal carinae almost reaching transverse carina anteriorly, indistinct next to transverse carina because of irregular wrinkles.

Fore wing with second recurrent vein (2m-cu) distinctly postfurcal, weakly pigmented in anterior 0.6. First abscissa of radius (Rs+2r) straight, distinctly longer than width of pterostigma. First and second abscissae of radius (Rs+2r and Rs) meeting at right angle. Intercubitus (2rs-m) slightly thickened, twice as long as abscissa of cubitus between intercubitus and second recurrent vein (abscissa of M between 2rs-m and 2m-cu). Metacarpus (R1) reaching ca. 0.7 the distance from distal corner of radial cell to

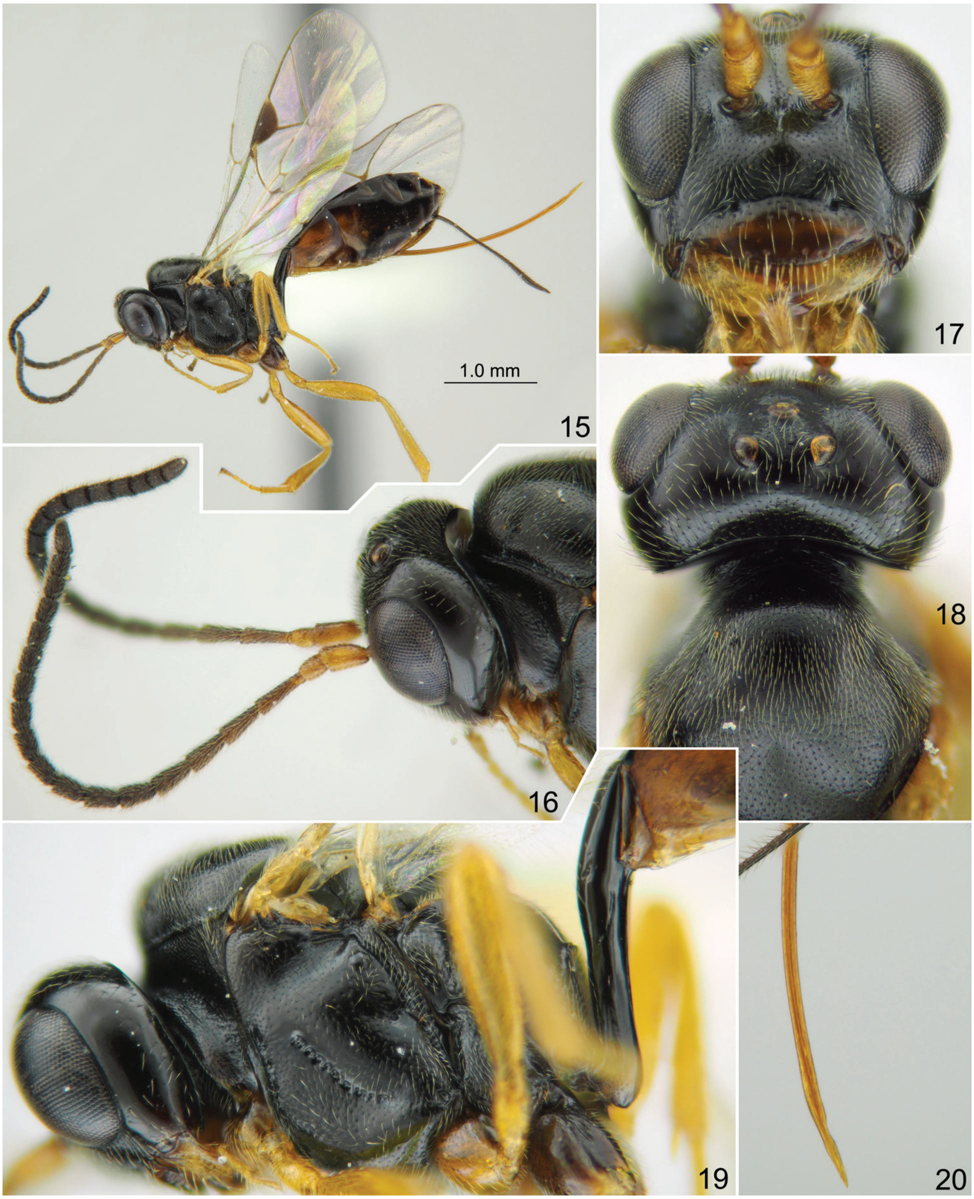

Figures 15–20. *Phradis belovi* sp. nov., holotype female **15** habitus, lateral view **16** head with antennae lateral view **17** head, front view **18** head and mesoscutum, dorsal view **19** head, mesosoma and base of metasoma, lateral view **20** apex of ovipositor, lateral view.

the tip of wing. Second abscissa of postnervulus (Cu&2cu-a) present but short, thus brachial cell is partly open posteriorly. Hind wing with nervellus (cu1&cu-a) straight, weakly reclivous. Legs slender. Tarsal claws slender, not pectinate.

First tergite ca. 4.1 × as long as posteriorly broad, smooth, without glymma but with sharp oblique groove (Fig. 19), with upper margin in lateral view straight in basal half and arcuate in apical half; petiole round in cross-section centrally. First tergite, in dorsal view, weakly and rather evenly widened from base towards apex, thus postpetiole is weakly separated from petiole. Second tergite 2.5 × as long as anteriorly broad. Thyridial depression distinct, ca. 2.5 × as long as broad, with posterior end somewhat pointed. Ovipositor weakly and evenly bent upwards over its total length, with weak dorsal subapical depression (Fig. 20); sheath twice as long as first tergite.

Head, mesosoma and first tergite of metasoma black; clypeus brown in lower 0.4 and dark brown in upper 0.4, with narrow transverse brownish yellow band. Palpi, mandible (teeth dark red) and tegula brownish yellow. Scape and pedicel of antenna yellow-brown, flagellum pale brown basally to black apically. Pterostigma brown. Legs brownish yellow; fore and mid coxae browish, hind coxa dark brown. Metasoma posterior to first tergite predominantly dark brown, tergites 2 and 3 laterally brown (Fig. 15).

Male. Unknown.

Etymology. The species is named after my friend, the well-known entomologist Vassili Belov (TAMU).

Material examined. Holotype female (TAMU), Mexico, Nuevo León, "3 mi. south Pacheco", taken at light, 3.VII.1974, coll. Clark, Murraw, Asche & Schaffner.

Distribution. Northeast Mexico (Nuevo León).

Genus *Stethantyx* Townes, 1971

Type species. *Stethantyx nearctica* Townes, 1971.

Large and almost exclusively Neotropical genus with ca. 50 described and many undescribed species. Three species of *Stethantyx* occur in America north of Mexico, including one species introduced from South America (Horstmann 2010), and six Mexican species were reviewed by Khalaim and Ruíz-Cancino (2013). Species of the genus are known as parasitoids of coleopteran hosts of the families Curculionidae and Nitidulidae.

Two new species of *Stethantyx* are described here from Mexico, raising the total number of known *Stethantyx* species in Mexico to eight. The both new species possess right-angled radial cell in the fore wing and belong to the species group *radiata* (see Khalaim et al. 2015), while other six Mexican species belong to the species group *nearctica*, as they have abscissae of radius (Rs+2r and Rs) meeting at obtuse angle (see Khalaim and Broad 2013, Khalaim et al. 2013).

Stethantyx covida Khalaim & Ruíz-Cancino, sp. nov.

http://zoobank.org/FCCA3517-3788-403B-9FC9-4ED17AF839EF

Figures 21–26

Differential diagnosis. The new species differs from other species of *Stethantyx* with a right-angled first and second abscissae of radius (Rs+2r and Rs) by the combination of highly polished head and mesosoma, sharp and strongly oblique foveate groove of mesopleuron (Fig. 23), propodeum with narrow basal area (Fig. 24), and very long and slender ovipositor (Fig. 21). It is very similar to *St. oaxacana* sp. nov., but differs from this species by the shape of the ovipositor (Fig. 26), and somewhat longer gena, thyridial depression and second tergite.

Description. Female. Body length 3.5 mm. Fore wing length 2.8 mm.

Head, in dorsal view, roundly constricted posterior to eyes; gena 0.9–1.0 × as long as eye width. Eyes glabrous. Clypeus lenticular (sometimes with lower margin slightly truncate), 3.2–3.4 × as broad as long, weakly convex in lateral view, with weak transverse ridge in lower 0.3–0.4, separated from face by sharp furrow; smooth, with fine punctures in upper part. Mandible slender, distinctly constricted in basal 0.3–0.4; upper tooth 2.0–2.5 × as long as the lower. Malar space 0.9–1.1 × as long as basal mandibular width. Antennal flagellum (Fig. 22) with 15–18 flagellomeres, filiform; flagellomeres 2–4 ca. 1.4–1.8 ×, subapical flagellomeres 1.1–1.3 × as long as broad; flagellomeres 4 to 6 bearing subapical finger-shaped structures on outer surface (hardly discernible in light microscope). Face weakly convex. Face, frons, and vertex subpolished; face and frons with very fine (sometimes indistinct) punctures. Gena polished, impunctate, or with very fine punctures in posterior part (near occipital carica). Occipital carina complete, evenly arcuate in dorsal view. Hypostomal carina present, complete.

Mesoscutum and mesopleuron very finely (sometimes indistinctly) punctate on smooth background; dorsolateral area of propodeum polished, impunctate. Notaulus with strong wrinkle on anterolateral side of mesoscutum. Scutellum with lateral longitudinal carinae at basal 0.3–0.5. Epicnemial carina not reaching front margin of mesopleuron, continuing above along front margin of mesopleuron, and vanishing there (Fig. 23). Foveate groove situated in anterior half of mesopleuron, deep, strongly oblique, almost straight, with distinct transverse wrinkles (Fig. 23). Propodeal spiracle small, adjacent to pleural carina or separated from it by one diameter of spiracle (Fig. 23). Propodeum with long and narrow basal area (basal longitudinal carinae parallel or weakly divergent anteriorly) which is 0.5–0.8 × (0.6 in holotype) as long as apical area (Fig. 24). Apical area flat, rounded to slightly pointed anteriorly; apical longitudinal carinae complete and reaching transverse carina anteriorly.

Fore wing with second recurrent vein (2m-cu) postfurcal, weakly pigmented in anterior part and distinct posteriorly. First abscissa of radius (Rs+2r) straight, longer than width of pterostigma. First and second abscissae of radius (Rs+2r and Rs) meeting at right or slightly acute angle. Intercubitus (2rs-m) slightly thickened, relatively long, distinctly longer than abscissa of cubitus between intercubitus and second recurrent vein (abscissa of M between 2rs-m and 2m-cu). Metacarpus (R1) short, not reaching apex of fore wing (Fig. 21). Second abscissa of postnervulus (Cu&2cu-a) present, thus brachial cell is closed posteriorly. Hind wing with nervellus (cu1&cu-a) weakly reclivous. Legs slender. Tarsal claws not pectinate.

First tergite 4.0 × as long as posteriorly broad, smooth, usually with longitudinal striae laterally before glymma and dorsally at apex of petiole; petiole slightly trapeziform in cross-section centrally; in dorsal view, postpetiole distinctly widened at base, wider than petiole and clearly separated from it; in lateral view, upper margin of tergite straight or weakly arcuate in basal 0.6–0.7 and arcuate in apical 0.3–0.4. Glymma

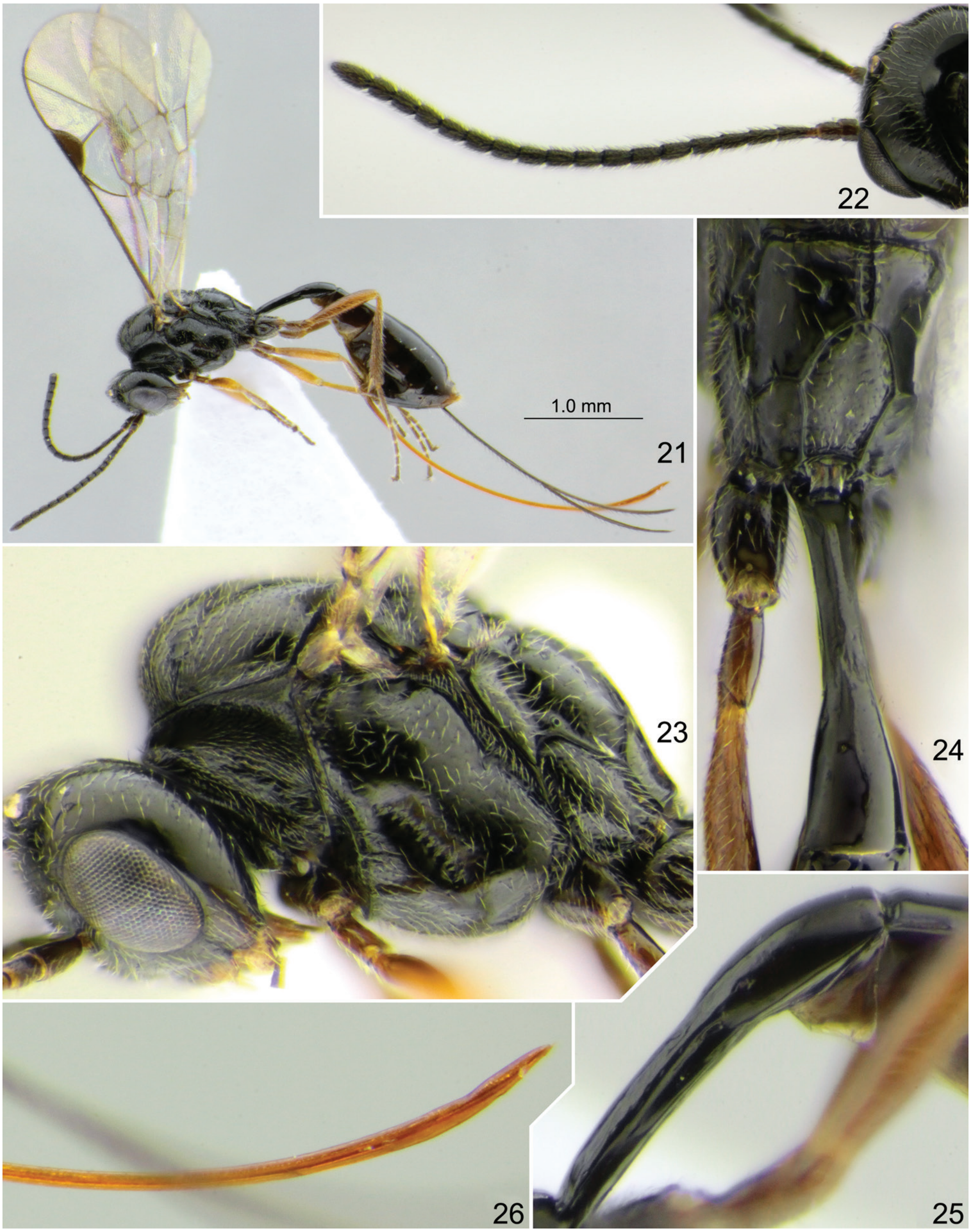

Figures 21–26. *Stethantyx covida* sp. nov., holotype female **21** habitus, lateral view **22** head with antennae, dorso-posterior view **23** head and mesosoma, lateral view **24** propodeum and first tergite, dorso-posterior view **25** first tergite, lateral view **26** apex of ovipositor, lateral view.

(Fig. 25) small but distinct, situated in apical 0.55 of tergite and joining by fine groove (sometimes indistinct in small specimens) with lower part of postpetiole. Second tergite ca. 1.7 × as long as anteriorly broad. Thyridial depression deep, 2.0–3.0 × as long as broad, with posterior end usually rounded. Ovipositor bent upwards over its total length, with weak dorsal subapical depression and without teeth ventrally (Fig. 26); sheath 2.7–3.5 × (3.2 in holotype) as long as first tergite.

Head, mesosoma and first tergite brownish black to black; clypeus brownish yellow in lower 0.4 and dark brown in upper part, but sometimes clypeus is more or less entirely brownish yellow. Palpi and mandible (teeth red) brownish yellow. Tegula brownish yellow to brown. Antenna dark brown to black, scape and pedicel sometimes yellow-brown ventrally. Pterostigma brown. Legs brownish yellow; coxae and trochanters sometimes strongly darkened with brown (to almost black), tibiae and tarsi sometimes weakly to strongly infuscate (Fig. 21). Metasoma entirely or predominantly dark brown, sometimes brown posteriorly and ventrally.

Male. Similar to female but malar space somewhat shorter than basal mandibular width; basal area of propodeum very narrow and usually longer; and second metasomal tergite and thyridial depression longer.

Variation. Two females from Nevado de Toluca (State of Mexico) possess second tergite 1.5–1.6 × as long as anteriorly broad. Epicnemial carina sometimes almost reaching front margin of mesopleuron. Foveate groove in small specimens sometimes weak.

Etymology. This abundant Mexican species is named after the Covid-19 (Coronavirus) because the taxon was described while the outbreak of this virus in Mexico.

Material examined. ***Holotype*** female (UAT), Mexico, Tamaulipas, 6 km NE of Miquihuana, 23°36.125'N, 99°42.45'W, 2200–2600 m, 24.X.2008, coll. A.I. Khalaim.

***Paratypes*. Mexico:** 5 females (2 in BMNH, 1 in UAT, 2 in ZISP), same data as holotype. 12 females, 1 male (10 females in UAT; 2 females, 1 male in ZISP), **Tamaulipas**, [NE of] Miquihuana, Km. 15 [of road] from La Peña, 2500 m, pine forest, 16.VIII.2000, coll. D.R. Kasparyan. 14 females (1 in BMNH, 1 in FSCA, 12 in UAT), Tamaulipas, [NE of] Miquihuana, Km. 21 [of road] La Peña – Joya, pine forest, 16.IX.2000, coll. C. Covarrubias Dimas. 1 female (UAT), Tamaulipas, [NE of] Miquihuana, Km. 13 [of road] Aserradero – La Peña, herbs, 28.VIII.1993, coll. E. Ruíz-Cancino. 1 female (UAT), Tamaulipas, [NE of] Miquihuana, Km. 18 [of road] La Peña – Aserradero, pine forest, herbs, 24.X.2008, coll. E. Ruíz-Cancino. 1 female (ZISP), **Hidalgo**, 8 km N of Pachuca de Soto, National Park El Chico, 20°11.4'N, 98°44.55'W, 2950–3000 m, 27.III.2014, coll. A.I. Khalaim. 2 females (BMNH, FSCA), Hidalgo, 8 km N of Pachuca de Soto, National Park El Chico, 20°11.4'N, 98°44.55'W, 2800–2900 m, 18–22.XII.2014, coll. A.I. Khalaim. 2 females, 1 male (1 female, 1 male in UAT; 1 female in ZISP), **Tlaxcala**, 15 km SSE of Apizaco, north slope of La Malinche volcano, 19°16.97'N, 98°02.52'W, 3300–3800 m, 2.IV.2016, coll. A.I. Khalaim. 7 males (1 in BMNH, 1 in FSCA, 4 in UAT, 1 in ZISP), Tlaxcala, 15 km SSE of Apizaco, north slope of La Malinche volcano, 2550–3000 m, 1–2.X.2016, coll. A.I. Khalaim & A.E. Humala. 2 females, 1 male (UAT), **Mexico** [State of], NW slope of Nevado de Toluca volcano, 3150–3830 m, 29.IX.2016, coll. A.I. Khalaim. 1 female, 1 male (ZISP), **Morelos**, N of Tepoztlán, path to El Tepozteco, 1800–2000 m, 11.X.2014, coll. A.I. Khalaim. 2 males (TAMU), **Guerrero**, 7 mi. SW of Filo de Caballo, 12.VII.1985, coll. J. Woolley & G. Zolnerowich. 1 female (TAMU), **Oaxaca**, Llano de las Flores, 8900 ft

(= 2715 m), 17–19.VII.1987, coll. R. Wharton. 2 females (TAMU), Oaxaca, 15 mi. (= 24 km) NE of Ixtlán de Juárez, Llano de las Flores, 21.VII.1985, coll. J.B. Woolley & G. Zolnerovich. 1 female (TAMU), Oaxaca, 10.8 mi. (= 17.4 km) S of El Punto, 6100 ft (= 1860 m), 19.VII.1987, coll. R. Wharton. 1 female (UNAM), Oaxaca, Santiago Comaltepec, 17.58429N, 96.49398W, 2332 m, 6.VI.2009, coll. H. Clebsch & A. Zaldívar. 1 female (UAT), 1 male (UNAM), same data but 29.XI–26.XII.2005 (head in female absent). 6 females, 12 males (5 females, 11 males in UNAM; 1 female, 1 male in UAT), Oaxaca, Santiago Comaltepec, 17.58424N, 96.49428W, 2427 m, humid oak-pine forest, Malaise trap, 12–20.VI.2007, coll. H. Clebsch. **Guatemala:** 1 female (UCR), Sacatepéquez [Department], Sumpango, Durwest Farm, 14°40'17"N, 90°43'11"W, 3–10.II.2007, coll. M. Hoddle.

Distribution. Northeast, central, and south Mexico (Tamaulipas, Hidalgo, Tlaxcala, Mexico, Guerrero, Oaxaca), Guatemala.

Stethantyx oaxacana Khalaim & Ruíz-Cancino, sp. nov.

http://zoobank.org/56BC0231-F72C-4D74-B9AC-DBBEC699674D
Figures 27–32

Differential diagnosis. The new species is very similar to *St. covida* sp. nov. but differs from this species in the shape of the ovipositor (Fig. 32), and shorter gena and second tergite. *Stethantyx oaxacana* sp. nov. also resembles *St. radiata* Khalaim & Sääksjärvi as both have similar shape of the ovipositor apex, but distinct in having clypeus separated from face by sharp furrow, less punctate head and mesosoma, and longer ovipositor.

Description. Female. Body length 3.4 mm. Fore wing length 2.7 mm.

Head, in dorsal view, roundly constricted posterior to eyes (Fig. 28); gena ca. 0.7 × as long as eye width. Eyes glabrous. Clypeus lenticular, ca. 2.8 × as broad as long, weakly convex in lateral view, separated from face by sharp furrow; smooth, with fine scattered punctures in upper part. Mandible slender, weakly constricted in basal half; upper tooth twice longer than the lower. Malar space 1.0–1.1 × as long as basal mandibular width. Antennal flagellum (Fig. 29) with 16–17 flagellomeres, filiform; subbasal flagellomeres 1.5–1.8 ×, subapical flagellomeres 1.2–1.3 × as long as broad; flagellomeres 4 to 6 bearing subapical finger-shaped structures on outer surface (hardly discernible in light microscope). Face weakly convex. Face and frons finely (sometimes indistinctly) punctate on smooth or slightly scabrous background. Vertex and gena polished, without distinct punctures. Occipital carina complete, evenly arcuate in dorsal view. Hypostomal carina present, complete.

Mesoscutum and mesopleuron finely punctate on smooth background. Notaulus with strong wrinkle on anterolateral side of mesoscutum. Scutellum with lateral longitudinal carinae at basal 0.3–0.5. Epicnemial carina not reaching front margin of mesopleuron, continuing above along front margin of mesopleuron and vanishing there (Fig. 30). Foveate groove situated in anterior half of mesopleuron, deep, strongly oblique, almost straight, with distinct transverse wrinkles (Fig. 30). Propodeal spiracle adjacent to pleural carina or separated from it by less than one diameter of spiracle (Fig. 30). Propodeum with rectangular or slightly widened anteriorly basal area which is 2.0–4.0 × (2.0 in holotype) as long as broad and 0.4–0.8 × (0.4 in holotype) as long as apical area (Fig. 31). Dorsolateral area polished, with fine punctures in holotype (Fig. 31) and impunctate in paratypes. Apical area flat, rounded anteriorly (Fig. 31); apical longitudinal carinae complete and reaching transverse carina anteriorly.

Fore wing with second recurrent vein (2m-cu) postfurcal, weakly pigmented in anterior part and distinct posteriorly. First abscissa of radius (Rs+2r) straight, longer than width of pterostigma. First and second abscissae of radius (Rs+2r and Rs) meeting at slightly acute angle. Intercubitus (2rs-m) slightly thickened, approximately twice longer than abscissa of cubitus between intercubitus and second recurrent vein (abscissa of M between 2rs-m and 2m-cu). Metacarpus (R1) not reaching apex of fore wing. Second abscissa of postnervulus (Cu&2cu-a) present, thus brachial cell is closed posteriorly. Hind wing with nervellus (cu1&cu-a) weakly reclivous. Legs slender. Tarsal claws not pectinate.

First tergite 3.7 × as long as posteriorly broad, smooth, sometimes with longitudinal striae laterally before glymma and dorsally at apex of petiole; petiole rounded or slightly trapeziform in cross-section centrally; in dorsal view, postpetiole distinctly widened at base, wider than petiole and clearly separated from it; in lateral view, upper margin of tergite weakly arcuate in basal 0.6 and stronger arcuate in apical 0.4. Glymma small but distinct, situated in apical 0.55 of tergite and joining by fine groove with lower part of postpetiole. Second tergite ca. 1.25 × as long as anteriorly broad. Thyridial depression deep, ca. 1.5 × as long as broad, with posterior end rounded. Ovipositor bent upwards over its total length, with two dorsal subapical teeth and approximately three very small teeth ventrally (Fig. 32); sheath 2.3–2.6 × as long as first tergite (2.6 × in holotype).

Head and mesosoma predominantly brown to dark reddish brown (paratypes) or more or less entirely black (holotype); lower part of gena (near mandible) yellowish. Palpi and mandible (teeth red) yellow. Clypeus yellow, sometimes brownish in upper part. Tegula yellow or brownish yellow. Scape and pedicel of antenna yellowish brown; flagellum brownish black. Pterostigma brown. Legs brownish yellow; hind coxa sometimes darkened with brown basally; apices of tibiae and tarsi sometimes infuscate. Metasoma more or less uniformly brown or dark brown in paratypes, or extensively yellow ventrally and posteriorly in holotype (Fig. 27).

Male. Unknown.

Variation. All paratypes are smaller (body length ca. 2.5 mm, fore wing length ca. 2.2 mm), paler and with weaker punctures than the holotype. Foveate groove of mesopleuron in paratypes is usually narrow and more or less straight. Shape and length of basal area of propodeum is very variable: 2.0 to 4.0 × as long as broad, and 0.4 to 0.8 × as long as apical area.

Etymology. The species is named after the type locality, [State of] Oaxaca.

Material examined. ***Holotype*** female (UNAM), Mexico, Oaxaca, Santiago Comaltepec, 17.58429N, 96.49398W, 2332 m, 6.VI.2009, coll. H. Clebsch & A. Zaldívar.

Figures 27–32. *Stethantyx oaxacana* sp. nov., holotype female **27** habitus, lateral view **28** head and mesoscutum, dorsal view **29** head with antennae, lateral view **30** head and mesosoma, lateral view **31** propodeum, dorsal view **32** apex of ovipositor, lateral view.

Paratypes. 7 females (3 in UNAM, 2 in UAT, 2 in ZISP), Mexico, Oaxaca, Santiago Comaltepec, 17.58424N, 96.49428W, 2427 m, Malaise trap, 12–20.VI.2007, coll. H. Clebsch.

Distribution. Mexico (Oaxaca).

Acknowledgements

We are thankful to Alejandro Zaldívar-Riverón (UNAM), James B. Woolley, John D. Oswald, and Karen Wright (TAMU) for the loan of specimens, and to Jing-Xian Liu (South China Agricultural University, Guangzhou, China) and Andrei E. Humala (Forest Research Institute, Karelian Research Centre, Russian Academy of Sciences, Petrozavodsk, Russia) for reviewing this manuscript. This study was performed in the frames of the PRODEP project "Taxonomical and biological studies of pests and natural enemies in Mexico", and the work of the senior author was partly supported by the Russian Foundation for Basic Research (grant no. 19-04-00027) and the State Research Project no. AAAA–A19–119020690101–6.

References

Alvarado M (2012) Discovery of the genus *Meggoleus* Townes, 1971 (Hymenoptera, Ichneumonidae, Tersilochinae) in Peru, with the description of two new species. ZooKeys 163: 83–90. https://doi.org/10.3897/zookeys.163.2291

Horstmann K (2010) Revisions of Nearctic Tersilochinae II. Genera *Allophrys* Förster, *Barycnemis* Förster, *Ctenophion* gen. nov., *Sathropterus* Förster, *Spinolochus* Horstmann and *Stethantyx* Townes (Hymenoptera, Ichneumonidae). Spixiana 33, 73–109.

Horstmann K (2013a) Revisions of Nearctic Tersilochinae IV. Genus *Phradis* Förster (Hymenoptera, Ichneumonidae). Spixiana 36(1): 67–92.

Horstmann K (2013b) Revisions of Nearctic Tersilochinae V. Genera *Allophroides* Horstmann and *Gelanes* Horstmann (partim) (Hymenoptera, Ichneumonidae). Spixiana 36(2): 227–261.

Khalaim AI (2007) First records of *Meggoleus*, *Heterocola* and *Phradis* (Hymenoptera: Ichneumonidae: Tersilochinae) from the Afrotropical region, with description of four new species. African Invertebrates 48(2): 101–110.

Khalaim AI (2011) Tersilochinae of South, Southeast and East Asia, excluding Mongolia and Japan (Hymenoptera: Ichneumonidae). Zoosystematica Rossica 20(1): 96–148.

Khalaim AI (2017) A new species of *Allophrys* Förster, 1869 (Hymenoptera: Ichneumonidae: Tersilochinae) with large propodeal spiracles from Indonesia. Proceedings of the Zoological Institute RAS 321(4): 365–370.

Khalaim AI (2019) Illustrated catalogue of North American species of *Ctenophion* Horstmann and *Phradis* Förster (Hymenoptera: Ichneumonidae: Tersilochinae). Russian Entomological Journal 28(4): 400–420.

Khalaim AI, Blank SM (2011) Review of the European species of the genus *Gelanes* Horstmann (Hymenoptera: Ichneumonidae: Tersilochinae), parasitoids of xyelid sawflies (Hymenoptera: Xyelidae). Proceedings of the Zoological Institute RAS 315(2): 154–166.

Khalaim AI, Broad GR (2012) Tersilochinae (Hymenoptera: Ichneumonidae) of Costa Rica, part 1. Genera *Allophrys* Förster, *Barycnemis* Förster and *Meggoleus* Townes. Zootaxa 3185: 36–52. https://doi.org/10.11646/zootaxa.3185.1.2

Khalaim AI, Broad GR (2013) Tersilochinae (Hymenoptera: Ichneumonidae) of Costa Rica, part 2. Genera *Megalochus* gen. nov. and *Stethantyx* Townes. Zootaxa 3693(2): 221–266. https://doi.org/10.11646/zootaxa.3693.2.8

Khalaim AI, Ruíz-Cancino E (2013) Mexican species of the genus *Stethantyx* Townes (Hymenoptera, Ichneumonidae, Tersilochinae). ZooKeys 360: 83–94. https://doi.org/10.3897/zookeys.360.6362

Khalaim AI, Ruíz-Cancino E (2017) Ichneumonidae (Hymenoptera) associated with xyelid sawflies (Hymenoptera, Xyelidae) in Mexico. Journal of Hymenoptera Research 58: 17–27. https://doi.org/10.3897/jhr.58.12919

Khalaim AI, Ruíz-Cancino E (2018) First record of the genera *Diaparsis* Förster and *Phradis* Förster (Hymenoptera, Ichneumonidae, Tersilochinae) from Mexico. Journal of Hymenoptera Research 63: 61–72. https://doi.org/10.3897/jhr.63.24491

Khalaim AI, Ruíz-Cancino E (2019) Mexican species of the genus *Probles* Förster (Hymenoptera: Ichneumonidae: Tersilochinae). Zootaxa 4619(2): 201–230. https://doi.org/10.11646/zootaxa.4619.2.1

Khalaim AI, Sääksjärvi IE, Bordera S (2013) Tersilochinae of Western Amazonia (Hymenoptera: Ichneumonidae). Genus *Stethantyx* Townes, part 1. Zootaxa 3741(3): 301–326. https://doi.org/10.11646/zootaxa.3741.3.1

Khalaim AI, Sääksjärvi IE, Bordera S (2015) Tersilochinae of Western Amazonia (Hymenoptera: Ichneumonidae). Genus *Stethantyx* Townes, part 2. Zootaxa 3981(1): 95–106. https://doi.org/10.11646/zootaxa.3981.1.4

Khalaim AI, Kasparyan DR, López-Ortega M (2018) New records and descriptions of Ichneumonidae (Hymenoptera) from Mexico. Zootaxa 4486(1): 1–30. https://doi.org/10.11646/zootaxa.4486.1.1

Townes HK (1969) The genera of Ichneumonidae, Part 1. Memoirs of the American Entomological Institute 11: 1–300. https://doi.org/10.1007/BF02027741

Townes HK (1971) The genera of Ichneumonidae, Part 4. Memoirs of the American Entomological Institute 17: 1–372.

Yu DSK, Achterberg C van, Horstmann K (2016) Taxapad 2016, Ichneumonoidea 2015. Database on flash-drive. Nepean, Ontario.

ZooKeys 974: 23–29 (2020)
doi: 10.3897/zookeys.974.55528
https://zookeys.pensoft.net

RESEARCH ARTICLE

A peer-reviewed open-access journal
ZooKeys
Launched to accelerate biodiversity research

A new species of *Cheiloneurus* Westwood (Hymenoptera, Encyrtidae) as a hyperparasitoid of the invasive cotton mealybug, *Phenacoccus solenopsis* Tinsley, in China

Zhuomiao Li[1], Tingting Yao[1], Zhihong Xu[2], Ling Meng[1], Baoping Li[1]

1 School of Plant Protection, Nanjing Agricultural University, No. 1 Weigang, Nanjing, Jiangsu 210095, China **2** *Department of Plant Protection, School of Agriculture and Food Science, Zhejiang Agriculture & Forestry University, Lin'an, Zhejiang 311300, China*

Corresponding author: Baoping Li (lbp@njau.edu.cn)

Academic editor: A. Köhler | Received 17 June 2020 | Accepted 3 September 2020 | Published 7 October 2020

http://zoobank.org/87F93B60-FD12-44CA-BE72-BCF1B20FCABA

Citation: Li Z, Yao T, Xu Z, Meng L, Li B (2020) A new species of *Cheiloneurus* Westwood (Hymenoptera, Encyrtidae) as a hyperparasitoid of the invasive cotton mealybug, *Phenacoccus solenopsis* Tinsley, in China. ZooKeys 974: 23–29. https://doi.org/10.3897/zookeys.974.55528

Abstract

A new species, *Cheiloneurus nankingensis* **sp. nov.**, from Eastern China is described. It is similar to *C. arabiacus* Hayat but distinct from it in a number of morphological characters. It is a hyperparasitoid with the encyrtid wasp *Aenasius arizonensis* Girault, 1915 as the primary host and the cotton mealybug *Phenacoccus solenopsis* Tinsley, 1898 (Hemiptera: Pseudococcidae) as the secondary host. A key to all seven species of *Cheiloneurus* known from China is presented.

Keywords

Aenasius arizonensis, *bambawalei*, biological control, hyperparasitism, Nanjing

Introduction

Hyperparasitoids are specialized natural enemies of primary parasitoids but their negative effects on biological control have often been overlooked. Hyperparasitoids may directly impact their primary parasitoid by parasitizing their offspring and host-feeding

(Sullivan 1987; Godfray 1994). Besides, the presence of hyperparasitoids may cause dispersal and patch leaving of their primary parasitoids to further influence biological control efficacy (Cusumano et al. 2019). Hyperparasitoids are often mistakenly regarded as primary parasitoids when they are collected from reared herbivorous hosts that have been parasitized. For example, while *Cheiloneurus* (Encyrtidae) has been recorded as a hyperparasitoid of the cotton mealybug *Phenacoccus solenopsis* Tinsley, 1898 (Hemiptera, Pseudococcidae) in North America (Fuchs et al. 1991), it was considered as a primary parasitoid of the mealybug in China (Li et al. 2020).

Phenacoccus solenopsis, native to North America, has spread to Asia over the past two decades (Tong et al. 2018). Since entering China, it has spread over a wide area and caused serious concern over its damage to a variety of economic crop plants (Wang et al. 2020). Biological control with natural enemies provides an alternative approach to managing this invasive pest. Numerous species of parasitoid wasps have been known attacking *P. solenopsis* in invaded Asia countries (Hayat 2009; Chen et al. 2011; Li et al. 2020). Yet few hyperparasitoids of the mealybug have been discovered in these areas.

Here, a hyperparasitoid wasp new to science is named *Cheiloneurus nankingensis* sp. nov. It was collected from rearing mummified *P. solenopsis* mealybugs on okra *Abelmoschus esculentus* (Linn.) Moench. Laboratory observation showed that *C. nankingensis* adults produce offspring when attacking the mealybugs that had been parasitized by *Aenasius arizonensis* Girault, 1915, but failed to do so when confined with healthy mealybugs, indicating that *A. arizonensis* is the host. This host parasitoid, having been synonymized with *A. bambawalei* Hayat, 2009, belongs to the subfamily Tetracneminae in Encyrtidae (Fallahzadeh et al. 2014). It was originally recorded in the USA and is now widespread in Asia where it is generally considered to be a potential biological control agent of the invasive cotton mealybug (Chen et al. 2011; Fallahzadeh et al. 2014; Aga et al. 2016; Li et al. 2020). Yet, its potential may be compromised by hyperparasitoids.

Cheiloneurus includes more than 140 species over the world, and all species, for which their biologies are known, are hyperparasitoids, attacking a wide range of parasitoid wasp taxa (Trjapitzin and Zuparko 2004). Six species of *Cheiloneurus* have been recorded from across mainland China, mostly with mealybugs as their secondary hosts; their primary hosts are unknown, except for *C. claviger* Thomson, 1876, which parasitizes *Microterys* encyrtid wasps (Xu and Huang 2004; Mita et al. 2016).

Materials and methods

Sample individuals of the cotton mealybug were collected from okra plants in a vegetable field and then maintained on potato *Solanum tuberosum* L. seedlings in an insectary. Parasitized mealybug mummies were individually placed in glass vials in which a cotton ball soaked with a 10% honey solution was provided as supplementary food. *Cheiloneurus* adults were mounted on slides following the methods described by Noyes (1982) for identification under a stereoscope (Nikon SMZ25, with NIS-Elements BR software for taking measurements and Zerene Stacker for processing photographs).

The terminology follows Noyes and Hayat (1984).

The following abbreviations are used in the description: POL, distance between the posterior ocelli; OOL, distance between a posterior ocellus and the corresponding eye margin; F1, F2, …, F6, first through sixth funicle segments; NAU, Nanjing Agricultural University, Nanjing, China.

Taxonomy

Cheiloneurus nankingensis Li & Xu, sp. nov.

http://zoobank.org/0A0CAA90-9BAD-4A04-8E4A-64851CE36387
Fig. 1[female], Fig. 2[male]

Type materials. ***Holotype.*** ♀; China, Jiangsu province: Nanjing city, NAU-affiliated Pailou Experiment station; alt. 18 m; 32°01'10"N, 118°51'21"E; October 2019; Zhuomiao Li leg. ***Paratypes.*** ♀; 15 individuals, same data as for holotype.

Deposition. The type specimens are deposited in the Department of Plant Protection, School of Agriculture and Food Science, Zhejiang Agri & Forest University, Li-an district, Hangzhou city, Zhejiang, China.

Etymology. The species name is derived from the name of the city, Nanjing, where the holotype was collected.

Distribution. All specimens were collected in an eastern suburb of Nanjing city, Jiangsu province, East China.

Description. ***Female.*** Holotype, body length 1.54 mm; other females ranged from 1.1 to 1.8 mm. Head dark brown, with purple sheen; ocelli reddish brown; compound eye dark brown; scape, pedicel yellowish brown; funicle and clava black, except first funicle segment with narrow strip of yellowish brown on ventral margin; pronotum and mesoscutum black with yellowish green sheen and silvery white setae; tegulae, axillae, scutellum yellowish brown except middle third of scutellum yellowish white; ventral and lateral sides of thorax dark brown with dark purple sheen; propodeum dark brown. Fore wing infuscated, with basal third, apex narrowly and rectangular area behind stigmal vein, hyaline; hyaline area in basal third with oblique infuscate streak; veins brown; hind wing hyaline. Fore and mid legs yellowish brown except middle part of mid tibia brown; hind femora and tibia brown except tibial base white.

Head: in dorsal view, 0.77 × as broad as high; head width 3.29 × frontovertex width; occipital margin rounded; ocelli arranged in equilateral triangle; POL and OOL 2.02 × and 0.30 × as long as diameter of anterior ocellus respectively; anterior ocellus separated with posterior ocelli by distance 1.01 × as long as POL; frontovertex with scaly reticulations. In frontal view, 0.79 × as broad as high; toruli separated by 1.93 × their own longest diameters; upper margin below lowest level of compound eye; toruli separated from clypeus by distance 0.73 × as long as longest diameter of torulus; mandible tridentate, teeth acute; maxillary palpi with four segments with rounded apex.

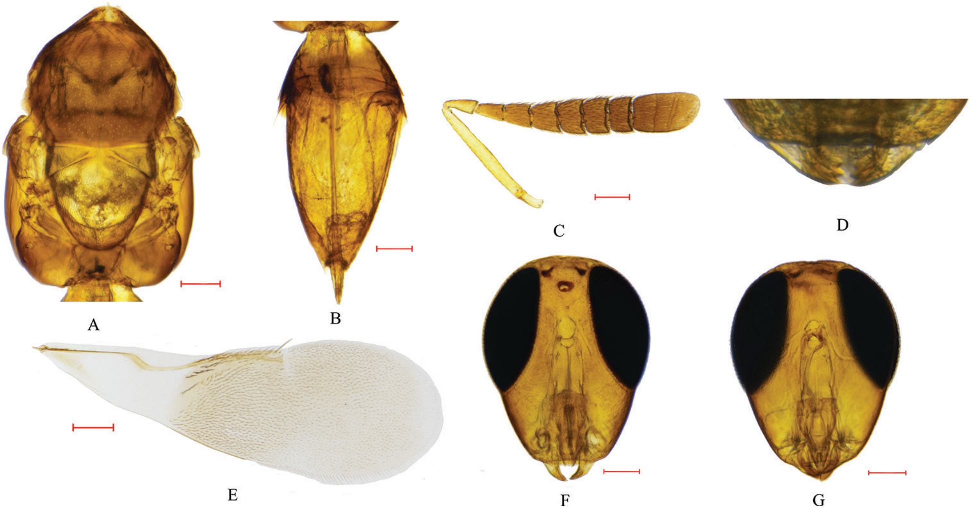

Figure 1. *Cheiloneurus nankingensis* sp. nov. (female, holotype) **A** mesosoma, dorsal view **B** metasoma, dorsal view **C** antennae **D** mandibles **E** fore wing **F** head, front view **G** head, ventral view. Scale bars: 0.10 mm.

Antennae: scape cylindrical, 8.27 × as long as broad; pedicel 2.23 × as long as wide and 1.26 × as long as F1. F6 shortest segment; F1 and F2 longer than wide, the ratio of length to width 1.60 and 1.13, respectively; F3–F6 wider than long, the ratio of length to width 0.87, 0.67, 0.67, 0.64, respectively; club 1.78 × as long as broad, slightly shorter than preceding three funicle segments combined, clava with second suture slightly oblique.

Mesosoma: mesoscutum with striated or scaly reticulations and usually with distinct silvery white setae; notauli virtually absent; axillae and scutellum flat and usually with sculpture scaly; apex of scutellum with a tuft of bristles (bristles are easily lost at making slide but their swelling bases are recognizable); hind margin of scutellum reaching base of propodeum; mesopleura smooth, reaching base of abdomen; propodeum smooth.

Fore wings: 3.01 × as long as broad, with uniform cilia except basal third; submarginal vein with about five setae; submarginal vein 3.90 × as long as stigmal vein; linea calva closed anteriorly by two or three lines of setae and posteriorly closed by 11 or 12 lines of hyaline setae.

Legs: a row of spines at apex of mid tibia; tibial spur 0.96 × as long asbasitarsus ; basitarsus longer than tarsal segments 2–4.

Metasoma: oblong in dorsal view. Ovipositor sheaths yellow. Exserted part of ovipositor sheaths (from slide) 0.15 × gaster length.

Measurements (from slide): length of mid tibia 0.65 mm, mesosoma 0.73 mm, metasoma 0.70 mm, forewing 1.25 mm.

Male. Length 1.07 mm. Body black. Antennae slender with radicle, scape and pedicel dark yellowish brown; funicle and clava black. Oval compound eye and ocelli black. Legs yellowish brown.

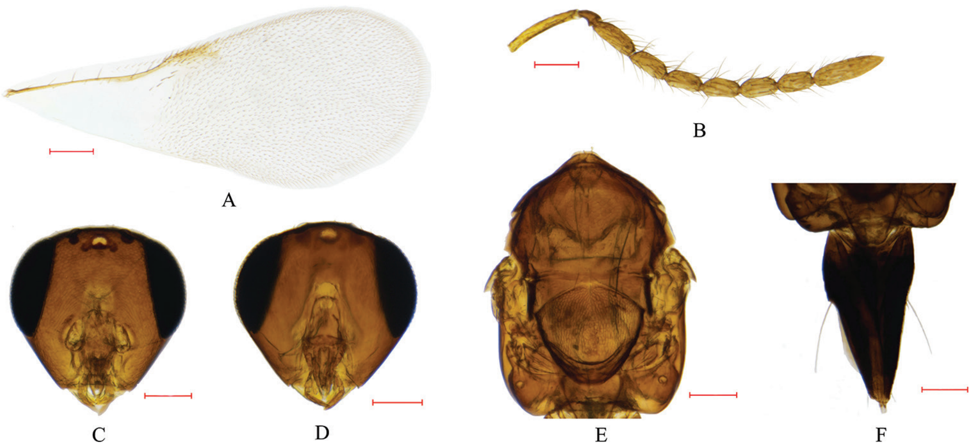

Figure 2. *Cheiloneurus nankingensis* sp. nov. (male) **A** fore wing **B** antennae **C** head, front view **D** head, ventral view **E** mesosoma, dorsal view **F** metasoma, dorsal view. Scale bars: 0.10 mm.

Head: in frontal view, approximately triangular with scaly reticulations, 0.97 × as broad as high; POL and OOL 3.00 × and 0.92 × as long as diameter of anterior ocellus, respectively; toruli separated by 0.83 × their own longest diameters; mandible bidentate; toruli diameters 0.69 × and 2.26 × as long as POL and OOL, respectively; distance between compound eyes 3.45 × as long as that between toruli.

Antennae: scape cylindrical, 6.53 × and 0.46 × as long as broad and head height, respectively; pedicel triangular; clava unsegmented, longer than F5–F6 combined; scape 3.35, 1.62, 1.95, 2.13, 2.14, 2.15, 2.18, and 1.05 times as long as pedicel, F1–F6, and clava, respectively; F1 slightly longer than F2–F6 separately; F2–F6 nearly same length; ratio of length to width 2.57, 2.20, 2.30, 2.22, 2.15, and 2.18 for F1 to F6, respectively.

Mesosoma: In dorsal view, 1.35 × as long as width; mesoscutum, axillae, and scutellum with sculpture scaly and similar to head sculpture; scutellum 0.97 × as long as height; setae and notauli virtually absent.

Fore wings: 2.42 × as long as broad; submarginal vein with about 13 setae; postmarginal and submarginal veins 0.58 × and 10.65 × as long as stigmal vein.

Legs: mid tibia with row of spines apically; spur 1.08 × as long as basitarsus.

Metanotum: nearly triangular in dorsal view. Shorter than thorax.

Measurements (from slide): mesosoma length 0.55 mm, metasoma length 0.43 mm, antennae 0.86 mm, and mid tibia length 0.43 mm.

Diagnosis. This new species resembles *C. arabiacus* Hayat, (2014) but differs from it in the following respects (compared with *C. arabiacus* in brackets): without an infuscate area below proximal half of parastigma (with it); scape cylindrical (slightly expanded in the middle); pedicel as long as F1 (longer than F1–F2 combined); F3 quadrate or slightly broader than long (F3 longer than broad); F4–F6 broader than long (F4, F5 quadrate); clava shorter than F4–F6 combined (longer than F4–F6 combined); head in frontal view higher than broad (broader than high); mandible with three acute teeth (with two acute and one round teeth).

Biology. Little has been known about biology of this new species. It is a hyperparasitoid with the encyrtid wasp *A. arizonensis* as the host, which is a primary and solitary parasitoid of the cotton mealybug *P. solenopsis*. This hyperparasitoid attacks only mealybugs that have already been parasitized by *A. arizonensis* and the number of offspring hyperparasitoids ermerging from a mummified mealybug ranges from one to 18. The prevalence of hyperparasitism by this wasp across the range of the cotton mealybug remains to be investigated.

Key to females of *Cheiloneurus* species known from China

1 Scutellum without a tuft of bristles at apex .... ***C. exitiosus* Perkins, 1906**
– Scutellum with a tuft of bristles at apex **2**
2 Scape cylindrical; clava slightly broader than funicle **3**
– Scape slightly expanded in the middle; clava clearly broader than funicle **5**
3 F1–F6 longer than wide, entirely whitish **4**
– Only F1–F2 longer than wide; funicle blackish .... ***C. nankingensis* sp. nov.**
4 Pedicel as long as F1; clava as long as F4–F6 combined ..... ***C. quercus* Mayr, 1876**
– Pedicel longer than F1; clava as long as F3–F6 combined ....
.... ***C. sinensis* Özdikmen, 2011**
5 Fore wing apex narrowly hyaline; funicle entirely blackish ....
.... ***C. axillaris* Hayat, Alam & Agarwal, 1975**
– Fore wing apex narrowly not hyaline; some funicular segments whitish **6**
6 F4–F5 whitish with a brown stripe on ventral margin ..... ***C. chinensis* Shi, 1993**
– F4–F5 entirely whitish .... ***C. claviger* Thomson, 1876**

Acknowledgements

We thank Jirui Wang at Zhejiang Agri & Forest University for processing the specimen deposition and offering suggestions for the study, Changhai Sun and Xinyu Ge for help with the photography, Jingya Liu for help in rearing mealybugs, and Jiajia Zhao for the information about the mealybug infestation site. This work was supported by the National Key R&D Program of China (2017YFE0104900).

References

Aga TM, Tambe VJ, Nagrare VS, Naikwadi B (2016) Parasitoid, *Aenasius arizonensis* (Girault) (Hymenoptera: Encyrtidae): Its biology, morphometrics, host stage preference and use in biological control. Journal of Biological Control 30(2): 91–98. https://doi.org/10.18641/jbc/30/2/95751

Chen HY, He LF, Zhen CH, Li P, Yi JH, Xu ZF (2011) Survey on the natural enemies of mealybug, *Phenacoccus solenopsis* Tinsley (Hemiptera: Pseudococcidae) from Guangdong and Hainan, China. Journal of Environmental Entomology 33(2): 269–272. https://en.cnki.com.cn/Article_en/CJFDTotal-KCTD201102023.htm

Cusumano A, Harvey JA, Bourne ME, Poelman EH, Boer J (2019) Exploiting chemical ecology to manage hyperparasitoids in biological control of arthropod pests. Pest Management Science 76: 432–443. https://doi.org/10.1002/ps.5679

Fallahzadeh M, Japoshvili G, Abdimaleki R, Saghaei N (2014) New records of Tetracneminae (Hymenoptera, Chalcidoidea, Encyrtidae) from Iran. Turkish Journal of Zoology 38: 515–518. https://doi.org/10.3906/zoo-1309-28

Fuchs TW, Stewart JW, Minzenmayer R, Rose M (1991) First record of *Phenacoccus solenopsis* Tinsley in cultivated cotton in the United States. Southwestern Entomologist 16: 215–221.

Godfray HCJ (1994) Parasitoids: Behavioral and Evolutionary Ecology. Princeton University Press, Princeton, New Jersey, 221 pp. https://doi.org/10.1515/9780691207025

Hayat M (2009) Description of a new species of *Aenasius* Walker (Hymenoptera: Encyrtidae), India. Biosystematica 3: 21–26.

Hayat M, Ahmad Z, Khan FR (2014) Encyrtidae (Hymenoptera: Chalcidoidea) from the Kingdom of Saudi Arabia. Zootaxa 3793(1): 22–24. https://doi.org/10.11646/zootaxa.3793.1.1

Li J, Deng J, Chen H, Yang L, Zhou Z, Jiaqng J, Huang L, Gui F, Chen J (2020) Investigation on the occurrence of parasitic wasps of *Phenacoccus solenopsis* Tinsley in Guangxi. Journal of Southern Agriculture 51(4): 853–861.

Mita T, Handa H, Higashiura Y, Japoshvili G (2016) First report of *Cheiloneurus exitiosus* (Perkins, 1906) and *Helegonatopus dimorphus* (Hoffer, 1954) (Hymenoptera: Encyrtidae) from Japan, with remarks on their abundance in rice paddies. Biodiversity Data Journal 4: e9230. https://doi.org/10.3897/BDJ.4.e9230

Noyes JS (1982) Collecting and preserving chalcid wasp (Hymenoptera: Chalcidoidea). Journal of Natural History 16: 315–334. https://doi.org/10.1080/00222938200770261

Noyes JS, Hayat M (1984) A review of the genera of Indo-Pacific Encyrtidae (Hymenoptera: Chalcidoidea). Bulletin of the British Museum (Natural History), Entomology 48(3): 131–395. https://www.biodiversitylibrary.org/page/2288550

Sullivan DJ (1987) Insect hyperparasitism. Annual Review of Entomology 32: 49–70. https://doi.org/10.1146/annurev.en.32.010187.000405

Trjapitzin VA, Zuparko RL (2004) A synopsis of the genus *Cheiloneurus* Westwood, 1833 (Hymenoptera: Chalcidoidea: Encyrtidae) of the New World. Russian Entomological Journal 13: 257–266.

Tong H, Ao Y, Li Z, Wang Y, Jiang M (2018) Invasion biology of the cotton mealybug, *Phenacoccus solenopsis* Tinsley: current knowledge and future directions. Journal of Integrative Agriculture 17: 60345–60347. http://lib.cqvip.com/Qikan/Article/Detail?id=7001765165.

Xu Z, Huang J (2004) Chinese Fauna of Parasitic Wasps on Scale Insects. Shanghai Scientific & Technical Publishers, Shanghai, 524 pp.

Wang Y, Dai T, Tian H, Wang F, Zhang G (2020) Range expansion of the invasive cotton mealybug, *Phenacoccus solenopsis* Tinsley: an increasing threat to agricultural and horticultural crops in China. Journal of Integrative Agriculture 19(3): 881–885. https://doi.org/10.1016/S2095-3119(19)62765-6

ZooKeys 974: 31–92 (2020)
doi: 10.3897/zookeys.974.54794
https://zookeys.pensoft.net

RESEARCH ARTICLE

A peer-reviewed open-access journal
ZooKeys
Launched to accelerate biodiversity research

An update and revision of the *Andrena* fauna of Morocco (Hymenoptera, Apoidea, Andrenidae) with the description of eleven new North African species

Thomas James Wood[1], Denis Michez[1], Diego Cejas[1],
Patrick Lhomme[1,2], Pierre Rasmont[1]

1 *Laboratoire de Zoologie, Université de Mons, 7000, Mons, Belgium* **2** *International Center of Agricultural Research in the Dry Areas, Rabat, Morocco*

Corresponding author: Thomas James Wood (thomasjames.wood@umons.ac.be)

Academic editor: Thorleif Dörfel | Received 27 May 2020 | Accepted 5 August 2020 | Published 7 October 2020

http://zoobank.org/9B888866-0F07-4DEC-AE7B-88DFB0A4621C

Citation: Wood TJ, Michez D, Cejas D, Lhomme P, Rasmont P (2020) An update and revision of the *Andrena* fauna of Morocco (Hymenoptera, Apoidea, Andrenidae) with the description of eleven new North African species. ZooKeys 974: 31–92. https://doi.org/10.3897/zookeys.974.54794

Abstract

Morocco has a diverse bee fauna, but one that has also been relatively understudied in recent years. Here a revision of the species-rich genus *Andrena* is presented that reveals eleven new species for science and substantially improves our understanding of North African *Andrena*. From Morocco, *Andrena* (*Aciandrena*) *semiadesus* Wood, **sp. nov.**, *Andrena* (*Aciandrena*) *triangulivalvis* Wood **sp. nov.**, *Andrena* (*Campylogaster*) *sparsipunctata* Wood **sp. nov.**, *Andrena* (*Carandrena*) *hebescens* Wood **sp. nov.**, *Andrena* (*Cnemidandrena*) *niveofacies* Wood **sp. nov.**, *Andrena* (*incertae sedis*) *tenebricorpus* Wood **sp. nov.**, *Andrena* (*Notandrena*) *acutidentis* Wood **sp. nov.**, *Andrena* (*Poliandrena*) *breviceps* Wood **sp. nov.**, and *Andrena* (*Poliandrena*) *farinosoides* Wood **sp. nov.** are described and their ecology is discussed. *Andrena* (*Aciandrena*) *astrella* Warncke, 1975 is synonymised with *Andrena* (*Aciandrena*) *fulica* Warncke, 1974 **syn. nov.** The unknown female of *Andrena* (*Nobandrena*) *ounifa* Warncke, 1974, and the unknown male of *Andrena* (*Poliandrena*) *guichardi* Warncke, 1980 are described. *Andrena* (*incertae sedis*) *gafsensis* Wood **sp. nov.** from Tunisia is described due to its similarity to *Andrena tenebricorpus*. *Andrena* (*Poecilandrena*) *nigriclypeus* Wood **sp. nov.** from Algeria is also described as it was collected within 10 km of the Moroccan border. A further 18 species are recorded in Morocco for the first time. *Andrena* (*Melandrena*) *nitida* (Müller, 1776) and *Andrena* (*Notandrena*) *nitidiuscula* Schenck, 1853 are removed from the Moroccan list due to historic problems in the application of these names to Mediterranean taxa.

Keywords

alpine, deserts, endemic, faunal list, pollen host plants, solitary bees, taxonomy

Introduction

Andrena are the second most speciose genus of bees worldwide after *Lasioglossum* (Ascher and Pickering 2020). The genus has a primarily Holarctic distribution and with the greatest diversity found in Mediterranean and xeric regions (Gusenleitner and Schwarz 2002). The Mediterranean basin of the Western Palearctic is therefore one of the hotspots of *Andrena* diversity, and new *Andrena* species continue to be described from North Africa and the Levant at regular intervals (e.g., Scheuchl 2009; Scheuchl and Gusenleitner 2009; Scheuchl et al. 2011; Schwenninger 2015; Pisanty et al. 2016; Pisanty et al. 2018). Compared to the Levant, the *Andrena* fauna of north-western Africa is historically better known and described thanks to a long history of taxonomic activity (e.g., Pérez 1895; Schmiedeknecht 1900; Saunders 1908; Alfken 1914; Schulthess 1924; Benoist 1961). The *Andrena* fauna of this region was later revised by Warncke (1967, 1974, 1980, 1983) who described many new species. Since then there has been relatively little work conducted on North African *Andrena* until recently (Scheuchl 2009; Scheuchl et al. 2011; Benarfa et al. 2013; Cherair et al. 2013; Schwenninger 2015; Djouama et al. 2016) as interest in the conservation, ecology, and taxonomy of wild bees has increased. However, nothing on the taxonomy of *Andrena* in Morocco has been published since 1980 (Warncke 1980), and a critical reappraisal of this rich fauna is therefore warranted.

Inspection of 5,685 female and 2,275 male *Andrena* specimens from contemporary and ongoing collections in Morocco and undetermined material from the Oberösterreich Landesmusum, Linz, the Naturalis Biodiversity Center, Leiden, and the personal collection of Maximillian Schwarz, Ansfelden, comprised 155 valid species, with many new records for Morocco and undescribed taxa. These are described herein, and the identity of several problematic taxa are reviewed.

Materials and methods

Identification was enabled through a comprehensive review of the literature in combination with visits to the Warncke collection in Linz as part of the lead author's ongoing review of West Palearctic *Andrena* species (Wood 2020; Wood et al. 2020a, b).

The subgeneric classification of *Andrena* continues to pose problems. Because of the very large number of species, taxonomic workers have largely been restricted to only a part of the global fauna (broadly, West Palearctic, Central and Eastern Palearctic, and Nearctic falling into three groups), and therefore a co-ordinated global system of subgeneric classification has not yet been possible. In both a Moroccan and West Palearctic context, the system of Warncke (1968a) is the most relevant, and so we broadly follow his assigned subgenera. However, though no globally consistent system currently exists, major steps towards such a reclassification have recently been made (Pisanty et al. 2020). Molecular analyses show that many existing *Andrena* subgenera are strongly polyphyletic (particularly groups such as *Poecilandrena* and *Poliandrena*), and are in need of deep revision. It is currently beyond the scope of this study to revise the subgeneric status of Moroccan *Andrena* taxa, but we take the opportunity to discuss problematic taxa, highlight outstanding areas of confusion, and to place newly described taxa with an appropriate degree of confidence in light of the findings of Pisanty et al. (2020).

Body length was measured from the vertical plane of the front of the head to the tip of the metasoma. Morphological terminology follows Michener (2007). Photographs were taken using an Olympus E-M1 Mark II with a 60 mm macro lens and were stacked using Zerene Stacker 1.04 (Zerene Systems, USA) and plates were prepared in GNU Image Manipulation Program (GIMP) 2.10.

In order to investigate a possible synonymy (see section on *Andrena alchata* Warncke, 1974), DNA was extracted and amplified from two specimens. DNA was extracted from two legs of each individual using a NucleoSpin Tissue (Macherey-Nagel, Düren Germany) extraction kit and following manufacturer´s instructions. The region selected for amplification was the LEP fragment within the mitochondrial gene cytochrome oxidase I (*cox1*), a region widely used in Hymenoptera taxonomy (Sheffield et al. 2009). However, as retrieving genetic information from pinned specimens can be challenging (Wandeler et al. 2007), a section within the fragment was targeted for amplification using primers LEP-F1 and LEP-R2 (Hebert et al. 2004). PCR profile consisted of an initial denaturation step at 94 °C for 3 min followed by 36 cycles of denaturation at 94 °C for 1 min, annealing temperature at 50 °C for 1 min and elongation at 72 °C for 1 min followed by a final extension at 72 °C for 10 min. Results of the PCR reaction were checked in a 1.5% agarose gel. Amplicons were sequenced using forward and reverse primers (Eurofins, Germany).

MSC	Maximillian Schwarz personal collection, Ansfelden, Linz, Austria
NMNL	National Museum of Natural History Naturalis, Leiden, the Netherlands
OÖLM	Oberösterreich Landesmusum, Linz, Austria
TJW	Thomas Wood personal collection, Mons, Belgium
UMONS	University of Mons collection, Mons, Belgium

Results

Description of new species

Andrena (*Aciandrena*) *semiadesus* Wood, sp. nov.

http://zoobank.org/235512E8-91EA-4A84-91B8-41F7727AE452
Figures 1–8

Material. ***Holotype*:** Morocco: Fès-Meknès, Laanoucer, 1456 m, 33.6166N, -4.7484W, 11–12.iv.2019, 1♂, white pan trap, leg. L. Hamroud & A. Sentil. Deposited in the OÖLM. ***Paratypes*:** Morocco: Fès-Meknès, Laanoucer, 1456 m, 11–12.iv.2019, 4♂, white and yellow pan traps, leg. L. Hamroud & A. Sentil; Drâa-Tafilalet, 20 km W Boudnib, 9.iv.1995, 2♂, 2♀, leg. Ma. Halada. Paratypes are deposited at the OÖLM, with a male and female retained in the personal collection of TJW.

Diagnosis. The finely shagreened propodeal triangle, the narrow facial foveae, the absence of longitudinal striations on the clypeus, and the yellow-marked clypeus in the male place this bee in the *Aciandrena*. The classification of *Aciandrena* and its relationship to *Micrandrena*, *Graecandrena*, and *Distandrena* is somewhat in flux, and the subgenus is currently polyphyletic (Pisanty et al. 2020). However, when excluding uncharacteristic taxa that are currently placed in the *Aciandrena* such as *A. janthina* Warncke, 1975 that clearly belong elsewhere (Pisanty et al. 2020), *A. semiadesus* meets the classical definition of *Aciandrena*. The male can be instantly separated from the other *Aciandrena* with yellow clypei because the yellow marking is diminished, it does not extend all the way to the clypeal margins, and the two dark spots that are usually found towards the centre of the clypeus in yellow-faced *Aciandrena* are absent as they instead are contiguous with black markings that extend in from the clypeal margins (Fig. 6). The genitalia are also noticeably more elongate, the capsule almost twice as long as wide, and with a broad penis valve, most other *Aciandrena* species with capsules only a little longer than wide and with a comparatively narrow penis valve (Figs 100, 102, 104, 126, 128, 130; Pisanty et al. 2016). The female is most similar to *A.* (*Graecandrena*) *totana* Warncke, 1974 as they both have a broad, shagreened, dull, moderately raised, and centrally slightly flattened sparsely punctate clypeus, but the tergites of *A. semiadesus* are completely impunctate and the foveae are narrower.

Description. Female: Body length 7 mm (Fig. 1). ***Head*:** Black, as wide as long (Fig. 2). Clypeus broad, slightly arched, dull, strongly shagreened with exception of apical margin where shagreenation is weaker, therefore weakly shining. Sparsely and shallowly punctured, punctures separated by 2–3 puncture diameters. Process of labrum semi-circular, weakly shining. Foveae in lower half deep, narrow, less than half the width of an antenna, very close to inner margin of compound eye. In upper half foveae widen to approximately the width of an antenna, at their widest still occupying less than half the distance between top of compound eye and lateral ocellus. Face, gena, and vertex with moderate brownish to whitish hairs, the longest of these roughly equal to ½ the length of the scape. Antennae dark, A5–12 lightened orange below, A3 equalling A4+5 combined. Gena slightly wider than width of compound eye, weakly longitudinally striate. Ocelloccipital distance short, less than 1/3 width of lateral ocellus. ***Mesosoma*:** Scutum and scutellum completely shagreened, weakly shining, punctures shallow and inconspicuous, punctures separated by 2–3 puncture diameters (Fig. 3). Propodeal triangle differentiated from rest of propodeum by larger and coarser shagreenation, weakly shining. Episternum and propodeum finely shagreened, dull. Episternum with sparse, long white hairs, these approaching ¾ of the length of the scape. Legs dark, tarsal segments becoming dark brown. Femoral and tibial scopa simple, white. Wings hyaline, venation light brown, stigma pale yellow, nervulus interstitial to slightly antefurcal. ***Metasoma*:** Tergites dark, margins lightened yellow (Fig. 4). Tergal discs strongly microreticulate, punctation extremely sparse and obscured. T2–4 laterally with very weak fringes of white hairs. T5–6 with golden hairs flanking pygidial plate, this rounded with raised margin, shagreened, weakly shining.

Male. Body length 6.5–7 mm (Fig. 5). ***Head*:** Black, wider than long. Clypeus slightly arched, ground colour black but with large yellow marking covering approxi-

Figures 1–8. *Andrena* (*Aciandrena*) *semiadesus* sp. nov. **1** female profile **2** female face **3** female dorsum **4** female tergites **5** male profile **6** male face **7** male tergites **8** male genitalia.

mately 90% of surface (Fig. 6). Yellow marking does not extend to base of clypeus. Laterad of clypeal centre, yellow marking reduced, two black triangular markings extending in towards the centre, giving marking a broad, inverted T-shape. In basal half, clypeus dull and shagreened, becoming shiny in apical half. Clypeal punctures shallow and irregular, separated by 2–5 puncture diameters. Process of labrum rectangular, twice as broad and long, shiny. Face, gena, and vertex with long white hairs, longest on underside of head, equalling length of the scape. Scape and pedicel black, following antennal segments dark brown to black, A3 longer than A4, shorter than A4+5 combined. Gena and ocelloccipital distance as in female. ***Mesosoma*:** Scutum and scutellum dull, strongly shagreened, sparsely and shallowly punctured, punctures separated by 1–4 puncture diameters. Propodeal triangle weakly marked, scarcely differentiated from propodeum, shagreened, slightly shining laterally. Mesosoma with white hairs, sparse on scutum, denser and longer on episternum, exceeding length of scape. Legs dark, only final tarsal segment slightly lightened to dark brown, pubescence white. Wings hyaline, venation brown, stigma brown, nervulus interstitial. ***Metasoma*:** Tergites as in female, but margins more strongly lightened, transparent whitish apically (Fig. 7). Tergal margins laterally with loose white hair bands of irregular length, very widely interrupted. Genitalia simple (Fig. 8), gonocoxites forming rounded dorsal lobes, gonostyli long, tapering to rounded end.

Distribution. Central and eastern Morocco (Fig. 145a).

Floral preferences. None recorded.

Etymology. The name *semi* (partly or partially) + *adesus* (eaten, worn, eroded) was chosen to illustrate the clypeus of the male, where the central yellow marking is laterally diminished by intruding black marks.

Andrena (*Aciandrena*) *triangulivalvis* Wood, sp. nov.

http://zoobank.org/FE3F09DD-2181-4E54-BA70-FEAABAAA6F52
Figures 9–12

Material. ***Holotype*:** Morocco: Drâa-Tafilalet, 20 km W Boudnib, 9.iv.1995, 1♂, leg. Ma. Halada. Deposited in the OÖLM. ***Paratypes*:** Morocco: Drâa-Tafilalet, 20 km W Boudnib, 9.iv.1995, 3♂, leg. Ma. Halada. Paratypes are deposited at the OÖLM, with a male retained in the personal collection of TJW.

Diagnosis. The male of *A. triangulivalvis* resembles other *Aciandrena* with a yellow polished clypeus such as *A. pratincola*. However, it can be instantly separated from all other *Aciandrena* with a yellow clypeus by the structure of the genitalia. Normal *Aciandrena* genitalia are simple, with a relatively narrow, unmodified penis valve (Figs 8, 100, 102, 104, 126, 128, 130; Warncke 1968b, 1972, 1974, 1975a; Pisanty et al. 2016). However, in *A. triangulivalvis* the penis valve is inflated and forms a triangle that sites between the broad gonostyli that have a slightly raised internal margin (Fig. 12).

Description. Female: Unknown.

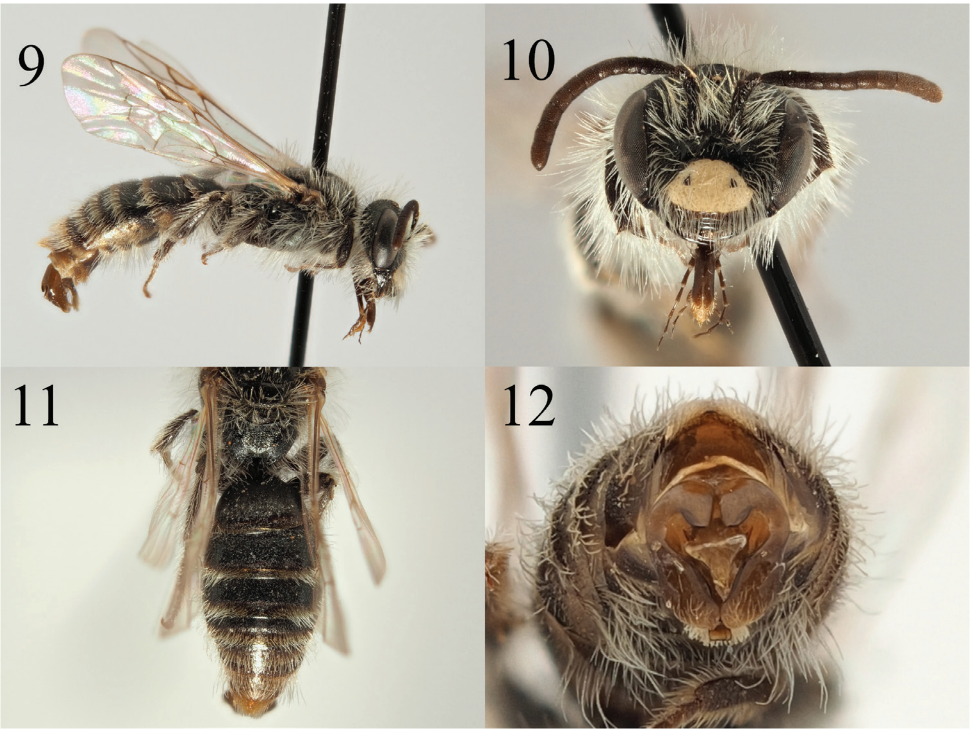

Figures 9–12. *Andrena* (*Aciandrena*) *triangulivalvis* sp. nov. **9** male profile **10** male face **11** male tergites **12** male genitalia.

Male. Body length 6 mm (Fig. 9). ***Head*:** Dark, close to black, instead a subtle faintly metallic dark green. Clypeus arched, completely pale yellow with the exception of two lateral small black triangular marks, polished and evenly punctured, punctures separated by 1–2 puncture diameters (Fig. 10). Process of labrum trapezoidal, fore margin emarginate. Gena as wide as width of compound eye. Face, gena, scape, and vertex with long white hairs, the longest achieving length of the scape. Antennae dark, A6–13 slightly lightened brown, A3 equalling A4+5. Ocelloccipital distance short, less than 1/3 width of lateral ocellus. ***Mesosoma*:** Scutum and scutellum dark, with slight metallic green-purple hints when viewed from an angle, strongly shagreened, weakly shining, sparsely and irregularly punctured, punctures separated by 1–3 puncture diameters. Propodeal triangle weakly marked, shagreened, slightly shining laterally, centrally weakly rugose. Episternum and propodeum strongly shagreened, obscurely punctured, dull. Scutum, scutellum, episternum, and propodeum with long white hairs, the longest exceeding the scape in length. Legs dark, tarsi lightened to brown, pubescence whitish. Wings hyaline, venation and stigma light brown, nervulus slightly antefurcal. ***Metasoma*:** Tergites dark, marginal areas light brown to yellow (Fig. 11). Tergal discs microreticulate, intensity of microreticulation diminishes from T1 onwards, T1 therefore dull, T4–5 weakly shining. T2–4 with weak lateral hair fringes, those on T5–6 extend across the whole margin but sparsely, never obscuring underlying surface. Genitalia compact, slightly longer than wide, gonocoxites forming pronounced points, penis valve strongly inflated basolaterally, forming a triangle (Fig. 12). Gonostyli with inner margin thickened and raised, medially forming a 135-degree angle, gonostyli apexes slightly restricted before forming rounded point.

Distribution. Eastern Morocco from the province of Drâa-Tafilalet (Fig. 145b).

Floral preferences. None recorded.

Etymology. The name *trianguli* (triangular) + *valvis* (valve) was chosen because of the remarkable male genitalia in which the penis valve is inflated and triangular in shape, strongly contrasting with other *Aciandrena* species.

Andrena **(*Campylogaster*)** ***sparsipunctata*** **Wood, sp. nov.**

http://zoobank.org/710F0923-3C28-4B47-B6C5-95F4CC4CD880
Figures 13–28

Material. ***Holotype*:** Morocco: Guelmim-Oued Noun, 10 km E Guelmim, 15–16.iv.1995, 1♀, leg. Ma. Halada. Deposited in the OÖLM. ***Paratypes*:** Morocco: Guelmim-Oued Noun, 10 km E Guelmim, 15–16.iv.1995, 1♂, 1♀, leg. Ma. Halada, OÖLM; Oriental, 10 km S Bouarfa, 20.v.1995, 2♂, leg. Ma. Halada, OÖLM. Paratypes are deposited in the OÖLM.

Diagnosis. *Andrena sparsipunctata* can be easily placed into the *Campylogaster* because of the large, dense, and clear punctures on the episternum combined with its large body size. However, recent evidence shows that *Campylogaster* is strongly polyphyletic, and the species in northwestern Africa do not fall close to *A.* (*Campylogaster*) *erberi* Morawitz, 1871, the type species of *Campylogaster* that differs by its tormentose pilosity. A new subgenus is probably needed for the species around *A. sparsipunctata* (Pisanty et al. 2020). Against this context, it is close to the two most widespread *Campylogaster* species in North Africa, *A. pruinosa* Erichson, 1835 ssp. *succinea* Dours, 1872 and *A. caroli* Pérez, 1895, both of which are also stained red over the majority of the metasoma. The female of *A. sparsipunctata* is instantly recognisable because the punctures of the first tergite are sparse, separated by 2–4 puncture diameters (Fig. 16) whereas in the other two species the punctures are dense and separated by 1–2 puncture diameters (Figs 18, 20). Moreover, the foveae of *A. sparsipunctata* females are narrow and depart from the inner eye margins so that at the top of the compound eye they are separated from the compound eye by a distance subequal to the width of a fovea itself (Fig. 15), whereas in the other two species the foveae are never clearly separated from the top of the compound eye (Figs 17, 19). The scutal hairs are also normal, not squamous (Fig. 15), strongly contrasting with the squamous hairs of the other two species (Figs 17, 19).

In males, *A. sparsipunctata* can be recognised by the shape of the labrum which is wide and rectangular (Fig. 23), whereas in *A. pruinosa* it is trapezoidal and markedly emarginate (Fig. 25). In *A. caroli* it is less strongly trapezoidal and emarginate (Fig. 27), but the tergites have well-marked and dense bands of short white hairs on the tergal

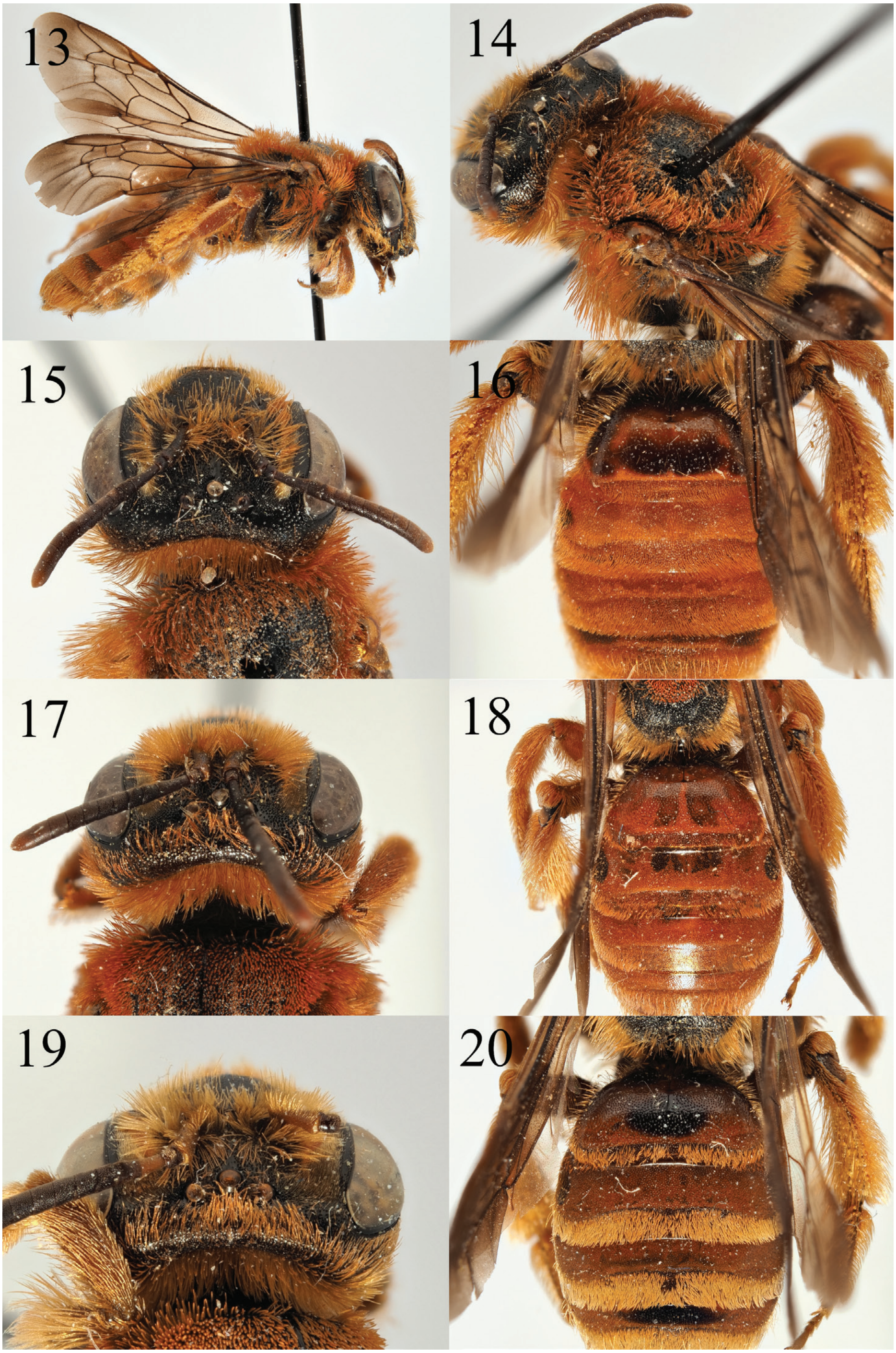

Figures 13–20. *Andrena* (*Campylogaster*) *sparsipunctata* sp. nov. **13** female profile **14** female mesonotum in semi-profile **15** female head dorsal view **16** female tergites. *Andrena* (*Campylogaster*) *pruinosa succinea* Dours, 1872 **17** female head dorsal view **18** female tergites. *Andrena caroli* Pérez, 1895 **19** female head dorsal view **20** female tergites.

margins (Fig. 28), whereas *A. sparsipunctata* has only a few scattered hairs on the tergal margins, never forming well-marked bands, as in *A. pruinosa* (Fig. 26).

Description. Female: Body length 12 mm (Fig. 13). ***Head*:** Black, a little wider than long. Clypeus domed, evenly and shallowly punctured, punctures separated by 0.5–1 puncture diameters. Clypeus surface weakly shining, fore margin slightly upturned. Process of labrum trapezoidal, with weak lateral striations, fore margin weakly and narrowly emarginate. Gena 1.2 times wider than width of compound eye, densely and deeply punctate, punctures extend to the vertex where they become much shallower and encircle two impunctate areas immediately adjacent to lateral ocelli, these areas equivalent to inter-ocellar area in size (Fig. 15). Gena and vertex with a mane of bright ginger hairs, achieving a maximum length of 2/3^{rds} of the length of the scape. Face, scape, and clypeus with shorter ginger hairs, these achieving a maximum length of ½ the length of the scape. Antennae dark, A3 apically and A4–12 lightened orange below, A3 longer than A4+5, shorter than A4+5+6. Foveae narrow, slightly narrower than the width of an antenna, close to the internal margin of compound eye below level of antennal insertions but diverging above so that at top of compound eye each fovea is separated by a distance subequal to its own width, area between a fovea and the internal margin of compound eye shiny and sparsely punctured. Ocelloccipital distance broad, two times the width of lateral ocellus. ***Mesosoma*:** Scutal punctures dense, punctures almost touching, underlying surface shiny. Scutum and scutellum with non-squamous hairs, these achieving a maximum length of ½ the length of the scape (Fig. 14). Episternum and propodeum with exception of propodeal triangle densely and evenly punctate, punctures separated by 0.5 puncture diameters, underlying surface finely and subtly shagreened, weakly shining. Propodeal triangle weakly rugose. Episternum and propodeum with normal ginger hairs, these achieving the length of the scape. Femora dark, tibia and tarsi orange. Femoral and tibial scopa orange. Wings slightly infuscate, venation dark, stigma slightly translucent. Nervulus interstitial. ***Metasoma*:** Tergites amber, becoming amber to dark brown on T1. T1 strongly contrasting with following tergites, T1 sparsely punctate, punctures separated by 2–4 puncture diameters, surface of disc clear of hairs, shining (Fig. 16). T2–4 densely punctured, punctures separated by 0.5–1 puncture diameters, covered in short ginger hair across entire surface. Tergal margins slightly depressed, covered in short ginger hairs that form weak apical fringes, poorly differentiated from hairs on discs of T2–4. T5–6 with long ginger-golden hairs flanking pygidial plate, pygidial plate simple, triangular, without raised margins.

Male. Body length 11–12 mm (Fig. 21). ***Head*:** Similar to female, wider than long, pubescence whitish throughout but probably faded. All punctation weaker and finer with exception of clypeus where it is equally strong as in the female. Labrum broadly rectangular, wider than long, fore margin straight, without emargination (Fig. 23). Mandibles long, crossing, very slightly bidentate with tiny internal tooth. Scape dark-orange, A2–13 evenly orange coloured, A3 equalling A4. Ocelloccipital distance broad, 1.5 times width of lateral ocellus. ***Mesosoma*:** Similar to female, punctation of the scutum and scutellum weaker, punctation of the episternum and propodeum absent, replaced by weak rugosity. Venation of wings amber, nervulus interstitial to antefurcal. ***Metasoma*:** Tergites amber, extent variable, becoming darker on centre of tergal discs,

Figures 21–28. *Andrena* (*Campylogaster*) *sparsipunctata* sp. nov. **21** male profile **22** male genitalia **23** male face and labrum **24** male tergites. *Andrena* (*Campylogaster*) *pruinosa succinea* Dours, 1872 **25** male face and labrum **26** male tergites. *Andrena caroli* Pérez, 1895 **27** male face and labrum **28** male tergites.

in some cases forming extensive dark bands across entire surface (Fig. 24). Punctation shallow and even, separated by 1–2 puncture diameters, not noticeably sparser on T1 compared to other tergites. Sternite 8 long, rectangular, three times longer than broad, covered in hairs, apex weakly emarginate. Genitalia simple (Fig. 22), gonocoxites slightly pointed, weakly separated from each other apically.

Distribution. Southern and eastern Morocco in desert environments (Fig. 145c).

Floral preferences. None recorded.

Remarks. There is uncertainty over the exact status of *A. pruinosa succinea*, as the North African animals differ in colouration of the metasoma and scutal hairs (red) from *A. pruinosa sensu stricto* (black-brown) from Spain. However, structural differences are minor (e.g., the shape of the foveae is the same), and molecular investigation is warranted. It is however clear that the name *succinea* cannot apply to the bees described here as the first tergite of females is much less densely punctured than *A. pruinosa* s.l. from either Spain or North Africa, and Dours (1872) makes no mention of contrasting tergal punctation in his description 'Abdomen… très-finement ponctué et hérissé de poils…'. The sampling locations of *A. sparsipunctata*, both found at the extreme edges of Morocco, may provide an explanation as to why this species has gone undetected to date.

Etymology. The name *sparsi* (sparse) + *punctata* (punctured) was chosen to illustrate the first tergite of females, which is much less densely punctate than the similarly coloured *A. pruinosa succinea* and *A. caroli*.

Andrena (*Carandrena*) *hebescens* Wood, sp. nov.

http://zoobank.org/BECF6642-E2D6-479D-A132-18F49B9725B6
Figures 29–40

Material. ***Holotype*:** Morocco: Guelmim-Oued Noun, 15–16.iv.1995, 1♀, leg. Ma. Halada. Deposited in the OÖLM. ***Paratypes*:** Morocco: Guelmim-Oued Noun, 15–16.iv.1995, 4♂, 6♀, leg. Ma. Halada, OÖLM; Souss-Massa, Tassademt, 50 km NE, Agadir, 19.iv.1996, 1♀, leg. M. Schwarz, OÖLM; Souss-Massa, Aoulouz-Taliouine, 19.iii.1988, 1♂, leg. H. Teunissen. Paratypes are deposited at the OÖLM and NMNL, with a male and female retained in the personal collection of TJW.

Diagnosis. The female of *A. hebescens* can be placed in the *Carandrena* because the dorsolateral angle of the pronotum has a transverse ridge, the propodeal triangle is shagreened and weakly rugose at the base, and there is almost no punctation on the metasoma, and the head has a typical *Carandrena* shape, broader than long, with the inner eye margins slightly converging below (Fig. 30). It is most similar to *A. euzona* Pérez, 1895 and *A. microthorax* Pérez, 1895 given its dark, non-metallic appearance (*A. aerinifrons* Dours, 1873, *A. bellidis* Pérez, 1895, *A. daphanea* Warncke, 1974, *A. deserta* Warncke, 1974, *A. nigroviridiula* Dours, 1873, and *A. reperta*, Warncke, 1974 with metallic green or blue integument, *A. binominata* Smith, 1853, *A. eremobia* Guiglia, 1933, and *A. leucophaea* Lepeletier, 1841 with partially red metasoma), dull domed clypeus, and white hair bands on the tergites (*A. eddaensis* Gusenleitner, 1998 and *A. decaocta* Warncke, 1967 with felt-like hair on the tergal discs). However, the scutum

Figures 29–34. *Andrena* (*Carandrena*) *hebescens* sp. nov. **29** female profile **30** female face **31** female dorsum **32** female tergites. *Andrena* (*Carandrena*) *euzona* Pérez, 1895 **33** female dorsum **34** female tergites.

is shagreened and only weakly shining (Fig. 31) whereas in *A. euzona* it is extensively smooth and shiny (Fig. 33), and the hair bands are narrower (Fig. 32) whereas in *A. euzona* they are wider (Fig. 34). The clypeus is also evenly punctured and shagreened, weakly shining with only a subtle impunctate mid-line whereas in *A. microthorax* it is shiny and strongly punctured with a conspicuous impunctate mid-line, particularly at the fore margin of the clypeus where it forms a broad impunctate triangle.

The male of *A. hebescens* has a yellow marking on the clypeus, but this is reduced in size and does not cover the entire clypeal surface, with two black markings that extend in from the clypeal margins giving the marking an inverted 'T' shape (Fig. 36).

The male is therefore superficially similar to *A. semiadesus*, but can be separated by the typical *Carandrena* head which is clearly wider (more than 1.5 times) than the width of a compound eye in *A. hebescens* (Figs 37, 38) but only slightly wider in *A. semiadesus* and lacking an angulate hind corner. The male of *A. microthorax* can have a yellow clypeal marking, but the scutum and tergites of this species are shiny, whereas in *A. hebescens* they are shagreened and at most, weakly shining (Fig. 39).

Description. Female: Body length 8 mm (Fig. 29). ***Head*:** Black, clearly wider than long (Fig. 30). Clypeus arched, shagreened, weakly shining. Clypeus evenly punctured with exception of a subtle, impunctate midline, punctures otherwise separated by 0.5–1 puncture diameters. Process of labrum trapezoidal, fore margin very weakly emarginate. Gena as wide as width of compound eye. Gena, face, and scape with moderately dense white hairs, the longest not achieving length of the scape. Vertex with whitish brown hairs of a similar length. Foveae normal, occupying half the distance between the compound eye and a lateral ocellus. Antennae dark, scape black, A2–4 apically lightened to orange, A5–12 predominantly orange ventrally, A3 exceeding A4+5, shorter than A4+5+6. Ocelloccipital distance short, less than 1/3 width of lateral ocellus. ***Mesosoma*:** Scutum dark, evenly and shallowly punctured, punctures separated by 1–2 puncture diameters, underlying surface shagreened, weakly shining (Fig. 31). Scutellum less densely punctured, punctures separated by 3–4 puncture diameters, shagreenation weaker, more strongly shining. Episternum and propodeum microreticulate, dull, propodeal triangle slightly more finely shagreened, weakly shining, distinct. Scutum and scutellum with faded light brownish hairs, episternum and propodeum with longer white hairs, the longest achieving the length of the scape. Legs dark, tarsi lightened brown, pubescence white, femoral and tibial scopa white, hairs simple. Wings hyaline, venation and stigma golden brown. Nervulus interstitial to slightly antefurcal. ***Metasoma*:** Tergites dark with wide lightened margins, apically translucent, basally yellowish (Fig. 32). Tergal discs microreticulate, weakly shining. T1 shallowly punctured, punctures separated by two puncture diameters. Following tergites weakly and obscurely punctured, punctures hidden by microreticulation. Tergal margins with dense white hairbands, on T1 widely interrupted, on T2–4 complete. T5+6 centrally with golden hairs flanking pygidial plate, laterally with white hairs. Sternites with plumose white hairs, forming loose fringes apically on hind margins.

Male. Body length 8 mm (Fig. 35). ***Head*:** Similar to female, clypeus slightly arched, evenly and shallowly punctured, punctures separated by one puncture diameter, no impunctate central line. Clypeus centrally with yellow mark, this not reaching the lateral or basal margin of the clypeus, laterally invaded by two black marks therefore forming a broad inverted T-shape (Fig. 36). Underlying surface weakly shagreened, moderately shiny. Process of labrum trapezoidal, fore margin inflated, slightly bulbous, very weakly emarginate. Antennae dark, A4–13 slightly lightened dark brown, A3 exceeding A4, shorter than A4+5. Gena enlarged, most 1.2 times wider than compound eye, non-carinate, with weakly angulate hind corner (Fig. 37). Gena, vertex, and face below the level of the antennal insertions with long white hair equalling length of the scape. Scape,

Figures 35–40. *Andrena* (*Carandrena*) *hebescens* sp. nov. **35** male profile **36** male face **37** male gena **38** male dorsum **39** male tergites **40** male genitalia.

frons, and inner margin of compound eyes with mixture of black and white hairs. Ocelloccipital distance short, 2/3 width of lateral ocellus. ***Mesosoma*:** Similar to female but scutum with stronger shagreenation, dull except for central shining line (Fig. 38). Scutellum centrally weakly shining, contrasting with the scutum. Episternum, propodeum, and mesosomal pubescence as in the female. Legs dark, tarsi lightened brown, with white pubescence. Wings hyaline, venation dark brown, stigma centrally light brown. Nervulus interstitial to slightly antefurcal. ***Metasoma*:** Similar to the female. Tergites more clearly punctured, punctures visible against the microreticulation with slightly raised margins giving the overall surface an uneven impression (Fig. 39). T1–5 consistently punctured, punctures separated by 3–4 puncture diameters. T2–4 laterally with weak fringes of white hair, T5–6 with complete fringes of whitish to golden hairs. Sternites forming loose white hair bands apically. Genitalia simple, of a typical *Carandrena* form, gonocoxites apically forming weak points, rounded, diverging apically (Fig. 40).

Distribution. South-western Morocco in the Souss valley (Fig. 145a).

Floral preferences. None recorded.

Etymology. The name *hebescens* was chosen because this member of the *Carandrena*, though morphologically similar to several species with metallic green colouration, is completely dark, therefore *heb-* (dull or blunt) + *escens* (becoming).

Andrena (*Cnemidandrena*) *niveofacies* Wood, sp. nov.

http://zoobank.org/E8892496-603A-4AD8-BB34-E5F63A35E60E
Figure 41–54

Material. ***Holotype*:** Morocco: Marrakesh-Safi, Asni, S Imlil, 2900 m, 24.viii.1992, 1♀, leg. Warncke [see Remarks]. Deposited in the OÖLM. ***Paratypes*:** Morocco: Marrakesh-Safi, Asni, S Imlil, 3300 m, 21.viii.1992, 1♂, leg. Warncke, OÖLM.

Diagnosis. *Andrena niveofacies* can easily be recognised as part of the *Cnemidandrena* because of the transverse ridge on the dorsolateral angle of the pronotum, the triangular hind tibiae in the female, the upturned process of the labrum in the male (Fig. 48), the thick and distinct hair bands on the metasoma (Figs 45, 46), and the late summer activity period.

Within the *Cnemidandrena*, *A. niveofacies* females have completely brown hair on the scutum (intermixed with black in *A. denticulata* (Kirby, 1802)), the galea is dull (shiny in *A. fuscipes* (Kirby, 1802)), T5–6 are black haired (light haired in *A. tridentata* (Kirby, 1802)), and the face is pale haired (black at least in part in *A. nigriceps* (Kirby, 1802) and *A. freygessneri* Alfken, 1904). The female *A. niveofacies* is most similar to *A. simillima* Smith, 1851 but is can be easily separated as it has strikingly bright white hairs on the face and gena (Fig. 43), these being buff-brown in *A. simillima*.

The male has a non-carinate gena (Fig. 49, carinate in *A. denticulata* and *A. tridentata*), the galea is dull (shining in *A. fuscipes*), S8 is short and relatively densely haired (long and sparsely haired in *A. freygessneri*, see illustrations in Ember 2001), and the face has bright white hairs, with no trace of black hairs on the discs of the tergites (face with brown hairs in *A. nigriceps*, T4–5 with black hairs basally). However, the male material also differs from *A. simillima* as A3+4 are equal in length, whereas in *A. simillima* A3 is a little longer than A4.

Description. Female: Body length 10 mm (Fig. 41). ***Head*:** Black, a little wider than long. Clypeus slightly arched, evenly and clearly punctured, punctures dense, separated by 0.5–1 puncture diameters with the exception of subtle central impunctate line than widens into a triangle immediately before fore margin of clypeus. Underlying surface weakly shagreened, slightly shining. Process of labrum trapezoidal, fore margin clearly emarginate. Gena slightly wider than width of

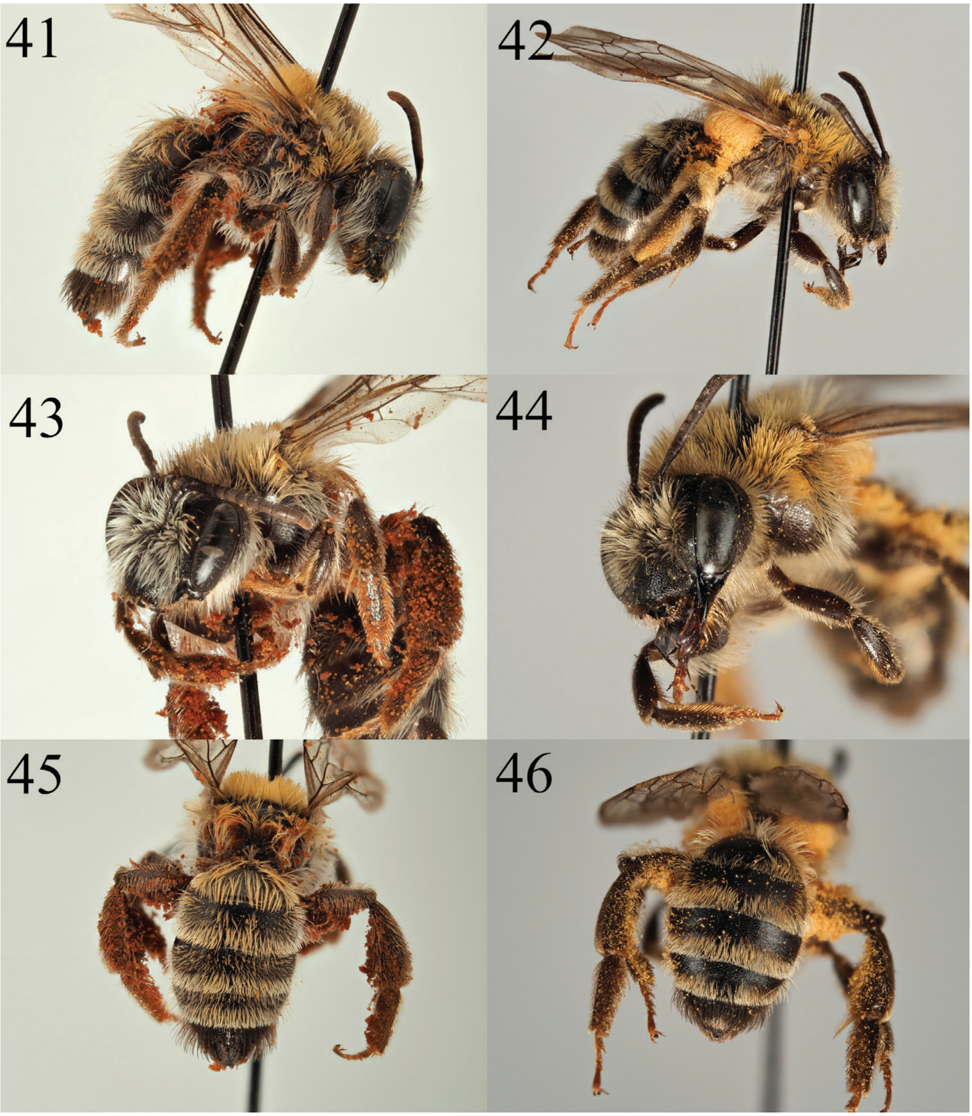

Figures 41–46. *Andrena* (*Cnemidandrena*) *niveofacies* sp. nov. **41** female profile **43** female face **45** female tergites. *Andrena* (*Cnemidandrena*) *simillima sischkai* Warncke, 1988 (holotype) **42** female profile **44** female face **46** female tergites.

compound eye. Gena, face, and scape with bright white hairs, longest achieving length of the scape (Fig. 43). Vertex with contrasting brown and black hairs of equal length. Foveae generally wide, occupying three quarters of distance between top of compound eye and lateral ocellus. Antennae black, ventral surface of A4–12 lightened brown, A3 slightly shorter than A4+5. Ocelloccipital distance equalling width of lateral ocellus. ***Mesosoma*:** Scutum densely punctate, punctures separated by 0.5 puncture diameters over majority of disc but becoming sparser towards rear in centre and on scutellum, here separated by one puncture diameter. Underlying surface microreticulate, but this weakens to become fine shagreenation, shining, centrally and laterally on scutum and particularly on scutellum. Episternum with microreticulation, dull. Propodeum laterally shagreened, weakly shining, posterolaterally microreticulate and dull with large shallow punctures, these absent from the propodeal triangle which is therefore well defined. Scutum, scutellum, and propodeum with buff-brown hairs of moderate length, contrasting with white hairs on episternum. Legs dark, tarsal segments lightened brown. Wings hyaline, venation black, stigma centrally dark brown. Nervulus clearly antefurcal. ***Metasoma*****:** Tergites black, microreticulate, weakly shining, moderately punctured, punctures separated by 1–2 puncture diameters (Fig. 45). T1 with long buff-brown hairs over whole disc and margin, T2–4 with clear buff-brown hair bands occupying marginal area, surface of disc with sparser and shorter hairs of same colour. T5–6 with black-brown hairs. S2–4 with sparse white hairs forming weak bands.

Male. Body length 10 mm (Fig. 47). ***Head*****:** As in the female, but clypeus without central impunctate line, process of labrum narrow and centrally upturned (Fig. 48). Galea dull (Fig. 49). Antennae dark, A4–13 lightened to dark brown below, A3 equalling A4. Gena wide, 1.5 times wider than width of compound eye, non-carinate, forming weak posterior angle. Face, gena, scape, and vertex all with long white hairs achieving length of the scape. Ocelloccipital distance broad, 1.5 times width of lateral ocellus. ***Mesosoma*****:** Scutum and scutellum as in female, microreticulation weaker so the whole surface appears shinier. Propodeal punctures weaker and shallower, slightly obscured by weak reticulation, contrast with the propodeal triangle as in the female. ***Metasoma*****:** As in female (Fig. 51), T2–5 with pale hair bands, T6 with brown apical fringe. S8 short and densely hairy (Fig. 53).

Distribution. Probably restricted to the High Atlas Mountains of Morocco. This material represents the first record of the subgenus *Cnemidandrena* from Morocco and more broadly the whole of North Africa (Fig. 145b).

Floral preferences. The single female had a full scopa (Fig. 43) comprising 95% *Cirsium*-type (Asteraceae: Cynareae) and 5% *Eryngium*-type (Apiaceae). It is too early to draw strong conclusions, as *Cnemidandrena* contain both oligolectic (*A. denticulata*, Asteraceae, Wood and Roberts 2017) and polylectic species (*A. freygessneri*, *A. nigriceps*, *A. simillima*; Wood and Roberts 2017; Else and Edwards 2018; Müller 2018).

Remarks. There has historically been uncertainty over the species status of taxa assigned to *A. simillima*. The former subspecies *A. freygessneri* was returned to species status by Ebmer (2001), but the status of *A. s. bremensis* Alfken, 1900 and *A. s. sischkai* Warncke, 1988 remain unclear. This latter subspecies is found in Bulgaria and Greece (Figs 42, 44, 46, 50, 52, 54; Warncke 1988) and the facial hairs are buff coloured as in the nominate form (Fig. 44), but the tergites are much less densely hairy and the hairs are shorter, giving the overall impression that the bee is darker (Figs 46, 52). It is likely that both taxa are distinct from *A. simillima*, but more work is required. Against this context, we describe *A. niveofacies* as a good species, not only because of the morphological differences but also because of the degree of geographical separation, with the *locus typicus* in the High Atlas approximately 1,600 km from the nearest *A. simillima* records in southern France.

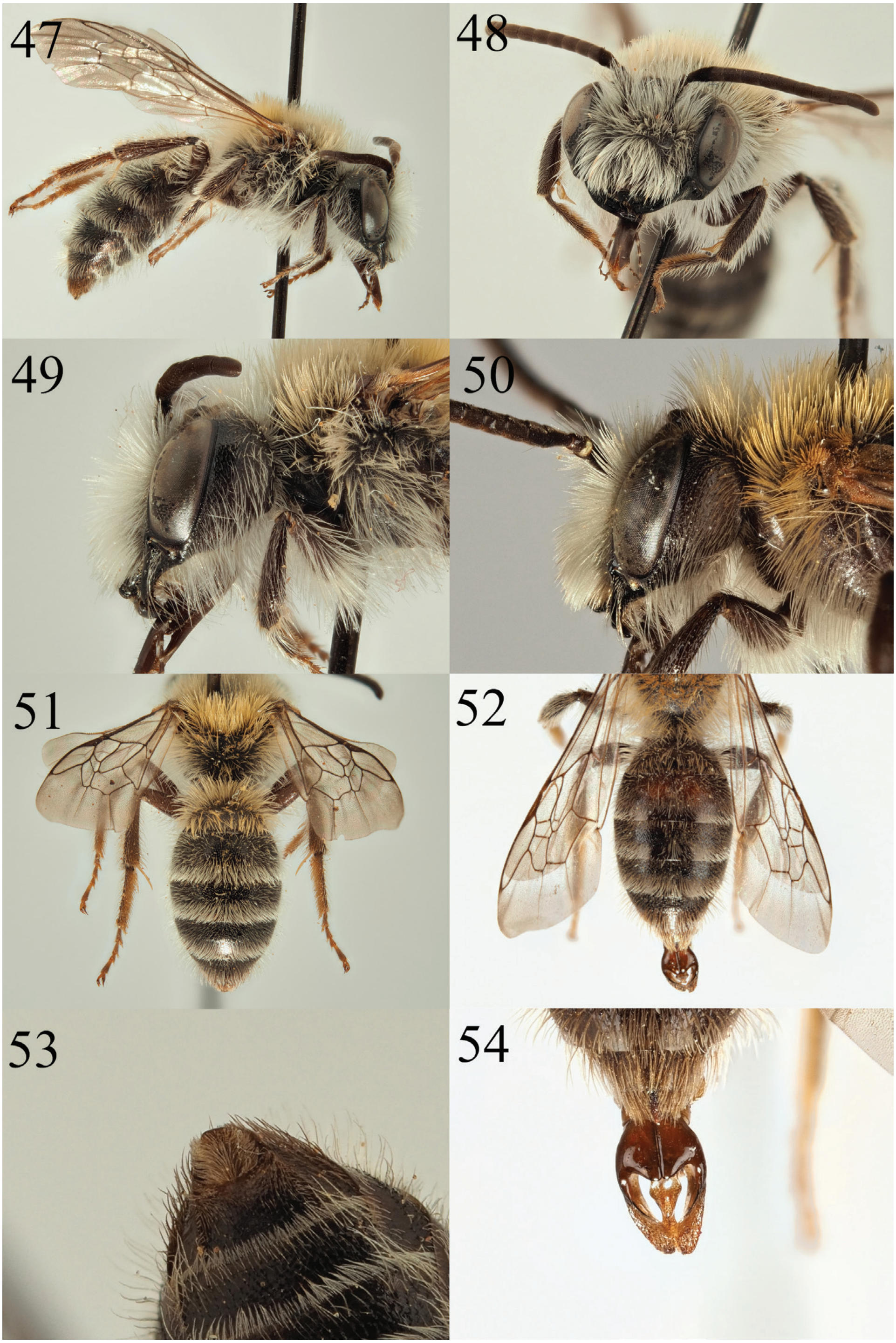

Figures 47–54. *Andrena* (*Cnemidandrena*) *niveofacies* sp. nov. **47** male profile **48** male face **49** male gena **51** male tergites **53** male sternite 8. *Andrena* (*Cnemidandrena*) *simillima sischkai* Warncke, 1988 (paratype) **50** male gena **52** male tergites **54** male genitalia.

The collection labels themselves are a small mystery, as they have the collector name Warncke struck through by hand (~~Warncke~~). They may have been used by a collector accompanying Warncke who used his spare preprinted labels, but if this is the case then their identity is not clear.

Etymology. The subspecific epithet *niveofacies* from *niveus* (snow) + *facies* (face) was chosen to illustrate the bright white facial hair.

Other material examined. (*Andrena simillima sischkai*): Greece: Olympus, 2000–2200 m, 18.viii.1978, 1♀, leg. K. Warncke, OÖLM (holotype); Bulgaria: mer., Pirin, Popina-Lka I (1350 m), 23–27.vii.1974, 1♂, leg. Dr. A. Hoffer, OÖLM (paratype); (*Andrena simillima simillima*): United Kingdom: Devon, Weston Cliff NT, Branscombe, 23.vii.1992, 1♀, leg. M. Edwards, TJW.

***Andrena* (*incertae sedis*) *gafsensis* Wood, sp. nov.**

http://zoobank.org/B4DDA0DB-D0BC-4675-B135-B20636594D00
Figures 55–62

Material. ***Holotype*:** Tunisia: 40 km NW Gafsa, 17.iv.1994, 1♀, leg. M. Schwarz. Deposited in the OÖLM. ***Paratypes*:** Tunisia: 40 km NW Gafsa, 17.iv.1994, 3♂, 1♀, leg. M. Schwarz. Paratypes are deposited at the OÖLM, with a male and female retained in the personal collection of TJW.

Diagnosis. Placement of this species into a subgenus is not immediately obvious. *Andrena gafsensis* is a small to medium sized *Andrena* with a strongly flattened clypeus that is extensively shiny in both the female (Fig. 56) and the male where it is coloured yellow, with this colouration extending onto the lower paraocular areas (Fig. 60). This pattern of yellow colouration is typically found in males from the subgenera *Holandrena* Pérez, 1980, *Ulandrena* Warncke, 1968, and *Nobandrena* Warncke, 1968. Specimens can quickly be separated from the first two because of the sculpturing of the episternum and propodeum (simple, not honeycomb-areolate) and from the second by the shape of the female hind tibial spur (straight not medially broadened) and the genitalia of the male (penis valve not inflated).

Nobandrena normally contains large species in the range of 13–14 mm in length, most of which have males with domed clypei which are extensively yellow-marked, with the yellow extending onto the lower paraocular areas. However, there are two smaller species *A. iliaca* Warncke, 1969 (7–8 mm, Turkey, Israel, and Jordan) and *A. ounifa* Warncke, 1974 (7–7.5 mm, Algeria, see below for new description of female) placed into the *Nobandrena* by Warncke where the male clypeus is shinier and flatter, whilst retaining the same colour pattern. This flattened clypeus can be seen in the female of *A. ounifa* which has a strongly flattened and shining clypeus in both the female (Fig. 94) and the male (Fig. 98). However, these two taxa clearly do not belong in the *Nobandrena*, with molecular analysis placing *A. iliaca* in the *Fuscandrena* (Pisanty et al. 2020). The position of *A. ounifa* is unclear without molecular work, and so confident placement of *A. gafsensis* is not possible at this time.

Given these problems, *Andrena gafsensis* is therefore best recognised in the female by the distinctive clypeal structure (Fig. 56), but then separated from *A. ounifa* by the short propodeum (Fig. 57) and by the colouration of the tergites which are almost completely red except for the basal parts of T1 and two lateral black spots on T2 (Fig. 58). The male can be recognised by the clypeal structure and colouration, but can also be separated by the short propodeum as in the female and by the structure of the genitalia (Fig. 62) which are most similar to *A. iliaca* but the gonocoxites form lateral points and the gonostyli lack an emargination in the outer margin.

Description. Female: Body length 9 mm (Fig. 55). ***Head*:** Black, as wide as long. Clypeus very slightly arched laterally, flattened over the majority of its area (Fig. 56). Laterally with punctures separated by one puncture diameter but only immediately adjacent to clypeal margin, remaining parts more sparsely punctured, punctures separated by 2–3 puncture diameters, underlying surface smooth and shiny. Process of labrum broad, trapezoidal, approximately twice as wide basally as long. Gena approximately width of compound eye. Gena, vertex, face, and scape with white hairs, the longest not exceeding length of the scape. Foveae of average width, occupying just over half the distance between top of compound eye and lateral ocellus. Antennae black, A4–12 extensively lightened orange below, A3 equalling A4+5+6. Ocelloccipital distance short, less than 1/3 width of lateral ocellus. ***Mesosoma*:** Scutum and scutellum densely punctured, punctures separated by 1–1.5 puncture diameters, underlying surface of the scutum shagreened anteriorly and laterally, shiny centrally, posteriorly and on scutellum. Episternum microreticulate, dull. Lateral faces of propodeum (propodeal corbicula) shagreened, weakly shining. Hind face of propodeum microreticulate and weakly rugose, rugosity outlining propodeal triangle which is rugose and therefore defined by change in texture (Fig. 57). Scutum and scutellum with short brown hair, at most achieving the length of A3. Episternum and propodeum with longer white hair, never exceeding length of the scape. Legs dark, tarsi lightened brown, pubescence brown to brownish white. Femoral scopa white, tibial scopa white to light brown. Wings hyaline, venation brown, stigma light brown. Nervulus slightly antefurcal. ***Metasoma*:** Tergites light red with exception of black basal and lateral parts of T1 and two black lateral spots on T2, and apex of T5 which is slightly lightened brown (Fig. 58). Sternites light red with exception of S1 and apical margins of S4–6. Tergites densely, finely, and evenly punctured, punctures separated by one puncture diameter. T2–4 with thin white hair bands of fine hairs, on T2–3 widely interrupted, on T4 complete. T5–6 with golden hairs flanking pygidial plate, laterally white. Pygidial plate with slightly raised margins, centrally with longitudinal slightly raised area.

Male. Body length 9–10 mm (Fig. 59). ***Head*:** Black, slightly wider than long. Clypeus very shallowly arched, essentially flat, ivory-coloured with exception of two faint dark spots centrally, yellow colouration extending onto bottom parts of paraocular areas (Fig. 60). Underlying clypeal surface shiny, moderately and shallowly punctured, punctures separated by 1–2 puncture diameters. Process of labrum trapezoidal, fore margin broadly and shallowly emarginate, shiny. Pubescence and antennal colouration as in female, A3 equalling A4+5. Ocelloccipital distance slightly shorter than width of

Figures 55–62. *Andrena* (*Nobandrena*) *gafsensis* sp. nov. **55** female profile **56** female face **57** female propodeum **58** female tergites **59** male profile **60** male face **61** male tergites **62** male genitalia.

lateral ocellus. ***Mesosoma*:** Scutum and scutellum dark, shagreened, dull laterally and anteriorly, weakly shining only centrally, moderately punctured, punctures separated by one puncture diameter. Sculpturing of episternum and propodeum as in female. Pubescence as in female. Wings hyaline, venation brown, stigma light brown. Nervulus clearly antefurcal. ***Metasoma*:** Tergites predominantly dark, tergal margins slightly depressed, lightened yellow to orange (Fig. 61). Tergites microreticulate, weakly shining, shallowly punctured, punctures separated by 1–2 puncture diameters. T2–5 with loose white hair fringes, that on T2 weakly interrupted, the following complete. T6 with fringe of longer white-golden hairs. Genitalia simple, gonocoxites diverging apically and forming points (Fig. 62). Sternite 8 short, densely hairy.

Distribution. Known only from the *locus typicus* in southern Tunisia.

Floral preferences. None recorded.

Etymology. Named after the nearest indicated town Gafsa in southern Tunisia.

***Andrena* (*incertae sedis*) *tenebricorpus* Wood, sp. nov.**

http://zoobank.org/6C1EA635-A7DD-418E-BC59-CF97AB02F508
Figures 63–66

Material. ***Holotype*:** Morocco: Guelmim-Oued Noun, 10 km E Guelmim, 15.iv.1995, 1♀, leg. Ma. Halada. Deposited in the OÖLM.

Diagnosis. *Andrena tenebricorpus* is very similar to *A. gafsensis* and faces the same problems of subgeneric classification, and is therefore also not currently placed in one until molecular data are available. Both species have a flattened and shiny clypeus (Fig. 64) and a short propodeum (Fig. 65), but differ most obviously in colour, with *A. tenebricorpus* having dark brown terga (Fig. 66) in strong contrast to the red terga of *A. gafsensis*. In terms of structural difference, in *A. tenebricorpus* the foveae are slightly wider, the hairs on the scutum and scutellum are relatively much shorter (compare Figs 57, 65) at the same time that the hair bands on the apical margins of the tergites are relatively much thicker (compare Figs 58, 66), suggesting that this is not as a result of abrasion, and the scopa are a dirty brown (Fig. 63) rather than white (Fig. 55).

In terms of overall colouration and appearance *A. tenebricorpus* is extremely similar to *A. guichardi* Warncke, 1980 (also found only in south-western Morocco) with the same dark to dark brownish tergal colouration with contrasting white hair bands (see Fig. 104). However, *A. tenebricorpus* can be clearly separated by the flattened clypeus (domed in *A. guichardi*), more densely punctate scutum (punctures separated by 1–2 puncture diameters, by 2–4 puncture diameters in *A. guichardi*, see Fig. 103), and by the propodeal triangle which is weakly differentiated only by sculpturing (clearly marked by a small raised carina in *A. guichardi*).

Description. Female: Body length 10 mm (Fig. 63). ***Head*:** Dark, as wide as long. Clypeus slightly arched laterally, broadly flattened on the disc, underlying surface laterally with shagreenation, the majority of disc shiny (Fig. 64). Moderately punctured, punctures separated by 1–2 puncture diameters, with generally impunctate line in centre

Figures 63–66. *Andrena* (*Nobandrena*) *tenebricorpus* sp. nov. **63** female profile **64** female face **65** female propodeum **66** female tergites.

of clypeus. Process of labrum trapezoidal with faint lateral striations, fore margin weakly emarginate, slightly bulging. Gena equal to width of compound eye. Gena, face, and scape with white hairs, longest not exceeding length of the scape. Vertex with mixture of whitish and yellowish hairs of same length as on rest of face. Foveae of average width, occupying slightly more than half of distance between top of compound eye and lateral ocellus. Antennae dark, A4 apically and A5–12 lightened orange below, A3 equalling A4+5. Ocelloccipital distance equalling width of lateral ocellus. ***Mesosoma*:** Scutum and scutellum densely punctured, punctures separated by 1–1.5 puncture diameters, underlying surface of the scutum shagreened anteriorly, elsewhere and on the scutellum shiny. Episternum microreticulate, dull. Lateral faces of the propodeum shagreened, weakly shining. Hind face of propodeum microreticulate and weakly rugose, rugosity outlining the propodeal triangle which is itself rugose and therefore defined by the change in texture between rugosities (Fig. 65). Scutum and scutellum with very short and fine hairs, scarcely longer than width of lateral ocellus. Episternum and propodeum with longer white hair, never exceeding length of the scape. Legs dark, tarsi brown, pubescence brown. Femoral scopa white, tibial scopa dirty brown. Wings hyaline, venation brown, stigma dark brown. Nervulus slightly antefurcal. ***Metasoma*:** Tergites dark brown throughout with exception of two lateral black spots on T2 (Fig. 66). Tergites densely, finely, and evenly punctured, punctures separated by one puncture diameter. T2–4 with dense white hair bands that obscure underlying surface, on T2 interrupted medially, on T3–4 complete. T5–6 with thick brown hairs flanking pygidial plate, with a few white hairs laterally. Pygidial plate with slightly raised margin, centrally flat.

Male. Unknown.

Distribution. South-western Morocco (Fig. 145b).

Floral preferences. None recorded.

Remarks. Whilst *A. tenebricorpus* is structurally very similar to *A. gafsensis*, the subtle morphological differences suggest that *A. tenebricorpus* is distinct. Moreover, the Souss valley to the Guelmim region is bio-climatically quite distinct to the deserts of southern Tunisia and hosts many unique bee species within Morocco itself, further suggesting a distinct specific identity.

Etymology. The name *tenebricorpus* from *tenebris* (dark) + *corpus* (body) was chosen because of the structural similarities between *A. tenebricorpus* and *A. gafsensis*, but without the same reddish colouration.

***Andrena* (*Notandrena*) *acutidentis* Wood, sp. nov.**

http://zoobank.org/4F7E28FC-64A4-43D8-AE09-3A7B7E63FA2F

Figures 67–76

Material. ***Holotype*:** Morocco: Souss-Massa, 10 km SE Ait Baha, 18.iv.1996, 1♀, leg. M. Schwarz. Deposited in the OÖLM. ***Paratypes*:** Morocco: Souss-Massa, 10 km SE Ait Baha, 18.iv.1996, 2♂, 2♀, leg. M. Schwarz; 20.iv.1996, 2♂, leg. M. Schwarz; Souss-Massa, 10 km W Tiznit, 6.v.1995, 5♂, 1♀, leg. Mi. Halada, OÖLM; Souss-Massa, 30 km SE Taliouine, 17.iv.1996, 3♀, leg. M. Schwarz, OÖLM; Souss-Massa, Biougra-Tafraout, 13.ii.1987, 1♂, leg H. Teunissen, NMNL. Paratypes are deposited at the OÖLM and NMNL, with a male and female retained in the personal collection of TJW.

Diagnosis. A small *Notandrena* recognised in the subgenus by the dorsolateral angle of the pronotum with a transverse ridge, the clearly punctured metasoma, and the weakly rugose (not shagreened) propodeal triangle. Because of its small size it can be placed into the *nitidiuscula* group, and it is most similar to *A. fulvicornis* Schenck, 1853 (see also species newly recorded for Morocco below). It differs by the clypeus which has a central, shining, impunctate line (Fig. 68, evenly punctured and shagreened in *A. fulvicornis*) and the shiny scutum and scutellum (Fig. 69, shagreened and dull in *A. fulvicornis*).

The male can easily be recognised as a *Notandrena* because of the greatly enlarged and carinate gena (Fig. 73) and the broadened apex of the gonostyli in combination with a punctured metasoma (Fig. 75). It can be further recognised within the *Notandrena* by the shape of the genitalia which are short and compact (Fig. 76), placing it close to species like *A. chrysosceles*, *A. fulvicornis*, *A. nitidiuscula*, and *A. pallitarsis* (see illustrations in Schmid-Egger and Scheuchl 1997). However, the apices of the gonostyli are produced into points whereas they are

Figures 67–70. *Andrena* (*Notandrena*) *acutidentis* sp. nov. **67** female profile **68** female face **69** female dorsum **70** female tergites.

rounded in the other species, the clypeus is yellow (Fig. 72, black in species like *A. fulvicornis* and *A. nitidiuscula*), and the apex of sternite 8 is also emarginate. The combination of these characters is unique.

Description. Female: Body length 8–8.5 mm (Fig. 67). ***Head*:** Black, head wider than long (Fig. 68). Clypeus broad, evenly arched, evenly punctured, punctured separated by one puncture diameter with the exception of clear impunctate line in centre equivalent to two puncture diameters. Underlying surface weakly shagreened, shining. Process of labrum trapezoidal, weakly emarginate. Gena broad, 1.2 times wider than width of compound eye, clearly and evenly punctured, punctures separated by one puncture diameter, underlying surface close to the compound eye shining, becoming shagreened towards the hind margin of the vertex, punctures becoming obscure. Gena, vertex, and face with moderate brown hairs, never exceeding the scape in length. Foveae of average width, occupying half distance between top of compound eye and lateral ocellus. Antennae dark, A4 apically and A5–12 lightened orange below, A3 slightly shorter than A4+5+6. Ocelloccipital distance short, ½ width of lateral ocellus. ***Mesosoma*:** Scutum and scutellum moderately densely punctured, punctures separated by 1–1.5 puncture diameters, underlying surface weakly shagreened, generally shiny (Fig. 69). Scutum and scutellum with short, fine, brownish hair. Episternum and propodeum microreticulate, dull, propodeal triangle clearly

Figures 71–76. *Andrena* (*Notandrena*) *acutidentis* sp. nov. **71** male profile **72** male face **73** male gena **74** male dorsum **75** male tergites **76** male genitalia.

marked by a faint carina, propodeal triangle weakly rugose. Episternum and propodeum with longer brownish-whitish hair, not exceeding length of the scape, propodeal corbiculae well defined. Legs dark, tarsi lightened brown, pubescence yellowish to whitish. Femoral and tibial scopa white. Wings hyaline, venation and stigma dark brown. Nervulus interstitial. ***Metasoma*:** Tergites dark, margins slightly lightened yellow to light brown (Fig. 70). T1 moderately punctured, puncture separated by 2–3 puncture diameters, T2–4 more densely punctured, punctures separated by 1–1.5 puncture diameters, underlying surface weakly shagreened, shining. T2–4 with thin hairbands of yellowish-white hairs, on T2+3 broadly interrupted, on T4 complete. T5+6 with a fringe of golden hairs.

Male. Body length 8 mm (Fig. 71). ***Head*:** Black, head wider than long (Fig. 72). Clypeus broad, evenly arched, entirely yellow with exception of two small dark triangles laterally. Process of labrum narrow, longer than broad, emarginate. Gena substantially wider than width of compound eye, angulate with distinct upper and lower corner, carinate (Fig. 73). Genal punctation and sculpturing as in female. Gena, face, vertex, and scape with white hairs, longest equalling scape in length. Antennae dark, A3 apically and A4–13 lightened orange below, A3 equalling A4+5. Ocelloccipital distance short, 2/3 width of lateral ocellus. ***Mesosoma*:** Mesosomal sculpturing and pubescence as in the female (Fig. 74). Legs brown, tarsi light brown, pubescence whitish. Wings hyaline, venation and stigma dark brown. Nervulus slightly antefurcal. ***Metasoma*:** Tergites brownish, punctation and sculpturing as in the female (Fig. 75). Tergites 2–4 with very thin and faint white hair bands, very broadly interrupted. Sternite 8 apically emarginate and bilobed. Genitalia short and compact (Fig. 76), gonocoxites not forming points, dorsal surface shagreened in a manner reminiscent of *Zonandrena*. Gonostyli forming a point.

Distribution. The Souss valley in south-western Morocco (Fig. 145d).

Floral preferences. None recorded. Other members of the *Notandrena* are associated with Apiaceae (Wood et al. 2020a).

Etymology. The name *acuti* (sharp) + *dentis* (teeth) was chosen because of the male genitalia where the apices of the gonostyli are produced into points in contrast to other members of this group where they are rounded.

***Andrena* (*Poecilandrena*) *nigriclypeus* Wood, sp. nov.**

http://zoobank.org/53B24FC1-90C7-41A2-8CB2-1AC4E226C2C5
Figures 77–82

Material. ***Holotype*:** Algeria: Tlemcen, 20 km N de Maghnia, Bab Taza, 34.968N, -1.7622W, 9.iv.1983, 1♂, leg. R. Leys & P. v. d. Hurk. Deposited in the NMNL.

Diagnosis. The subgenus *Poecilandrena* is poorly defined and has been treated as a wastebasket for species with few apomorphies (Pisanty et al. 2018), and so unsurprisingly it has been found to be strongly polyphyletic, containing at least five clades (Pisanty et al. 2020), and in future revisions, only the *labiata* and *viridescens* groups are likely to remain in the *Poecilandrena*. However, until this point it is desirable to keep superficially similar species together, even if the subgenus itself is clearly polyphyletic, so that they may be dealt with together in future revisions. Based on the criteria outlined by Pisanty et al. (2018), *A. nigriclypeus* can be placed into the *Poecilandrena sensu lato* by the combination of small body size (< 10 mm), red marked abdomen, non-carinate pronotum, mesepisternum weakly areolate with large, spaced shallow punctures, propodeal triangle moderately rugose, genal area not broadened, and sternite eight columnar.

Currently only one species of *Poecilandrena sensu lato* is known from North Africa, the similarly red-marked *A. maximiliani* Scheuchl, 2009 which was described from

Figures 77–82. *Andrena* (*Poecilandrena*) *nigriclypeus* sp. nov. **77** male profile **78** male face **79** male dorsum **80** male tergites **81** male sternite eight **82** male genitalia.

Tunisia (see Scheuchl 2009 for discussion of previous unconfirmed records of *Poecilandrena* from North Africa). *Andrena nigriclypeus* is similar to *A. maximiliani* as both have male genitalia with pronounced but apically truncate (square-ended) gonocoxal teeth. However, it can be easily separated because the clypeus is black, not yellow, and the gonostyli are completely different, small and narrow and with a shallow emargination in the outer edge before the apex whereas in *A. maximiliani* they are long, broad, and flattened. The only other similar species is *A. paradisaea* Warncke, 1975 from Turkey which has a red abdomen and a black clypeus in the male. However, this species has clearly hooked hind tibial spurs and the genitalia are completely different with a broad-based penis valve, spatula-shaped gonostyli with an evenly rounded outer margin, and pointed gonocoxal teeth (see photograph in Pisanty et al. 2018: fig. 122).

Description. Female: Unknown.

Male. Body length 8 mm (Fig. 77). ***Head*:** Black, slightly broader than long (Fig. 78). Clypeus domed, centrally slightly flattened therefore appearing weakly three-faced. Front 2/3^{rds} weakly shagreened, broadly shiny, basal 1/3 and lateral areas strongly shagreened, dull. Shiny area unevenly punctured, punctures separated by 1–2 puncture diameters, puncture density increases slightly in dull areas, punctures separated by one puncture diameter. Process of labrum rectangular, two times broader than long. Gena and vertex with white hairs, turning to black hairs on gena behind dorsal 1/3 of compound eyes (Fig. 79). Scape with short white hairs, lower paraocular areas and areas around the antennal insertions with mixture of black and white hairs. None of the facial pubescence exceeds scape in length. A1–3 dark, A4–13 dark brown, A3 equalling A4+5. Ocelloccipital distance short, ½ width of lateral ocellus. ***Mesosoma*:** Scutum and scutellum densely shagreened, dull, slightly shiny centrally. Surface evenly and weakly punctured, punctures separated by 1–2 puncture diameters. Episternum and propodeum strongly microreticulate, with weak raised reticulation, very weakly shining. Episternum with very shallow wide punctures between raised reticulation. Propodeal triangle well-marked with raised external carina, internal surface with weakly raised longitudinal rugosity. Legs dark, tarsal segments 2–5 on first two pairs of legs and all segments including the basitarsi on hind legs lightened dark red-orange (Fig. 77). Wings hyaline, venation amber, nervulus interstitial. ***Metasoma*:** T1 predominantly dark, red-marked only on apical margin, T2–4 red, T5–6 black (Fig. 80). T2–5 with apical margins lightened yellow, slightly hyaline apically. All tergites densely and uniformly punctate, punctures separated by 0.5 puncture diameters, underlying surface finely shagreened, weakly shining. T6+7 with short golden hairs. S8 arched, centrally at vertical apex of the arch with a patch of dense yellowish hairs, remaining part of relatively hairless sternite narrowly projecting beyond (Fig. 81). Genitalia simple, gonocoxites with pronounced but apically truncate and square-ended teeth (Fig. 82). Penis valve triangular basally with slightly raised winged margins. Gonostyli narrow, apically strongly truncate with a shallow emargination in outer margin (Fig. 82).

Distribution. North-western Algeria close to the Moroccan border (Fig. 145d).

Floral preferences. None recorded.

Etymology. The name *nigri* (black) + *clypeus* (clypeus) was chosen because of the entirely black male clypeus, which is unusual within small red-marked *Andrena* species.

Andrena (*Poliandrena*) *breviceps* Wood, sp. nov.

http://zoobank.org/8F5F1214-8FDB-404D-BB5C-E9C0F7E8031B
Figures 83–86

Material. ***Holotype*:** Morocco: Drâa-Tafilalet, 10 km N Erfoud, 10.iv.1995, 1♀, leg. Ma. Halada. Deposited in the OÖLM. ***Paratypes*:** Morocco: Drâa-Tafilalet, 10 km N Erfoud, 10.iv.1995, 2♀, leg. Ma. Halada, OÖLM; Drâa-Tafilalet, 20 km E Agdz, 20.iv.1995, 2♀, leg. Mi. Halada, OÖLM; Drâa-Tafilalet, Tagounite, 60 km S Zagora, 23.iv.1995, 1♀, leg. Ma. Halada, OÖLM. Paratypes are deposited at the OÖLM with a female retained in the personal collection of TJW.

Diagnosis. The subgenus *Poliandrena* Warncke, 1968 is currently unsatisfactorily defined (females keying out in three places in Warncke's 1968a key) and will probably be broken up in the future as it has been shown to be strongly polyphyletic (Pisanty et al. 2020). It predominantly contains Mediterranean species that have heads that are short and broad (Fig. 84), short facial foveae, strongly punctate metasomas (Fig. 86), and often show a propodeal triangle that is defined by an external carina and internal rugosity (but not honeycomb-areolate, Warncke 1968a). As such, members of the *Poliandrena* are often recognised by their similarity to each other rather than by a single character *per se*, in other words a wastebasket taxon.

Andrena breviceps is small relative to the rest of the *Poliandrena*, comparable in size to *A. marsae* Schmiedeknecht, 1900 and *A. laurivora* Warncke, 1974, two of the smallest *Poliandrena*, but *A. breviceps* can easily be separated from them by the colour of the tergites which are dark brown (red in *A. marsae*, dark metallic green-blue in *A. laurivora*) and the sculpturing of the scutum which is shiny and (relatively within the *Poliandrena*) sparsely punctate, punctures separated by 2–3 puncture diameters (Fig. 75, separated by less than ½ a puncture diameter in *A. marsae* and by one puncture diameter in *A. laurivora*, underlying integument shagreened, with a metallic glint). It is also similar to the larger *A. relata* Warncke, 1967 which is newly recorded for Morocco (see below) because of their similar dark tergites and general appearance. However, it can also be separated using the same scutal punctation character (in *A. relata* punctures dense laterally, centrally separated by at most two puncture diameters) and also by the clypeus where *A. breviceps* has a central longitudinal impunctate line that is not present in *A. relata*. Overall, the shiny and relatively sparsely punctate scutum (Fig. 75) in combination with its small size should allow separation from other *Poliandrena* from North Africa.

Description. Female: Body length 8.5–9 mm (Fig. 83). ***Head*:** Black, clearly wider than long (Fig. 84). Clypeus broad, arched, with large punctures, punctures separated by one puncture diameter except for a central slightly raised impunctate line, underlying surface uneven, slightly but irregularly raised between punctures, shining. Process of labrum broadly trapezoidal, fore margin weakly emarginate. Gena as wide as width of compound eye. Gena, vertex, face, and scape with moderately dense white hairs, longest of these not exceeding length of the scape. Foveae moderately broad, occupying 2/3 of distance between the of compound eye and lateral ocellus, of normal length, not extending below the level of the antennal insertions. Antennae bright, scape and pedicel dark, A3 apically marked with orange, A4–12 predominantly orange, A3 exceeding A4+5, shorter than A4+5+6. Ocelloccipital distance short, ½ width of lateral ocellus. ***Mesosoma*:** Scutum and scutellum moderately punctured, punctures separated by 1–2 puncture diameters, underlying surface shiny, very weakly shagreened laterally and anteriorly (Fig. 85). Margins of scutum and scutellum with short, dense whitish hairs, these extending only very sparsely onto

Figures 83–86. *Andrena* (*Poliandrena*) *breviceps* sp. nov. **83** female profile **84** female head **85** female dorsum **86** female tergites.

the disc. Episternum and propodeum microreticulate, dull, propodeum with weak rugosity, propodeal triangle defined with small but clear slightly raised carina, propodeal triangle with sparse and weak rugosity centrally. Episternum and propodeum with white hairs, longest not exceeding length of the scape. Legs dark, tarsi lightened brown, pubescence whitish to brownish. Femoral and tibial scopa white. Wings hyaline, venation and stigma brown. Nervulus antefurcal. ***Metasoma*:** Tergites brownish, margins slightly depressed, lightened white to yellow, apically translucent (Fig. 86). Tergites densely, evenly, and finely punctate, punctures separated by one puncture diameter, underlying surface very weakly shagreened, shining. T1 with two small lateral hair patches of white hair on apical margin, T2–4 apically with complete white hair bands obscuring underlying surface. T5–6 with golden hairs flanking pygidial plate. Pygidial plate rounded triangular, flat, without raised margin.

Male. Unknown.

Distribution. The eastern Moroccan desert in the province of Drâa-Tafilalet (Fig. 145c).

Floral preferences. None recorded.

Etymology. The name *brevi* (short) + *ceps* (head) was chosen because of the particularly short and wide head of this species, even within the *Poliandrena*.

***Andrena* (*Poliandrena*) *farinosoides* Wood, sp. nov.**

http://zoobank.org/184F4B1C-A3C6-48A8-96D6-560CC9A9379A
Figures 87–98

Material. ***Holotype*:** Morocco: Oriental, 40 km S Guercif, 15–17.v.1995, 1♀, leg. Ma. Halada. Deposited in the OÖLM. ***Paratypes*:** Morocco: Oriental, 40 km S Guercif, 15–17.v.1995, 2♂, 24♀, leg. Ma. Halada, OÖLM; Drâa-Tafilalet, 30 km E Midelt, 13.v.1995, 1♀, leg. Mi. Halada, OÖLM; Drâa-Tafilalet, 10 km N Rich, 2♀, leg. Mi. Halada, OÖLM. Paratypes are deposited at the OÖLM with three females retained in the personal collection of TJW.

Diagnosis. *Andrena farinosoides* can also be placed in the *Poliandrena* because of its short and broad head (Fig. 88), short facial foveae, strongly punctate metasoma (Fig. 91), and propodeal triangle marked by a carina and internal rugosity (but not honeycomb-areolate). It can be recognised within the *Poliandrena* as very similar to *A. farinosa* Pérez, 1895 from Spain and France (Gusenleitner and Schwarz 2002) but the two species differ in the pubescence of the abdomen and the scutal punctation. In addition to thick hair bands on the tergal margins (Figs 90, 92), *A. farinosa* also has short hairs on the tergal discs forming a sparse velvety pubescence when viewed laterally (Fig. 94, not as dense as in *A. eddaensis* or *A. decaocta*). In contrast, *A. farinosoides* has only a few short hairs on the tergal discs, not forming a velvety pubescence (Fig. 93). In addition, the scutum of *A. farinosoides* is clearly less densely punctate, with punctures separated by one puncture diameter, punctures denser and almost confluent in *A. farinosa*.

Diagnosis of the male is more difficult, but both *A. farinosa* and *A. farinosoides* are in the group with dark, densely punctate tergites and black (not yellow) clypei with an upturned fore margin (Fig. 96). The male of *A. farinosoides* is then less densely and more finely punctate on the scutum (punctures separated by one puncture diameter) whereas *A. farinosa* has larger punctures that are separated by less than a puncture diameter (Fig. 97).

Description. Female: Body length 8.5–9.5 mm (Fig. 87). ***Head*:** Black, clearly wider than long (Fig. 88). Clypeus broad, slightly arched, densely and evenly punctured, punctures separated by ½ a puncture diameter. Process of labrum broad, trapezoidal, twice as wide as long, fore margin compressed and slightly upturned, surface with weak transverse striations. Gena slightly narrower than width of compound eye. Gena, face, and scape with dense white hairs, longest not achieving ¾ of length of the scape, hairs on the vertex of similar length but becoming yellowish. Foveae normal, occupying half of distance between top of compound eye and lateral ocellus. Antennae dark, A5–12 lightened orange below, A3 long, slightly shorter than A4+5+6. Ocelloccipital distance short, less than 1/3 width of lateral ocellus. ***Mesosoma*:** Scutum and scutellum densely punctured, punctures separated by one puncture diameter, underlying surface smooth and shiny (Fig. 89). Margins of scutum and scutellum with short whitish-brownish hairs, densest on the margins and becoming sparser as hairs move into centre of the disc. Episternum and propodeum with weak rugosity, dull, propodeal triangle clearly defined by raised carina, propodeal triangle itself rugose with

Figures 87–94. *Andrena* (*Poliandrena*) *farinosoides* sp. nov. **87** female profile **88** female face **89** female dorsum **90** female tergites **91** female tergites in lateral view. *Andrena* (*Poliandrena*) *farinosa* Pérez, 1895 (paralectotype) **92** female dorsum **93** female tergites **94** female tergites in lateral view.

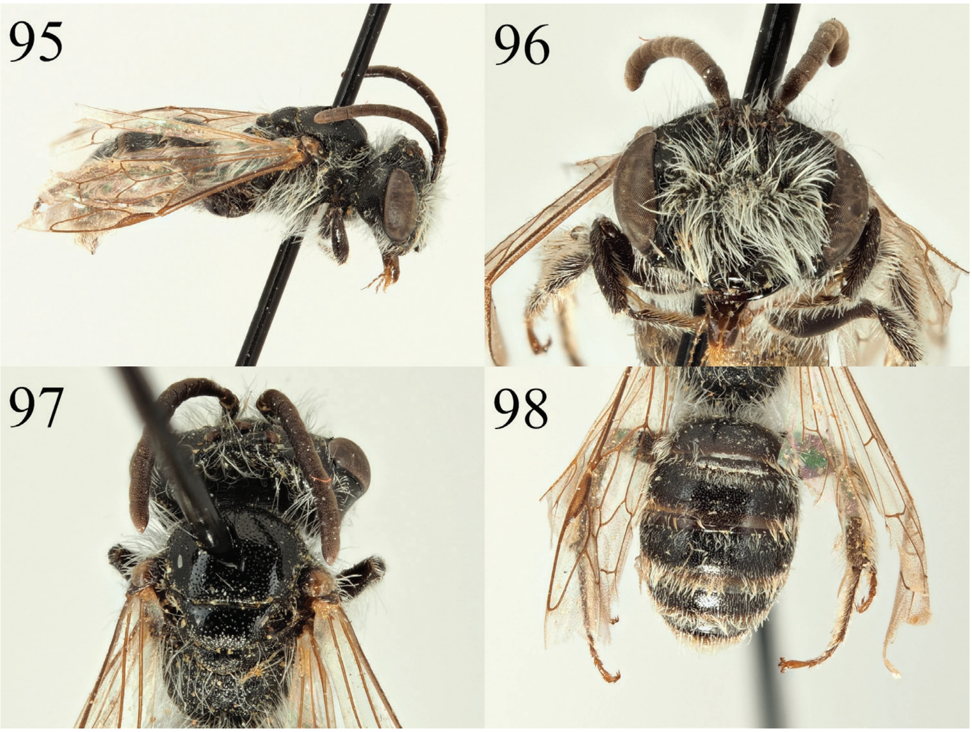

Figures 95–98. *Andrena* (*Poliandrena*) *farinosoides* sp. nov. **95** male profile **96** male head **97** male dorsum **98** male tergites.

weak longitudinal carinae. Episternum and propodeum with white hairs, not exceeding ¾ length of scape. Legs dark, tarsi lightened brown, pubescence light brown to whitish. Femoral and tibial scopa white. Wings hyaline, venation and stigma light brown. Nervulus interstitial. ***Metasoma*:** Tergites dark, margins depressed and slightly lightened to brown (Fig. 91). Tergites densely and evenly punctured, punctures separated by ½ puncture diameter. T1–4 with thick white hair bands that exceed length of margins, completely obscuring underlying surface, all bands complete in fresh individuals. T5 and T6 with golden hairs flanking pygidial plate, white haired laterally. Pygidial plate rounded triangular, without raised margin, very subtly domed centrally.

Male. Body length 7 mm (Fig. 85). ***Head*:** Black, clearly wider than long (Fig. 96). Clypeus broadly flattened, with clear upturned fore margin. Clypeus densely and evenly punctured as in female. Gena thickened, slightly wider than the width of compound eye. Gena, face, vertex, and scape with white hairs, longest equalling length of the scape. Antennae dark, A4–13 lightened brown below, A3 slightly shorter than A4+5. Ocelloccipital distance short, ½ width of lateral ocellus. ***Mesosoma*:** Similar to female, scutum and scutellum evenly punctured, punctures separated by one puncture diameter, underlying surface shiny, contrasting with the episternum and propodeum that are reticulate, dull (Fig. 97). Legs dark, tarsi lightened brown, pubescence white. Wings hyaline, venation and stigma light brown. Nervulus interstitial.

***Metasoma*:** Similar to female, tergites dark, margins lightened yellow to brown, apically whitish translucent (Fig. 98). Tergites densely and evenly punctate, punctures separated by one puncture diameter.

Distribution. The eastern Moroccan desert in the provinces of Oriental and Drâa-Tafilalet (Fig. 145d).

Floral preferences. None recorded.

Etymology. Given the similarity to *A. farinosa*, the name *A. farinosoides* (*farinosa* + *oides*, form or likeness) was chosen to illustrate this close link.

Other material examined. (*Andrena farinosa*): Spain: Barcelona, [no date], 1♀, designated paratype [technically paralectotype] by Warncke, Warncke Colln., OÖLM (illustrated Figs 90, 92, 94); 80 km SW Valencia, Muela de Cortes reserve, 14.v.2003, 4♂, 13♀, leg. J. Halada, OÖLM; Lleida, Granadella, 450 m, 23.v.1983, 2♂, 1♀, leg. H. Teunissen, NMNL; Maella, 23.v.1983, 1♂, leg. H. Teunissen, NMNL; Murcia, Pto. de Jumilla, 19.v.2003, 1♀, leg. J. Halada, OÖLM; Murcia, Sierra de Españula, 11.v.2003, 5♂, 3♀, leg. J. Halada, OÖLM; Taragona, Bellaguarda, 683 m, 1.vi.2019, 1♀, leg. W. Klein, NMNL; Zaragoza, Codos, 5.vi.1985, 2♂, leg. H. Teunissen, NMNL.

Additional taxonomic changes and updates

Andrena (*Aciandrena*) *fulica* Warncke, 1974

Figures 99–104

Andrena (*Aciandrena*) *astrella* ssp. *fulica* Warncke, 1974: p44
Andrena (*Aciandrena*) *astrella* Warncke, 1975: 305. syn. nov.

Material examined, males only, black faced and therefore nominally *A. fulica*. Tunisia: Tunis, 1898, 1♂, leg. O. Schmiedeknecht (paratype *A. fulica*), OÖLM; Morocco: Fès-Meknès, Ifrane environs, 9.v.1997, 1♂, leg. K. Deneš, OÖLM (illustrated Figs 99, 100); Spain: Benidorm, 20.iv.1982, 1♂, NMNL.

Material examined, males only, yellow face and therefore nominally *A. astrella*. Morocco: Fès-Meknès, Ifrane environs, 9.v.1997, 1♂, leg. K. Deneš, OÖLM (illustrated Figs 101, 102); Portugal: Algarve, Altura, near Monte Gordo, 24.iv.2016, 1♂, leg. Wood, TJW Colln.; Algarve, Pêra, Praia Grande, 2.iv.2015, 2♂, leg. Wood, TJW Colln.; Spain: Rivas [Madrid], 1♂, leg. Dusmet (paratype *A. astrella*), OÖLM; 40 km W Malaga, Yunquera, 800 m, 29.iv.2003, 2♂, leg. J. Halada, OÖLM; 50 km W Almería, Berja, 21.iv.2003, 10♂, leg. J. Halada, OÖLM; Alicante, Elche, 23.iv.1982, 1♂, NMNL; Altea, 10 km N Benidorm, 15.iv.1982, 1♂, NMNL; Benidorm, 20.iv.1982, 1♂, NMNL; Ávila, Hoyos del Espino, 1400 m, 19.v.1995, 1♂, leg. H. & J.E. Wiering, NMNL; Ávila, Hoyocasero, 1350 m, 2 km W, 10.v.1995, 1♂, leg. H. & J.E. Wiering, NMNL; 80 km SW Valencia, Muela de Cortes reserve, 14.v.2003, 2♂, leg. J. Halada, OÖLM; E-Sierra Nevada, near Alboloduy, 7.v.2003, 3♂, leg. J. Halada, OÖLM; Sierra Alhamilla, 5 km E Nijar, 20.iv.2003, 1♂, leg. J. Halada, OÖLM; Sierra Alhamilla, Lucainena, 25.iv.2003, 10♂, leg. J. Halada, OÖLM; Sierra de Nevada,

Figures 99–104. *Andrena* (*Aciandrena*) *fulica* Warncke, 1974 **99** male face **100** male genitalia. *Andrena* (*Aciandrena*) *fulica astrella* Warncke, 1975 (Morocco) **101** male face **102** male genitalia (Spain) **103** male face **104** male genitalia.

Ohanes env., 5.v.2003, 5♂, leg. J. Halada, OÖLM; S-Sierra Nevada, env. Lanjaron, 4.v.2003, 5♂, leg. J. Halada, OÖLM (illustrated Figs 103, 104).

Distribution and remarks. *Andrena fulica* (Morocco, Algeria, and Tunisia) and *A. astrella* (Spain and Portugal) were both described by Warncke, with *A. fulica* described as *A. astrella* ssp. *fulica* (Warncke, 1974) despite being formally published before *A. astrella* (Warncke 1975b), this problem arising due to differences in publishing speed between the two journals, with the paper on Iberian *Andrena* originally submitted in 1971. The most recent global treatment listed them as distinct (Gusenleitner and Schwarz 2002).

The two species can be rapidly recognised within the *Aciandrena* because they have punctured tergites with the punctures extending onto the tergal margins, a character that is unique within this subgenus. According to Warncke (1974), *Andrena fulica* is characterised as having finer tergal punctation and, importantly, a black clypeus in the male sex (Fig. 99), whereas in *A. astrella* the male clypeus is yellow (Figs 101, 103). The description of *A. fulica* by Warncke (1974) is extremely short, just two sentences for the female and two short sentences for the male which read: '♂ wie beim ♀ feiner punktiert. Clypeus dunkel gefärbt!'.

Inspection of *Aciandrena* males from Ifrane in Morocco (9.v.1997) revealed the two colour forms in sympatry, though unfortunately only two specimens in total (one *A. fulica*, one *A. astrella*) were collected during this sampling making an assessment of variation impossible. Additionally, specimens from Benidorm in Spain (20.iv.1982) also showed the two colour forms in sympatry. Across all Iberian material studied, 46/47 (97.8%) males showed a consistently yellow clypeus. Inspection of the genitalia showed no obvious differences between the two Ifrane specimens (Figs 100, 102), and neither specimen shows obvious differences from the genitalia of Spanish specimens (Fig. 104).

Aciandrena do not always show consistent clypeal colouration. In the recently described *A.* (*Aciandrena*) *abruptifovea* Wood, 2020, a series of six males from the same type locality site collected on the same day vary considerably in colouration from a clypeus with 80% yellow coverage, to 40%, to entirely black (Wood et al. 2020b). Given the extremely similar genitalia and the fact that both colour forms can be found together in both Iberia and North Africa, we synonymise *A. astrella* with *A. fulica*, with *A. fulica* taking priority as senior synonym as it was published first.

***Andrena* (*Nobandrena*) *ounifa* Warncke, 1974**

Figs 105–112

Material examined. Morocco: Drâa-Tafilalet, Errachidia, 11.iv.1995, 2♀, leg. Ma. Halada, one female deposited in the OÖLM, with one female retained in the personal collection of TJW.

Distribution and remarks. Previously known only from the type locality in the western Algerian part of the Sahara Desert. The specimens from Errachidia are approximately 350 kilometres to the west. They agree with the male in size, the flattened and shiny clypeus (Figs 106, 108), the length of the propodeum (Figs 107, 111), and general structural characters. The female differs most strongly from classical *Nobandrena* (see Warncke 1968a) in the shape of the foveae which are long and very narrow, narrower than the width of an antenna (Fig. 106) and on the tergites it lacks the impressed centre line on T(2)3–4. In common with *A. iliaca* which was also placed in the *Nobandrena* by Warncke, it has a long propodeum with a flat, granular dorsal surface. Molecular work places *A. iliaca* within the *Fuscandrena* (Pisanty et al. 2020), and it

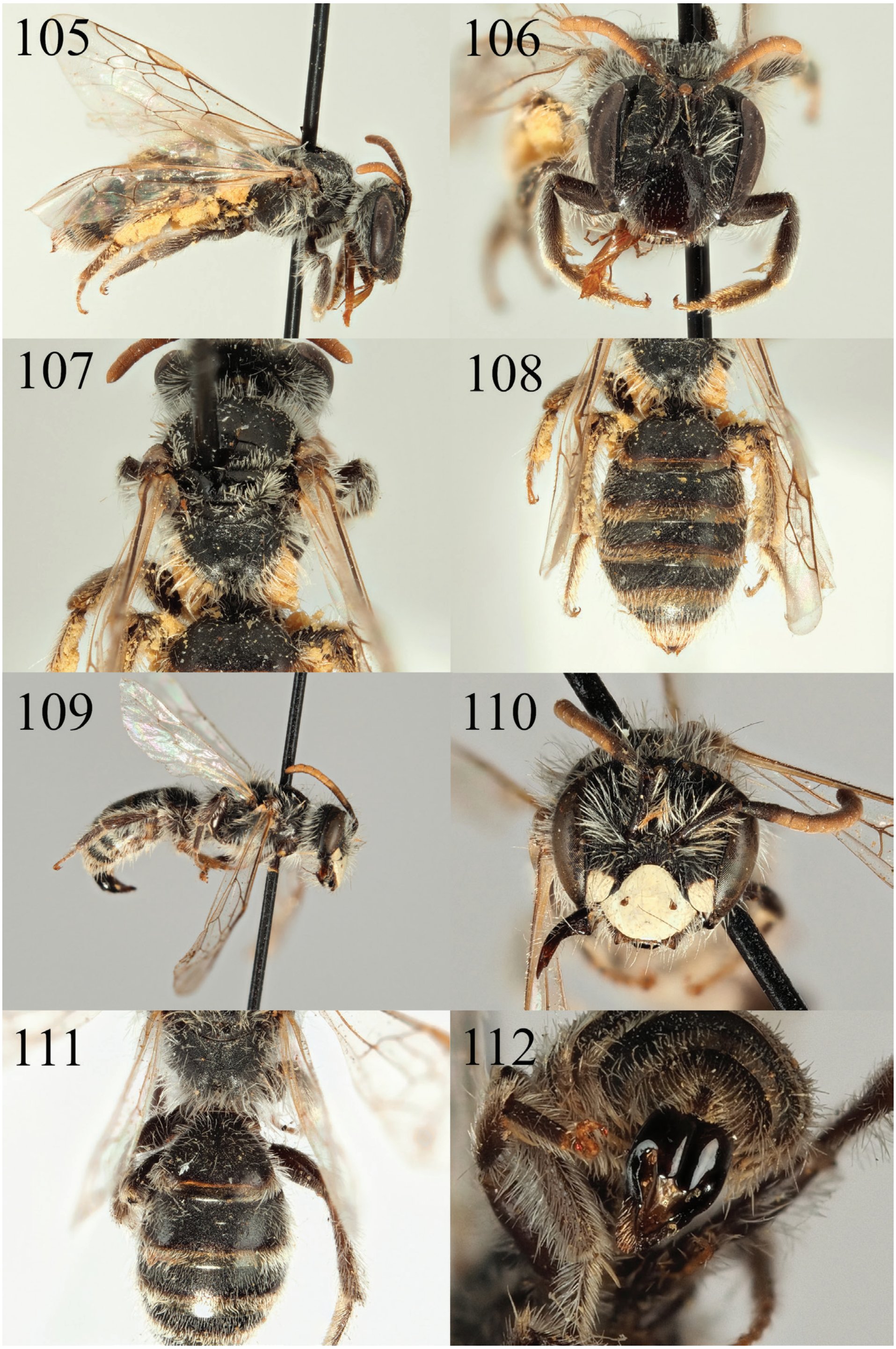

Figures 105–112. *Andrena* (*Nobandrena*) *ounifa* Warncke, 1974 **105** female profile **106** female face **107** female propodeum **108** female tergites **109** male (holotype) profile **110** male face **111** male tergites **112** male genitalia.

may be moved there in future, but without molecular data this move is premature, though it clearly does not belong in the *Nobandrena*. The holotype male is illustrated here for comparison (Figs 109–112). A single pollen load contained pure *Raphanus*-type pollen (Brassicaceae).

Description. Female: Body length 7.5 mm (Fig. 105). ***Head*****:** Black, clearly longer than wide (Fig. 106). Clypeus strongly flattened, strongly shining, weakly shagreened only on margins, moderately punctured, punctures separated by 2–3 puncture diameters. Process of labrum weakly trapezoidal, almost triangular, broad, twice as wide as long. Gena slightly narrower than width of compound eye with sparse, short white hair extending to vertex. Foveae long, narrow, narrower than width of scape, separated from inner margin of compound eye by less than their own width. Antenna dark, A4–12 extensively lightened orange below, A7–12 almost entirely orange, A3 slightly exceeding A4+5 in length. Ocelloccipital distance extremely short, linear, almost non-existent. ***Mesosoma*****:** Scutum strongly shagreened, dull to weakly shining centrally, strongly contrasting with shiny scutellum. Scutum and scutellum moderately punctured, punctures separated by 2–3 puncture diameters, with short whitish-brown pubescence. Episternum and propodeum strongly shagreened, dull. Dorsal area of propodeum longer than scutellum, propodeal triangle indicated by an increase in granular size of shagreenation (Fig. 107). Episternum and propodeum with white hair, longest attaining ¾ of length of the scape. Legs dark, tarsi lightened brown, pubescence whitish-brownish. Femoral and tibial scopa white. Wings hyaline, venation brown, stigma light brown. Nervulus interstitial. ***Metasoma*****:** Tergites dark, margins clearly lightened yellow to dark orange, apically partly translucent (Fig. 108). Tergal discs microreticulate, dull. Tergal discs and margins with sparse white hair, T5 apically and T6 with short golden hairs flanking the pygidial plate. T5 basally with long white hairs, these overlaying but not obscuring the apical golden hairs. Pygidial plate narrow, centrally with a longitudinal slightly raised area.

Other material examined. Algeria: Beni Ounif, 6.iii.[year unknown], 1♂, leg. Weber, OÖLM (holotype), illustrated Figs 109–112.

Andrena (*Poliandrena*) *guichardi* Warncke, 1980

Figures 113–116

Material examined. Morocco: Guelmim-Oued Noun, 15–16.iv.1995, 3♂, 1♀, leg. Ma. Halada, OÖLM; Souss-Massa, 10 km S Taroudant, 12.iv.1995, 1♀, leg. Ma. Halada, allotype male and one other male deposited in the OÖLM, with one male and one female retained in the personal collection of TJW.

Distribution and remarks. Known only from south-western Morocco (Warncke 1980). Gusenleitner and Schwarz (2002) provided comments on the appearance of the male but this was not a formal description and so one is provided here. *Andrena guichardi* can be easily recognised within the *Poliandrena* by the extremely shiny and very sparsely punctate scutum (Fig. 115).

Figures 113–116. *Andrena* (*Poliandrena*) *guichardi* Warncke, 1980 **113** male profile **114** male face **115** male dorsum **116** male tergites.

Description. Male: Body length 9 mm (Fig. 113). ***Head*:** Black, clearly wider than long. Clypeus slightly arched, predominantly yellow but with two dark triangular marks intruding laterally (Fig. 114). Underlying surface smooth and shiny, densely punctured, punctures separated by one puncture diameter except centrally where there is a small impunctate circular area. Process of labrum narrow, weakly emarginate, shiny. Gena slightly wider than the width of a compound eye. Gena, face, vertex, and scape with long white hairs, equalling length of the scape. Antennae dark, A3 apically and A4–12 completely lightened orange below, A3 exceeding A4, shorter than A4+5. Ocelloccipital distance broad, two times wides than width of lateral ocellus. Surface of galea shagreened, dull. ***Mesosoma*:** Scutum and scutellum sparsely punctate, punctures separated by 2–4 puncture diameters, underlying surface very smooth and shiny (Fig. 115). Episternum weakly reticulate, underlying surface weakly shining. Propodeum microreticulate, dull, propodeal triangle marked by small but clearly defined slightly raised carina, internal structure weakly and finely rugose. Scutum, scutellum, episternum, and propodeum with long white hairs, these often exceeding the length of the scape. Legs dark, tarsi lightened brown, pubescence white. Wings hyaline, venation and stigma brown, nervulus antefurcal. ***Metasoma*:** Tergites dark brownish, margins lightened whitish, apically translucent (Fig. 116). Tergal discs very weakly reticulate, shining, tergites densely and finely punctured, punctures separated by one puncture diameter. T1–5 with loose white hair bands, on T1 interrupted, T2–5 complete. T6–7 centrally with golden fringe of hairs. S2–5 with apical fringes of white hair.

Other material examined. Morocco: Sidi-Ifni, within 100 m of the sea, 31.iii.1974, 1♀, leg. K.M. Guichard & G.R. Else, OÖLM (***paratype***).

Andrena (*Truncandrena*) *alchata* Warncke, 1974

Material examined. *Andrena alchata*: Algeria: Maison Carrée, Alger, 1♂, leg. Dr. J. Bequaert, OÖLM (***holotype***); *Andrena doursana agadira*: Morocco: S-Marokko, Agadir, 20.ii.1977, 1♀, OÖLM (***holotype***); *Andrena doursana citreola* Warncke, 1975: Spain: Vaciamadrid, 25.v.1919, 1♀, leg. Dusmet, OÖLM (***holotype***); Morocco: Azrou Ras el Ma, 30.iii.1923, 1♀, leg. Schulthess, OÖLM (***paratype***); Rez Dj. Zalagh, 25.iii.1923, 1♂, leg. Schulthess, OÖLM (***paratype***).

New material. *Andrena alchata*: Morocco: Fès-Meknès, Laanoucer, 33.6167, -4.7489, 2.v.2018, 1♂, 3♀, leg P. Lhomme & A. Sentil; 33.6708, -4.8527, 2–3.v.2018, 1♀, white pan trap, leg P. Lhomme & A. Sentil; 33.6699, -4.8673, 10–11.v.2018, 1♂, 1♀, yellow pan trap, leg P. Lhomme & O. Ihsane; 33.7099, -4.8431, 15–16.v.2018, 1♀, white pan trap, leg. P. Lhomme & O. Ihsane; 7099, -4.8431, 15–16.v.2018, 1♀, white pan trap, leg. P. Lhomme; Casablanca-Settat, Oueled Sghir, 32.8230, -7.6421, 23.ii.2018, 1♂, 1♀, A. Sentil & I.E. Abdouni, all UMONS.

Distribution. *Andrena alchata* is known from Morocco and Algeria and was only described from the male sex (Warncke 1974); the subspecies *A. doursana agadira* was known only from south-western Morocco and was described only from the female sex (Warncke 1980), though the presence of putative males was noted.

Remarks. Sampling at both Laanoucer and Oueled Sghir in northern Morocco resulted in the capture of males of *A. alchata* and females corresponding to *A. doursana agadira* on the wing at the same time. Other *Truncandrena* species were present, with females of *Andrena ferrugineicrus* Dours, 1872 and *A. schmiedeknechti* Magretti, 1883 captured at Laanoucer and males and females of *Andrena varia* Pérez, 1895 at Oueled Sghir. However, no males or females of *A. doursana citreola* Warncke, 1975, the form occurring in this part of Morocco, were recorded. This situation raised the possibility that *A. alchata* and *A. doursana agadira* are actually synonymous.

Captured females are darker than *A. d. citreola* (compare Figs 117, 118) and can be separated by the colouration of the hairs of T5–6 flanking the pygidial plate which are dark brown (Fig. 119) not light brown as in *A. d. citreola* (Fig. 120). The contrast of these hairs against the abdomen is greater in *A. d. citreola* as the underlying integument is lighter and weakly metallic green (see also Fig. 118) with overlying pale hair bands, whereas in captured females the integument is dark and the hair bands are darker (Fig. 119). The colouration of the hairs on the frons and along the inner margin of the compound eye are also important; these are a mixture of brown and black in captured females (Fig. 121), and white to light brown in *A. d. citreola* s.s. (Fig. 122). In these characters, captured females match *A. d. agadira* perfectly (Warncke 1980).

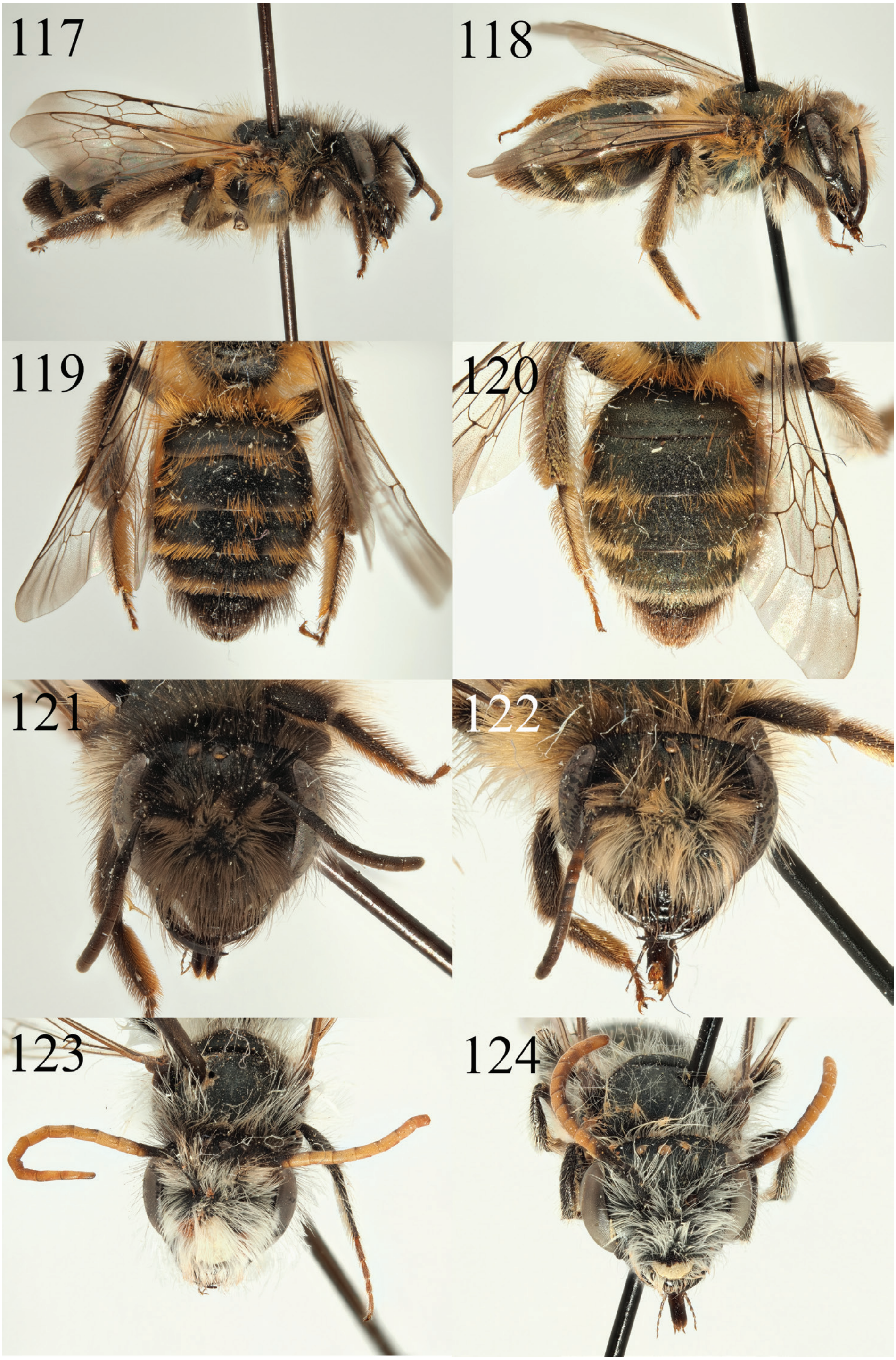

Figures 117–124. *Andrena* (*Truncandrena*) *alchata* Warncke, 1974 **117** female profile **119** female tergites **121** female face **123** male face. *Andrena* (*Truncandrena*) *doursana citreola* Warncke, 1975 **118** female profile **120** female tergites **122** female face **124** male face.

Warncke did not describe male of *A. d. agadira*, commenting that they were indistinguishable from other *A. doursana* subspecies. In contrast, males of *A. alchata* are easy to distinguish as the white markings on the face of *A. alchata* are much more extensive, covering the clypeus and the lower paraocular areas (Fig. 123) whereas in *A. d. citreola* the single white marking is small and is restricted to the very tip of the clypeus which forms a clear raised protrusion (Fig. 124). There are also genitalia differences, in *A. alchata* the outer margin of the gonostyli is curved inwards (evenly rounded in *A. d. citreola*), and the penis valve is comparatively wider.

A female corresponding to *A. d. agadira* and a male *A. alchata* were selected from the same site (Laanoucer, 2.v.2018) for molecular investigation. A *cox1* fragment of 263 base pairs was obtained after sequencing. A complete homology between the sequences of the female (GENBANK SUB7440720) and the *A. alchata* male (SUB7440720) was found, confirming their conspecificity. However, this result raises a difficult issue, as Warncke believed the males of *A. d. agadira* to be identical to other *A. doursana* subspecies. This therefore means that either *A. alchata* and *A. d. agadira* are not synonymous, and simply very similar morphologically in the female sex, or the undescribed *A. d. agadira* males are incorrectly associated with the type series females. Given this uncertainty, it is not appropriate to propose synonymy between *A. d. agadira* and *A. alchata* until genetic sequences can be obtained from the *locus typicus* to clarify sex associations in this region. What is clear is that captured females represent *A. alchata*, but given the large degree of variation in the colour of *Truncandrena* pubescence, it is possible that they simply resemble females of *A. d. agadira*. As such, we do not describe females here until this situation can be clarified further.

Other species newly recorded for the Moroccan fauna

***Andrena* (*Aciandrena*) *pratincola* Warncke, 1974**

Material examined. Morocco: Guelmim-Oued Noun, 10 km E Guelmim, 15–16.iv.1995, 5♂, leg. Ma. Halada, OÖLM; Drâa-Tafilalet, 20 km W Boudnib, 9.iv.1995, 1♂, leg. Ma. Halada, OÖLM.

Distribution and remarks. Previously recorded from Egypt and Tunisia (Gusenleitner and Schwarz 2002), this species has red tergites in the female sex but the male is fairly generic within the *Aciandrena*; it has an almost completely yellow and polished clypeus with loose white hair (Fig. 127), the tergites are dull, the nervulus is pronouncedly antefurcal, and the genitalia are simple (Fig. 128, also illustrated in Warncke 1974). Material from Morocco was entirely male and so comparison with the female type was not possible, but all other characters in the male sex were a good match (Figs 115, 126). These records considerably extend the range of *A. pratincola* to the west. The species may be found in the Algerian part of the Sahara but more survey effort is required.

Other material examined. Egypt: Min. Agr. Egypt, Dekhela, 20.ii.1917, 1♂, leg. Storey, OÖLM (paratype, illustrated Fig. 121); Ikingi, Mariout, 18.iii.1935, 1♀, leg. W. Wittmer, OÖLM (holotype); Matruh, 21.iii.1933, 1♂, leg. H. Priesner, OÖLM (paratype, illustrated Fig. 122).

Figures 125–130. *Andrena* (*Aciandrena*) *pratincola* Warncke, 1974 (Morocco) **125** male face **126** male genitalia (Egypt, Paratype) **127** male face **128** male genitalia *Andrena* (*Aciandrena*) *varicornis* Pérez, 1895 **129** male face **130** male genitalia.

Andrena (*Aciandrena*) *varicornis* Pérez, 1895

Material examined. Morocco: Oriental, 70 km S Oujda, 8.iv.1995, 1♂, leg. Ma. Halada, OÖLM.

Distribution and remarks. Known from Algeria, Tunisia, Egypt, and Israel (Gusenleitner and Schwarz 2002; Pisanty et al. 2018), so the presence of this species in eastern Morocco is not unexpected. The male is unique within the *Aciandrena* in that the yellow markings on the clypeus extend on to the lower paraocular areas (Fig. 129), and additionally the tips of the gonostyli are produced into points (Fig. 130).

***Andrena* (*Andrena*) *synadelpha* Perkins, 1914**

Material examined. Morocco: Fès-Meknès, Ifrane environs, 1700 m, 10.v.1997, 1♀, leg. P. Průdek; South of Azrou, 25.iv.2017, 1♂, M. Snižek, both OÖLM.

Distribution and remarks. This is a predominantly central and northern European bee, but there are isolated southern populations in upland areas of Spain, Portugal, and Turkey (Gusenleitner and Schwarz 2002; Wood et al. 2020a). *Andrena synadelpha* is polylectic, but it prefers pollen from trees and shrubs of broadleaf woodland such as *Acer*, *Rubus*, *Crataegus*, *Quercus*, *Rhamnus*, *Frangula* and *Ilex* (Wood and Roberts 2017). Its presence in the Middle Atlas is therefore unexpected, but it has precedence. *Andrena haemorrhoa* (Fabricius, 1781), another predominantly central and northern European bee which is able to live as far north as the Arctic circle, was also recently found in the Ouled Nail mountains of Algeria at an elevation of 761 meters (Cherair et al. 2013). It remains to be seen if there are more typically 'European' *Andrena* species that persist in the mountains of North Africa, presumably having been isolated at the end of the Ice Age as the lowland areas of North Africa returned to a more arid climate.

***Andrena* (*Avandrena*) *melacana* Warncke, 1967**

Replacement name for *Andrena melaleuca* Friese, 1922 nec *Andrena melaleuca* Pérez, 1895

Material examined. Morocco: Fès-Meknès, 12 km east of Ifrane, 9.v.1997, 1♀, leg. J. Halada, OÖLM; Fès-Meknès, Laanoucer, 1417 m, 3.v.2018, 1♂, leg. A. Sentil & P. Lhomme, UMONS.

Distribution and remarks. Previously known from Algeria, Tunisia, and Libya (Gusenleitner and Schwarz 2002). This species is part of the *Avandrena* group that, like the *Pallandrena*, appear to be associated with Geraniaceae. Records of *A. avara* Warncke, 1967 and *A. panurgina* Desteffani, 1889 in Portugal have been made exclusively from *Erodium*, and pollen removed from the scopa from *A. melacana* comprised entirely of *Erodium*-type pollen (Figs 131, 132). *Andrena melacana* can be easily distinguished from *A. avara* and *A. panurgina* as the hind femora lacks spines (Warncke 1980) and the male genitalia are completely different.

***Andrena* (*Carandrena*) *leucophaea* Lepeletier, 1841**

Material examined. Morocco: Fès-Meknès, Azrou, 20 km south, 23.iv.2009, 1♀, E. & P. Hajdaj, OÖLM.

Distribution and remarks. A West Mediterranean species, found in Algeria, Italy, Spain, and Tunisia (Gusenleitner and Schwarz 2002), and recently Portugal (Wood et al. 2020a). In Portugal, the bee has been recorded between January and March, and so it may have been missed by previous collectors in lowland areas of Morocco.

Andrena (*Cryptandrena*) *rotundata* Pérez, 1895

Material examined. Morocco: Fès-Meknès, Bhalil, 10 km NW Sefrou, 28.v.1995, 1♀, leg. Ma. Halada; Fès-Meknès, El-Menzel, 30 km E Sefrou, 29.v.1995, 2♀, leg. Mi. Halada, all OÖLM.

Distribution and remarks. Known from Algeria, Italy (Sardinia), and Tunisia (Gusenleitner and Schwarz 2002). This species is very similar to *A. ventricosa* Dours, 1873 but differs by the less dense scutal punctures. Given the very slight differences between *A. rotundata*, *A. ventricosa*, and the more eastern *A. brumanensis* Friese, 1899, this group could benefit from molecular examination.

Andrena (*Distandrena*) *merimna* Saunders, 1908

Material examined. Morocco: Drâa-Tafilalet, Er-Rich, 1253 meters, 28.ii.2019, 3♂, 2♀, *Moricandia foleyi*, leg. O. Ihsane; Fès-Meknès, Laanoucer, 1387 meters, 11.v.2018, 1♀, leg. P. Lhomme & O. Ihsane, all UMONS.

Distribution and remarks. Previously known only from Algeria and Tunisia (Gusenleitner and Schwarz 2002). At 9 mm in length, this one of the larger *Distandrena* species, almost as large as *Andrena fria* Warncke, 1975 which is restricted to Spain. Female Moroccan material is very slightly more striate centrally on the clypeus than comparative material from Algeria and Tunisia, but the male genitalia are a clear match.

Other material examined. Algeria: Biskra, 3.ii.1997, 1♀, OÖLM; Tunisia: 30 km N Foum Tatahouine, 15.ii.1992, 1♀, leg. Warncke, OÖLM; 21.ii.1992, 1♂, leg. Warncke, OÖLM.

Andrena (*Margandrena*) *menahemella* Scheuchl & Pisanty, 2016

Material examined. Morocco: Fès-Meknès, south of Azrou, 25.iv.2017, 1♀, leg. M. Snižek, OÖLM; Fès-Meknès, Laanoucer, 1416 m, 11–12.iv.2019, 1♀, white pan trap; 1♀, yellow pan trap, both leg. L. Hamroud & A. Sentil, UMONS; Fès-Meknès, Ain Leuh, Azrou S, 17.iii.1990, 6♀, leg. H. Teunissen, NMNL, Leiden; Fès-Meknès, Col du Zad, 1800 m, 4.iii.1989, 1♀, 2100 m, 10.iii.1989, 2♀, all leg. H. Teunissen, NMNL, Leiden.

Distribution and remarks. Previously known only from central Israel (Pisanty et al. 2016, Figs 141–144). Specimens were collected at altitude from the Middle Atlas, and were also found in collections at Linz and Leiden. Specimens collected from

Morocco conform to the description of *A. menahemella* with the following differences: In addition to T2+3 and S2+3, T4 is basally red and S4 is almost entirely red. There are no central black spots in T2 or T3 (compare Figs 140, 144). The outer side of the hind tibia has uniformly dark hairs (compare Figs 137, 141), and the nervulus slightly antefurcal. The hairs on the thorax are generally darker (Figs 142, 143), rather than yellowish (Figs 138, 139), contributing to an overall darker appearance.

Whilst overall the Moroccan material has more extensive reddish tergal margins and darker pubescence, the lack of any major structural differences mean that we consider this material to be conspecific with that from Israel, despite the large degree of geographic separation. This record extends the range of *A. menahemella* some 3,600 km to the west, giving a disjunct distribution of Morocco and Israel with no records from Algeria, Tunisia, Libya, or Egypt. However, this situation is not unprecedented amongst *Andrena*, with *Andrena aegyptiaca* Friese, 1899 showing a disjunct distribution being absent from much of the central part of North Africa (Gusenleitner and Schwarz 2002).

Floral preferences. As the two known specimens were caught in pan traps, no information on floral preferences is available. This reflects the situation in Israel, where females are known only from pan traps (Pisanty et al. 2016). The pollen preferences of *Margandrena* are incompletely known (Standfuss and Standfuss 2010; Gogala 2011). For species that fly in the winter through to the spring, they seem to be associated with monocotyledons such as *Bellevalia* (Asparagaceae), *Colchium* (Colchicaceae), and *Crocus* (Iridaceae) (Mavromoustakis 1952, 1958; Scheuchl and Gusenleitner 2009). However, as very little detailed pollen work has been conducted on this group it is difficult to come to firm conclusions. *Andrena menahemella* should be searched for on monocotyledons in northern Morocco during March and April.

Other material examined. Israel: Netiv Italamed He, 16.ii.2010, 1♀, leg. G. Pisanty, OÖLM (paratype, illustrated Figs 141–144).

Andrena (*Micrandrena*) *icterina* Warncke, 1974

Material examined. Morocco: Fès-Meknès, Laanoucer, 1474 meters, 2–3.v.2018, 1♀, yellow pan trap; 33.6234, -4.9002, 11.v.2018, 2♀, all leg. P. Lhomme & O. Ihsane, UMONS.

Distribution and remarks. Described from Algeria (Warncke 1974) and is also known from southern Spain (Dardon et al. 2014). Warncke originally compared *A. icterina* to the central European *Andrena strohmella* Stöckhert, 1928 and suggested an association between the two species. In a revision of *Micrandrena* species from Iberia, Dardon et al. (2014) redescribed the type of *A. icterina* noting that the distinctive carina of *A. strohmella* found on the sides of tergite 1 is absent. However, in our material the carina is present, but weak. On examination of the type material we found that the carina is present, but equally weak when compared to *A. strohmella*.

Other material examined. Algeria: Teniet, 10.v.1895, 1♀, OÖLM (holotype).

***Andrena* (*Micrandrena*) *saxonica* Stoeckhert, 1935**

Material examined. Morocco: Tangier-Tétouan-Al Hoceima, Issaguen, 150 km SE Tanger, 1550 m, 12.v.2015, 1♀, leg. Mucska, OÖLM; Fès-Meknès, Ifrane environs, 1700 m, 10.v.1997, 1♀, leg. P. Průdek, OÖLM.

Distribution and remarks. Known from central Europe south into Spain and Greece (Gusenleitner and Schwarz 2002), and recently southern Spain (Dardon et al. 2014) and Portugal (Wood et al. 2020a). This bee is a specialist of *Ornithogalum* (Westrich 2010) and has been overlooked in southern Iberia where it is generally associated with wooded upland areas.

***Andrena* (*Orandrena*) *monilia* Warncke, 1967**

Material examined. Morocco: Souss-Massa, 10 km W Tiznit, 6.v.1995, 2♀, leg. Mi. Halada, OÖKM; Fès-Meknès, Laanoucer, 33.6302, -4.8847, 2–3.v.2018, 1♂; 10–11.v.2018, 2♀; 15–16.v.2018, 2♀, all caught in yellow pan traps, leg. P. Lhomme & O. Ihsane; Fès-Meknès, Laanoucer, 33.6150, -4.7752, 11–12.iv.2019, 1♀, white pan trap, leg. L. Hamroud & A. Sentil, UMONS.

Distribution and remarks. Originally described from central Spain (Warncke 1967) but found also in Tunisia (Warncke 1980) and the Near East (Warncke 1969, 1976), the species was recently reported from Algeria (Benarfa et al. 2013). The presence of this species in Morocco continues to fill in the distributional gap across North Africa between Spain and the Near East.

Other material examined. Spain: Montarco, 10.v.1933, leg. Dusmet, 1♀, OÖLM (holotype).

***Andrena* (*Pallandrena*) *byrsicola* Schmiedeknecht, 1900**

Material examined. Morocco: Fès-Meknès, 12 km east of Ifrane, 9.v.1997, 1♂, 20♀, leg. J. Halada; Fès-Meknès, Ifrane environs, 9.v.1997, 2♂, 18♀, leg. K. Deneš; Fès-Meknès, Tissa environs, 8.v.1997, 1♀, leg. K. Deneš, all OÖLM.

Distribution and remarks. This taxon has been poorly recorded and documented, leading to nomenclatural confusion. It is part of the *Pallandrena* subgenus that is characterised by females with plumose scopa on the ventral side of the tibiae (Fig. 133), smooth hind femora (contrast *Chlorandrena*), and a deeply incised labrum.

The bee is similar to *Andrena braunsiana* Friese, 1887 which is found in central Europe eastwards to Greece, Turkey and the Caucasus (Gusenleitner and Schwarz 2002). However, both the scutum (Fig. 134) and the tergites (Fig. 135) are much less strongly punctured. In Schmiedeknecht's original description he wrote 'Abdomen nitidum, sparsim et subtilier punctlatum, depressionibus latis apicalibus fere laevibus' which corresponds very well to this material. In German, Schmiedeknecht draws parallels

Figures 131–136. *Andrena* (*Avandrena*) *melacana* Warncke, 1967 **131** female scopa **132** female scopa. *Andrena* (*Pallandrena*) *byrsicola* Schmiedeknecht, 1900 **133** female scopa **134** female scutum **135** female tergites **136** female scopa with pollen.

with members of the *Chlorandrena* in general impression, but notes the differences including the wide reddish margins of the tergites.

Confusion exists over this taxon because the location of the type of Schmiedeknecht collected from Tunisia is unclear and it may be lost (Gusenleitner and Schwarz 2002), and furthermore Warncke (1967) described *Andrena oblita* Warncke, 1967 from southern Italy (females, including holotype) and Tunisia (males). Grünwaldt (unpublished manuscript) examined the type series of *A. oblita* and compared it to material including a male of *A. byrsicola* collected by Schmiedeknecht from Tunis (non-type material). He found that Tunisian *A. oblita* males were identical to *A. byrsicola*, but that Italian females were identical to *A. braunsiana* females. At this moment, it is not possible to confirm these observations and to propose a formal synonymy, but both male and female Moroccan material is consistent with Schmiedeknecht's description of *A. byrsicola*, and this taxon is likely restricted to Morocco, Algeria, and Tunisia (Kuhlmann et al. 2020).

Floral preferences. There are no flower records associated with these specimens, but the unusual modified tibial scopa of the *Pallandrena* suggests some kind of floral specialisation. None of the specimens had full pollen loads, but fragments could be removed from four females (Fig. 136). Some samples were contaminated with *Cistus*-type pollen, but the dominant pollen was Geraniaceae, probably *Erodium* (84.5%). Visual inspection of the scopa of specimens of *A.* (*Pallandrena*) *pallidicincta* Brullé, 1832 from Greece showed the presence of similar large Geraniaceae-type grains, and *A. pallidicincta* and *A.* (*Pallandrena*) *christineae* Dubitzky, 2006 from Lebanon are associated with *Geranium* species (Wood et al. 2020b). It is likely that this *Andrena* clade are specialists of Geraniaceae, but more evidence is required.

Andrena (*Parandrenella*) *tebessana* Scheuchl, Benarfa & Louadi, 2011

Material examined. Morocco: Souss-Massa, 30 km north of Tafraoute (Tafraut), 7.v.1995, 1♀, leg. Ma. Halada, OÖLM; Béni Mellal-Khénifra, Khenifra env., 11.v.1997, 1♀, leg. K. Deneš, OÖLM; Casablanca-Settat, Oueled Sghir, 23.ii.2018, 8♂, 11♀; 27.iii.2018, 18♀; 4–5.iv.2018, 1♀, yellow pan trap, all leg. A. Sentil & El Abdouni, UMONS; Casablanca-Settat, Mzamza, Janoubia, 32.9524, -7.5142, 2♀, 6.v.2019, *Sinapis arvensis*, leg. A. Sentil, UMONS; Fès-Meknès, Sidi Youssef Ben Ahmed, 29.iii.2018, 1♀, leg. P. Lhomme & O. Ihsane, UMONS; Fès-Meknès, Laanoucer, 33.6150, -4.7752, 25.iv.2019, 1♀, leg. L. Hamroud & P. Lhomme, UMONS.

Distribution and remarks. This species was previously known only from a small region of Tunisia and eastern Algeria (Scheuchl et al. 2011). The discovery of this species in northern Morocco extends the range of this species approximately 1,500 km to the west. It is surprising that it has not previously been detected in Morocco because these records come from four quite geographically different provinces.

Other material examined. Algeria: Tébessa, Ouenza, 24.iii.2009, 1♀, OÖLM (holotype).

Andrena (*Poliandrena*) *melaleuca* Pérez, 1895

Material examined. Morocco: Fès-Meknès, Aghbalou, Akourar, 9.v.2019, 1♀, *Marrubium vulgare*, leg. L. Hamroud & A. Sentil, UMONS.

Distribution and remarks. Known from Algeria, Tunisia, and Libya (Gusenleitner and Schwarz 2002), this bee is similar to *A. macroptera* Warncke, 1974 and *A. corax*

Figures 137–144. *Andrena* (*Margandrena*) *menahemella* Scheuchl & Pisanty, 2016 (Israel) **137** female profile **138** female face **139** female dorsum **140** female tergites (Morocco) **141** female profile **142** female face **143** female dorsum **144** female tergites.

Warncke, 1967 but has a slimmer body shape than the former and has hairbands on the metasoma in contrast to the latter, as well as more subtle morphological differences in the structure of the integument.

Andrena (*Poliandrena*) *relata* Warncke, 1967

Material examined. Morocco: Oriental, 40 km south of Guercif, 15–17.v.1995, 100♀, leg. Ma. Halada, OÖLM; Fès-Meknès, Ifkern, 25 km E Boulemane, 24.v.1995, 2♀, leg. Ma. Halada, OÖLM

Distribution and remarks. Previously known only from Spain (Gusenleitner and Schwarz 2002), a very long series of this species was collected in eastern Morocco. Though not previously recorded from North Africa, this material matches the holotype perfectly. In Iberia, *A. relata* is known from eastern and southern Spain including from the provinces of Almería and Murcia which are the driest and most desert-like habitat in Europe, so its presence in the similarly desertic regions south of Guercif and east of Boulemane is ecologically consistent.

Other material examined. Spain: Aragon, Albarracín, 5.vi.1925, 1♀, OÖLM (***holotype***); Albacete, Almansa, 25.v.1983, 1♀, leg. H. Teunissen, NMNL; Granada, Pantano de Cubillas, 27.v.1982, 1♀, leg. R. Leys, NMNL; Granada, Pantano de los Bermejales, 26.v.1982, 1♀, leg. R. Leys, NMNL; Almería, Sierra de Maria, 25 km W Lorca, 10.v.2003, 1♂, 6♀, leg. J. Halada, OÖLM; Granada, S-Sierra Nevada, env. Lanjaron, 4.v.2003, 3♀, leg. J. Halada, OÖLM; Zaragoza, Vera de Moncayo, 15.v.1995, 1♂, 1♀, leg. H. & J.E. Wiering, NMNL.

Andrena (*Simandrena*) *selena* Gusenleitner, 1994

Material examined. Morocco: Souss-Massa, 20 km north Foum-Zguid, 29–30.iv.1995, 1♀, leg. Ma. Halada, OÖLM; Drâa-Tafilalet, 5 km south of Zagora, 25.iv.1995, 1♀, leg. Ma. Halada, OÖLM.

Distribution and remarks. Described from desert regions of eastern Algeria, Tunisia, and Egypt (Sinai, Gusenleitner 1994), these records substantially extend the range of this species to the west in the same manner as for *A. tebessana*.

Andrena (*Ulandrena*) *speciosa* Friese, 1899

Material examined. Morocco: Fès-Meknès, 20 km north of Missour, 14.v.1995, 1♀, leg. Ma. Halada, OÖLM.

Distribution and remarks. Previously known from Syria, Jordan, and Israel through North Africa to Algeria (Gusenleitner and Schwarz 2002). There are only two *Ulandrena* in north-western Africa, and *A. speciosa* is instantly separable in the female sex from *A.* (*Ulandrena*) *tadorna* Warncke, 1974 as the former has a yellow clypeus and lower paraocular areas, whereas those of the latter are completely black.

Species removed from the Moroccan fauna

Andrena (*Melandrena*) *nitida* (Müller, 1776)

Discussion. *Andrena nitida* was recorded from Morocco by Warncke (1974) under the name *Andrena nitida mixtura* Warncke, 1967. This subspecies was described from Portugal and Spain under the name *Andrena limata* Smith, 1853 *mixtura* (Warncke, 1967). However, Warncke transferred this subspecies into combination with *A. nitida* (Warncke 1974, 1976) without any apparent justification. Examination of the type series of *A. n. mixtura* shows that its original placement was justified based on its bivoltine behaviour and the darker colouration of its tergal and scopal hairs (Wood et al. 2020a), and that therefore records of *A. n. mixtura* from North Africa (none of which are part of the type series) refer to *A. limata* and that *A. nitida* should be removed from the Moroccan list.

Material examined. Warncke Collection, OÖLM (*Andrena nitida mixtura*): Morocco: Ifrane, 18.vii.1931, 1♀, leg. A. Nadig; Koudia, 19.iii.1969, 1♀, leg. J.N. Tasei; Portugal: Carcavelhos, 29.iv.1956, 1♀, leg. N.F. d'Andrade (holotype); Coimbra, Ponte da Portela, 30.iii.1968, 1♂, leg. M.A. Diniz; Spain: Catalonia, Arenys, 15.iv.1929, 1♀, leg. Zariquiey (paratype); Playa de Aro, Gerona, 1♀, leg. H. Pochon (paratype); Catalonia, Beceite, 16.vii.1923, 1♀, leg. Zariquiey (paratype); Alicante, Orihuela, 30.v.1925, 1♀, leg. Andréu (paratype); 8.iv.1925, 1♀, leg. Andréu; 16.vi.1949, 1♂, leg. Andréu; (illegible), 8.vi.1912, 1♂, leg. J.M. Dusmet y Alonso; Barcelona, 7.vii.1898, 1♂; Tunisia: 2 km E Menzel Bourguiba, 28.iii.1976, 1♀, leg. P. Robinson.

Andrena (*Notandrena*) *fulvicornis* Schenck, 1853

Material examined. Morocco: Souss-Massa, 10 km S Taroudant, 12.iv.1995, 1♀, leg. Mi. Halada, OÖLM; Tangier-Tétouan-Al Hoceima, 3 km Wm Bni Hadifa, 800 m, 15.v.1995, 1♀, leg. Aßmuth, Sanetra & Schulz, OÖLM; Fès-Meknès, 5 km SE Azrou, 31.v.1995, 2♂, leg. Ma. Halada, OÖLM; Drâa-Tafilalet, Ait sais, 23–26.v.2019, 5♀, leg. O. Ihsane, Y. Bencharki, UMONS; Béni Mellal-Khénifra, Aoulou env., 17.v.1997, 1♀, leg. J. Halada, OÖLM; Fès-Meknès, Bhalil, 10 km NW Sefrou, 28.v.1995, 12♂, 24♀, leg. Ma. Halada, OÖLM; Rabat-Salé-Kénitra, Bouknadel, 28.v.2019, 4♀, leg. I. El Abdouni & P. Lhomme, UMONS; Fès-Meknès, Fes, 23.v.1930, 1♂, leg. Werner, OÖLM; Rabat-Salé-Kénitra, Haddada, 12.vi.2018, 1♀; 8.iv-3.vi.2019, 2♀, leg. I. El Abdouni, P. Lhomme & A. Sentil, UMONS; Fès-Meknès, Ifrane, 1670 m, 11.v.2015, 1♀; leg. K. Deneš, OÖLM; Rabat-Salé-Kénitra, Kenitra, 22.vi.1987, 1♂, leg. M. Schwarz, MSC; Fès-Meknès, Laanoucer, 15.v.2018, 1♂, leg. P. Lhomme & O. Ihsane, UMONS; Lot Journu, Abjelil, 8.v.1997, 1♂, leg. P. Průdek, OÖLM; Casablanca-Settat, Mzamza Janoubia, 6–31.v.2019, 12♂, 15♀, leg. A. Sentil, UMONS; Drâa-Tafilalet, Mzizl, 22.v.2019, 1♀, leg. O. Ihsane & Y. Bencharki, UMONS; Fès-Meknès, Oued Sebou, riv, near El-Menzel, 24–27.v.1999, 1♂, 30♀, leg. P. & V. Průdek, OÖLM; Casablanca-Settat, Oueled Sghir, 23.ii-20.vi.2018, 1♂, 2♀, 10.iii-29.vi.2019, 7♂, 10♀, leg. A. Sentil, I. El Abdouni & M. Chokri, UMONS; Drâa-Tafilalet, Sidi Boukil, 24.iv-22.v.2019, 1♂, 18♀, leg. O. Ihsane & Y. Bencharki, UMONS; Drâa-Tafilalet, Tabia, 24.v.2019, 3♀, O. Ihsane & Y. Bencharki, UMONS; Fès-Meknès, Tazzeka N.P., Bab-Bou-Idir env., 28.v.1999, 1♀, leg. P. Průdek, OÖLM.

Distribution and remarks. *Andrena fulvicornis* was described by Schenck in the same publication as *A. nitidiuscula* (Schenck 1853). Warncke (1967) considered the two to be synonymous under the name *A. nitidiuscula nitidiuscula* (though without formal synonymy, see Schmid-Egger and Doczkal 1995), the name for European populations and as separated from *A. nitidiuscula nigellata* Pérez, 1895 found in North Africa and the Near East (Warncke 1967; see map in Gusenleitner and Schwarz 2002), and this position persisted in future publications (Schmid-Egger and Doczkal 1995).

Schmid-Egger and Doczkal (1995) resurrected the name *A. fulvicornis* as valid on the basis of morphological differences, specifically the strength of the depressed line on the anterior part of the scutum, the density and position of punctures on the scutellum, and the colour of the hind basitarsi. There are also ecological differences, as in southern Germany *A. fulvicornis* is bivoltine whereas *nitidiuscula* is univoltine and flies only in the summer. This differentiation is also supported by more recent genetic work (Benon and Praz 2016). Whilst this distinction was clarified in central Europe, it has not yet been applied across the Mediterranean where the broader concept of Warncke (1967) has been followed in the absence of revisionary work.

At Linz, all examined material in the Warncke Collection from Algeria, Egypt, Morocco, Portugal, Spain, and Tunisia (variably identified by Warncke as *A. nitidiuscula* or *A. nitidiuscula nigellata* depending on sampling location) conformed to *Andrena fulvicornis sensu* Schmid-Egger and Doczkal. Overall, examination of 273 specimens of this species pair from Iberia and North Africa revealed 272 *A. fulvicornis* [Algeria (2), Egypt (1), Morocco (161), Portugal (57), Spain (16), Tunisia (35)] and a single specimen of *A. nitidiuscula* from Portugal (Wood et al. 2020a). On this basis, *A. nitidiuscula* is removed from the Moroccan list and replaced by *A. fulvicornis*.

The identity of taxa from this complex described from North Africa previously considered as *A. nitidiuscula nigellata sensu* Warncke (1967) need to be investigated, specifically *A. nigellata* [Algeria], *A. rostellata* Pérez, 1903 [Algeria], *A. rubrosignata* Saunders, 1908 [Algeria], and *A. lucens* var. *algira* Friese, 1922 [Tunisia]. Based on the North African material examined to date, it is likely that they conform to *A. fulvicornis*, but this must be confirmed by type examination. The status of other names currently in synonymy with *A. nitidiuscula* described from parts of southern Europe including Italy (*Andrena gascheti* Pérez, 1903), Spain (*Andrena divergens* Pérez, 1903), and southern France (*Andrena petroselini* Pérez, 1903, see Gusenleitner and Schwarz 2002) needs to be assessed as they could potentially refer to either *A. nitidiuscula* or *A. fulvicornis*. *Andrena franconica* [Southwestern France] Stoeckhert, 1922 and *A. petroselini* were considered by Stoeckhert (1930) to be synonymous with *A. fulvicornis*.

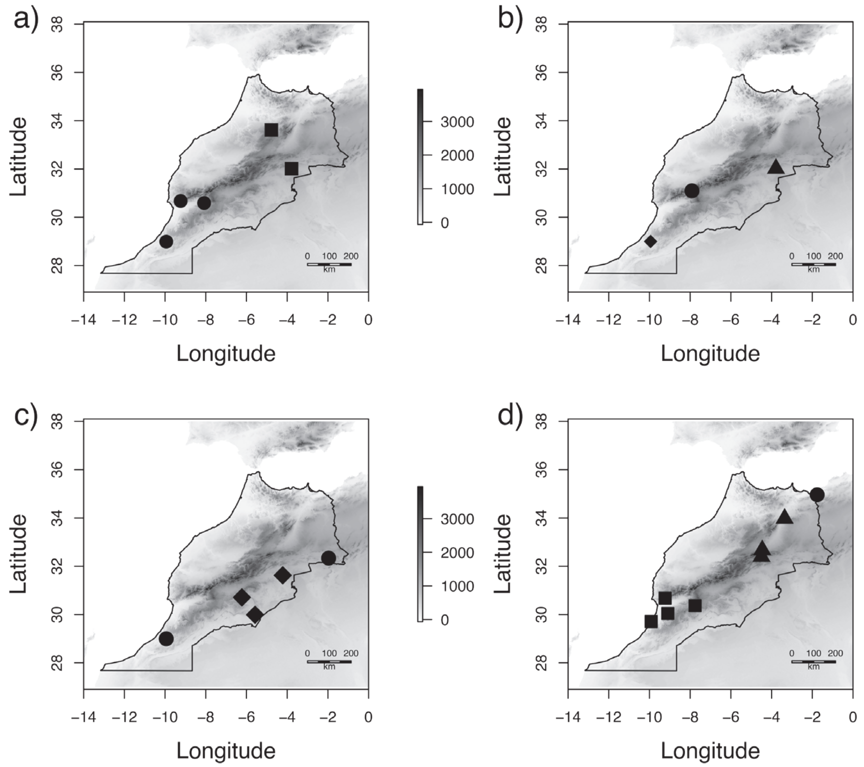

Figure 145. Distribution of sampling locations of newly described species **A** *Andrena hebescens* (circles), *Andrena semiadesus* (squares) **B** *Andrena tenebricorpus* (diamond), *Andrena niveofacies* (circle), *Andrena triangulivalvis* (triangle) **C** *Andrena sparsipunctata* (circles), *Andrena breviceps* (diamonds) **D** *Andrena acutidentis* (squares), *Andrena farinosoides* (triangles), *Andrena nigriclypeus* (circle). Relief is indicated by shading, measured in meters above sea level.

True *A. nitidiuscula* is almost certainly absent from North Africa, and indeed may be rare in hot areas of Mediterranean Europe, being restricted to areas with a cooler microclimate such as the coastline of northern Portugal (Wood et al. 2020a). There is likely to be broad overlap between the two taxa from southern Germany (Schmid-Egger and Doczkal 1995) to Iberia (Wood et al. 2020a) and probably other areas of southern Europe, though *A. fulvicornis* is probably rare in cooler areas such as Switzerland (Benon and Praz 2016). In northern Europe it is highly likely that only *A. nitidiuscula* is present, with no bivoltine behaviour in this species group ever observed in Britain for example (Else and Edwards 2018).

Other material examined. Senckenberg, Frankfurt (*Andrena fulvicornis*): *no collection details*, 1♀ (Neotype, designated Schwenninger 2012); (*Andrena nitidiuscula*): *no collection details*, 1♀ (Lectotype, designated Schwenninger 2013); Warncke Collection, OÖLM (all conforming to *Andrena fulvicornis*): Algeria: Algiers, 2.v.1913, 1♀; Oran, 1895, 1♂, leg. Schmiedeknecht; Egypt: Kerdasa [Kirdasah], 19.v.1929, 1♂, leg. H. Priesner; Portugal: Carcavelos, 13.vi.1953, 1♀, leg. N.F. d'Andrade; Évora, 3.vii.1953, 1♀, leg. N.F. d'Andrade; Sintra, 31.v.1953, ♀, leg. N.F. d'Andrade; Spain: Aranjuez, 26.v.1912, 1♀, leg. Dusmet; Huesca, Benasque, 12.vii.1907, 1♀; Segovia, Madrona, 30.vii.1968, 1♀, leg. K. Warncke; Sierra de Arecena, Rio Odiel dei Calanas, 25.iv.1981, 1♀, M. Kühbander; Tunisia: Tunis, 1898, 1♂, leg. Schmiedeknecht; other collections (*Andrena fulvicornis*): Tunisia: 30 km N Gabes, 10.iv.1994, 33♀, leg. M. Schwarz, M. Schwarz Colln.; Zana, 6.iv.1965, 1♀, leg. R.T. Simon Thomas, NMNL, ZMA.INS.5087405

Conclusions

This work increases the number of *Andrena* species known from Morocco by 26, a richness increase of almost 17%. The presence of species previously known only from varying combinations of Spain, Algeria, Tunisia, Libya, Egypt, and Israel, including recently described species like *A. menahemella*, *A. selena*, and *A. tebessana*, previously undescribed species, and species more typically known from Europe such as *A. synadelpha* indicates that our knowledge of North African *Andrena* remains incomplete.

Morocco has previously been identified not only as an area supporting a rich bee fauna but also as a hotspot of bee diversity and endemism (Patiny and Michez 2007; Patiny et al. 2009). However, it is likely that several of the desert species (*A. breviceps*, *A. farinosoides*, *A. semiadesus*, *A. sparsipunctata*, and *A. triangulivalvis*) will also be present in Algeria. Species found in the Souss valley and further south (*A. acutidentis*, *A. hebescens*, and *A. tenebricorpus*) are more likely to truly be endemic, as they align more closely with the distribution of Moroccan endemics like *Camptopoeum nadigi* (Warncke, 1972), *Rophites theryi* Benoist, 1930, *Panurgus acutus* Patiny, 2002, and *Panurgus minor* Warncke, 1972 which clearly have western and Atlantic distributions within Morocco itself (Patiny and Michez 2007).

The distribution of sampling locations for species newly described for science (Fig. 145) shows that most were collected in desert areas, mainly in the eastern provinces of Oriental and Drâa-Tafilalet, and in the southern provinces of Guelmim-Oued Noun and Souss-Massa (the Drâa and Souss valleys). Considering the history of bee recording in Morocco, these southern and eastern areas are the most difficult to reach, and would not have been visited by historical collectors and taxonomists in the 19th and early 20th century. The papers of Pérez (1895), Schmiedeknecht (1900), Saunders (1908), and Alfken (1914) focused primarily on the more coastal and northern areas of North Africa that naturally were easiest to reach and therefore be visited by European collectors. Though Warncke (1974, 1980) described species collected from the Drâa and Souss valleys (e.g., *A. guichardi*), these collections were clearly not exhaustive. Other recent collecting efforts show that these desert areas are highly likely to contain further undescribed species from other bee groups; for example, a new species of *Osmia* endemic to the Souss valley was just described, (Müller 2020) and other taxonomic work has revealed a major range expansion for the poorly known genus *Borgatomelissa* (Panurginiae) that was recently found in

Morocco for the first time (Ortiz-Sánchez and Patiny 2019), being previously known from the Arabian Peninsula and East Africa to Mauritania across the Sahelo-Sudanian belt.

There are many outstanding problems in North African *Andrena* arising from the large number of subspecies described or erected by Warncke such as in *A. pandosa* Warncke, 1968 and *A. medeninensis* Pérez, 1895 that require focused taxonomic attention to resolve satisfactorily, and which are beyond the scope of this paper. Dealing with these species complexes should form the base for future taxonomic research on *Andrena* in this region.

Acknowledgements

We would like to thank Ahlam Sentil, Insafe El Abdouni, Laila Hamroud, Oumayma Ihsane, and Youssef Ben Charki for their significant contribution towards the contemporary insect collections, and to Dr. Stefanie Christmann, leader of the ICARDA Pollination project in Morocco that made all recent sampling possible. Our thanks to Fritz Gusenleitner, Esther Ockermüller, Martin Schwarz for access to the Warncke Collection and hospitality at Linz, to Frederique Bakker for access to *Andrena* material from Naturalis, and to Maximillian Schwarz for the loan of material from his collection. Our thanks also go to Christophe Praz and Romain Le Divelec for helpful discussion on Mediterranean *Andrena*, and to Christian Schmid-Egger, Gideon Pisanty, and an anonymous reviewer whose comments greatly improved the manuscript. This research was funded by the Federal German Ministry for the Environment, Nature Conservation and Nuclear Safety (BMU) through the International Climate Initiative (IKI). It was also partly supported by the "Fonds de la Recherche Scientifique – FNRS" and the "Research Foundation of Flanders – FWO" under EOS Project (n°3094785).

References

Alfken JD (1914) Beitrag zur Kenntnis der Bienenfauna von Algerien. Mémoires de la Société Entomologique de Belgique 22: 185–237.

Amiet F, Herrmann M, Müller A, Neumeyer R (2010) Apidae 6: *Andrena*, *Melitturga*, *Panurginus*, *Panurgus*. Centre Suisse de Cartographie de la Faune (CSCF)/Schweizerische Entomologische Gesellschaft (SEG), Neuchâtel, 318 pp.

Ascher JS, Pickering J (2020) Discover Life bee species guide and world checklist (Hymenoptera: Apoidea: Anthophila). http://www.discoverlife.org/mp/20q?guide=Apoidea_species

Benarfa N, Louadi K, Scheuchl E (2013) Liste taxonomique des abeilles du genre *Andrena* (Hymenoptera: Apoidea: Andrenidae) du Nord-Est algérien avec les commentaires et les ajouts aux autres régions du pays. Annales de la Société entomologique de France 49: 383–397. https://doi.org/10.1080/00379271.2014.893643

Benoist R (1961) Hyménoptères récoltés par une mission Suisse au Maroc (1947) Apidae, genre *Andrena*. Bulletin de la Société des Sciences naturelles et physiques du Maroc 41: 85–95.

Benon D, Praz C (2016) Deux nouvelles espèces d'abeilles sauvages pour l'entomofaune suisse: observation d'*Andrena florivaga* Eversmann, 1852 et *Andrena fulvicornis* Schenck, 1853 dans les pâturages jurassiens. Entomo Helvetica 9: 69–78.

Cherair EH, Scheuchl E, Doumandji S, Louadi K (2013) A new record and a new subspecies of *Andrena haemorrhoa* (Fabricius, 1781). African Entomology 21: 287–293. https://doi.org/10.4001/003.021.0224

Dardon MJ, Torres F, Ornosa C (2014) The subgenus (*Micrandrena*) (Hymenoptera: Andrenidae) in the Iberian Peninsula. Zootaxa 3872: 467–497. https://doi.org/10.11646/zootaxa.3872.5.3

Djouama H, Louadi K, Scheuchl E (2016) Inventaire préliminaire du genre *Andrena* (Hymenoptera: Apoidea, Andrenidae) de quelques localités sahariennes de l'est de l'Algérie. Annales de la Société entomologique de France 52: 300–310. https://doi.org/10.1080/00379271.2017.1279571

Dours JA (1872) Hyménoptères nouveaux du bassin Mediterranéen. Revue et magasin de zoologie pure et appliquée 23: 293–311, 349–359, 396–399, 419–434.

Ebmer AW (2001) Hymenopterologische Notizen aus Österreich – 14 (Insecta: Hymenoptera: Apoidea). Linzer biologische Beiträge 33: 435–460.

Else GR, Edwards ME (2018) Handbook of the Bees of the British Isles. The Ray Society, London, 775 pp.

Gogala A (2011) Some interesting notes on the *Andrena* species in Slovenia (Hymenoptera: Andrenidae). Acta Entomologica Slovenica 19: 29–35.

Gusenleitner F (1994) *Andrena selena* nov. spec., eine neue Art aus der *Andrena dorsata*-Gruppe (Hymenoptera: Apoidea: Andrenidae). Linzer biologische Beiträge 26: 923–930.

Gusenleitner F, Schwarz M (2002) Weltweite Checkliste der Bienengattung *Andrena* mit Bemerkungen und Ergänzungen zu paläarktischen Arten (Hymenoptera, Apidae, Andreninae, *Andrena*). Entomofauna Supplement 10: 1–1280.

Hebert PD, Penton EH, Burns JM, Janzen DH, Hallwachs W (2004) Ten species in one: DNA barcoding reveals cryptic species in the neotropical skipper butterfly *Astraptes fulgerator*. Proceedings of the National Academy of Sciences 101: 14812–14817. https://doi.org/10.1073/pnas.0406166101

Kuhlmann M et al. [co-authors as listed in "Contributors"] (2020) Checklist of the Western Palaearctic Bees (Hymenoptera: Apoidea: Anthophila). http://westpalbees.myspecies.info

Mavromoustakis GA (1952) On the Bees (Hymenoptera, Apoidea) of Cyprus. – Part III. Annals and Magazine of Natural History 5: 814–843. https://doi.org/10.1080/00222935208654357

Mavromoustakis GA (1958) New bees of the genera *Andrena* and *Nomada* from the island Cyprus (Hymenoptera: Apoidea), part II. Beiträge zur Entomologie 8: 212–219.

Michener CD (2007) The Bees of the World (2nd edn.). Johns Hopkins University Press, Baltimore, 953 pp.

Müller A (2018) Pollen host selection by predominantly alpine bee species of the genera *Andrena*, *Panurginus*, *Dufourea*, *Megachile*, *Hoplitis* and *Osmia* (Hymenoptera, Apoidea). Alpine Entomology 2: 101–113. https://doi.org/10.3897/alpento.2.29250

Müller A (2020) Palaearctic *Osmia* bees of the subgenera *Hemiosmia*, *Tergosmia* and *Erythrosmia* (Megachilidae, Osmiini): biology, taxonomy and key to species. Zootaxa 4778: 201–236. https://doi.org/10.11646/zootaxa.4778.2.1

Nieto A, Roberts SPM, Kemp J, Rasmont P, Kuhlmann M, Criado MG, Biesmeijer JC, Bogusch P, Dathe HH, PD la Rúa, Meulemeester TD, Dehon M, Dewulf A, Ortiz-Sánchez FJ, Lhomme P, Pauly A, Potts SG, Praz C, Quaranta M, Radchenko VG, Scheuchl E, Smit J, Straka J, Terzo M, Tomozii B, Window J, Michez D (2014) European Red List of bees. Publication Office of the European Union, Luxembourg.

Ortiz-Sánchez FJ, Patiny S (2019) A new species of *Borgatomelissa* Patiny, 2000 from eastern Morocco: *Borgatomelissa flavimaura* n. sp. (Hymenoptera, Andrenidae). Annales de la Société entomologique de France 55: 454–457. https://doi.org/10.1080/00379271.2019.1652115

Patiny S, Michez D (2007) Biogeography of bees (Hymenoptera, Apoidea) in Sahara and the Arabian deserts. Insect Systematics and Evolution 38: 19–34. https://doi.org/10.1163/187631207788784012

Patiny S, Michez D, Kuhlmann M, Pauly A, Barbier Y (2009) Factors limiting the species richness of bees in Saharan Africa. Bulletin of Entomological Research 99: 337–346. https://doi.org/10.1017/S0007485308006433

Pérez J (1895) Espèces Nouvelles de Mellifères de Barbarie. (Diagnoses préliminaires). Gounouilhou, Bordeaux, 65 pp.

Pisanty G, Richter R, Martin T, Dettman J, Cardinal S (2020) Molecular phylogeny and historical biogeography of andrenine bees (Hymenoptera: Andrenidae). bioRxiv. https://doi.org/10.1101/2020.06.09.103556

Pisanty G, Scheuchl E, Dorchin N (2016) Eight new species of *Andrena* Fabricius (Hymenoptera: Apoidea: Andrenidae) from Israel – a Mediterranean hotspot for wild bees. Zootaxa 4189: 485–515. https://doi.org/10.11646/zootaxa.4189.3.3

Pisanty G, Scheuchl E, Dorchin N (2018) Taxonomic review of the subgenus *Andrena* (*Poecilandrena*) (Hymenoptera: Andrenidae) in Israel and the Levant. Zootaxa 4374: 151–188. https://doi.org/10.11646/zootaxa.4374.2.1

Praz C, Müller A, Genoud D (2019) Hidden diversity in European bees: *Andrena amieti* sp. n., a new Alpine bee species related to *Andrena bicolor* (Fabricius, 1775) (Hymenoptera, Apoidea, Andrenidae). Alpine Entomology 3: 11–38. https://doi.org/10.3897/alpento.3.29675

Saunders E (1908) Hymenoptera aculeata collected in Algeria by the Rev. A. E. Eaton, M.A., F.E.S., and the Rev. Francis David Morice, M.A., F.E.S. Part III. Anthophila. Transactions of the Entomological Society of London 56: 177–274. https://doi.org/10.1111/j.1365-2311.1908.tb02145.x

Schenck A (1853) Nachtrag zu der Beschreibung nassauischer Bienenarten. Jahrbücher des Nassauischen Vereins für Naturkunde 9: 88–306.

Scheuchl E (2009) *Andrena maximiliani* nov. sp., eine neue *Andrena*-Art aus Tunesien (Hymenoptera: Apidae: Andrenidae). Linzer biologische Beiträge 41: 963–968.

Scheuchl E, Benarfa N, Louadi K (2011) Description of a new *Andrena* species from Algeria (Hymenoptera: Apoidea: Andrenidae). Entomofauna 32: 221–232.

Scheuchl E, Gusenleitner F (2009) *Andrena* (*Margandrena*) *elsei* nov. sp., eine neue türkische Sandbienenart (Hymenoptera, Apidae, Andreninae). Linzer biologische Beiträge 41: 947–962.

Schmiedeknecht O (1900) Neue Hymenopteren aus Nord – Afrika. Természetrajzi Füzetek kiadja a Magyar nemzeti Muzeum 23: 220–247.

Schmid-Egger C, Doczkal D (1995) Der taxonomische Status von *Andrena fulvicornis* Schenck, 1853 (Hymenoptera: Apidae). Entomofauna 16: 1–12.

Schmid-Egger C, Scheuchl E (1997) Illustrierte Bestimmungstabellen der Wildbienen Deutschlands und Österreichs und Berücksichtigung der Arten der Schweiz. Band III Andrenidae. Apollo Books, Denmark, 180 pp.

Schulthess A (1924) Contribution à la connaissance de la faune des Hyménoptères de l'Afrique du Nord. Bulletin de la Société d'Histoire Naturelle de l'Afrique du Nord 15: 293–320.

Schwenninger HR (2015) Revision of the Western Palaearctic species of the *Andrena taraxaci*-group with description of four new species (Hymenoptera: Andrenidae). Stuttgarter Beiträge zur Naturkunde A, Neue Serie 8: 251–270.

Sheffield CS, Hebert PD, Kevan PG, Packer L (2009) DNA barcoding a regional bee (Hymenoptera: Apoidea) fauna and its potential for ecological studies. Molecular Ecology Resources 9: 196–207. https://doi.org/10.1111/j.1755-0998.2009.02645.x

Standfuss K, Standfuss L (2010) *Andrena pellucens* Pérez, 1895 und *Nomada argentata* Herrich-Schäffer, 1839 in Griechenland (Hymenoptera, Andrenidae et Apidae). Bembix, Zeitschrift für Hymenopterologie 30: 35–40.

Stoeckhert E (1930) *Andrena* F. In: Schmiedeknecht O (Ed.) (1930) Die Hymenopteren Mitteleuropas (2nd edn.), 986–1053.

Wandeler P, Hoeck PE, Keller LF (2007) Back to the future: museum specimens in population genetics. Trends in Ecology & Evolution 22: 634–642. https://doi.org/10.1016/j.tree.2007.08.017

Warncke K (1967) Beitrag zur Klärung paläarktischer *Andrena*-Arten. Eos 43: 171–318.

Warncke K (1968a) Die Untergattungen der westpaläarktischen Bienengattung Andrena F. Memórias e Estudos do Museu Zoológico da Universidade de Coimbra 307: 1–110.

Warncke K (1968b) Zur Kenntnis der Bienengattung *Andrena* F. auf der Kanarischen Inseln. Notulae Entomologicae 47: 63–80.

Warncke K (1969) A contribution to the knowledge of the genus *Andrena* (Apoidea) in Israel. Israel Journal of Entomology 4: 377–408.

Warncke K (1974) Beitrag zur Kenntnis und Verbreitung der Sandbienen in Nordafrika (Hymenoptera, Apoidea, *Andrena*). Mitteilungen aus dem Zoologischen Museum in Berlin 50: 3–54.

Warncke K (1975a) Die Sandbienen der Türkei. Teil A. Mitteilungen der Münchner Entomologischen Gesellschaft 64: 81–116.

Warncke K (1975b) Die Bienengattung *Andrena* F., in Iberien (Hym. Apidae). Teil A. Eos 49: 293–314.

Warncke K (1976) Die Bienengattung Andrena F., 1775, in Iberien (Hym. Apidae). Teil B. Eos 50: 119–223.

Warncke K (1980) Zur Verbreitung der Bienengattung *Andrena* F. in Tunesien. Mitteilungen der Münchner Entomologischen Gesellschaft 70: 86–87.

Warncke K (1983) Beitrag zur Kenntnis der Bienen, besonders an Tamarisken, in der nördlichen und zentralen Sahara Algeriens (Hym., Apidae). Bollettino del Museo Civico di Storia Naturale di Venezia 33: 203–214.

Warncke K (1988) Isolierte Bienenvorkommen auf dem Olymp in Griechenland (Hymenoptera, Apidae). Linzer biologische Beiträge 20: 83–117.

Westrich P (2010) Untersuchungen zum Blütenbesuch von Bienen (Hymenoptera, Apidae) an *Ornithogalum* s. l. (Milchstern, Hyacinthaceae). Eucera 3: 1–17.

Wood TJ, Roberts SPM (2017) An assessment of historical and contemporary diet breadth in polylectic *Andrena* bee species. Biological Conservation 215: 72–80. https://doi.org/10.1016/j.biocon.2017.09.009

Wood TJ (2020) Description of a remarkable new *Andrena* species (Hymenoptera: Andrenidae) from Syria. Zoology in the Middle East 66: 262–268. https://doi.org/10.1080/09397140.2020.1782580

Wood TJ, Boustani M, Rasmont P (2020b) A revision of the *Andrena* (Hymenoptera: Andrenidae) of Lebanon with the description of six new species. Annales de la Société entomologique de France. [in press]

Wood TJ, Cross I, Baldock DW (2020a) Updates to the bee fauna of Portugal with the description of three new Iberian *Andrena* species (Hymenoptera: Apoidea: Anthophila). Zootaxa 4790: 201–228. https://doi.org/10.11646/zootaxa.4790.2.1

ZooKeys 974: 93–119 (2020)
doi: 10.3897/zookeys.974.56059
https://zookeys.pensoft.net

RESEARCH ARTICLE

A peer-reviewed open-access journal
ZooKeys
Launched to accelerate biodiversity research

On Chinese Trachyphloeini with description of four new species (Coleoptera, Curculionidae, Entiminae)

Li Ren[1], Roman Borovec[2], Runzhi Zhang[1,3]

1 *Key Laboratory of Zoological Systematics and Evolution, Institute of Zoology, Chinese Academy of Sciences, No. 1 Beichen West Road, Chaoyang District, Beijing 100101, China* **2** *Czech University of Life Sciences Prague, Faculty of Forestry and Wood Sciences, Department of Forest Protection and Entomology, Kamýcká 1176, CZ-165 21 Praha 6-Suchdol, Czech Republic* **3** *University of Chinese Academy of Sciences, Beijing 100049, China*

Corresponding author: Runzhi Zhang (zhangrz@ioz.ac.cn)

Academic editor: M. Alonso-Zarazaga | Received 1 July 2020 | Accepted 14 August 2020 | Published 7 October 2020

http://zoobank.org/A7F28C32-A064-4CAB-8F66-74462E6D54A4

Citation: Ren L, Borovec R, Zhang R (2020) On Chinese Trachyphloeini with description of four new species (Coleoptera, Curculionidae, Entiminae). ZooKeys 974: 93–119. https://doi.org/10.3897/zookeys.974.56059

Abstract

Rhinodontodes alashanensis **sp. nov.**, *Trachyphloeosoma honza* **sp. nov.**, *T. jirka* **sp. nov.,** and *T. martin* **sp. nov.** are described from China, illustrated and compared with similar species. The genus *Rhinodontodes* and the species *Rhinodontodes subsignatus* Voss, 1967 and *Rhinodontus mongolicus* Borovec, 2003 are recorded from China for the first time. Keys to all Chinese genera of Trachyphloeini, and to the Chinese species of *Rhinodontodes* and *Trachyphloeosoma*, are provided.

Keywords

New taxa, taxonomy, *Rhinodontodes*, *Rhinodontus*, *Trachyphloeosoma*, weevil

Introduction

The Trachyphloeini Gistel, 1848 is a medium-sized tribe of entimines containing small wingless, terricolous species with body size 1.3–6.8 mm, having limited ability to migrate. They are mostly xerothermophilous, associated with steppe habitats, xeric grasslands, stony or sandy places, ranging to sandy semideserts (Borovec 2009). Only species of three genera from East Asia, *Pseudocneorhinus* Roelofs, 1873, *Trachyphilus* Faust, 1887 and *Trachyphloeosoma* Wollaston, 1869, are collected from forest litter (O´Brien 1984, Sawada et al. 1999, Morimoto 2015). The tribe is known primarily from the Palaearctic region, with only several genera known also from North America, South Africa, and Oriental region, but the tribal position of South African Trachyphloeini must be clarified. In the Palaearctic Region, the tribe is distributed from the Iberian Peninsula and north-western Africa up to Japan; the genera *Trachyphloeus* Germar, 1817 and *Romualdius* Borovec, 2009 occur in the whole of Europe and eastwards up to Kazakhstan, but the majority of genera have a much smaller area. At present, 13 genera with 363 species are known from the Palaearctic region (Alonso-Zarazaga et al. 2017).

Chinese Trachyphloeini have not been mentioned in literature very often due their cryptic way of life and difficulties in their collection. The majority of the species of the tribe, 67%, are known from the western Palaearctic region; 25% are known from Japan due Morimoto´s revision of the genus *Trachyphilus* (Morimoto 2015), and only 8% are known from China (Alonso-Zarazaga et al. 2017). However, the Himalo-Chinese region is home to a distinctive, peculiar, and specific terricolous fauna of Trachyphloeini, although there are not as many species as in the western subregion. Study of material deposited in the Institute of Zoology in Beijing, as well as newly collected material by several specialists focused on litter associated beetles, has increased our knowledge of the Chinese fauna. The first part of the results of our examination of this very interesting material was published in a previous article (Ren et al., 2019); the present paper adds additional information about other genera of Trachyphloeini.

Materials and methods

The body length of specimens was measured in profile from the anterior margin of the eyes to the apex of the elytra, excluding the rostrum, as customary for curculionids. Rostral length was measured in dorsal view from the anterior margin of eyes to the anterior margin of the epistome and the rostral width was its maximum width. Pronotal and elytral length was measured along the mid-line length in dorsal view, width was the maximum width as measured in dorsal view. Entire abdomens were separated from the specimens and were macerated in 10% KOH for 7–10 days to remove soft tissues. They were then washed in distilled water. Internal abdominal segments were carefully separated from each other. Dissected female genitalia were embedded in Solakryl BMX, and dried male genitalia were glued to the same mounting card as the insect. The terminology of the rostrum and the terminalia follows Oberprieler et al. (2014).

Acronyms for depositories of the material are as follows:

IZCAS	Institute of Zoology, Chinese Academy of Sciences;
NMPC	Národní muzeum, Prague, Czech Republic;
RBSC	Roman Borovec collection, Sloupno, Czech Republic;
ZIN	Zoological Institute of the USSR Academy of Sciences, Saint Petersburg, Russia.

Taxonomy

Rhinodontodes Voss, 1967

Rhinodontodes Voss, 1967: 276 (original description); Alonso-Zarazaga and Lyal 1999: 183 (catalogue); Borovec 2003: 31 (note); Borovec 2009: 76 (redescription of the genus); Alonso-Zarazaga et al. 2017: 403 (catalogue).

Remarks. The genus was described by Voss (1967) for a single species, *Rhinodontodes subsignatus* Voss, 1967, based on a single specimen from Mongolia. The holotype was later examined by Borovec (2003) and until recently was the only specimen of the genus known. We now have access to 21 more specimens of this genus, mainly from the collections of IZCAS and ZIN, and we are able to discuss characters used for the definition of *Rhinodontodes*. Voss described the genus as similar to *Rhinodontus* in its elongated epistome, but distinguishable by tarsomere 3 being wider than tarsomere 2, claws parallel in basal half, apical part of protibiae not distinctly enlarged laterally, rounded, without spines and narrower pronotum, 1.34–1.42 × as wide as long, with anterior margin not distinctly narrower than posterior one. Borovec (2009) in his phylogenetic analysis of the tribe Trachyphloeini confirmed *Rhinodontodes* as related to *Rhinodontus* and *Pseudocneorhinus*, sharing the character states of epistome projected anteriorly and ocular lobes with short setae with *Rhinodontus*, and having as an autapomorphy, rostrum continuous with head, not separated by any furrow. Some of the characters previously used to distinguish *Rhinodontodes* are not unique, in comparison with newly known *Pseudocneorhinus* described in Ren et al. (2019). Males of *P. bifasciatus* Roelofs, 1880 also have the epistome projected anteriorly (Borovec 2009: figs 55, 61), creating a striking tooth, and *P. glaber* Ren, Borovec, Zhang, 2019 also have weak ocular lobes with very short setae and, especially, have a long rostrum and epifrons constricted in the middle. These two species thus show characters very similar to the shape of the rostrum of *Rhinodontodes*. Thus, *Rhinodontodes* seems to be more closely related to *Pseudocneorhinus* than was previously assumed. Study of further material of both genera will confirm whether the two genera are separate or should be placed in synonymy. Presently, *Rhinodontodes* can be distinguished from *Pseudocneorhinus* mainly by the rostrum and head being on the same level and the protibiae being laterally weakly enlarged (Borovec 2009: fig. 58).

Rhinodontodes alashanensis sp. nov.

http://zoobank.org/CEF06CD7-8A76-411D-BF30-4371F691F530
Figs 1–4, 25–27, 52

Type locality. Alashan, Bayanhaotezhen (China: Inner Mongolia).

Material examined. ***Holotype.*** China – **Inner Mongolia Autonomous Region** • 1 ♂; Алашанъ, Дын-юань-ин, V.08 ек. Козлова [Alashan, Ding-yuan-ying (now

Bayanhaotezhen), v.1908, Kozlov's expedition]; Pseudocneorhinus alashanicus Typ. m.; G. Suvorov det.; ZIN. *Paratypes*. CHINA – **Inner Mongolia Autonomous Region** • 1 ♂ 1 ♀; same data as for holotype; ZIN.

Description. Body length: 3.94–4.31 mm, holotype 3.94 mm.

Body (Figs 1–4) dark brownish, epistome, mucros, and claws reddish brown, fringe of setae on protibiae yellowish. Appressed scales covering antennae, head, pronotum, elytra and legs, except antennal clubs; scales on elytra oval, wider than long, densely and finely longitudinally striate, very dense, imbricate, six or seven scales across interval width, light brownish on disc with small, irregularly scattered dark brownish and greyish spots and with light greyish stripe along lateral margins, occupying three lateral intervals and very short apical part of elytra. Pronotum and head with rostrum with oval appressed scales standing on their edges and visible only as special structure of narrow short lines, only short flat area behind frons with the same appressed scales as elytra. Semi-appressed elytral setae subspatulate to spatulate, in holotype more slender than in paratypes, approximately as long as half of width of one interval, densely and finely longitudinally striate, creating one regular row on each interval, distance between two setae 2 × length of one seta. Pronotum and head with rostrum with almost identical semi-appressed setae, irregularly scattered, on pronotum transversely directed, on rostrum shorter than on elytra and longitudinally directed. Antennal scapes and femora with semi-appressed setae, funicles, tibiae and tarsi with semi-erect, moderately long setae, prominent from outline. Clubs densely and finely setose.

Rostrum (Figs 1–4, 25) 1.17–1.22 × as long as wide, from base slightly, regularly enlarged apicad with straight sides, at apex only slightly wider than at base. Epifrons at basal third distinctly tapered apicad, then weakly enlarged apicad, in both parts with slightly convex sides, at apex distinctly narrower than at base, longitudinally shallowly depressed. Epistome long and conspicuous, distinct in dorsal and lateral view, as wide as apex of rostrum or slightly wider, separated from frons by very narrow carina, in females U-shaped, slender, lengthily exceeding anterior rostral margin, with tips directed anteriad, in males V-shaped, wider, less exceeding anterior rostral margin, with tips directed obliquely, laterally. Frons flat, squamose, bearing in lateral parts four or five pairs of stout apical setae, obliquely directed anteriad. Scrobes in dorsal view visible in apical third of rostrum as narrow furrows; in lateral view narrow, subparallel-sided, weakly curved, directed towards middle of eyes, visible as short furrow only in apical half of rostrum, in basal half with margins weakly indicated. Rostrum in lateral view somewhat convex, separated from head by shallow transverse depression. Eyes almost flat, hardly prominent from outline of head. Head distinctly enlarged basad.

Antennae slender; scapes faintly regularly curved, approximately equally long as funicles, at basal two thirds weakly and regularly enlarged apicad, at apical third enlarged somewhat more, at apex equally wide as clubs. Funicles with segments 1 and 2 conical, long, funicle segment 1 slightly longer and wider than segment 2, in males more slender than in females; in males funicle 1 1.7–1.8 × as long as wide; segment 2 1.8–1.9 × as long as wide; segment 3 1.1 × as long as wide; segments 4 and 5 isodiametric; segment 6 1.1 × as wide as long; segment 7 1.4 × as wide as long; in females funicle 1 1.7–1.8 × as long as wide; segment 2 1.6–1.7 × as long as wide; segment 3 and 4 1.2 × as wide as long; segment 5 1.3 × as wide as long; segment 6 1.4 × as wide as long; segment 7 1.6 × as wide as long.

Pronotum (Figs 1–4) 1.34–1.36 × as wide as long, widest just behind the midlength, with rounded sides, more strongly tapered anteriad than posteriad, behind anterior margin weakly constricted. Disc regularly convex. Base arched. Pronotum in lateral view moderately convex, ocular lobes developed.

Elytra (Figs 1–4) 1.26–1.30 × as long as wide, oval, widest at midlength, with regularly rounded sides; shoulders regularly rounded; basal margin arched. Striae narrow, punctured, punctures hidden by appressed scales; stria 1 at base distinctly curved outwards, sutural interval at base distinctly enlarged. Interval almost flat, equally wide and elevated. Elytra in lateral view convex.

Protibiae moderately long and slender, mesally distinctly, laterally weakly enlarged, at apex rounded, with fringe of short and fine yellowish setae, mucronate, inner margin of protibiae and metatibiae with 2–3 very small, black, almost indistinct teeth; metatibial corbels densely squamose. Tarsi slender; tarsomere 2 1.2–1.3 × as wide as long; tarsomere 3 1.5–1.6 × as wide as long and 1.4 × as wide as tarsomere 2; onychium (tarsomere 5) 1.4–1.6 × as long as tarsomere 3. Claws fused at basal third, moderately and regularly divergent apicad.

Penis (Fig. 26) short and wide, 1.91 × as long as wide, in ventral view at base and at apex approximately equally wide, parallel-sided with slightly concave sides; apex regularly rounded to small, regular triangular prolongation; in lateral view wide, regularly curved, subcrescent-shaped, with slender and short apical elongation.

Female genitalia. Sternite VIII umbrella-shaped with short apodeme. Gonocoxites not examined. Spermatheca (Fig. 28) with long, regularly and distinctly curved cornu; corpus large; ramus subsquare, nodulus smaller, subtriangular.

Biology. Unknown.

Distribution. China, Inner Mongolia (Fig. 52).

Etymology. Patronymic, name is derived from the name of type locality.

Differential diagnosis. *Rhinodontodes alashanensis* is similar to the only other known species of the genus, *R. subsignatus* Voss, 1967. It is possible to distinguish the two species by the following key:

1 Larger body size, 4.5–5.4 mm. Epistome short, with points narrower than rostrum at apex, in females V-shaped, moderately robust, slightly exceeding anterior margin of rostrum (Figs 5–8). Pronotum wider, 1.37–1.41 × as wide as long (Figs 5–8). Penis with long apical part (Fig. 27). China, Inner, Mongolia; Mongolia.. ***R. subsignatus* Voss**

– Smaller body size, 3.9–4.3 mm. Epistome long, with tips as wide or wider than rostrum at apex, in females U-shaped, slender, distinctly exceeding anterior margin of rostrum (Figs 1–4). Pronotum narrower, 1.34–1.36 × as wide as long (Figs 1–4). Penis with short apical part (Fig. 26). China, Inner Mongolia.. ***R. alashanensis* sp. nov.**

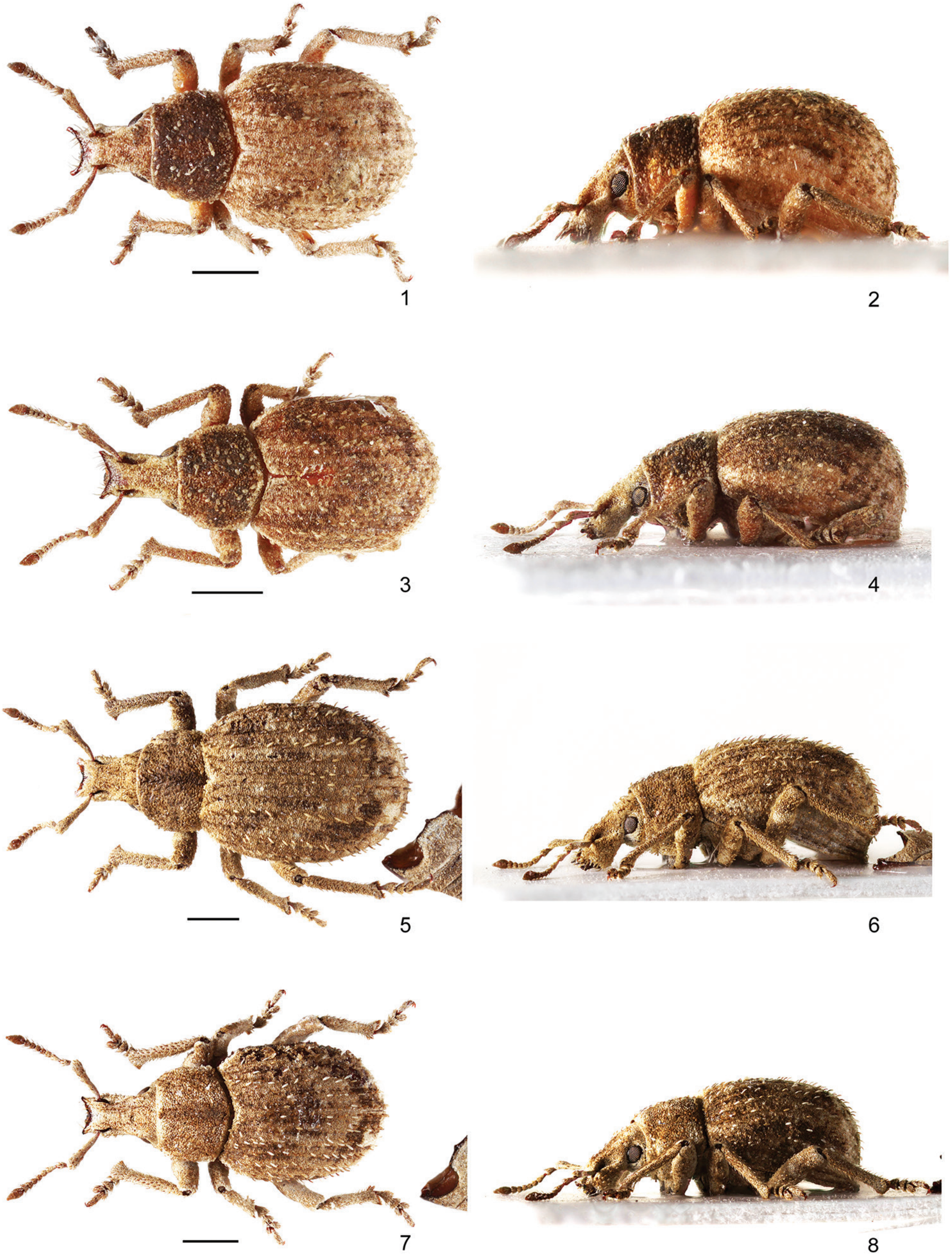

Figures 1–8. Habitus of species of *Rhinodontodes*: **1, 2** *R. alashanensis* sp. nov., female, paratype, dorsal and lateral view **3, 4** *R. alashanensis* sp. nov., male, holotype, dorsal and lateral view **5, 6** *R. subsignatus*, female, dorsal and lateral view **7, 8** *R. subsignatus*, male, dorsal and lateral view. Scale bars: 1 mm.

Rhinodontodes subsignatus Voss, 1967

Figs 5–8, 27, 29, 52

Rhinodontodes subsignatus Voss, 1967: 277 (original description); Alonso-Zarazaga and Lyal 1999: 183 (catalogue); Borovec 2003: 49 (type examination); Borovec 2009: 76 (check-list); Alonso-Zarazaga et al. 2017: 403 (catalogue).

Material examined. China – **Inner Mongolia Autonomous Region** • 2 ♂♂ 2 ♀♀; 阿拉善左旗贺兰山水磨沟正沟 [Alxa Zuoqi, Helan Mountains, Shuimogou Zhenggou]; 27 Jul. 2010; 黄鑫磊 [X.L. Huang leg.]; IZCAS, IOZ(E)1965104, IOZ(E)1965108, IOZ(E)1965105, IOZ(E)1965110; • 3 ♀♀; 阿拉善左旗贺兰山哈拉乌青树湾 [Alxa Zuoqi, Helan Mountains, Halawu, Qingshuwan]; 30 Jul. 2010; 黄鑫磊 [X.L. Huang leg.]; IZCAS, IOZ(E)1965107, IOZ(E)1965109, IOZ(E)1965113; • 1 ♀; 阿拉善左旗贺兰山主峰峰顶 [Alxa Zuoqi, the main top of Helan Mountains]; 3134 m a.s.l.; 17 Aug. 2010; 38°49.8'N, 105°56.4'E; 林美英 [M.Y. Lin leg.]; IZCAS, IOZ(E)1965112; • 1 ♂; 阿拉善左旗贺兰山水磨沟正沟 [Alxa Zuoqi, Helan Mountains, Shuimogou Zhenggou]; 2025 m a.s.l.; 16 Aug. 2010; 38°55.8'N, 105°53.4'E; 林美英 [M.Y. Lin leg.]; IZCAS, IOZ(E)1965114 • 2 ♀♀; 阿拉善左旗贺兰山强岗岭 [Alxa Zuoqi, Helan Mountains, Qianggangling]; 8 Aug. 2010; 黄鑫磊 [X.L. Huang leg.]; IZCAS, IOZ(E)1965106, IOZ(E)1965111; • 1 ♂ 1 ♀; 阿拉善左旗贺兰山古拉本 [Alxa Zuoqi, Helan Mountains, Gulaben]; 6 Aug. 2010; 黄鑫磊 [X.L. Huang leg.]; IZCAS, IOZ(E)1965102, IOZ(E)1965101; • 1 ♀; 阿拉善左旗贺兰山北寺 [Alxa Zuoqi, Helan Mountains, Beisi]; 13 Aug. 2010; 黄鑫磊 [X.L. Huang leg.]; IZCAS, IOZ(E)1965103; • 1 ♀; 阿拉善左旗贺兰山水磨沟 [Alxa Zuoqi, Helan Mountains, Shuimogou]; 25 Jul. 2010; 黄鑫磊 [X.L. Huang leg.]; IZCAS, IOZ(E)1941122.

Mongolia • 1 ♀; 40 km W Dalanzadgad, Gobi Gurvansaikhan NP, Yolyn am env.; 28–30 Jun. 2003; 1700–2000 m a.s.l.; Z. Jindra leg.; RBSC; • 2 ♀♀; Bayan-Chong, Aimak, Ich-Bogdo-Ula, srednegorie [central mountains]; 2500 m a.s.l.; 3 Jul. 1973; G. Medvedev leg.; ZIN.

Remarks. The eighteen specimens examined of *R. subsignatus* come from Mongolia and also from China, Inner Mongolia Autonomous Region. The four males and 11 females from China differ somewhat from the three females from Mongolia, which share with the holotype slender, subparallel-sided, semi-erect elytral setae, while material from Mongolia has wider, subspatulate, semi-appressed elytral setae. Mongolian and Chinese specimens are almost identical in all other characters thus we assume the shape of elytral setae is a variable character of the species. This is the first record of *R. subsignatus* from China (Fig. 52).

Rhinodontus Faust, 1890

Rhinodontus Faust, 1890: 455 (original description); Alonso-Zarazaga and Lyal 1999: 183 (catalogue); Borovec 2003: 32 (genus revision); Borovec 2009: 76 (check-list); Alonso-Zarazaga et al. 2017: 403 (catalogue).

Remarks. The genus is well defined and distinguished by apex of protibiae strikingly enlarged laterally, armed with wide spines, epistome long, rostrum short and wide, distinctly enlarged before eyes and body wide and robust. It was described as monotypic by Faust (1890) and studied later by Voss (1967) and Borovec (2003). *Rhinodontus* currently contains five valid species from China and Mongolia (Alonso-Zarazaga et al. 2017). Among material from IZCAS and ZIN we discovered specimens which add to our knowledge distribution of the species, which were previously known from only a limited number of specimens.

Rhinodontus crassiscapus Borovec, 2003

Figs 9, 10, 30

Rhinodontus crassiscapus Borovec, 2003: 38 (original description); Borovec 2009: 76 (check-list); Alonso-Zarazaga et al. 2017: 403 (catalogue).

Material examined. China – **Qinghai Prov.** • 2 ♀♀; Ю. скл. хр. Бурхан-Будда: дол. оз. Алык-нор. 30.V.1900. Експ. Козлова. [southern slope of the mountains Burchan-Buddha, valley of the lake Alake Hu. 30.v.1900; Kozlov's expedition]; ZIN.

Remarks. This species was described based on three females from China, Xinjiang and Gansu. This is the first additional locality since the original description.

Rhinodontus crassiscapus differs from all other species of the genus by its very short, distally thickened scape and by its long raised elytral setae being longer than one half of the interval width.

Rhinodontus ignarus Faust, 1890

Figs 11, 12, 31, 32

Rhinodontus ignarus Faust, 1890: 455 (original description); Alonso-Zarazaga and Lyal 1999: 183 (catalogue); Borovec 2003: 32 (redescription); Borovec 2009: 76 (check-list); Alonso-Zarazaga et al. 2017: 403 (catalogue).
Rhinodontus proximus centralis Voss, 1967: 276 (original description).

Material examined. China – **Inner Mongolia Autonomous Region** • 2 ♀♀; 阿拉善左旗贺兰山哈拉乌青树湾 [Alxa Zuoqi, Helan Mountains, Halawu, Qingshuwan]; 30 Jul. 2010; 黄鑫磊 [X.L. Huang leg.]; IZCAS, IOZ(E)1965140, IOZ(E)1965142; • 1 ♀; 阿拉善左旗贺兰山强岗岭 [Alxa Zuoqi, Helan Mountains, Qianggangling]; 8 Aug. 2010; 黄鑫磊 [X.L. Huang leg.]; IZCAS, IOZ(E)1965141; • 6 ♀♀; 阿拉善左旗贺兰山哈拉乌主峰 [Alxa Zuoqi, Helan Mountains, the main top of Halawu]; 1 Aug. 2010; 黄鑫磊 [X.L. Huang leg.]; IZCAS, IOZ(E)1965143–1965148.

Mongolia • 1 ♀, Centralnyi Aimak, Dzorgol-Khairkhan, 30 km NE Undzhul; 16 Jul. 1973; G. Medvedev leg.; ZIN; • 1 ♀; Centralnyi Aimak, Dzorgol-Khairkhan, Uver-Undzhul-Ul hill; 16 Jul. 1973; G. Medvedev leg.; ZIN.


9


10


11


12


13


14


15


16

Figures 9–16. Habitus of species of *Rhinodontus*: **9, 10** *R. crassiscapus*, female, dorsal and lateral view **11, 12** *R. ignarus*, female, dorsal and lateral view **13, 14** *R. mongolicus*, female, dorsal and lateral view **15, 16** *R. proximus*, female, dorsal and lateral view. Scale bars: 1 mm.

Remarks. Nine females from China (Inner Mongolia) have the spermatheca with a shorter ramus and more slender collum and nine spines at the protibial apex in comparison with previously known material, including the type specimens, of the species having only eight spines. Due to the lack of males of this population we currently retain it as conspecific with *R. ignarus*.

Rhinodontus mongolicus Borovec, 2003

Figs 13, 14, 33, 53

Rhinodontus mongolicus Borovec, 2003: 36 (original description); Borovec 2009: 76 (check-list); Alonso-Zarazaga et al. 2017: 403 (catalogue).

Material examined. China – **Inner Mongolia Autonomous Region** • 1 ♀; 阿拉善左旗贺兰山哈拉乌主峰[Alxa Zuoqi, Helan Mountains, the main top of Halawu]; 1 Aug. 2010; 黄鑫磊 [X.L. Huang leg.]; IZCAS, IOZ(E)1965118; • 1 ♀; 阿拉善左旗贺兰山强岗岭 [Alxa Zuoqi, Helan Mountains, Qianggangling]; 8 Aug. 2010; 黄鑫磊 [X.L. Huang leg.]; IZCAS, IOZ(E)1965131; • 1 ♀; 阿拉善左旗贺兰山水磨沟正沟 [Alxa Zuoqi, Helan Mountains, Shuimogou Zhenggou]; 27 Jul. 2010; 黄鑫磊 [X.L. Huang leg.]; IZCAS, IOZ(E)1965133; • 1♀; 阿拉善左旗贺兰山哈拉乌青树湾 [Alxa Zuoqi, Helan Mountains, Halawu, Qingshuwan]; 30 Jul. 2010; 黄鑫磊 [X.L. Huang leg.]; IZCAS, IOZ(E)1965137; • 1 ♀; 阿拉善左旗贺兰山水磨沟 [Alxa Zuoqi, Helan Mountains, Shuimogou]; 25 Jul. 2010; 黄鑫磊 [X.L. Huang leg.]; IZCAS, IOZ(E)1941074.

Mongolia • 1 ♀; Uver Khangaiskyi Aimak, Arc-Bogdo Mts., 20 km S Khovda; 12–13 Aug. 1967; Kerzhner leg.; ZIN; • 1 ♀; Ara-Khangaiskyi Aimak, 20 km NE Tevshrulakh; 17 Jun. 1975; Emelianov leg.; ZIN; • 1 ♀; Uver Khangaiskyi Aimak, Orkhon, 15 km W Bat-Ulgyi; 22 Sept. 1981; Korolas leg.; ZIN.

Remarks. The species was described based on 17 females from Mongolia, Ulaan Baatar and these are the first additional specimens since the original description. This is also the first record of the species in China (Fig. 53). *Rhinodontus mongolicus* is very easy distinguishable from all other species of *Rhinodontus* by the prominent sulci covering eyes in dorsal view and by the slender antennal scape.

Rhinodontus proximus Voss, 1967

Figs 15, 16, 34

Rhinodontus proximus Voss, 1967: 275 (original description); Borovec 2003: 34 (redescription); Borovec 2009: 76 (check-list); Alonso-Zarazaga et al. 2017: 403 (catalogue).

Material examined. China – **Inner Mongolia Autonomous Region** • 1 ♀; 阿拉善左旗贺兰山南寺雪岭子[Alxa Zuoqi, Helan Mountains, Nansi, Xuelingzi]; 11 Aug. 2010; 黄鑫磊 [X.L. Huang leg.]; IZCAS, IOZ(E)1965149; • 4 ♀♀; 阿拉善左旗

水磨沟 [Alxa Zuoqi, Helan Mountains, Shuimogou]; 25 Jul. 2010; 黄鑫磊 [X.L. Huang leg.]; IZCAS, IOZ(E)1941092–1941095. – **Gansu Prov. [Kan-Ssu Prov.]** • 1 ♀; 1884; O. Potanin leg.; ZIN.

Mongolia • 1 ♀; Bayankhongor aym., Khangayan Nuruu Mts., Tsagaan-Ovoo 25 km W; 45°55.1'N, 101°10.4'E; 2050 m, a.s.l.; 8 Jun. 2013; M. Košťál leg.; MKBC; • 2 ♀♀; Uver Khangaisk Aimak, Arc-Bogdo Mts., 20 km S Khovda; 12–13 Aug. 1967; Kerzchner leg.; ZIN; • 2 ♀♀; Iuzhno-Gob. Aimak, Ukh-Shankhai; 12 Jun. 1972; ZIN; • 3 ♀♀; Iuzhno-Gob. Aimak, 25 km SW Bulgan; 5 Aug. 1971; ZIN; • 1 ♀; Iuzhno-Gob. Aimak, Navtgar-Ul hill, 35 km NW Iamat-Ul; 9 Aug. 1971; Emelianov leg.; ZIN; • 3 ♀♀; Vostochno-Gob. Aimak, Nomt-Ul hill, 30 km SSE Shokhoi-Nur lake; 26 Jun. 1971; Emelianov & Kozlov leg.; ZIN; • 1 ♀; Baian-Kchongor. Aimak, 20 km ESE Uldzint; 9 Jul. 1970; Emelianov leg.; ZIN; • 2 ♀♀; Iuzhno-Gob. Aimak, Tachilga-Ul hill, 35 km NNE Dalan-Deadagad; 10 Aug. 1971; Kerzhner leg.; ZIN; • 1 ♀; Centralnyi Aimak, Dzorgol-Khairkhan, Uver-Undzhul-Ul hill; 16 Jul. 1973; G. Medvedev leg.; ZIN; • 1 ♀; Iuzhno-Gob. Aimak, Khuryn-Khalkha-Nur, 25 km W Noën; 20 Jun. 1973; G. Medvedev leg.; ZIN.

Remarks. This species was described from four specimens from two localities in Mongolia, later recorded also from China. It is very similar to *R. ignarus*, but differs by possessing eight or nine spines at apex of protibia, tarsal claws connate only in the very short basal part, and also the more slender antenna.

Rhinodontus sawadai Borovec, 2003

Figs 17, 18, 35

Rhinodontus sawadai Borovec, 2003: 40 (original description).

Rhinodontus sawadai: Borovec 2009: 76 (check-list); Alonso-Zarazaga et al. 2017: 403 (catalogue).

Material examined. China – **Xinjiang Autonomous Region** • 1 ♀; Polu; 13 May 1890; ZIN.

Remarks. This species was described based on three females from China, Xinjiang; this is the first additional specimen since the original description. *Rhinodontus sawadai* can be distinguished from other species of the genus by its wider rostrum, curved scape, missing prominences above eyes, and less enlarged outside apex of protibia.

Trachyphloeosoma Wollaston, 1869

Trachyphloeosoma Wollaston, 1869: 414 (original description); Zimmerman 1956: 27 (review of genus); Alonso-Zarazaga and Lyal 1999: 183 (catalogue); Borovec 2009: 52 (redescription of genus); Borovec 2014: 11 (revision of genus); Morimoto 2015: 343 (review of Japanese species); Alonso-Zarazaga et al. 2017: 406 (catalogue).

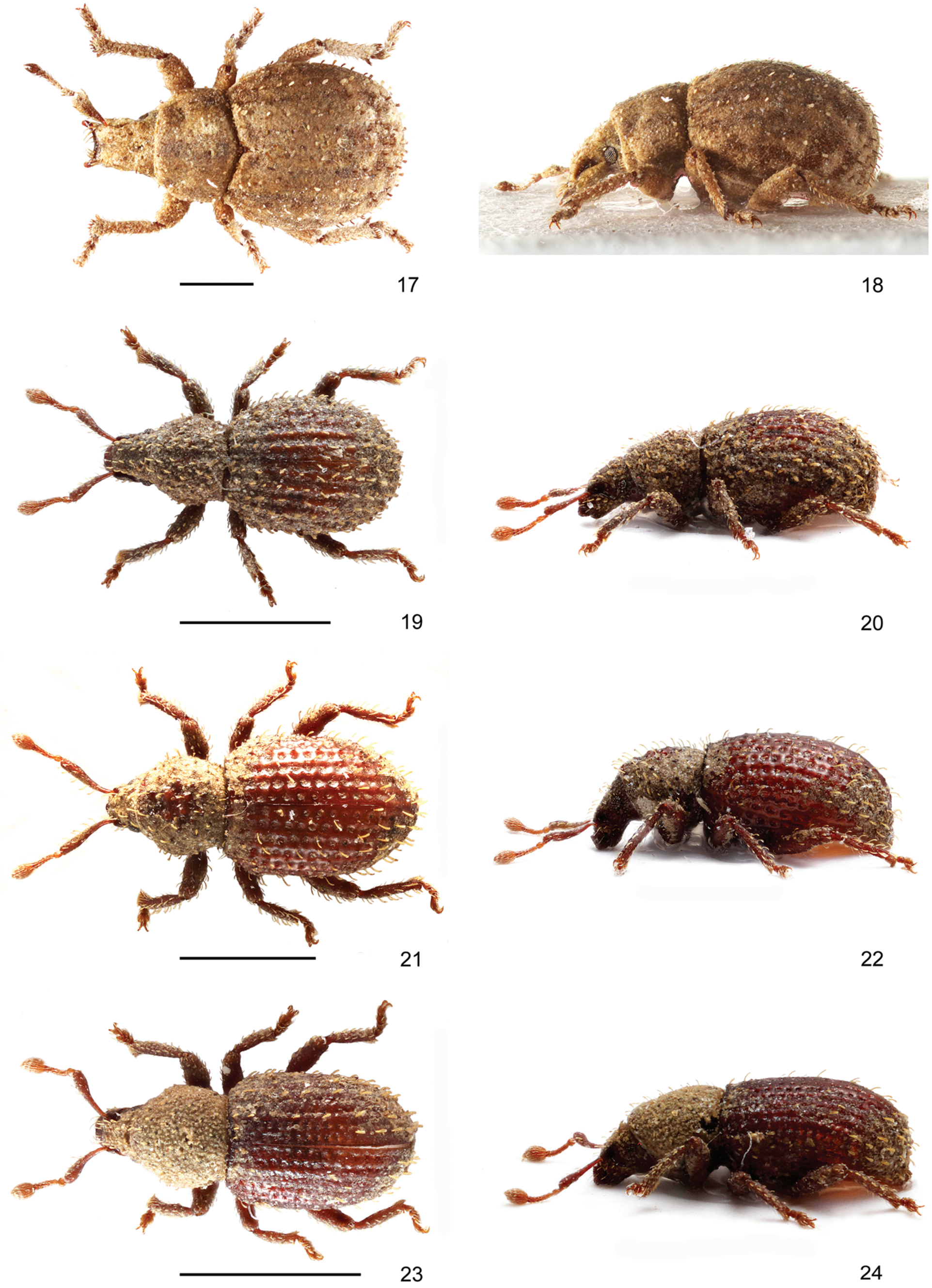

Figures 17–24. Habitus of species of *Rhinodontus* and *Trachyphloeosoma*: **17, 18** *Rhinodontus sawadai*, female, dorsal and lateral view **19, 20** *Trachyphloeosoma honza* sp. nov., paratype, female, dorsal and lateral view **21, 22** *T. jirka* sp. nov., paratype, female, dorsal and lateral view **23, 24** *T. martin* sp. nov., paratype, female, dorsal and lateral view. Scale bars: 1 mm.

Figure 25. Head of *Rhinodontodes alashanensis*, sp. nov., dorsal view, arrows indicate the epistome.

Remarks. This genus was described by Wollaston based on material from the island of St. Helena. Additional species were described later, and the present number of valid species is five. The genus was redescribed and compared to all other Palaearctic Trachyphloeini by Borovec (2009), then subsequently revised by Borovec (2014), based on material from China, Vietnam, Japan, Korea, and the Moluccas. Morimoto (2015), in his monography of Japanese Entiminae, surveyed the Japanese species of the genus. China is the most northwestern part of the range of the genus, and *Trachyphloeosoma* was first recorded from this country only in 2009 by Borovec, based on one male from Yunnan, and subsequently by Borovec (2014) based on several additional specimens of the same species. Following examination of some newly sifted material from China, and comparing this with Morimoto's (2015) review of the genus from the Japanese islands, we can state that the species collected in China are new to science. We can thus correct the name of the species so far recorded from China. This newly collected material from China was erroneously identified as *T. advena* Zimmerman, 1956 and was listed under this name in the Palaearctic catalogue (Alonso-Zarazaga et al. 2017). After dissection and thorough examination, we are able to recognise the specimens as distinct from *T. advena* and belonging to three different species, which are described below.

Trachyphloeosoma honza **sp. nov.**

http://zoobank.org/F296C5F2-B37B-4170-A85F-581BC127CD91
Figs 19, 20, 36, 40, 42, 44, 48, 54

Trachyphloeosoma advena: Borovec 2009: 78 (check-list); Borovec 2014: 12 (note); Alonso-Zarazaga et al. 2017: 406 (catalogue). **non** Zimmermann, 1956.

Type locality. China, Yunnan, Lunan.

Material examined. ***Holotype.*** China – **Yunnan Prov.** • 1 ♂; Lunan – env., Stone Forest; 29 Jul. 1995; Z. Jindra leg.; NMPC. *Paratypes.* CHINA – **Yunnan Prov.** • 10 ♀♀; 14 km SE Tengchong, Renjiafen env.; 24°56.43'N, 98°35.52'E; 2145 m a.s.l.; (CH06) 23 Jun. 2016; J. Hájek & J. Růžička leg.; sift ♯05, border of old orchard, wet debris under trees; NMPC; • 2 ♀♀; same data as for preceding; RBSC; • 1 ♀; same data as for preceding; IZCAS; • 2 ♀♀; Tengchong city, Laifeng Shan Forest Park; 25°01.24'N, 98°28.94'E; 1800 m a.s.l.; (CH05) 22 Jun. 2016; J. Hájek & J. Růžička leg.; sift ♯04, dense mixed forest above tombs near track, wet debris in terrain depressions; NMPC.

Description. Body length: 1.87–2.39 mm, holotype 2.13 mm.

Body (Figs 19, 20) unicoloured piceous brown, antennae and legs slightly paler, reddish brown. The entire body except for frons, antennal funicles with clubs and tarsi covered with a brownish earth-like incrustation which conceals most of the surface; rounded appressed scales, covering the whole body, very hardly visible through this incrustation. Elytra with one conspicuous, dense row of erect, subspatulate setae on each interval, starting just from the base; setae approximately as long as half width of one interval, slightly enlarged apicad, distance between two setae slightly longer than length of one seta. Pronotum and head with rostrum with similar setae, less than half as long as elytral ones, densely irregularly scattered, anteriorly directed. Antennal scapes, femora and tibiae with long, erect, very slender setae, distinctly prominent from outline of scapes and legs.

Rostrum (Figs 19, 20, 36) 1.25–1.31 × wider than long, at base 1.18–1.23 × wider than at apex, evenly tapered anteriad with almost straight sides, at short basal part with shallowly concave sides; in profile short and wide, convex. Epifrons distinctly tapered anteriad with straight sides, at level of antennal insertion narrow, 0.65–0.68 × as wide as corresponding width of rostrum, with ill-defined, shallow, longitudinal furrow. Frons conspicuous, glabrous, smooth and shiny, posteriorly continuous with epifrons. Epistome indistinct. Antennal scrobes in dorsal view fully visible as furrows, reaching eyes; in lateral view with dorsal margin directed towards middle of eye and ventral margin deeply below ventral margin of eye. Eyes small, in dorsal view protruding from outline of head; in lateral view placed in dorsal third, distance from dorsal margin of head longer than diameter of eye.

Antennae moderately long, scapes slightly exceeding anterior margin of pronotum and longer than funicle, weakly regularly curved, in apical half slightly gradually thickened to apex, at apex 0.7–0.8 × as wide as club. Funicle segment 1 bead-shaped, 1.5–1.6 × longer than wide and 1.3–1.4 × longer than segment 2, which is 1.5–1.6 × longer than wide; segments 3–7 successively wider, segment 3 and 4 1.3–1.4 ×, segment 5–6 1.6–1.7 ×, segment 7 1.9–2.0 × wider than long. Clubs ovoid, large, 1.4–1.5 × longer than wide.

Pronotum (Figs 19, 20) 1.17–1.22 × wider than long, widest at midlength, with distinctly rounded sides; anterior margin distinctly narrower than posterior one; disc flatly and irregularly granulate; in lateral view pronotum slightly convex, anterior margin strongly obliquely directed back beneath towards coxae.

Elytra (Figs 19, 20) oval, 1.23–1.29 × longer than wide, widest at midlength, with regularly rounded sides. Striae coarsely punctate, wider than intervals, striae only slightly impressed between punctures; separation of punctures much shorter than their diameters. Intervals very narrow, somewhat convex, smooth.

Protibiae (Fig. 40) short and robust, 4.8–5.2 × longer than wide at midlength, at apical quarter indistinctly curved inwards with mesal edge slightly bisinuate, apically bluntly truncate, with dense fringe of fine but long yellowish setae, shorter in mesal than in lateral part and with long and slender yellowish mucro. Tarsi short, tarsomere 2 1.4–1.5 × wider than long; tarsomere 3 1.2–1.3 × wider than long and 1.3–1.4 × wider than tarsomere 2; onychium (tarsomere 5) 1.1 × as long as tarsomere 3, widened apicad with very long, strongly divaricate claws, almost as long as exceeding part of onychium.

Abdominal ventrites 1.09–1.12 × longer than wide, sparsely roughly punctate; ventrite 2 slightly longer than ventrite 1 and distinctly longer than ventrites 3 and 4 combined; suture between ventrites 1 and 2 sinuous, the others straight. Metaventral process as wide as transverse diameter of metacoxa.

Penis (Fig. 42) short, 1.57 × as long as wide, subparallel-sided, slightly evenly enlarged apicad, in apical part shortly subtriangular, tip rounded, sides of tip shallowly concave; in lateral view moderately wide, ventral side almost straight, dorsal side irregularly rounded, tip pointed and curved upwards.

Female genitalia. Spermatheca with short and moderately wide cornu; corpus large, elongated; ramus and collum developed, identically sized, short and wide (Fig. 44). Sternite VIII with plate 1.5–1.6 × longer than wide, rhombic, without any fenestra (Fig. 48). Gonocoxites of ovipositor very slender and long, basally enlarged, in apical part rod-shaped, bearing slender and long, cylindrical stylus with apical setae.

Bionomics. The majority of the material was collected by sifting wet debris under trees along the border of an old orchard.

Etymology. The new species is dedicated to one of the collectors and a very good friend of the second author, Dr. Jan Růžička (University of Life Science, Prague). The Czech name Jan has its nickname "Honza". The specific name is a noun in apposition.

Distribution. China, Yunnan (Fig. 54).

Differential diagnosis. *Trachyphloeosoma honza* sp. nov. shares with *T. martin* sp. nov. short and robust protibiae, short and wide rostrum and subspatulate setae. It is easily distinguished from *T. martin* sp. nov. by elytral setae on all elytral intervals, dorsal margin of antennal scrobes directed towards middle of eye and female sternite VIII lacking fenestra, while *T. martin* sp. nov. has elytral setae only on odd intervals, dorsal margin of scrobes directed above dorsal margin of eye and female sternite VIII with longitudinal fenestra. In comparison with non-Chinese species, *T. honza* sp. nov. is similar to *T. advena* Zimmerman, 1956, known from Japan, Korea and introduced to U.S.A. and *T. ryukyuensis* Morimoto, 2015, known from Japan, in the funicle being 7-segmented and body covered by appressed setae and elytra with raised setae on all intervals. It is possible to distinguish *T. honza* sp. nov. from both by short subspatulate setae, distinctly shorter than width of an elytral interval (long piliform setae on elytra, approximately as long as width of interval in *T. advena* and *T. ryukyuensis*), elytral setae distinctly bent backwards in lateral view (perpendicularly erect in *T. advena* and *T. ryukyuensis*) and plate of sternite VIII in females without fenestra (with fenestra in *T. advena* and *T. ryukyuensis*).

Trachyphloeosoma jirka **sp. nov.**

http://zoobank.org/766B872B-D8F0-4E20-8DD4-D27E44BAEA02
Figs 21, 22, 37, 41, 45, 49, 54

Type locality. China, Jiangxi, Jinggangshan Mts., Xiangzhou.

Material examined. ***Holotype.*** China – **Jiangxi Prov.** • 1 ♀; Jinggangshan Mts., Xiangzhou (forested valley S of the village); 26°35.5'N, 114°16.0'E; 374 m a.s.l.; 26 Apr. 2011; Fikáček & Hájek leg.; sifting, accumulation of moist leaf litter along the stream and on the steep slope above the stream in the sparse secondary forest; [MF08]; NMPC. ***Paratypes.*** China – **Jiangxi Prov.** • 1 ♀; the same data as holotype; NMPC; • 1 ♀; same data as holotype; IZCAS.

Description. Body length: 2.06–2.44 mm, holotype 2.06 mm.

Body (Figs 21, 22) including antennae and legs unicoloured piceous brown. The entire body except for frons, antennal funicles with clubs and tarsi covered with a brownish earth-like incrustation which conceals most of the surface; appressed scales, covering the whole body, with hardly visible shape, but in lateral parts rounded, finely densely striolate. Elytra with one conspicuous, dense row of long erect setae on each interval, starting from the base; setae as long as width of one interval, very slender, slightly and evenly enlarged apicad, distance between two setae slightly longer than length of one seta. Pronotum and head with rostrum with identically long and shaped setae as elytral setae, densely irregularly scattered, anteriorly directed. Antennal scapes, femora and tibiae with long, erect, very slender setae, distinctly prominent from outline of scapes and legs.

Rostrum (Figs 21, 22, 37) 1.12–1.18 × wider than long, at base 1.18–1.20 × wider than at apex, evenly tapered anteriad, at basal half with straight sides; in profile moderately long and slender, convex, at apex distinctly declined. Epifrons in basal half distinctly tapered anteriad, in apical half almost parallel-sided, narrow, 0.61–0.67 × as wide as rostrum in corresponding part, with ill-defined, slender, longitudinal furrow. Frons conspicuous, smooth, shiny, angularly declined from epifrons. Epistome small, short, indistinct, just at apical portion of rostrum, posteriorly narrowly carinate. Antennal scrobes in dorsal view visible as wide furrows, reaching

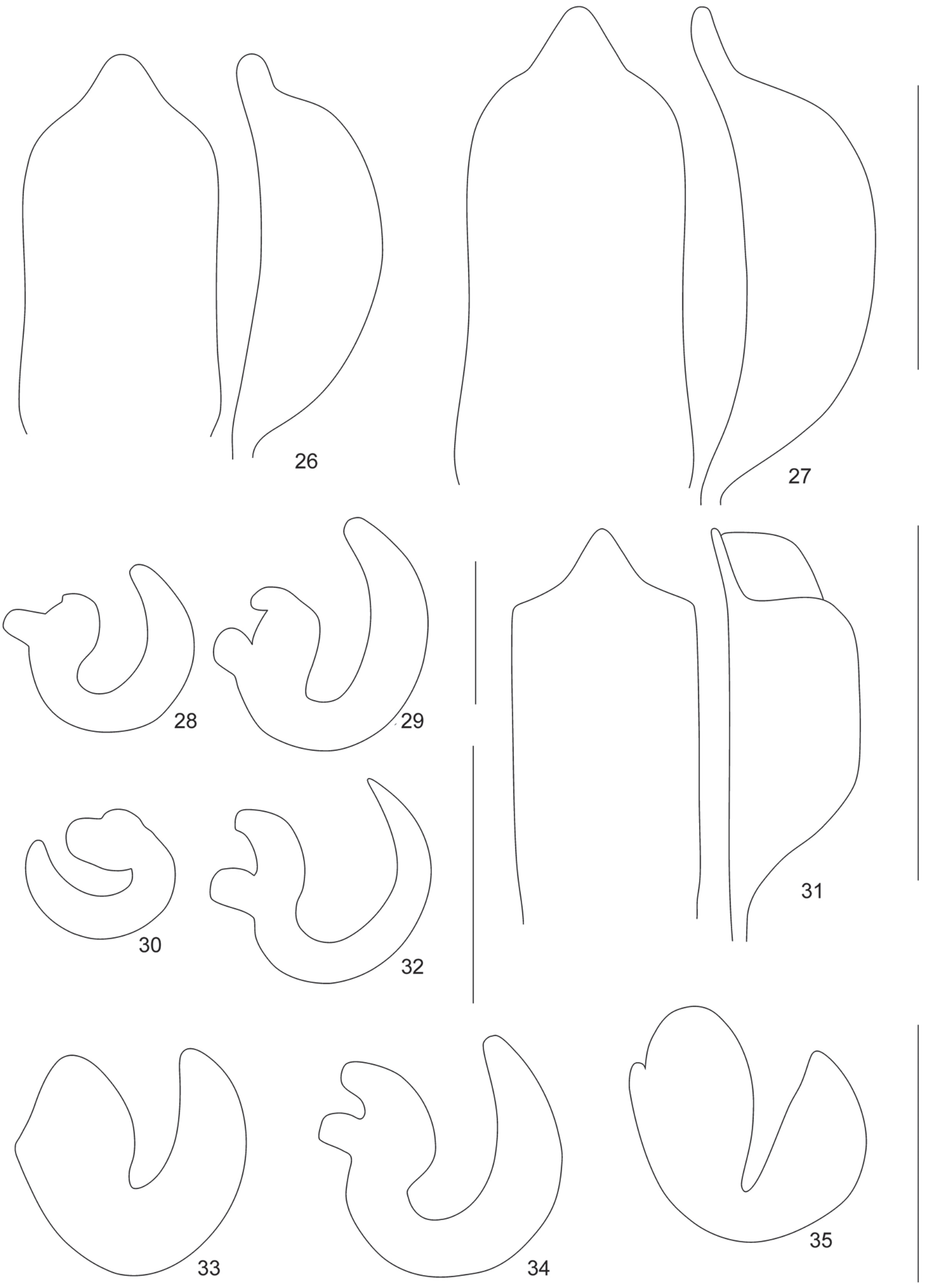

Figures 26–35. Genitalia of *Rhinodontodes* and *Rhinodontus*: **26** Penis of *Rhinodontodes alashanensis* sp. nov., dorsal and lateral view **27** Penis of *Rhinodontodes subsignatus*, dorsal and lateral view **28** Spermatheca of *Rhinodontodes alashanensis* sp. nov. **29** Spermatheca of *Rhinodontodes subsignatus* **30** Spermatheca of *Rhinodontus crassiscapus* **31** Penis of *Rhinodontus ignarus*, dorsal and lateral view **32** Spermatheca of *Rhinodontus ignarus* **33** Spermatheca of *Rhinodontus mongolicus* **34** Spermatheca of *Rhinodontus proximus* **35** Spermatheca of *Rhinodontus sawadai*. Scale bars: 0.50 mm (**26, 27, 31**); 0.25 mm (**28–30, 32–35**).

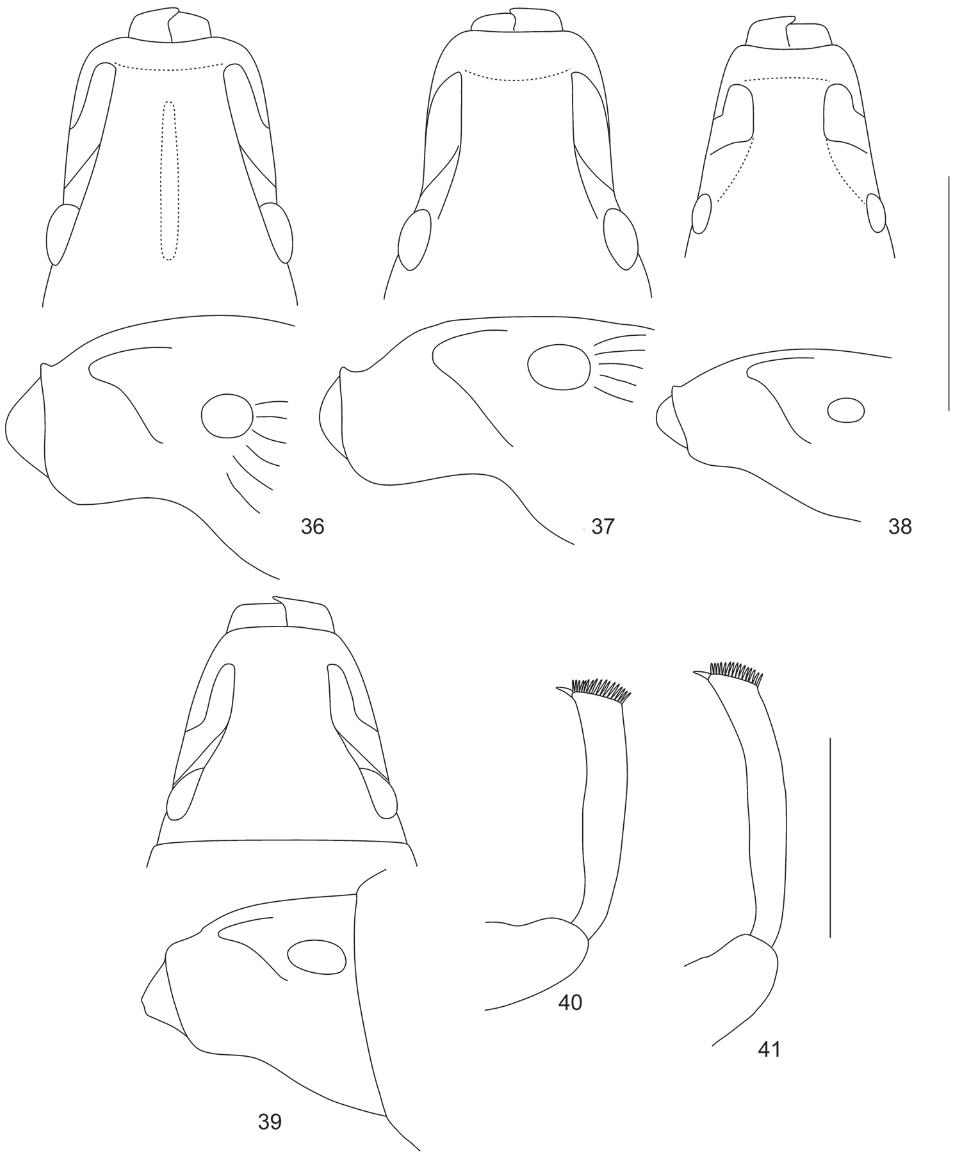

Figures 36–41. Head with rostrum in dorsal and lateral view of *Trachyphloeosoma* species: **36** *T. honza* sp. nov. **37** *T. jirka* sp. nov. **38** *T. martin* sp. nov. **39** *T. roelofsi*; Protibiae of *Trachyphloeosoma* species: **40** *T. honza* sp. nov. **41** *T. jirka* sp. nov. Scale bars: 0.50 mm (**36–41**).

eyes; in lateral view distinctly subtriangular, strikingly enlarged posteriad with dorsal margin directed above dorsal margin of eye and ventral margin deeply below ventral margin of eye. Eyes small, in dorsal view hardly protruding from outline of head; in lateral view placed subdorsally, distance from dorsal margin of head shorter than diameter of eye.

Antennae moderately long, scapes slightly exceeding anterior margin of pronotum and distinctly longer than funicle, weakly curved in basal third, in apical half slightly gradually thickened to apex, at apex 0.7–0.8 × as wide as club. Funicle segment 1 bead-shaped, 1.3–1.4 × longer than wide and 1.4–1.5 × longer than segment 2, this is short, 1.1–1.2 × longer than wide; segments 3–7 slightly successively wider, segment 3 and 4 1.3–1.4 ×, segment 5–6 1.5–1.6 ×, segment 7 1.7–1.8 × wider than long. Clubs ovoid, large, 1.6–1.7 × longer than wide.

Pronotum (Figs 21, 22) 1.21–1.28 × wider than long, widest at anterior third, with distinctly rounded sides, slightly constricted behind anterior margin; disc flatly and irregularly granulate, among granules irregularly punctate with rough and fine punctures; in lateral view pronotum slightly convex, anterior margin strongly obliquely directed back beneath towards coxae.

Elytra (Figs 21, 22) oval, 1.42–1.46 × longer than wide, widest at midlength, with regularly rounded sides. Striae coarsely punctate, twice as wide as intervals, striae not impressed between the punctures; separations of punctures much less than their diameters. Intervals very narrow, flat, shiny.

Protibiae (Fig. 41) long and slender, 6.1–6.3 × longer than wide at midlength, at apical quarter conspicuously curved inwards with mesal edge slightly bisinuate, apically obliquely subtruncate, with dense fringe of fine but long yellowish setae, shorter in mesal than in lateral part, with long and slender yellowish mucro. Tarsi short, tarsomere 2 1.4–1.5 × wider than long; tarsomere 3 1.3–1.4 × wider than long and 1.4–1.5 × wider than tarsomere 2; tarsomere 5 1.1 × as long as tarsomere 3, evenly widened apicad with very long, strongly divaricate claws, approximately as long as part of onychium (tarsomere 5) projecting beyond lobes of tarsomere 3.

Abdominal ventrites sparsely roughly punctate; ventrite 2 slightly longer than ventrite 1 and distinctly longer than ventrites 3 and 4 combined; suture between ventrites 1 and 2 sinuate, the others straight. Metaventral process as wide as transverse diameter of metacoxa.

Female genitalia. Spermatheca with very slender and irregularly distorted cornu; corpus large, elongate; ramus not developed; collum very small, hump-shaped, shorter than wide (Fig. 45). Sternite VIII with plate 2.0–2.2 × longer than wide, rhombic, without any fenestra (Fig. 49). Gonocoxites of ovipositor very slender and long, basally enlarged, in apical part rod-shaped, bearing slender and long cylindrical stylus with apical setae.

Bionomics. This species was collected by sifting in sparse secondary forest.

Etymology. This species is dedicated to Dr. Jiří Hájek, curator of National Museum in Prague, who loaned us very interesting material of *Trachyphloeosoma* for study and also collected the specimens of this species. The nickname of Jiří is "Jirka" in the Czech language. The specific name is a noun in apposition.

Distribution. China, Jiangxi (Fig. 54).

Differential diagnosis. *Trachyphloeosoma jirka* sp. nov. is easily distinguishable among Chinese *Trachyphloeosoma* species by its long and slender protibiae, distinctly curved inwards at apical part, long piliform setae as long on pronotum as on elytra, long

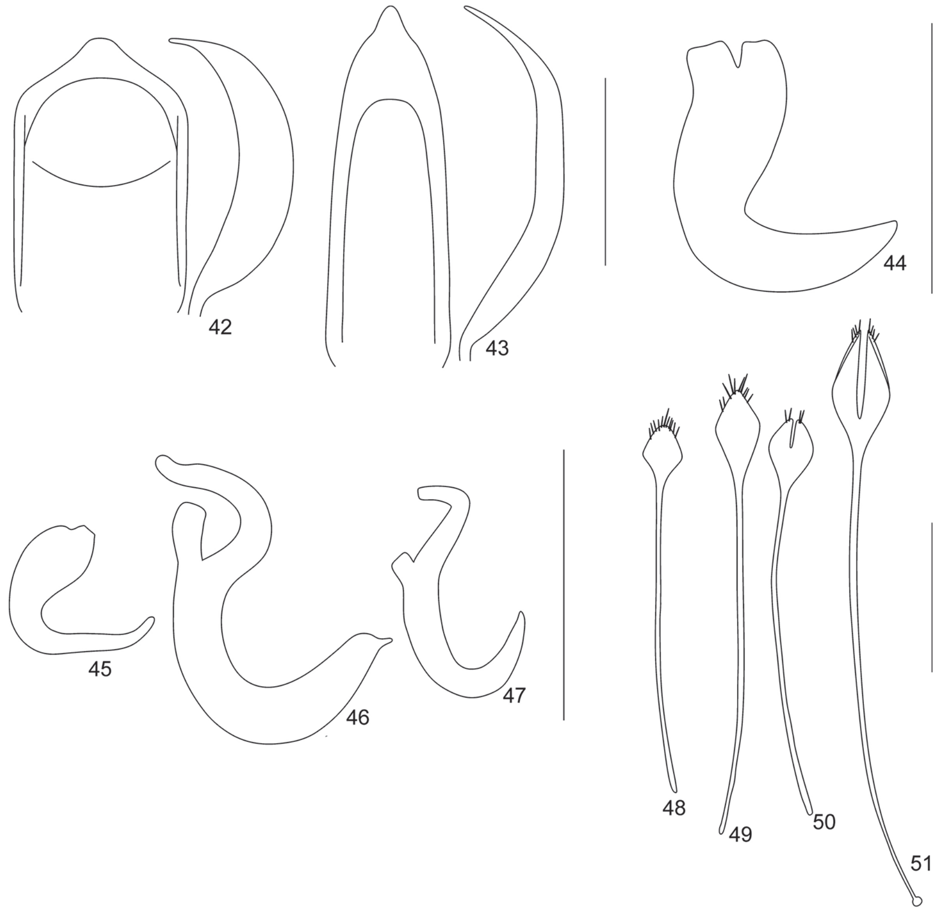

Figures 42–51. Terminalia of *Trachyphloeosoma* species: **42** Penis of *T. honza* sp. nov., dorsal and lateral view **43** Penis of *T. martin* sp. nov., dorsal and lateral view **44** Spermatheca of *T. honza* sp. nov. **45** Spermatheca of *T. jirka* sp. nov. **46** Spermatheca of *T. martin* sp. nov. **47** Spermatheca of *T. roelofsi* **48** Sternite VIII of *T. honza* sp. nov. **49** Sternite VIII of *T. jirka* sp. nov. **50** Sternite VIII of *T. martin* sp. nov. **51** Sternite VIII of *T. roelofsi*. Scale bars: 0.25 mm (**42–47**); 0.5 mm (**48–51**).

and slender rostrum with frons distinctly declined downwards, subdorsal eyes and long and slender plate of female sternite VIII. In comparison with non-Chinese species, *T. jirka* sp. nov. is, in the funicle 7-segmented, body covered by appressed setae and elytra with raised setae on all intervals similar to *T. advena* Zimmerman, 1956, known from Japan, Korea and introduced to U.S.A. and *T. ryukyuensis* Morimoto, 2015, known from Japan. It is possible to distinguish it from both by erect setae on pronotum equal in length to elytral setae (distinctly shorter in *T. advena* and *T. ryukyuensis*), elytra long, oval, 1.42–1.46 × longer than wide (oval, 1.26–1.31 × longer than wide long in *T. advena* and *T. ryukyuensis*) and protibiae slender, distinctly curved inwards at apical portion (short and robust, only slightly curved in *T. advena* and *T. ryukyuensis*) and also plate of sternite VIII in females without fenestra (with fenestra in *T. advena* and *T. ryukyuensis*).

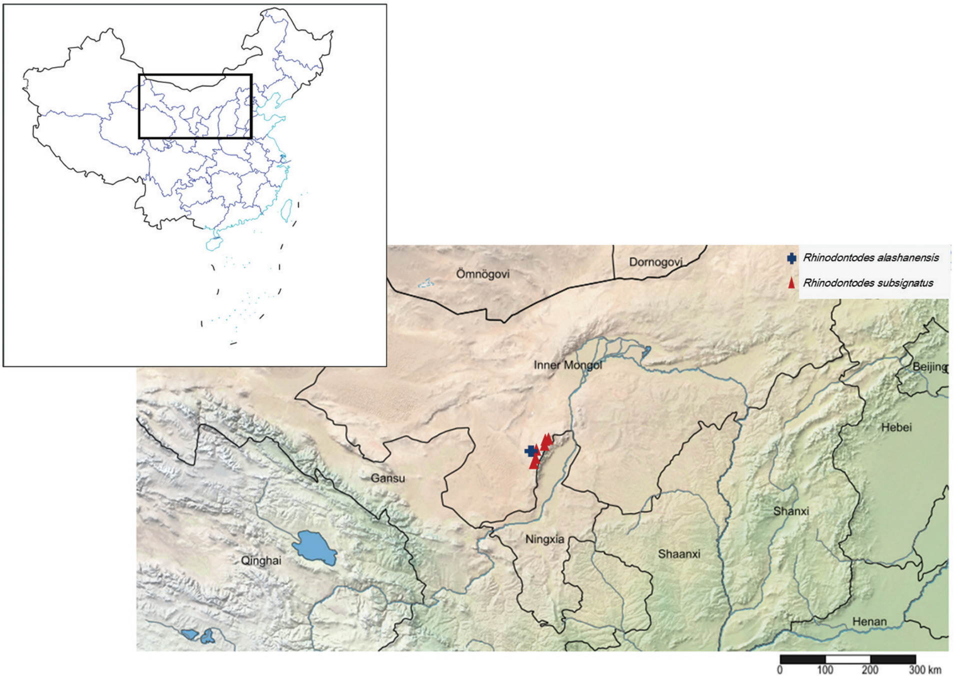

Figure 52. Geographical distribution of new species and new record of *Rhinodontodes* in China.

Trachyphloeosoma martin sp. nov.

http://zoobank.org/0F81305F-227E-49C0-95E3-B4FB14BB3F1C
Figs 23, 24, 38, 43, 46, 50, 54

Type locality. China, Hainan, Limushan Mts.

Material examined. ***Holotype.*** China – **Hainan Prov.** • 1 ♂; Limushan Mts., mountains above frst. admin. Centre; 19°10.5–19°10.9'N, 109°44–109°45'E; 650–900 m a.s.l.; 6 May 2011; Fikáček leg.; sifting – small accumulations of moist leaf litter along an on the trail in secondary forest partly with *Cyathea* and bamboo; MF19; NMPC. ***Paratypes.*** China – **Hainan Prov.** • 1 ♀; the same data as holotype; NMPC; • 1 ♀; same data as for preceding; IZCAS.

Description. Body length: 1.63–2.31 mm, holotype 1.63 mm.

Body (Figs 23, 24) including antennae and legs unicoloured piceous brown. Entire body except of frons, antennal funicles with clubs and tarsi covered with a brownish earth-like incrustation which conceals integument; rounded scales with hardly visible shape, but at least on pronotum, head and rostrum irregularly star-shaped. Elytra with one conspicuous dense row of erect, subspatulate setae only on odd-numbered intervals; setae almost as long as width of one interval, enlarged apicad, distance between two setae distinctly longer than length of one seta. Pronotum and head with rostrum with similar setae, approximately half length of elytral setae, densely irregularly scattered, anteriorly directed. Antennal scapes, femora and tibiae with short, erect, very slender setae, prominent from outline of scapes and legs.

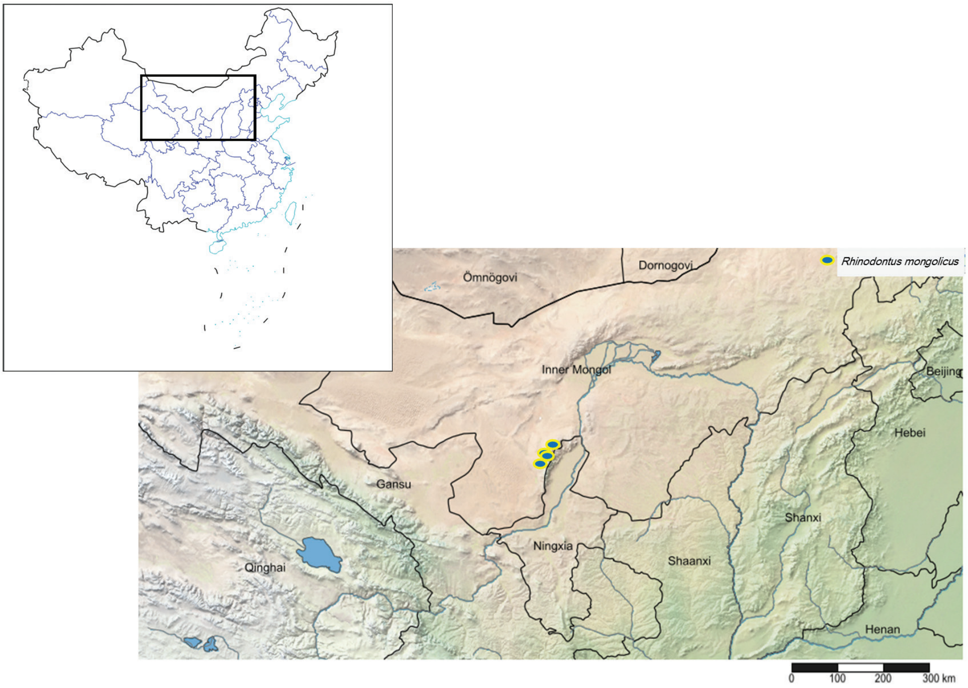

Figure 53. Geographical distribution of new record species of *Rhinodontus* in China.

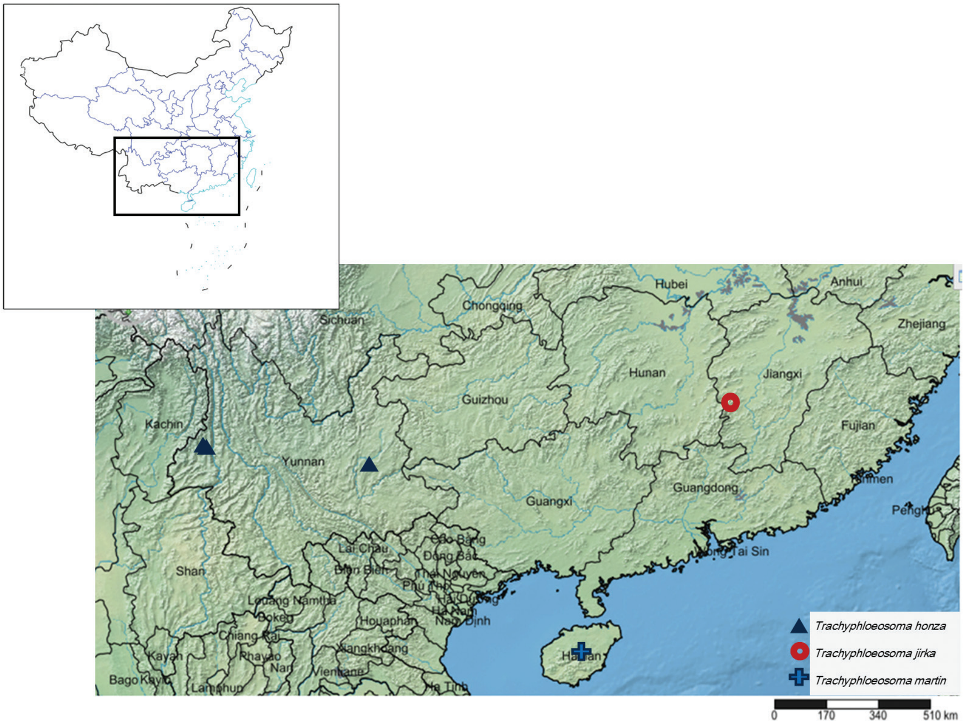

Figure 54. Geographical distribution of new species of *Trachyphloeosoma* in China.

Rostrum (Figs 23, 24, 38) 1.38–1.42 × wider than long, at base 1.23–1.28 × wider than at apex, evenly tapered anteriad with straight sides; in profile short and wide, convex. Epifrons in basal half distinctly tapered anteriad, in apical half almost parallel-sided, narrow, 0.62–0.67 × as wide as rostrum in corresponding part, with ill-defined, longitudinal furrow. Frons glabrous, smooth and shiny, posteriorly continuous with epifrons. Epistome indistinct. Antennal scrobes in dorsal view visible as furrows, not reaching eyes; in lateral view distinctly subtriangular, short, strikingly enlarged posteriad with dorsal margin directed above dorsal margin of eye and ventral margin deeply below ventral margin of eye. Eyes very small, in dorsal view hardly protruding from outline of head; in lateral view placed in dorsal third, distance from dorsal margin of head distinctly longer than diameter of eye.

Antennae moderately long, scapes slightly exceeding anterior margin of pronotum and longer than funicle, weakly regularly curved, in apical half slightly gradually thickened to apex, at apex 0.7–0.8 × as wide as club. Funicle segment 1 wide, bead-shaped, 1.3–1.4 × longer than wide and 1.6–1.7 × longer than segment 2, which is short, 1.1–1.2 × longer than wide; segments 3–7 slightly successively wider, segments 3–5 1.6–1.7 ×, segment 6 1.6–1.7 ×, segment 7 1.7–1.8 × wider than long. Clubs ovoid, large, 1.5–1.6 × longer than wide.

Pronotum (Figs 23, 24) narrow, 1.07–1.11 × wider than long, widest at anterior third, with distinctly rounded sides, constricted behind anterior margin; disc regularly domed, indistinctly granulate; pronotum slightly convex in lateral view, anterior margin strongly obliquely directed back beneath towards coxae.

Elytra (Figs 23, 24) elongated, 1.44–1.48 × longer than wide, widest at midlength, with regularly rounded sides. Striae coarsely punctate, twice as wide as intervals, striae not impressed between punctures; separation of punctures much less than their diameters. Intervals very narrow, flat, shiny.

Protibiae short and robust, 5.0–5.3 × longer than wide at midlength, at apical quarter slightly curved inwards with mesal edge slightly bisinuate, apically obliquely subtruncate, with a dense fringe fine of long yellowish setae, shorter in mesal than in lateral part, with long and slender yellowish mucro. Tarsi short, tarsomere 2 1.6–1.7 × wider than long; tarsomere 3 1.3–1.4 × wider than long and 1.4 × wider than tarsomere 2; onychium (tarsomere 5) as long as tarsomere 3, strikingly widened apicad with very long, strongly divaricate claws, as long as part of onychium projecting beyond lobes of tarsomere 3.

Abdominal ventrites 1.14–1.19 × longer than wide, sparsely roughly punctate; ventrite 2 slightly longer than ventrite 1 and distinctly longer than ventrites 3 and 4 combined; suture between ventrites 1 and 2 sinuate, the others straight. Metaventral process as wide as transverse diameter of metacoxa.

Penis (Fig. 43) long and slender, 2.91 × as long as wide, subparallel-sided with straight sides, slightly evenly tapered apicad; tip long, subtriangular with slightly concave sides; in lateral view slender, distinctly irregularly curved, tip pointed.

Female genitalia. Spermatheca with long and irregularly curved cornu; corpus slender, indistinct; ramus developed, short or tubular; collum very long, distinctly irregularly curved (Fig. 46). Sternite VIII with plate 1.5–1.7 × longer than wide, rhombic, with distinct, slender, longitudinal fenestra reaching midlength of plate (Fig. 50). Gonocoxites of ovipositor very slender and long, basally enlarged, in apical part rod-shaped, bearing slender and long, cylindrical stylus with apical setae.

Bionomics. Type material was sifted from leaf litter in secondary forest partly with *Cyathea* and bamboo.

Etymology. This species is named after the curator of the National Museum in Prague and also the collector of the type specimens, Dr. Martin Fikáček. The specific name is a noun in apposition.

Distribution. China, Hainan (Fig. 54).

Differential diagnosis. *Trachyphloeosoma martin* sp. nov. is very easily recognizable among Chinese species by the elytral raised setae only on odd-numbered intervals and also by the pronotum being somewhat longer, only slightly wider than long, not distinctly granulate on disc, almost flat. Within the genus, *Trachyphloeosoma martin* sp. nov. is similar only to *T. roelofsi* Sharp, 1896 from Japan and *T. setosum* (Wollaston, 1869) known from St. Helena, where it is apparently introduced (but region of origin not yet known). *Trachyphloeosoma martin* sp. nov. is similar to them in having raised elytral setae only on odd intervals, but distinguished from them by a more slender and longer rostrum, 1.38–1.42 × wider than long (1.56–1.73 × in *T. roelofsi* and *T. setosum*), longer and more slender elytra, 1.44–1.48 × longer than wide, (1.19–1.27 × in *T. roelofsi* and *T. setosum*), and also by the different shape of the spermatheca, with collum distinctly longer than wide (isodiametric in *T. roelofsi*), or long and irregularly curved cornu (short and regularly curved in *T. setosum*).

***Trachyphloeosoma roelofsi* Sharp, 1896**

Figs 39, 47, 51

Trachyphloeops setosus Roelofs 1873: 166 (**non** Wollaston, 1869).

Trachyphloeosoma roelofsi Sharp, 1896: 92 (nomen novum for *Trachyphloeops setosus* Roelofs); Morimoto 2015: 346 (review of Japanese species).

Trachyphloeosoma setosum: Zimmerman 1956: 27 (review of genus); Borovec 2009: 78 (check-list); Borovec 2014: 20 (revision of genus); Alonso-Zarazaga et al. 2017: 403 (catalogue).

Material examined. China – **Taiwan** • 1 ♀; TianMu Gudao Hik. Trail (Taipei) Beitou Twnsh., Taipei Co., S. Samau Mt.; 3 Jan. 2009; S. Vít leg.; dead leaves; NMPC; • 1 ♀; Rd. Jhuzihhu/Shuiwei, Yangmingshan Mts., slopes E of Mt. Datun, Taipei Co.; 650 m a.s.l.; 24 Oct. 2007; S. Vít leg.; putresc. base of Cryptomeria (?); NMPC.

Remarks. This species was described by Sharp from Nagasaki, Japan. Zimmerman (1956) compared the series of *Trachyphloeosoma setosum* Wollaston, 1869 from St. Helena with Sharp´s material of *T. roelofsi* from Japan and found the two series represent only one species and placed them in synonymy. However, Morimoto (2015) resurrected the name *T. roelofsi* as an independent species, and distinguished it from *T. setosus* Wollaston from St. Helena. *Trachyphloeosoma roelofsi* is thus known from Japan and Taiwan, while *T. setosus* is assumed as a species introduced to St. Helena without knowledge of its original country.

Key to Chinese *Trachyphloeosoma* species

1 Protibiae long and slender, 6.1–6.3 × longer than wide at midlength, at apical portion distinctly inwardly curved (Fig. 41). Elytral setae piliform, as long as setae on pronotum (Fig. 22). Rostrum long and slender, 1.12–1.18 × wider than long (Fig. 37). Frons distinctly declined from epifrons (Fig. 37). Distance between head and eye shorter than diameter of eye in profile (Fig. 37). Plate of female sternite VIII more elongate, rhombic, 2.0–2.2 × longer than wide, lacking fenestra (Fig. 49). China: Jiangxi.. ***T. jirka*** **sp. nov.**

– Protibiae short and robust, 4.8–5.3 × longer than wide at midlength, at apical portion only slightly inwardly curved (Fig. 40). Elytral setae subspatulate, twice as long as setae on pronotum (Figs 20, 24). Rostrum short and wide, 1.25–1.42 × wider than long (Figs 36, 38, 39). Frons continuous with epifrons (Figs 36, 38, 39). Distance between head and eye longer than diameter of eye in profile (Figs 36, 38, 39). Plate of female sternite VIII proportionally shorter, rhombic, 1.5–1.7 × longer than wide, if twice longer than wide, then with fenestra (Figs 48, 50, 51)..**2**

2 Elytral setae on all elytral intervals, half as long as width of interval (Fig. 19). Epifrons with straight sides (Fig. 36). Dorsal margin of antennal scrobes directed towards middle of eye (Fig. 36). Pronotum shorter, 1.17–1.22 × wider than long, widest at midlength, distinctly granulate (Fig. 36). Penis short and wide, in profile wide (Fig. 42). Spermatheca with ramus and collum equally sized (Fig. 44). Female sternite VIII lacking fenestra (Fig. 48). China: Yunnan ***T. honza*** **sp. nov.**

– Elytral setae on odd-numbered elytral intervals only, almost as long as width of interval (Fig. 23). Epifrons with concave sides (Figs 38, 39). Dorsal margin of antennal scrobes directed above eye (Figs 38, 39). Pronotum slightly longer, 1.07–1.15 × wider than long, widest at anterior third, almost flat (Fig. 23). Penis long and slender, slender in profile (Fig. 43). Spermatheca with collum distinctly longer than ramus (Figs 46, 47). Female sternite VIII with distinct slender fenestra (Figs 50, 51)..**3**

3 Rostrum more slender, 1.38–1.42 × wider than long (Fig. 38). Eyes smaller, in profile with greater distance from dorsal margin of head (Fig. 38). Elytra oval, 1.44–1.48 × longer than wide. Spermatheca with ramus distinctly longer than wide (Fig. 46). Female sternite VIII with plate 1.5–1.7 × longer than wide and fenestra reaching midlength of plate (Fig. 50). China: Hainan.......................... .... ***T. martin*** **sp. nov.**

– Rostrum wider, 1.56–1.73 × wider than long (Fig. 39). Eyes larger, in profile nearer to dorsal margin of head (Fig. 39). Elytra suboval, 1.19–1.27 × longer than wide. Spermatheca with ramus isodiametric (Fig. 47). Female sternite VIII with plate twice as long as wide and fenestra reaching basal part of plate (Fig. 51). China, Taiwan; Japan.. ***T. roelofsi*** **Sharp**

Key to Chinese genera of Trachyphloeini

1 Anterior margin of pronotum with postocular lobes in lateral view. Claws connate in short basal part **2**

– Anterior margin of pronotum straight or oblique in lateral view, without postocular lobes. Claws free **4**

2 Epistome conspicuous in dorsal as well as in lateral view, projecting as two teeth from outline of head. Postocular lobes with short fringe of setae **3**

– Epistome inconspicuous, not projecting from outline of the head. Postocular lobes without setae. 2.6–6.8 mm .... ***Pseudocneorhinus* Roelofs**

3 Rostrum before eyes enlarged, wider than long. Apex of protibiae enlarged laterally, with stout spines. Claws divaricate. Length 2.9–4.1 mm .... ***Rhinodontus* Faust**

– Rostrum very feebly enlarged anteriad, almost parallel-sided, longer than wide. Apex of protibiae feebly enlarged laterally, with slender, bristle-shaped spines. Claws almost parallel-sided, feebly divaricate. Length 3.8–4.9 mm .... ***Rhinodontodes* Voss**

4 Genae glabrous, longitudinally striate. Antennal scrobes in lateral view gently enlarged posteriad, dorsal margin directed towards ventral margin of eye. Rostrum as long as wide, or slightly wider than long. Length 3.0 mm ...... ***Trachyphilus* Faust**

– Genae squamose, lacking striae. Antennal scrobes in lateral view enlarged posteriad, subtriangular; dorsal margin directed towards dorsal margin of eye. Rostrum wider than long. Length 1.7–2.3 mm .... ***Trachyphloeosoma* Wollaston**

Acknowledgements

We want to thank all colleagues for the loan of material used for this study: Jiří Hájek (NMPC) and Boris Korotyaev (ZIN). Special thanks to Christopher H. C. Lyal (Natural History Museum, London) for linguistic help on the manuscript. We sincerely thank Miguel A. Alonso-Zarazaga (Madrid, Spain) for his help and efforts on searching for the type locality of new species. This research was supported by the National Natural Science Foundation of China (31872260), and the Special Foundation for National Science and Technology Basic Research Program of China (2019FY100400). The second author was supported by grant IGA No. A_19_01 of the Czech University of Life Sciences Prague, Faculty of Forestry and Wood Sciences.

References

Alonso-Zarazaga MA, Lyal CHC (1999) A world catalogue of families and genera of Curculionoidea (Insecta: Coleoptera) (excluding Scolytidae and Platypodidae). Entomopraxis, Barcelona SCP, 315 pp.

Alonso-Zarazaga MA, Barrios H, Borovec R, Bouchard P, Caldara R, Colonnelli E, Gültekin L, Hlaváč P, Korotyaev B, Lyal CHC, Machado A, Meregalli M, Pierotti H, Ren L, Sánchez-Ruiz M, Sforzi A, Silfverberg H, Skuhrovec J, Trýzna M, Velázquez de Castro AJ, Yunakov NN (2017) Cooperative catalogue of palaearctic Coleoptera Curculionoidea. Monografías electrónicas SEA 8: 1–729. http://sea-entomologia.org/PDF/MeSEA_8_Catalogue_Palaeartic_Curculionoidea.pdf

Borovec R (2003) Revision of genera *Rhinodontus* and *Trachyphilus* (Coleoptera: Curculionidae: Entiminae: Trachyphloeini). Klapalekiana 39: 31–51.

Borovec R (2009) Revision of the Palaearctic supraspecific taxa of the tribe Trachyphloeini (Coleoptera: Curculionidae: Entiminae). Klapalekiana 45: 1–97.

Borovec R (2013) Trachyphloeini, In: Löbl I, Smetana A (Eds) Catalogue of Palaearctic Coleoptera. Vol. 8. Curculionoidea 2. Leiden, Brill, 414–422.

Borovec R (2014) Study on Trachyphloeini of Oriental region (Coleoptera: Curculionidae: Entiminae). Studies and Reports, Taxonomical Series 10: 1–39.

Faust J (1890) Insecta, a Cl. G. N. Potanin in China et in Mongolia novissime lecta. XV. Curculionidae. Horae Societatis Entomologicae Rossicae 24: 421–476. https://www.biodiversitylibrary.org/page/27529476

Morimoto K (2015) [new taxa] In: Morimoto K, Nakamura T, Kannô K. Curculionidae: Entiminae (Part 2) (Coleoptera). The Insects of Japan, Volume 4. Fukuoka, Touka Shobo, 758 pp.

O'Brien CW (1984) *Trachyphloeosoma advena* Zimmerman, new to the continental United States, with a key to U. S. genera of Trachyphloeini (Coleoptera: Curculionidae: Otiorhynchinae). The Coleopterists Bulletin 38: 181–184.

Oberprieler RG, Anderson RS, Marvaldi AE (2014) 3. Curculionoidea Latreille, 1802: Introduction, Phylogeny. In: Leschen RAB, Beutel RG (Eds) Handbook of Zoology, Arthropoda: Insecta; Coleoptera, Beetles, Volume 3: Morphology and systematics (Phytophaga). Walter de Gruyter, Berlin/Boston, 675 pp.

Ren L, Borovec R, Zhang R (2019) On the genus *Pseudocneorhinus* (Coleoptera, Curculionidae, Entiminae), with descriptions of five new species from China. ZooKeys 853: 57–86. https://doi.org/10.3897/zookeys.853.33311

Sawada Y, Hirowatari T, Ishii M (1999) Species diversity of edaphic beetle communities in the Coppice of Mt. Mikusayama, Central Japan. Japanese Journal of Entomology 2: 161–178. [in Japanese, English abstr.]

Sharp D (1896) The *Rhynchophorous* Coleoptera of Japan. Part IV. Otiorhynchidae and Sitonides, and a genus of doubtful position from the Kurile Islands. Transactions of the Entomological Society of London 1: 81–115. https://doi.org/10.1111/j.1365-2311.1896.tb00958.x

Voss E (1967) Ergebnisse der zoologischen Forschungen von Dr. Kaszab in der Mongolei. 119. Attelabidae, Apionidae, Curculionidae (Coleoptera). (194. Beitrag zur Kenntnis der Curculioniden). Entomologische Abhandlungen Staatliches Museum für Tierkunde Dresden 34: 249–328.

Wollaston TV (1869) On the Coleoptera of St. Helena (Continued). Annals and Magazine of Natural History 24: 401–417. https://doi.org/10.1080/00222936908696087

Zimmerman EC (1956) On *Trachyphloeosoma* and a new species from Hawaii (Coleoptera. Curculionidae). The Coleopterists Bulletin 10: 27–31. https://www.jstor.org/stable/3999054

ZooKeys 974: 121–130 (2020)
doi: 10.3897/zookeys.974.55934
https://zookeys.pensoft.net

SHORT COMMUNICATION

A peer-reviewed open-access journal
ZooKeys
Launched to accelerate biodiversity research

A non-exhaustive survey revealed possible genetic similarity in mitochondrial adaptive evolution of marine fish species in the northwestern Pacific

Linlin Zhao[1], Tianzi Wang[2], Fangyuan Qu[1], Zhiqiang Han[2]

1 *The First Institute of Oceanography, Ministry of Natural Resources, Qingdao, China* **2** *Fishery College, Zhejiang Ocean University, Zhoushan, China*

Corresponding author: Zhiqiang Han (d6339124@163.com)

Academic editor: N. Bogutskaya | Received 28 June 2020 | Accepted 25 August 2020 | Published 7 October 2020

http://zoobank.org/9DC221A9-656F-4BC9-A9A1-301E3FDC4C8B

Citation: Zhao L, Wang T, Qu F, Han Z (2020) A non-exhaustive survey revealed possible genetic similarity in mitochondrial adaptive evolution of marine fish species in the northwestern Pacific. ZooKeys 974: 121–130. https://doi.org/10.3897/zookeys.974.55934

Abstract

Mitochondrial coding genes involved in the oxidative phosphorylation pathway play vitally important roles in energy production and thermal adaptation. Investigating the underlying molecular mechanism of mitochondrial adaptive evolution is crucial for understanding biodiversity and ecological radiation. In this study, we collated population genetic studies of marine fish species in the northwestern Pacific based on mitochondrial cytochrome *b* gene sequences, to investigate whether similar patterns could be detected in mitochondrial adaptive evolution. After filtering, nine studies containing eight marine fish species (*Ammodytes personatus*, *Boleophthalmus pectinirostris*, *Larimichthys polyactis*, *Mugil cephalus*, *Pampus argenteus*, *Platycephalus* sp.1, *Sebastiscus marmoratus*, and *Trachidermus fasciatus*) belonging to eight different families were retained. Multiple codon-based approaches were used to identify potential sites under selection in each species. By comparison, our results showed that the posterior part of the mitochondrial cytochrome *b* gene (particularly codon 372 and its neighboring sites) seemed to be involved in the adaptive evolution process, suggesting potential genetic similarity among distantly related species. We also summarized four types of adaptive patterns in the reviewed species, and suggest that the level of genetic differentiation and mitochondrial adaptive evolution might be correlated. Further studies are needed to confirm such relationship by detecting RNA-level evidence and investigating more species and samples.

Keywords

Cytochrome *b* gene, genetic similarity, marine fish, Northwestern Pacific, population genetics

Introduction

Understanding adaptive evolution of marine organisms is a focus topic in evolutionary biology, and can also provide essential information for fishery management and conservation (Postma and van Noordwijk 2005; Palsbøll et al. 2007). In marine realm, due to a lack of physical barriers, most environmental factors are relatively homogeneous compared to the terrestrial environment (Gleason and Burton 2016), and temperature is thought to be the most significant variable among different latitudinal gradients (Silva et al. 2014; Xu et al. 2017). Marine species with a wide latitudinal distribution normally experience various degrees of thermal tolerance across the distribution ranges, which could result in thermally adaptive evolution. In turn, genetic variations resulting from thermal adaptation could help organisms adapt to a local environment, and simultaneously contribute to genetic differentiation among geographically distant populations (Silva et al. 2014). Divergent local adaptation may generate barriers to population connectivity and ultimately lead to ecological speciation (Schluter and Rambaut 1996; Momigliano et al. 2017). It can be assumed that adaptive sites would be fixed among populations during the adaptation process, resulting in and maintaining genetic differentiation. Consequently, intraspecific adaptive evolution could be relatively easy to detect when population differentiation is weak (Lamichhaney et al. 2017). When strong genetic differentiation was maintained, strict purifying selection and relaxed positive selection might buffer the adaptation differentiation scenario (Nosil et al. 2009; Forester et al. 2016).

Given the relatively fast mutation rate, mitochondrial cytochrome *b* (cytb) and the non-coding control region are the most two mitochondrial genes investigated in population genetics of marine fish species (Guo et al. 2004). In the mitochondrial genome, protein coding genes involved in the oxidative phosphorylation (OXPHOS) pathway play vital important roles in energy production and respiration (Ruiz-Pesini et al. 2004; Sun et al. 2011). However, despite the important function of energy production and thermoregulation, mitochondrial DNA has been considered as an evolutionary bystander in population genetics and phylogenetics (Ballard and Pichaud 2014). Until now, limited numbers of studies have shown evidence for mitochondrial adaptive evolution in marine organisms (but see Sun et al. 2011; Caballero et al. 2015; Jacobsen et al. 2016). Among them, species-specific patterns were detected in mitochondrial adaptive evolution, suggesting varied genetic mechanisms. In contrary, our previous studies consistently revealed that adaptive sites were detected in the posterior part of mitochondrial cytb gene (Xu et al. 2017, 2018), to some extent suggesting potential genetic similarity in adaptive evolution of cytb gene. To confirm such potential similarity, here we collated population genetic studies of marine fish species in the northwestern Pacific based on mitochondrial cytb gene sequences and detect genetic adaptive sites by using population-based approaches. Our findings provide supplementary information for the evolutionary biology of marine organisms.

Methods

Literature collation

Considering that our major research field is population genetics of marine fish in the northwestern Pacific, we searched population genetics papers based on mitochondrial cytb gene sequences by using the search terms "population genetics", "cytochrome *b* or cytb", "marine fish species" and "northwestern Pacific" in Google Scholar and China National Knowledge Infrastructure (CNKI) literature databases. Our previous studies revealed few genetic variations in the front half of the cytb gene (Xu et al. 2017, 2018), suggesting the front part of the cytb gene is relatively conserved and unsuitable for population genetic analyses. Given that, papers only analyzing the front part of cytb gene sequences were excluded. In addition, papers with unreleased sequence data were also excluded. After filtering, nine papers containing eight marine fish species (*Ammodytes personatus* Girard, 1856; *Boleophthalmus pectinirostris* (Linnaeus, 1758); *Larimichthys polyactis* (Bleeker, 1877); *Mugil cephalus* Linnaeus, 1758; *Pampus argenteus* (Euphrasen, 1788); *Platycephalus* sp. 1 (sensu Nakabo, 2002); *Sebastiscus marmoratus* (Cuvier, 1829); and *Trachidermus fasciatus* Heckel, 1837) were retained (Table 1). The cytb gene sequences were downloaded from GenBank. We also downloaded cytb gene sequences of *Larimichthys crocea* (Richardson, 1846) (GenBank accessions: EU346914–EU346932), the sister species of *L. polyactis*, to investigate interspecific mitochondrial adaptive evolution.

Analyses of adaptive evolution

For each of the nine species, sequences were aligned using MAFFT method in Unipro UGENE v1.12.0 software (Okonechnikov et al. 2012). MEGA 6.0 software (Tamura

Table 1. General information of reviewed marine species in this study.

Order	Family	Species	Latitudinal range	GenBank accession	NH[2]	Reference
Perciformes	Sciaenidae	*Larimichthys polyactis*	39.8–27.2N	FJ609001–FJ609137; JN601196–JN601289	231	Huang 2011; Wu et al. 2009
	Gobiidae	*Boleophthalmus pectinirostris*	34.8–20.8N	KF384522–KF384638, KF415515	118	Chen et al. 2015
	Ammodytidae	*Ammodytes personatus*	45.5–35.9N	MK112908–MK113077	170	Deng et al. 2019
	Stromateidae	*Pampus argenteus*	19.2–11.6N[1]	JF790202–JF790259, KJ630414–KJ630460	105	Sun et al. 2012
Scorpaeniformes	Sebastidae	*Sebastiscus marmoratus*	37.9–21.5N	KX374371–KX374400, KX722503–KX722509	30	Xu et al. 2017
	Platycephalidae	*Platycephalus* sp.1	35.5–21.4N	MG913953–MG913986	34	Xu et al. 2018
	Cottidae	*Trachidermus fasciatus*	39.8–30.4N	JX079997–JX080027, KC701150–KC701194	76	Gao et al. 2013
Mugiliformes	Mugilidae	*Mugil cephalus*	32.7–22.0N	EU083809–EU083903	95	Ke et al. 2009

Note: [1] individuals under accessions KJ630414–KJ630460 were not included in this range. [2] NH: number of haplotypes.

et al. 2013) was applied to detect fixed adaptive sites based on branches of neighbor-joining topologies. For natural selection tests, the best fitting substitution model was firstly tested using the Model Selection algorithm implemented in HYPHY package on the DataMonkey server (Kosakovsky Pond et al. 2005; Delport et al. 2010) and used in the following selection tests on the DataMonkey server. To detect putatively adaptive sites, six codon-based selection tests were applied for selection inference to the data: CODEML (Yang 2007), SLAC (single likelihood ancestor counting, Kosakovsky Pond and Frost 2005), FEL (fixed effects likelihood, Kosakovsky Pond and Frost 2005), IFEL (internal fixed effects likelihood, Kosakovsky Pond et al. 2006), FUBAR (fast unconstrained Bayesian approximation, Murrell et al. 2013) and MEME (mixed effects model of evolution, Murrell et al. 2012) algorithms. Among them, CODEML algorithm was analyzed in PAML package (Yang 2007) and SLAC, FEL, IFEL, FUBAR and MEME algorithms were implemented in HYPHY package on the DataMonkey server. All these methods were applied to prevent against our results being an artifact of a particular methodology or a set of assumptions. Positively selected sites detected in at least two tests were considered to be positively adaptive sites. Significance was assessed by posterior probability (pp) >0.9 (FUBAR) and P-value <0.05 (SLAC, FEL, IFEL and MEME).

Results and discussion

A total of 987 mitochondrial cytb complete gene sequences were downloaded from the GenBank database for intraspecific analyses (Table 1). We also downloaded 19 *Larimichthys crocea* sequences for interspecific comparison with *L. polyactis*. No positively and fixed adaptive sites were detected in *L. polyactis* and *B. pectinirostris* based on the selection tests. Conversely, positively and/or fixed adaptive sites were detected in the remaining six species, including both positively and fixed adaptive sites in *P. argenteus* (Table 1). Previous studies revealed that the population differentiation was weak in *L. polyactis*, due to a high migration ability (Xiao et al. 2009). High migration ability could facilitate population connectivity and lead to population panmixia, especially in marine realms (Moody et al. 2015). Adaptive evolution of *L. polyactis* might be impeded by the high gene flow among populations. For *B. pectinirostris*, population differentiation mainly resulted from 13 non-synonymous substitutions (sites 102, 168, 219, 249, 330, 429, 468, 489, 531, 592, 735, 828, 846). As a result, no positively or fixed adaptive sites were detected in *B. pectinirostris*. *Pampus argenteus* was the only species with both positively and fixed adaptive sites. Considering the relatively wide sampling range (samples from South China Sea, the Bay of Bengal, and the Arabian Sea), physical barriers such as the Malaya and India peninsulas might force *P. argenteus* to split into different ecotypes (Sun et al. 2012). The same results were also detected in *Engraulis encrasicolus* (Silva et al. 2014). Based on the cytb haplotype sequences in Silva et al. (2014), we identified codon 368 as the positive fixed adaptive site among *E. encrasicolus* populations. Considering the trans-equatorial sampling range, *E. encrasicolus* might also split into different ecotypes (Le Moan et al. 2016). Positive and fixed adaptive sites contribute to and largely maintain intraspecific differentiation (Pearse et al. 2014; MacPherson and Nuismer 2017; Lai et al. 2019). Our results also revealed that positively adaptive sites could be detected when genetic differentiation was weak, and that fixed adaptive sites can be detected when strong genetic differentiation occurred (Table 2). Such a conclusion is consistent with different stages of ecological speciation (Rundle and Nosil 2005; Schluter and Conte 2009; Schluter 2009). Under this process, adaptive evolution caused by natural selection acts in contrasting directions between distinct environments, which drives the fixation of different alleles each advantageous in one environment but not in the other. Population differentiation would strengthen as they accumulate a different series of mutations (Schluter and Conte 2009).

It is worth noting that codon 372 and its neighbors in cytb gene are likely favored in adaptation in the reviewed species. Codon 372 was identified as an adaptive site in four out of six species (codon 314 in *P.* sp.1 and codon 352, 371 in *A. personatus*) (Table 2). In *E. encrasicolus*, codon 368 was also identified as an adaptive site (Silva et al. 2014). Furthermore, interspecific adaptive evolution analyses were also implemented based on cytb gene sequences of *L. polyactis* (GenBank accessions: FJ609001–FJ609019) and *L. crocea* (GenBank accessions: EU346914–EU346932). Similarly, we detected codon 372 as one of the fixed adaptive sites between the two closely related species. It should be noted that the individuals collected in Sun et al. (2012) possibly contained more than one valid *Pampus* species (Li et al. 2019). Therefore, the detected positively adaptive sites in *Pampus argenteus* herein should be considered as interspecific adaptive sites, mirroring the results between *L. polyactis* and *L. crocea*. Our previous study revealed codon 372 of cytb gene in *S. marmoratus* was situated in the last transmembrane domain, which is functionally important in the energy metabolism pathways (Xu et al. 2017). For the interspecific comparison between *L. polyactis* and *L.*

Table 2. Results of adaptive evolution analyses of reviewed marine species in this study.

Species	Model	Genetic background	Purifying site[1]	Positively adaptive site[2]	Fixed adaptive site[3]
Larimichthys polyactis	012032	Weak genetic differentiation	121 codons	Undetected	Undetected
Sebastiscus marmoratus	010010	Weak genetic differentiation	Codon 287	Codon 372	Undetected
Platycephalus sp.1	010000	Weak genetic differentiation	12 codons	Codon 314	Undetected
Trachidermus fasciatus	010020	Weak genetic differentiation	26 codons	Codon 372	Undetected
Boleophthalmus pectinirostris	010010	Strong genetic differentiation	50 codons	Undetected	Undetected
Ammodytes personatus	010020	Strong genetic differentiation	143 codons	Undetected	Codon 352, 371
Pampus argenteus	010010	Strong genetic differentiation	100 codons	Codon 320, 374	Codon 4, 14, 158, 214, 233, 240, 246, 320, 327, 356, 365, 366, 372, 376
Mugil cephalus	010010	Strong genetic differentiation	42 codons	Undetected	Codon 3, 234, 239, 303, 320, 323, 369, 372

Note: [1] sites were detected under purifying selection in at least one selection test; [2] sites were detected under positive selection in at least two selection test; and [3] sites were non-synonymous substitutions and fixed in certain branches.

crocea, as *L. crocea* is better adapted than *L. polyactis* in warmer environments (Xiao et al. 2009; Xu et al. 2018), the detected interspecific substitutions might be also associated with the thermal adaptation of *L. crocea*. Therefore, codon 372 of cytb gene and its neighboring sites might be associated with metabolic processes and play important roles in thermal adaptation. Although the reviewed species are distantly related, they showed similar or identical adaptive sites in the mitochondrial cytb gene, suggesting potential genetic convergence. However, no evidence of convergent nucleotide or amino acid substitution was detected. More species and evidence (e.g., RNA-level gene expression evidence) are warranted to further confirm potential adaptive convergence. Compared to positively adaptive sites, the relatively high levels of purifying selected sites might be due to the strict functional constraints of the mitochondrial cytb gene (Sun et al. 2011), suggesting relaxed purifying selection in mitochondrial cytb gene sequences. Large numbers of genetic variations can provide fundamental sources for the evolution of population differentiation and reproductive isolation (Schluter and Conte 2009). This might be an alternative reason as to why relatively more purifying selected sites were detected in the reviewed species.

Adaptive evolution is ubiquitous. Due to environmental deviation, intraspecific differentiation would arise in distinct populations to adapt to the local environment. Adaptive evolution may also generate barriers to population connectivity and ultimately lead to further ecological differentiation (Nosil et al. 2009). For instance, strong reproductive isolation was detected in European flounders (*Platichthys flesus*) in the Baltic, which exhibit rapid ecological speciation due to salinity adaptation (Momigliano et al. 2017). However, evidence for ecological speciation in the marine realm is scarce, especially associated with reproductive isolation (Momigliano et al. 2017). In the present study, the reviewed species revealed serial stages of genetic divergence: from panmixia to strong population differentiation. By integrating genetic background information and the results of adaptive analyses, we tentatively identify four types of adaptive patterns of the reviewed species, from weak genetic differentiation to strong genetic differentiation (Table 3). It is plausible that adaptive evolution probably played an important role in maintaining and facilitating population differentiation, particularly in one of the reviewed species, *A. personatus*, of which different evolutionary lineages were sympatrically distributed (Han et al. 2012; Deng et al. 2019). Further population genomic and transcriptomic approaches are warranted to assess genome-wide adaptive patterns and demographic histories of these species.

Table 3. Summary of the four types of adaptive patterns of the reviewed species in this study.

	Genetic background	Adaptive pattern	Examples in this study
Type I	weak and non-significant genetic differentiation	Undetected	*Larimichthys polyactis*
Type II	weak but significant genetic differentiation	Detected	*Sebastiscus marmoratus*, *Platycephalus* sp.1, *Trachidermus fasciatus*
Type III	synonymous substitution inducted strong genetic differentiation	Undetected	*Boleophthalmus pectinirostris*
Type IV	non-synonymous substitution induced strong genetic differentiation	Detected	*Ammodytes personatus*, *Pampus argenteus*, *Mugil cephalus*

Acknowledgements

This work was supported by the National Key Research and Development Program of China (2017YFA0604902) and National Natural Science Foundation of China (41706187).

References

Ballard JWO, Pichaud N (2014) Mitochondrial DNA: more than an evolutionary bystander. Functional Ecology 28: 218–231. https://doi.org/10.1111/1365-2435.12177

Bryant D, Moulton V (2004) Neighbor-Net: an agglomerative method for the construction of phylogenetic networks. Molecular Biology and Evolution 21: 255–265. https://doi.org/10.1093/molbev/msh018

Caballero S, Duchêne S, Garavito MF, Slikas B, Baker CS (2015) Initial evidence for adaptive selection on the NADH subunit two of freshwater dolphins by analyses of mitochondrial genomes. PLoS ONE 10(5): e0123543. https://doi.org/10.1371/journal.pone.0123543

Chen W, Hong WS, Chen SX, Wang Q, Zhang QY. (2015) Population genetic structure and demographic history of the mudskipper *Boleophthalmus pectinirostris* on the northwestern pacific coast. Environmental Biology of Fishes 98: 845–856. https://doi.org/10.1007/s10641-014-0320-1

Delport W, Poon AFY, Frost SDW, Kosakovsky Pond SL (2010) Datamonkey 2010: a suite of phylogenetic analysis tools for evolutionary biology. Bioinformatics 26: 2455–2457. https://doi.org/10.1093/bioinformatics/btq429

Deng ZC, Xu SY, Gao TX, Han ZQ (2019) Thermal adaptation of Japanese sand lance (*Ammodytes personatus*) in different ocean currents revealed by cytochrome *b* gene. Marine and Freshwater Research 70: 1484–1491. https://doi.org/10.1071/MF18473

Forester BR, Jones MR, Joost S, Landguth EL, Lasky JR (2016) Detecting spatial genetic signatures of local adaptation in heterogeneous landscapes. Molecular Ecology 25: 104–120. https://doi.org/10.1111/mec.13476

Gao TX, Bi XX, Zhao LL, Li CJ (2013) Population genetic structure of roughskin sculpin *Trachidermus fasciatus* based on the mitochondrial *Cytb* sequence. Acta Hydrobiol Sinica 37: 199–207. [In Chinese with English abstract]

Gleason LU, Burton RS (2016) Genomic evidence for ecological divergence against a background of population homogeneity in the marine snail *Chlorostoma funebralis*. Molecular Ecology 25: 3557–3573. https://doi.org/10.1111/mec.13703

Guo XH, Liu SJ, Liu Q, Liu Y (2004) New progresses on mitochondrial DNA in fish. Acta Genetica Sinica 31: 983–1000. [In Chinese with English abstract]

Han ZQ, Yanagimoto T, Zhang Y, Gao TX (2012) Phylogeography study of *Ammodytes personatus* in northwestern Pacific: Pleistocene isolation, temperature and current conducted secondary contact. PLoS ONE 7(5): e37425. https://doi.org/10.1371/journal.pone.0037425

Huang H (2011) Morphological variation and genetic diversity of five populations of small yellow croaker (*Larimichthys polyactis*). Master thesis, Nanjing, China: Nanjing Agricultural University. [In Chinese with English abstract]

Jacobsen MW, da Fonseca RR, Bernatchez L, Hansen MM (2016) Comparative analysis of complete mitochondrial genomes suggests that relaxed purifying selection is driving high nonsynonymous evolutionary rate of the NADH2 gene in whitefish (*Coregonus* ssp.), Molecular Phylogenetics and Evolution 95: 161–170. https://doi.org/10.1016/j.ympev.2015.11.008

Ke HM, Lin WW, Kao HW (2009) Genetic diversity and differentiation of gray mullet (*Mugil cephalus*) in the coastal waters of Taiwan. Zoological Science 26: 421–429. https://doi.org/10.2108/zsj.26.421

Kosakovsky Pond SL, Frost SDW (2005) Not so different after all: a comparison of methods for detecting amino acid sites under selection. Molecular Biology and Evolution 22: 1208–1222. https://doi.org/10.1093/molbev/msi105

Kosakovsky Pond SL, Frost SDW, Grossman Z, Gravenor MB, Richman DD, Brown AJL (2006) Adaptation to different human populations by HIV-1 revealed by codon-based analyses. PLoS Computational Biology 2: e62. https://doi.org/10.1371/journal.pcbi.0020062

Kosakovsky Pond SL, Frost SDW, Muse SV (2005) HyPhy: hypothesis testing using phylogenies. Bioinformatics 21: 676–679. https://doi.org/10.1093/bioinformatics/bti079

Lai YT, Yeung CKL, Omland KE, Pang EL, Hao Y, Liao BY, Cao HF, Zhang BW, Yeh CF, Hung CM, Hung HY, Yang MY, Liang W, Hsu YC, Yao CT, Dong L, Lin K, Li SH (2019) Standing genetic variation as the predominant source for adaptation of a songbird. Proceedings of the National Academy of Sciences of the United States of America 116: 2152–2157. https://doi.org/10.1073/pnas.1813597116

Lamichhaney S, Fuentes-Pardo AP, Rafati N, Ryman N, McCracken GR, Bourne C, Singh R, Ruzzante DE, Andersson L (2017) Parallel adaptive evolution of geographically distant herring populations on both sides of the North Atlantic Ocean. Proceedings of the National Academy of Sciences of the United States of America 114: E3452–E3461. https://doi.org/10.1073/pnas.1617728114

Le Moan A, Gagnaire PA, Bonhomme F (2016) Parallel genetic divergence among coastal-marine ecotype pairs of European anchovy explained by differential introgression after secondary contact. Molecular Ecology 25: 3187–3202. https://doi.org/10.1111/mec.13627

Li Y, Zhou YD, Li PF, Gao TX, Lin LS (2019) Species identification and cryptic diversity in *Pampus* species as inferred from morphological and molecular characteristics. Marine Biodiversity 49: 2521–2534. https://doi.org/10.1007/s12526-019-00976-6

MacPherson A, Nuismer SL (2017) The probability of parallel genetic evolution from standing genetic variation. Journal of Evolutionary Biology 30: 326–337. https://doi.org/10.1111/jeb.13006

Momigliano P, Jokinen H, Fraimout A, Florin AB, Norkko A, Merilä J (2017) Extraordinarily rapid speciation in a marine fish. Proceedings of the National Academy of Sciences of the United States of America 114: 6074–6079. https://doi.org/10.1073/pnas.1615109114

Moody KN, Hunter SN, Childress MJ, Blob RW, Schoenfuss HL, Blum MJ, Ptacek MB (2015) Local adaptation despite high gene flow in the waterfall-climbing Hawaiian goby, *Sicyopterus stimpsoni*. Molecular Ecology 24: 545–563. https://doi.org/10.1111/mec.13016

Murrell B, Moola S, Mabona A, Weighill T, Sheward D, Kosakovsky Pond SL, Scheffler K (2013) FUBAR: a fast, unconstrained bayesian approximation for inferring selection. Molecular Biology and Evolution 30: 1196–1205. https://doi.org/10.1093/molbev/mst030

Murrell B, Wertheim JO, Moola S, Weighill T, Scheffler K, Kosakovsky Pond SL (2012) Detecting individual sites subject to episodic diversifying selection. PLoS Genetics 8: e1002764. https://doi.org/10.1371/journal.pgen.1002764

Nosil P, Harmon LJ, Seehausen O (2009) Ecological explanations for (incomplete) speciation. Trends in Ecology and Evolution 24: 145–156. https://doi.org/10.1016/j.tree.2008.10.011

Okonechnikov K, Golosova O, Fursov M (2012) Unipro UGENE: a unified bioinformatics toolkit. Bioinformatics 28: 1166–1167. https://doi.org/10.1093/bioinformatics/bts091

Palsbøll PJ, Berube M, Allendorf FW (2007) Identification of management units using population genetic data. Trends in Ecology and Evolution 22: 11–16. https://doi.org/10.1016/j.tree.2006.09.003

Pearse DE, Miller MR, Abadía-Cardoso A, Garza JC (2014) Rapid parallel evolution of standing variation in a single, complex, genomic region is associated with life history in steelhead/rainbow trout. Proceedings of the Royal Society B-Biological Sciences 281: 20140012. https://doi.org/10.1098/rspb.2014.0012

Postma E, van Noordwijk AJ (2005) Gene flow maintains a large genetic difference in clutch size at a small spatial scale. Nature 433: 65–68. https://doi.org/10.1038/nature03083

Ruiz-Pesini E, Mishmar D, Brandon M, Procaccio V, Wallace DC (2004) Effects of purifying and adaptive selection on regional variation in human mtDNA. Science 303: 223–226. https://doi.org/10.1126/science.1088434

Rundle HD, Nosil P (2005) Ecological speciation. Ecology Letters 8: 336–352. https://doi.org/10.1111/j.1461-0248.2004.00715.x

Schluter D, Conte GL (2009) Genetics and ecological speciation. Proceedings of the National Academy of Sciences of the United States of America 106: 9955–9962. https://doi.org/10.1073/pnas.0901264106

Schluter D, Rambaut A (1996) Ecological speciation in postglacial fishes. Philosophical Transactions of the Royal Society B-Biological Sciences 351: 807–814. https://doi.org/10.1098/rstb.1996.0075

Schluter D (2009) Evidence for ecological speciation and its alternative. Science 323: 737–741. https://doi.org/10.1126/science.1160006

Silva G, Lima FP, Martel P, Castilho R (2014) Thermal adaptation and clinal mitochondrial DNA variation of European anchovy. Proceedings of the Royal Society B-Biological Sciences 281: 20141093. https://doi.org/10.1098/rspb.2014.1093

Sun P, Shi ZH, Yin F, Peng SM (2012) Population genetic structure and demographic history of *Pampus argenteus* in the Indo-West Pacific inferred from mitochondrial cytochrome *b* sequences. Biochemical Systematics and Ecology 43: 54–63. https://doi.org/10.1016/j.bse.2012.02.028

Sun YB, Shen YY, Irwin DM, Zhang YP (2011) Evaluating the roles of energetic functional constraints on teleost mitochondrial-encoded protein evolution. Molecular Biology and Evolution 28: 39–44. https://doi.org/10.1093/molbev/msq256

Tamura K, Stecher G, Peterson D, Filipski A, Kumar S (2013) MEGA6: molecular evolutionary genetics analysis version 6.0. Molecular Biology and Evolution 30: 2725–2729. https://doi.org/10.1093/molbev/mst197

Wu RX, Liu SF, Zhuang ZM, Jin XS, Su YQ, Tang QS (2009) Population genetic structure of *Larimichthys polyactis* in Yellow Sea and East China Sea based on mitochondrial Cyt *b* gene sequences. Progress in Natural Science 19: 924–930. [In Chinese with English abstract]

Xiao YS, Zhang Y, Gao TX, Yanagimoto T, Yabe M, Sakurai Y (2009) Genetic diversity in the mtDNA control region and population structure in the small yellow croaker *Larimichthys polyactis*. Environmental Biology of Fishes 85: 303–314. https://doi.org/10.1007/s10641-009-9497-0

Xu K, Xu H, Han Z (2018) Genome-wide identification of Hsp70 genes in the large yellow croaker (*Larimichthys crocea*) and their regulated expression under cold and heat stress. Genes 9: 590. https://doi.org/10.3390/genes9120590

Xu SY, Sun DR, Song N, Gao TX, Han ZQ, Shui BN (2017) Local adaptation shapes pattern of mitochondrial population structure in *Sebastiscus marmoratus*. Environmental Biology of Fishes 100: 763–774. https://doi.org/10.1007/s10641-017-0602-5

Xu SY, Wang ZY, Zhang Y, Gao TX, Zou JW, Zhang XM (2018) Evidence for intra-mitochondrial variation in population genetic structure of *Platycephalus* sp.1 In the Northwestern Pacific. Mitochondrial DNA Part A 30: 281–288. https://doi.org/10.1080/24701394.2018.1484119

Yang ZH (2007) PAML 4: phylogenetic analysis by maximum likelihood. Molecular Biology and Evolution 24: 1586–1591. https://doi.org/10.1093/molbev/msm088

ZooKeys 974: 131–159 (2020)
doi: 10.3897/zookeys.974.56070
https://zookeys.pensoft.net

RESEARCH ARTICLE

A peer-reviewed open-access journal
ZooKeys
Launched to accelerate biodiversity research

Description of a new horned toad of *Megophrys* Kuhl & Van Hasselt, 1822 (Anura, Megophryidae) from southwest China

Haijun Su[1*], Shengchao Shi[2*], Yanqing Wu[3], Guangrong Li[4], Xiaogang Yao[4], Bin Wang[2], Shize Li[2]

1 *College of Forestry, Guizhou University, Guiyang 550002, China* **2** *Chengdu Institute of Biology, Chinese Academy of Sciences, Chengdu 610041, China* **3** *Nanjing Institute of Environmental Sciences, Ministry of Ecology and Environment of China, Nanjing 210042, China* **4** *Kuankuoshui National Nature Reserve Administration, Suiyang 563300, China*

Corresponding author: Shize Li (976722439@qq.com); Bin Wang (wangbin@cib.ac.cn)

Academic editor: Anthony Herrel | Received 1 July 2020 | Accepted 24 August 2020 | Published 7 October 2020

http://zoobank.org/42BA600C-5E98-4408-8C4E-2CC8339D582A

Citation: Su H, Shi S, Wu Y, Li G, Yao X, Wang B, Li S (2020) Description of a new horned toad of *Megophrys* Kuhl & Van Hasselt, 1822 (Anura, Megophryidae) from southwest China. ZooKeys 974: 131–159. https://doi.org/10.3897/zookeys.974.56070

Abstract

A new species of the genus *Megophrys* is described from Guizhou Province, China. Molecular phylogenetic analyses supported the new species as an independent clade nested into the *Megophrys*. The new species could be distinguished from its congeners by a combination of the following characters: body size moderate (SVL 49.3–58.2 mm in males); vomerine ridges present distinctly, vomerine teeth present; tongue feebly notched behind; tympanum distinctly visible, oval; two metacarpal tubercles in hand; toes with one-third webbing and wide lateral fringes; heels overlapped when thighs are positioned at right angles to the body; tibiotarsal articulation reaching the level between tympanum and eye when leg stretched forward; an internal single subgular vocal sac present in male; in breeding male, the nuptial pads with large and sparse black nuptial spines present on the dorsal bases of the first two fingers.

Keywords

China, molecular phylogenetic analysis, morphology, new species, taxonomy

---

* Contributed equally as the first author.

Introduction

The toad genus *Megophrys* Kuhl & Van Hasselt, 1822 (Anura; Megophryidae) is widely distributed in eastern and central China, throughout southeastern Asia, and extending to the islands of the Sunda Shelf and the Philippines (Frost 2020). The taxonomic assignments of the taxa in this group have been debated for a long time (e.g., Tian and Hu 1983; Dubois 1987; Lathrop 1997; Rao and Yang 1997; Jiang et al. 2003; Delorme et al. 2006; Fei et al. 2009; Chen et al. 2016; Fei and Ye 2016; Deuti et al. 2017; Mahony et al. 2017; Frost 2020). Regardless, molecular phylogenetic studies indicate the group as a monophyletic group (Chen et al. 2017; Mahony et al. 2017; Li et al. 2018b; Liu et al. 2018, 2020; Wang et al. 2020), and thus some studies regarded it as a large genus, *Megophrys sensu lato* (Mahony et al. 2017; Li et al. 2018b; Liu et al. 2018, 2020; Wang et al. 2020; Frost 2020) while other studies divided the taxon into different genera and subgenera (Chen et al. 2017; Fei and Ye 2016; Liu et al. 2018).

The genus *Megophrys* currently contains 106 species, of which 50 species have been described in the last decade (Frost 2020). Many cryptic species were indicated in the genus by molecular phylogenetic frameworks (Chen et al. 2017; Liu et al. 2018). In recent years, four species were described from Guizhou Province, China: *Megophrys liboensis* Zhang, Li, Xiao, Li ,Pan, Wang, Zhang & Zhou, 2017, *Megophrys leishanensis* Li, Xu, Liu, Jiang, Wei & Wang, 2018, *Megophrys jiangi* Liu, Li, Wei, Xu, Cheng, Wang & Wu, 2020, and *Megophrys chishuiensis* Xu, Li, Liu, Wei, & Wang, 2020. However, many areas have not been well investigated in this province, and it is expected that there are still cryptic species of the toads in the region.

During field surveys in the Huanglian Nature Reserve, Tongzi County, and Kuankuoshui National Nature Reserve, Suiyang County in Guizhou Province, China, we collected a number of *Megophrys* specimens. Molecular phylogenetic analyses, morphological comparisons, and bioacoustics data support it as an undescribed species.

Materials and methods

Sampling

A total of nine molecular samples were collected in this study: five adult males of the undescribed species from two localities of Guizhou Province, China, two *M. sangzhiensis* and two *M. spinata* (Table 1; Fig. 1). In the field, the toads were euthanized using isoflurane, and the specimens were fixed in 75 % ethanol. Tissue samples were taken and preserved separately in 99% ethanol prior to fixation. The specimens were deposited in Chengdu Institute of Biology, Chinese Academy of Sciences (**CIB, CAS**).

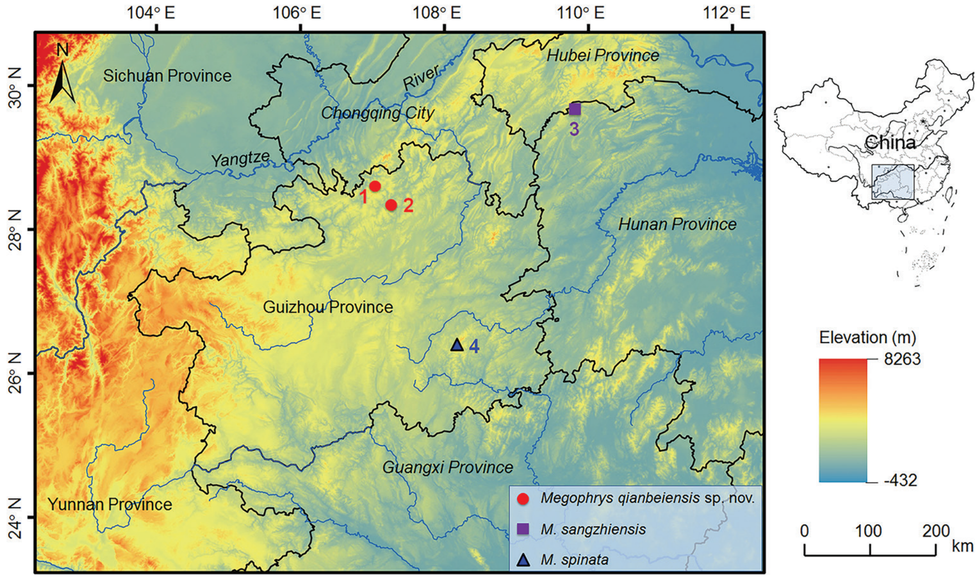

Figure 1. Sampling localities of *Megophrys qianbeiensis* sp. nov., *M. sangzhiensis* and *M. spinata* in China. 1. Huanglian Nature Reserve, Tongzi County, Guizhou Province; 2. Kuankuoshui National Nature Reserve, Suiyang County, Guizhou Province; 3. Badagong Mountain, Hunan Province, China; 4. Leigong Mountain, Guizhou Province.

Molecular data and phylogenetic analyses

Total DNA was extracted using a standard phenol-chloroform extraction protocol (Sambrook et al. 1989). Two fragments of the mitochondrial 16S rRNA (16S) and cytochromeoxidase subunit I (COI) genes were amplified. For 16S, the primers P7 (5'-CGCCTGTTTACCAAAAACAT-3') and P8 (5'-CCGGTCTGAACTCAGATCACGT-3') were used following Simon et al. (1994), and for COI, Chmf4 (5'-TYTCWACWAAYCAYAAAGAYATCGG-3') and Chmr4 (5'-ACYTCRGGRTGRCCRAARAATCA-3') were used following Che et al. (2012). Gene fragments were amplified under the following conditions: an initial denaturing step at 95 °C for 4 min; 36 cycles of denaturing at 95 °C for 30 s, annealing at 52 °C (for 16S)/47 °C (for COI) for 40 s and extending at 72 °C for 70 s. Sequencing was conducted using an ABI3730 automated DNA sequencer in Shanghai DNA BioTechnologies Co., Ltd. (Shanghai, China). New sequences were deposited in GenBank (for accession numbers see Table 1).

For molecular analyses, the available sequence data for congeners of *Megophrys* were downloaded from GenBank (Table 1), primarily from previous studies (Chen et al. 2017; Liu et al. 2018). For phylogenetic analyses, corresponding sequences of one *Leptobrachella oshanensis* (Liu, 1950) and one *Leptobrachium boringii* (Liu, 1945) were also downloaded (Table 1), and used as outgroups according to Mahony et al. (2017). Sequences were assembled and aligned using the Clustalw module in BioEdit v.7.0.9.0

Table 1. Information for samples used in molecular phylogenetic analyses in this study.

ID	Species	Voucher number	Locality	GenBank accession number	
				16S	COI
1	*Megophrys qianbeiensis* sp. nov.	CIBTZ20190608015	Huanglian Nature Reserve, Guizhou, China	MT651553	MT654520
2	*Megophrys qianbeiensis* sp. nov.	CIBTZ20190608017	Huanglian Nature Reserve, Guizhou, China	MT651554	MT654521
3	*Megophrys qianbeiensis* sp. nov.	CIBTZ20160715003	Huanglian Nature Reserve, Guizhou, China	MT651555	MT654522
4	*Megophrys qianbeiensis* sp. nov.	CIBKKS20180722002	Huanglian Nature Reserve, Guizhou, China	MT651556	MT654523
5	*Megophrys qianbeiensis* sp. nov.	CIBKKS20180722001	Kuankuoshui Nature Reserve, Guizhou, China	MT651557	MT654524
6	*Megophrys sangzhiensis*	CIBSZ2012062005	Badagongshan Nature Reserve, Hunan, China	MT651558	MT654525
7	*Megophrys sangzhiensis*	CIBSZ2012062008	Badagongshan Nature Reserve, Hunan, China	MT651559	MT654526
8	*Megophrys sangzhiensis*	SYSa004307	Zhangjiajie, Hunan, China	MH406798	MH406260
9	*Megophrys spinata*	CIBLS20190801001	Leigong Shan, Guizhou, China	MT651551	MT654518
10	*Megophrys spinata*	CIBLS20190801002	Leigong Shan, Guizhou, China	MT651552	MT654519
11	*Megophrys spinata*	SYSa002227	Leigong Shan, Guizhou, China	MH406676	MH406116
12	*Megophrys binlingensis*	KIZ025807	Wawu Shan, Sichuan, China	KX811852	KX812115
13	*Megophrys binlingensis*	SYSa005313	Wawu Shan, Sichuan, China	MH406892	MH406354
14	*Megophrys binlingensis*	SYSa005314	Wawu Shan, Sichuan, China	MH406893	MH406355
15	*Megophrys binchuanensis*	KIZ019441	Jizu Shan, Yunnan, China	KX811849	KX812112
16	*Megophrys palpebralespinosa*	KIZ011603	Pu Hu Nature Reserve, Thanh Hoa, Vietnam	KX811888	KX812137
17	*Megophrys omeimontis*	KIZ025765	Emei Shan, Sichuan, China	KX811884	KX812136
18	*Megophrys angka*	KIZ040591	Kiew Mae Pan nature trail, Chiang Mai, Thailand	MN508052	–
19	*Megophrys wuliangshanensis*	KIZ046812	Huangcaoling, Yunnan, China	KX811881	KX812129
20	*Megophrys daweimontis*	KIZ048997	Dawei Shan, Yunnan, China	KX811867	KX812125
21	*Megophrys jingdongensis*	KIZ-LC0805067	Huanglianshan National Nature Reserve, Yunnan, China	KX811872	KX812131
22	*Megophrys fansipanensis*	VNMN 2018.01	Lao Cai, Sa Pa, Vietnam	MH514886	–
23	*Megophrys hoanglienensis*	VNMN 2018.02	Lao Cai, Sa Pa, Vietnam	MH514889	–
24	*Megophrys minor*	KIZ01939	Qingcheng Shan, Sichuan, China	KX811896	KX812145
25	*Megophrys jiangi*	CIBKKS20180722006	Kuankuosui Nature Reserve, Guizhou, China	MN107743	MN107748
26	*Megophrys chishuiensis*	CIBCS20190518031	Chishui Nature Reserve, Guizhou, China	MN954707	MN928958
27	*Megophrys dongguanensis*	SYS a001972	Yinping Shan, Guangdong, China	MK524098	MK524129
28	*Megophrys nankunensis*	SYS a004498	Nankun Shan, Guangdong, China	MK524108	MK524139
29	*Megophrys cheni*	SYS a001427	Jinggang Shan, Jiangxi, China	KJ560391	–
30	*Megophrys obesa*	SYS a002272	Heishiding Nature Reserve, Guangdong, China	KJ579122	–
31	*Megophrys ombrophila*	KRM18	Wuyishan, Fujian, China	KX856404	–
32	*Megophrys wugongensis*	SYS a002610	Wugongshan Scenic Area, Jiangxi, China	MK524114	MK524145
33	*Megophrys lini*	SYS a002370	Suichuan, Jiangxi, China	KJ560412	–
34	*Megophrys xiangnanensis*	SYS a002874	Yangming Shan, Hunan, China	MH406713	MH406165
35	*Megophrys nanlingensis*	SYS a001959	Nanling Nature Reserve, Guangdong, China	MK524111	MK524142
36	*Megophrys kuatunensis*	SYS a001579	Wuyi Shan, Fujian, China	KJ560376	–
37	*Megophrys jinggangensis*	KIZ07132	Chashan Forest Farm, Jiangxi, China	KX811840	KX812108
38	*Megophrys lishuiensis*	WYF00169	Lishui, Zhejiang, China	KY021418	–
39	*Megophrys xianjuensis*	CIBXJ190505	Xianju, Zhejiang, China	MN563753	MN563769
40	*Megophrys wushanensis*	KIZ045469	Guangwu Shan, Sichuan, China	KX811838	KX812094
41	*Megophrys baolongensis*	KIZ019216	Baolong, Chongqing, China	KX811813	KX812093
42	*Megophrys leishanensis*	CIBLS20171101001	Leigong Shan, Guizhou, China	MK005310	MK005306
43	*Megophrys yangmingensis*	SYS a002877	Yangming Shan, Hunan, China	MH406716	MH406168
44	*Megophrys shimentaina*	SYS a002077	Shimentai Nature Reserve, Guangdong, China	MH406655	MH406092
45	*Megophrys jiulianensis*	SYS a002107	Jiulian Shan, Jiangxi, China	MK524099	MK524130
46	*Megophrys shunhuangensis*	HNNU16SH02	Shunhuang Mountains, Hunan, China	MK836037	–
47	*Megophrys mirabilis*	SYS a002192	Huaping Nature Reserve, Guangxi, China	MH406669	MH406109
48	*Megophrys tuberogranulata*	Tissue ID: YPX10987	Badagongshan Nature Reserve, Hunan, China	KX811823	KX812095
49	*Megophrys huangshanensis*	KIZ022004	Huang Shan, Anhui, China	KX811821	KX812107
50	*Megophrys boettgeri*	Tissue ID: YPXJK033	Wuyi Shan, Fujian, China	KX811814	KX812104
51	*Megophrys liboensis*	GNUG:20160408003	Libo, Guizhou, China	MF285262	–
52	*Megophrys mufumontana*	SYS a006391	Mufu Shan, Hunan, China	MK524105	MK524136
53	*Megophrys brachykolos*	ROM 16634	Hong Kong, China	KX811897	KX812150
54	*Megophrys acuta*	SYS a001957	Heishiding Nature Reserve, Guangdong, China	KJ579118	–
55	*Megophrys gerti*	ITBCZ 1108	Nui Chua National Park, Ninh Thuan, Vietnam	KX811917	KX812161
56	*Megophrys elfina*	ZMMU ABV-00454	Bidoup Mountain, Lam Dong, Vietnam	KY425379	–

ID	Species	Voucher number	Locality	GenBank accession number	
				16S	COI
57	*Megophrys synoria*	FMNH 262778	O'Reang, Mondolkiri, Cambodia	KY022198	–
58	*Megophrys hansi*	KIZ010360	Phong Dien Nature Reserve, Thua Thien Hue, Vietnam	KX811913	KX812155
59	*Megophrys microstoma*	KIZ048799	Xiaoqiaogou Nature Reserve, Yunnan, China	KX811914	KX812156
60	*Megophrys pachyproctus*	KIZ010978	Beibeng, Xizang, China	KX811908	KX812153
61	*Megophrys baluensis*	ZMH A13125	Gunung Kinabalu National Park, Kogopan Trail, Malaysia	KJ831310	–
62	*Megophrys stejnegeri*	KU 314303	Pasonanca Natural Park, Zamboanga, Philippines	KX811922	KX812052
63	*Megophrys ligayae*	ZMMU NAP-05015	Palawan, Philippines	KX811919	KX812051
64	*Megophrys kobayashii*	UNIMAS 8148	Gunung Kinabalu National Park, Sabah, Malaysia	KJ831313	–
65	*Megophrys nasuta*	KIZ019419	Malaysia	KX811921	KX812054
66	*Megophrys edwardinae*	FMNH 273694	Bintulu, Sarawak, Malaysia	KX811918	KX812050
67	*Megophrys aceras*	KIZ025467	Khao Nan National Park, Nakhon Si Thammarat, Thailand	KX811925	KX812159
68	*Megophrys dringi*	UNIMAS 8943	Gunung Mulu National Park, Sarawak, Malaysia	KJ831317	–
69	*Megophrys maosonensis*	KIZ016045	Xiaoqiaogou Nature Reserve, Yunnan, China	KX811780	KX812080
70	*Megophrys mangshanensis*	KIZ021786	Nanling National Forest Park, Guangdong, China	KX811790	KX812079
71	*Megophrys flavipunctata*	SDBDU2009.297	East Khasi Hills dist., Meghalaya	KY022307	MH647536
72	*Megophrys glandulosa*	KIZ048439	Husa, Yunnan, China	KX811762	KX812075
73	*Megophrys medogensis*	KIZ06621	Beibeng, Xizang, China	KX811767	KX812082
74	*Megophrys periosa*	BNHS 6061	West Kameng dist., Arunachal Pradesh, IN	KY022309	MH647528
75	*Megophrys himalayana*	SDBDU2009.75	East Siang dist., Arunachal Pradesh, IN	KY022311	–
76	*Megophrys sanu*	K5198/ZSI11393	–	KX894679	–
77	*Megophrys zhangi*	KIZ014278	Zhangmu, Xizang, China	KX811765	KX812084
78	*Megophrys katabhako*	ZSIA11799	–	KX894669	–
79	*Megophrys major*	SYSa002961	Zhushihe, Yunnan, China	MH406728	MH406180
80	*Megophrys oreocrypta*	BNHS 6046	West Garo Hills dist., Meghalaya	KY022306	–
81	*Megophrys auralensis*	NCSM 79599	Aural, Kampong Speu, Cambodia	KX811807	–
82	*Megophrys parva*	SYSa003042	Zhushihe, Yunnan, China	MH406737	MH406189
83	*Megophrys nankiangensis*	CIB ZYC517	Nanjiang, Sichuan, China	KX811900	–
84	*Megophrys wawuensis*	KIZ025799	Wawu Shan, Sichuan, China	KX811902	KX812062
85	*Megophrys gigantica*	SYSa003933	Wuliang shan, Yunnan, China	MH406775	MH406235
86	*Megophrys shapingensis*	KIZ014512	Liziping Nature Reserve, Sichuan, China	KX811904	KX812060
87	*Megophrys montana*	LSUMZ 81916	Sukabumi, Java, Indonesia	KX811927	KX812163
88	*Megophrys lancip*	MZB:Amp:22233	–	KY679891	–
89	*Megophrys feae*	KIZ046706	Huangcaoling, Yunnan, China	KX811810	KX812056
90	*Megophrys chuannanensis*	CIB20050081	Hejiang, Sichuan, China	KM504261	–
91	*Megophrys carinense*	Tissue ID: YPX20455	Dayao Shan, Guangxi, China	KX811811	KX812057
92	*Megophrys popei*	SYS a000589	Naling Nature Reserve, Guangdong, China	KM504251	–
93	*Megophrys intermedia*	ZFMK 87596	U Bo, Phong Nha-Ke Bang NP, Vietnam	HQ588950	–
94	*Leptobrachium boringii*	Tissue ID: YPX37539	Emei Shan, Sichuan, China	KX811930	KX812164
95	*Leptobrachella oshanensis*	KIZ025778	Emei Shan, Sichuan, China	KX811928	KX812166

(Hall 1999) with default settings. Alignments were checked by eye and revised manually if necessary. For phylogenetic analyses of mitochondrial DNA, the dataset concatenated with 16S and COI gene sequences. To avoid under- or over-parameterization (Lemmon and Moriarty 2004; McGuire et al. 2007), the best partition scheme and the best evolutionary model for each partition were chosen for the phylogenetic analyses using PARTITIONFINDER v. 1.1.1 (Robert et al. 2012). In this analysis, 16S gene and each codon position of COI gene were defined, and Bayesian Inference Criteria was used. As a result, the analysis suggested that the best partition scheme is16S gene/each codon position of COI gene, and selected GTR + G + I model as the best model for each partition. Phylogenetic analyses were conducted using maximum likelihood (ML) and Bayesian Inference (BI) methods, implemented in PhyML v. 3.0 (Guindon et al. 2010) and MrBayes v. 3.12 (Ronquist and Huelsenbeck 2003), respectively. For the ML tree, branch supports were drawn from 10,000 nonparametric bootstrap replicates. In BI, two runs each with four Markov chains were simultaneously run for 50 million generations with sampling every 1,000 generations. The first 25 % trees were removed as the "burn-in" stage followed by calculations of Bayesian posterior probabilities and the 50% majority-rule consensus of the post burn-in trees sampled at stationarity.

Morphological comparisons

In total, 16 specimens including six males of the undescribed species, five males of *M. sangzhiensis*, and five males of *M. spinata* were measured (for voucher information see Table 2). The terminology and methods followed Fei et al. (2009). Measurements were taken with a dial caliper to 0.1 mm. Twenty-one morphometric characters of adult specimens were measured:

ED	eye diameter (distance from the anterior corner to the posterior corner of the eye);
FL	foot length (distance from tarsus to the tip of fourth toe);
HDL	head length (distance from the tip of the snout to the articulation of jaw);
HDW	maximum head width (greatest width between the left and right articulations of jaw);
HLL	hindlimb length (maximum length from the vent to the distal tip of the Toe IV);
IAE	distance between posterior corner of eyes;
IFE	distance between anterior corner of eyes;
IND	internasal distance (minimum distance between the inner margins of the external nares);
IOD	interorbital distance (minimum distance between the inner edges of the upper eyelids);
LAL	length of lower arm and hand (distance from the elbow to the distal end of the Finger IV);
LW	lower arm width (maximum width of the lower arm);
NED	nasal to eye distance (distance between the nasal and the anterior corner of the eye);
NSD	nasal to snout distance (distance between the nasal the posterior edge of the vent);
SVL	snout-vent length (distance from the tip of the snout to the posterior edge of the vent);
SL	snout length (distance from the tip of the snout to the anterior corner of the eye);
TFL	length of foot and tarsus (distance from the tibiotarsal articulation to the distal end of the Toe IV);
THL	thigh length (distance from vent to knee);
TL	tibia length (distance from knee to tarsus);
TW	maximal tibia width;
TYD	maximal tympanum diameter;
UEW	upper eyelid width (greatest width of the upper eyelid margins measured perpendicular to the anterior-posterior axis).

Table 2. Measurements of the adult specimens of *Megophrys qianbeiensis* sp. nov., *M. spinata*, and *M. sangzhiensis*. Units are given in mm. See abbreviations for the morphological characters in Materials and methods section.

Species	Voucher number	Sex	SVL	HDL	HDW	SL	NED	NSD	IND	IOD	ED	UEW	LAL	LW	HLL	THL	TL	TW	TFL	FL	TYD	IFE	IAE
Megophrys qianbeiensis sp. nov.	CIBTZ20190608016	male	58.2	16.5	21.0	6.7	2.7	3.9	7.5	5.1	6.9	6.2	25.0	6.7	89.3	27.9	32.4	8.2	40.7	28.2	4.3	10.1	16.4
Megophrys qianbeiensis sp. nov.	CIBTZ20190608018	male	55.1	14.9	20.6	6.9	3.0	4.0	7.0	4.2	6.5	5.1	25.0	6.5	93.0	28.4	30.6	8.7	44.0	29.1	3.5	9.0	16.0
Megophrys qianbeiensis sp. nov.	CIBTZ20190608017	male	56.3	14.6	19.2	7.2	3.2	3.6	6.7	4.3	6.5	5.3	24.0	6.9	87.0	27.6	28.0	7.8	38.3	25.7	3.2	10.9	15.0
Megophrys qianbeiensis sp. nov.	CIBTZ20160715003	male	54.1	17.0	20.8	6.9	3.4	3.7	6.3	4.5	6.9	6.0	25.4	5.7	93.7	27.0	30.8	7.8	43.7	29.4	3.5	10.4	15.8
Megophrys qianbeiensis sp. nov.	CIBTZ20190608015	male	52.6	15.3	19.4	6.8	2.4	4.3	6.9	3.7	5.9	5.5	24.1	7.4	86.9	24.1	28.3	8.3	41.4	28.0	3.3	10.0	15.7
Megophrys qianbeiensis sp. nov.	CIBKKS20180722001	male	49.3	15.5	18.3	6.8	3.0	3.5	5.7	5.3	5.4	5.3	20.4	6.6	76.9	24.5	25.0	7.0	34.5	24.5	3.4	7.8	14.0
M. spinata	CIBLS20190801002	male	56.2	14.9	18.4	6.0	3.0	3.4	5.8	4.2	5.1	6.1	24.2	5.5	93.7	27.4	29.9	6.1	40.8	28.6	2.7	9.1	14.0
M. spinata	CIBLS20190801004	male	53.5	14.5	19.1	7.1	2.8	4.1	6.0	5.0	5.7	5.0	24.1	5.9	99.0	29.8	30.4	8.0	43.1	28.1	2.8	9.6	14.4
M. spinata	CIBLS20190801001	male	54.8	14.6	18.6	6.7	2.8	3.9	6.0	4.8	5.8	4.5	24.3	6.1	87.7	27.6	28.9	7.0	39.7	26.4	2.8	9.2	14.2
M. spinata	CIBLS20190801003	male	51.2	14.3	18.8	6.6	2.9	3.6	6.1	5.2	6.0	5.1	25.1	6.5	93.0	26.1	29.6	7.7	41.6	29.6	2.5	9.1	14.0
M. spinata	CIBLS20160610008	male	53.8	15.8	18.4	5.7	2.7	3.8	6.3	5.3	5.5	4.5	24.0	7.4	85.7	26.9	29.0	6.0	39.2	27.9	2.9	8.5	14.3
M. sangzhiensis	CIBSZ2012062005	male	59.8	17.8	20.6	7.2	3.1	4.1	7.3	4.8	7.1	5.7	26.6	6.6	105.0	31.6	32.6	7.8	46.1	29.4	3.1	10.4	16.1
M. sangzhiensis	CIBSZ2012062008	male	58.8	17.8	21.5	7.6	3.0	4.4	7.3	4.7	7.4	6.1	26.8	6.2	97.3	30.3	31.6	7.8	42.9	26.7	3.4	10.9	17.3
M. sangzhiensis	CIBSZ2012062006	male	59.5	16.1	21.0	8.2	3.5	4.6	7.7	5.0	6.7	6.1	26.6	6.3	99.8	27.9	32.3	7.3	43.8	29.2	3.4	10.1	17.3
M. sangzhiensis	CIBSZ2012062019	male	57.4	18.0	20.9	7.3	3.5	3.7	6.8	5.0	6.4	5.1	26.2	6.1	99.5	30.2	32.6	8.1	43.2	29.9	3.7	10.4	17.3
M. sangzhiensis	CIBSZ2012062007	male	56.1	16.1	20.0	6.6	3.9	4.1	6.9	5.8	6.1	5.7	28.2	6.7	100.0	28.0	32.0	7.5	44.9	29.4	3.4	9.4	16.2

In order to reduce the impact of allometry, the correct value from the ratio of each character to SVL was calculated, and then was log-transformed for subsequent morphometric analyses. One-way analysis of variance (ANOVA) was used to test the significance of differences on morphometric characters between different species. The significance level was set at 0.05. To show the spatial distribution of different species on the morphometric characters, principal component analyses (PCA) were performed. These analyses were carried out in the R (R Development Core Team 2008). The new species was also compared with all other *Megophrys* species on morphology. Comparative data were obtained from related species as described in literature (Table 3).

Table 3. References for morphological characters for congeners of the genus *Megophrys*.

Species	Literature
M. aceras Boulenger, 1903	Boulenger 1903
M. acuta Wang, Li & Jin, 2014	Li et al. 2014
M. ancrae Mahony, Teeling & Biju, 2013	Mahony et al. 2013
M. angka Wu, Suwannapoom, Poyarkov, Chen, Pawangkhanant, Xu, Jin, Murphy & Che, 2019	Wu et al. 2019
M. auralensis Ohler, Swan & Daltry, 2002	Ohler et al. 2002
M. baluensis (Boulenger, 1899)	Boulenger 1899a
M. baolongensis Ye, Fei & Xie, 2007	Ye et al. 2007
M. binchuanensis Ye & Fei, 1995	Ye and Fei 1995
M. binlingensis Jiang, Fei & Ye, 2009	Fei et al. 2009
M. boettgeri (Boulenger, 1899)	Boulenger 1899b
M. brachykolos Inger & Romer, 1961	Inger and Romer 1961
M. carinense (Boulenger, 1889)	Boulenger 1889
M. caobangensis Nguyen, Pham, Nguyen, Luong, & Ziegler, 2020	Nguyen et al. 2020
M. caudoprocta Shen, 1994	Shen. 1994
M. cheni (Wang & Liu, 2014)	Wang et al. 2014
M. chishuiensis Xu, Li, Liu, Wei & Wang, 2020	Xu et al. 2020
M. chuannanensis (Fei, Ye & Huang, 2001)	Fei et al. 2001
M. damrei Mahony, 2011	Mahony 2011
M. daweimontis Rao & Yang, 1997	Rao and Yang 1997
M. dongguanensis Wang & Wang, 2019	Wang et al. 2019b
M. dringi Inger, Stuebing & Tan, 1995	Inger et al. 1995
M. edwardinae Inger, 1989	Inger 1989
M. elfina Poyarkov, Duong, Orlov, Gogoleva, Vassilieva, Nguyen, Nguyen, Nguyen, Che & Mahony, 2017	Poyarkov et al. 2017
M. fansipanensis Tapley, Cutajar, Mahony, Nguyen, Dau, Luong, Le, Nguyen, Nguyen, Portway, Luong & Rowley, 2018	Tapley et al. 2018
M. feae Boulenger, 1887	Boulenger 1887
M. feii Yang, Wang & Wang, 2018	Yang et al. 2018
M. flavipunctata Mahony, Kamei, Teeling & Biju, 2018	Mahony et al. 2018
M. gerti (Ohler, 2003)	Ohler 2003
M. gigantica Liu, Hu & Yang, 1960	Liu et al. 1960
M. glandulosa Fei, Ye & Huang, 1990	Fei et al. 1990
M. hansi (Ohler, 2003)	Ohler 2003
M. himalayana Mahony, Kamei, Teeling & Biju, 2018	Mahony et al. 2018
M. hoanglienensis Tapley, Cutajar, Mahony, Nguyen, Dau, Luong, Le, Nguyen, Nguyen, Portway, Luong & Rowley, 2018	Tapley et al. 2018
M. huangshanensis Fei & Ye, 2005	Fei and Ye 2005
M. insularis (Wang, Liu, Lyu, Zeng & Wang, 2017)	Wang et al. 2017a
M. intermedia Smith, 1921	Smith 1921
M. jiangi Liu, Li, Wei, Xu, Cheng, Wang & Wu, 2020	Liu et al. 2020
M. jingdongensis Fei & Ye, 1983	Fei et al. 1983
M. jinggangensis (Wang, 2012)	Wang et al. 2012
M. jiulianensis Wang, Zeng, Lyu & Wang, 2019	Wang et al. 2019b
M. kalimantanensis Munir, Hamidy, Matsui, Iskandar, Sidik & Shimada, 2019	Munir et al. 2019
M. kobayashii Malkmus & Matsui, 1997	Malkmus and Matsui 1997

Species	Literature
M. koui Mahony, Foley, Biju & Teeling, 2017	Mahony et al. 2017
M. kuatunensis Pope, 1929	Pope 1929
M. lancip Munir, Hamidy, Farajallah & Smith, 2018	Munir et al. 2018
M. leishanensis Li, Xu, Liu, Jiang, Wei & Wang, 2018	Li et al. 2018b
M. lekaguli Stuart, Chuaynkern, Chan-ard & Inger, 2006	Stuart et al. 2006
M. liboensis (Zhang, Li, Xiao, Li, Pan, Wang, Zhang & Zhou, 2017)	Zhang et al. 2017
M. ligayae Taylor, 1920	Taylor 1920
M. lini (Wang & Yang, 2014)	Wang et al. 2014
M. lishuiensis (Wang, Liu & Jiang, 2017)	Wang et al. 2017b
M. longipes Boulenger, 1886	Boulenger 1886
M. major Boulenger, 1908	Boulenger 1908
M. mangshanensis Fei & Ye, 1990	Fei et al. 2012
M. maosonensis Bourret, 1937	Bourret 1937
M. medogensis Fei, Ye & Huang, 1983	Fei et al. 1983
M. megacephala Mahony, Sengupta, Kamei & Biju, 2011	Mahony et al. 2011
M. microstoma (Boulenger, 1903)	Boulenger 1903
M. minor Stejneger, 1926	Stejneger 1926
M. mirabilis Lyu, Wang & Zhao, 2020	Lyu et al. 2020
M. montana Kuhl & Van Hasselt, 1822	Kuhl and Van Hasselt 1822
M. monticola (Günther, 1864)	Günther 1864
M. mufumontana Wang, Lyu & Wang, 2019	Wang et al. 2019b
M. nankiangensis Liu & Hu, 1966	Hu and Liu 1966
M. nankunensis Wang, Zeng & Wang, 2019	Wang et al. 2019b
M. nanlingensis Lyu, Wang, Liu & Wang, 2019	Wang et al. 2019b
M. nasuta (Schlegel, 1858)	Schlegel 1858
M. obesa Wang, Li & Zhao, 2014	Wang et al. 2014
M. ombrophila Messenger & Dahn, 2019	Messenger et al. 2019
M. omeimontis Liu, 1950	Liu 1950
M. oreocrypta Mahony, Kamei, Teeling & Biju, 2018	Mahony et al. 2018
M. oropedion Mahony, Teeling & Biju, 2013	Mahony et al. 2013
M. orientalis Li, Lyu, Wang & Wang, 2020	Li et al. 2020
M. pachyproctus Huang, 1981	Huang and Fei 1981
M. palpebralespinosa Bourret, 1937	Bourret 1937
M. parallela Inger & Iskandar, 2005	Inger and Iskandar 2005
M. parva (Boulenger, 1893)	Boulenger 1893
M. periosa Mahony, Kamei, Teeling & Biju, 2018	Mahony et al. 2018
M. popei (Zhao, Yang, Chen, Chen & Wang, 2014)	Zhao et al. 2014
M. robusta Boulenger, 1908	Boulenger 1908
M. rubrimera Tapley, Cutajar, Mahony, Chung, Dau, Nguyen, Luong & Rowley, 2017	Tapley et al. 2017
M. sangzhiensis Jiang, Ye & Fei, 2008	Jiang et al. 2008
M. serchhipii (Mathew & Sen, 2007)	Mathew and Sen 2007
M. shapingensis Liu, 1950	Liu 1950
M. shimentaina Lyu, Liu & Wang, 2020	Lyu et al. 2020
M. shuichengensis Tian & Sun, 1995	Tian and Sun 1995
M. shunhuangensis Wang, Deng, Liu, Wu & Liu, 2019	Wang et al. 2019a
M. spinata Liu & Hu, 1973	Hu et al. 1973
M. stejnegeri Taylor, 1920	Taylor 1920
M. synoria (Stuart, Sok & Neang, 2006)	Stuart et al. 2006
M. takensis Mahony, 2011	Mahony 2011
M. tuberogranulata Shen, Mo & Li, 2010	Mo et al. 2010
M. vegrandis Mahony, Teeling, Biju, 2013	Mahony et al. 2013
M. wawuensis Fei, Jiang & Zheng, 2001	Fei et al. 2012
M. wugongensis Wang, Lyu & Wang, 2019	Wang et al. 2019b
M. wuliangshanensis Ye & Fei, 1995	Ye and Fei 1995
M. wushanensis Ye & Fei, 1995	Ye and Fei 1995
M. xianjuensis Wang, Wu, Peng, Shi, Lu & Wu, 2020	Wang et al. 2020
M. xiangnanensis Lyu, Zeng & Wang, 2020	Lyu et al. 2020
M. yangmingensis Lyu, Zeng & Wang, 2020	Lyu et al. 2020
M. zhangi Ye & Fei, 1992	Ye and Fei 2012
M. zunhebotoensis (Mathew & Sen, 2007)	Mathew and Sen 2007

Bioacoustics analyses

The advertisement calls of the undescribed species were recorded from the holotype specimen CIBTZ20190608017 in a stream at ambient air temperature of 20.5 °C and air humidity of 87 % in the field on 8 June 2019 in Huanglian Nature Reserve, Tongzi County, Guizhou Province, China. The advertisement calls of *M. sangzhiensis* were recorded from the specimen CIBSZ2012062005 in a stream at ambient air temperature of 18.5 °C and air humidity of 85 % in the field on 20 June 2012 in Sangzhi County, Hunan Province, China. The advertisement calls of *M. spinata* were recorded from the specimen CIBLS20190801001 in a stream at ambient air temperature of 19.0 °C and air humidity of 85 % in the field on 1 August 2019 in Leishan County, Guizhou Province, China. SONY PCM-D50 digital sound recorder was used to record within 20 cm of the calling individual. The sound files in wave format were resampled at 48 kHz with sampling depth 24 bits. The sonograms and waveforms were generated by WaveSurfer software (Sjöander and Beskow 2000) from which all parameters and characters were measured. Ambient temperature was taken by a digital hygrothermograph.

Results

Phylogenetic analyses

Aligned sequence matrix of 16S+COI contains 1104 bp. ML and BI trees had almost consistent topology though relationships of some lineages were unresolved (Fig. 2). In trees, the undescribed species was clustered as an independent clade and sister to a clade in comprising of *M. sangzhiensis* and *M. spinata* (Fig. 2).

Genetic distances on COI gene with uncorrected *p*-distance model between all samples of the undescribed species were below 0.2%. The genetic distance between the undescribed species and its closest related species *M. sangzhiensis* was 4.3 % on COI gene, which was higher or at the same level with those among many pairs of congeners, for example, 3.6 % between *M. spinata* and *M. sangzhiensis*, 1.8% between *M. huangshanensis* and *M. boettgeri*, and 4.3 % between *M. maosonensis* and *M. mangshanensis* (Suppl. material 1: Table S1).

Morphological comparisons

In PCA for males, the total variation of the first two principal components was 63.2 %. In males on the two-dimensional plots of PC1 vs. PC2, the undescribed species could be distinctly separated from *M. sangzhiensis* and *M. spinata* (Fig. 3). The results of one-way ANOVA indicated that in males, the undescribed species was significantly different from *M. sangzhiensis* and *M. spinata* on many morphometric characters (all *p*-values < 0.05; Table 4). More detailed descriptions of results from morphological comparisons between the undescribed species and its congeners were presented in the following sections for describing the new species.

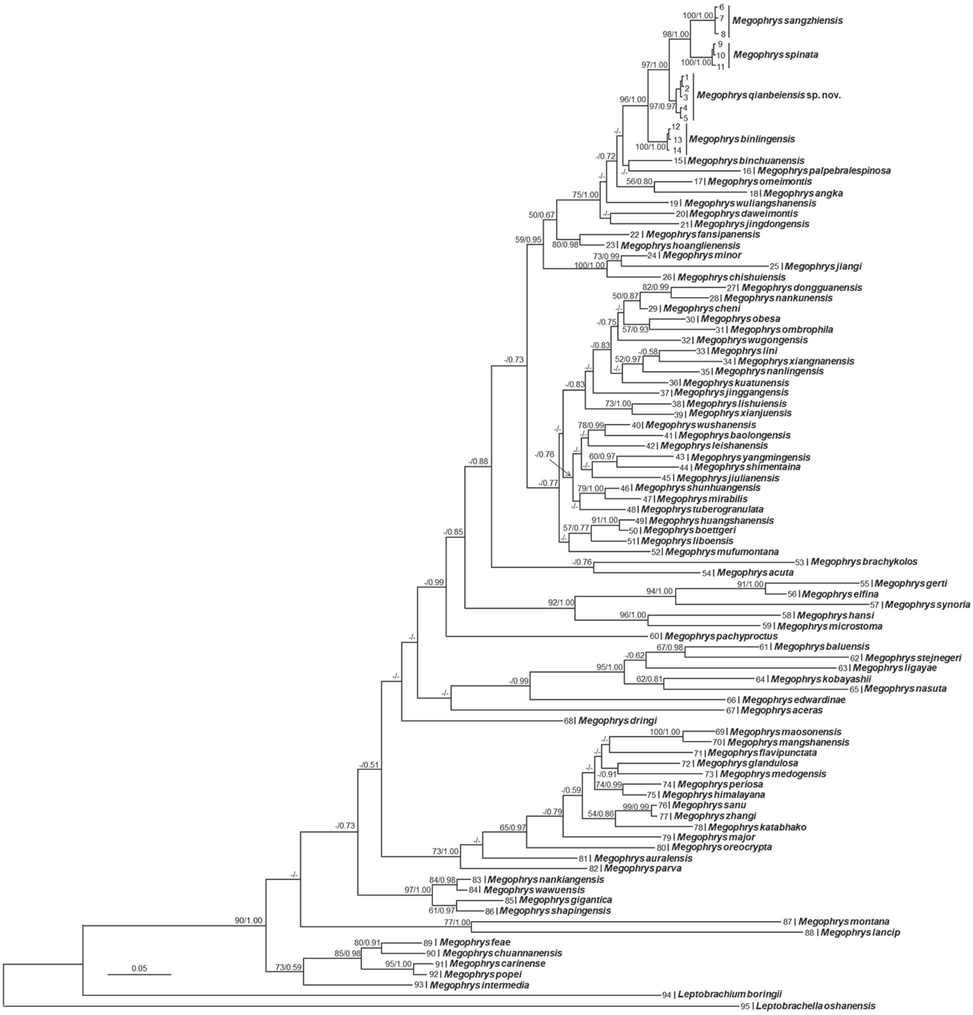

Figure 2. Bayesian Inference (BI) tree of the genus *Megophrys* reconstructed based on the 16S rRNA and COI gene sequences. Bayesian posterior probability resulted from BI analyses/ML bootstrap supports from Maximum Likelihood analyses were denoted beside each node. Samples 1–90 refer to Table 1.

Bioacoustics comparisons

There were many differences in sonograms and waveforms of calls between the undescribed species, *M. sangzhiensis*, and *M. spinata* (Fig. 4; Table 5). Firstly, in the note interval, the undescribed species were shorter than those of both *M. sangzhiensis* and *M. spinata*. Secondly, the dominant frequency of call in the undescribed species was lower than both of *M. sangzhiensis* and *M. spinata*. Thirdly, the amplitude of the undescribed species beginning with moderately high energy pulses, increasing slightly to a maximum by approximately mid note, and then decreasing towards the end of each note, in *M. sangzhiensis* beginning with maximum energy pulses and then decreasing towards the end of note, and in *M. spinata* beginning with lower energy pulses, then

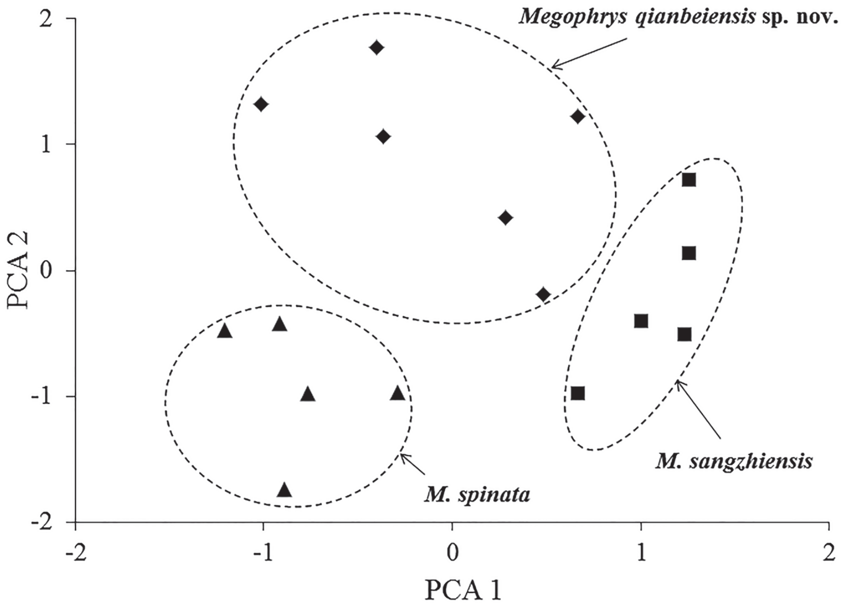

Figure 3. Plots of the first principal component (PCA1) versus the second (PCA2) for *Megophrys qianbeiensis* sp. nov., *M. sangzhiensis*, and *M. spinata* from principal component analyses.

Table 4. Morphometric comparisons between *Megophrys qianbeiensis* sp. nov., *M. sangzhiensis*, and *M. spinata*. Units given in mm. Abbreviations for the species name: MQ, *Megophrys qianbeiensis* sp. nov.; MSZ, *M. sangzhiensis*; MSP, *M. spinata*. See abbreviations for morphometric characters in Materials and methods section.

	***Megophrys qianbeiensis* sp. nov.**		***M. sangzhiensis***		***M. spinata***		***p*-value from ANOVA in male**	
	males (N = 6)		**males (N = 5)**		**males (N = 5)**			
	Range	**Mean ± SD**	**Range**	**Mean ± SD**	**Range**	**Mean ± SD**	**MQ vs. MSZ**	**MQ vs. MSP**
SVL	49.3–58.2	54.3 ± 3.09	56.1–59.8	58.3 ± 1.56	51.2–56.2	53.9 ± 1.84	0.029	0.851
HDL	14.6–17.0	15.6 ± 0.93	16.1–18.0	17.2 ± 0.96	14.3–15.8	14.8 ± 0.59	0.027	0.124
HDW	18.3–21.0	19.9 ± 1.08	20.0–21.5	20.8 ± 0.55	18.4–19.1	18.7 ± 0.30	0.123	0.037
SL	6.7–7.2	6.9 ± 0.17	6.6–8.2	7.4 ± 0.58	5.7–7.1	6.4 ± 0.56	0.067	0.085
TYD	3.2–4.3	3.5 ± 0.39	3.1–3.7	3.4 ± 0.21	2.5–2.9	2.7 ± 0.15	0.639	0.001
IFE	7.8–10.9	9.7 ± 1.13	9.4–10.9	10.2 ± 0.54	8.5–9.6	9.1 ± 0.39	0.340	0.348
IAE	14.0–16.4	15.5 ± 0.86	16.1–17.3	16.8 ± 0.62	14.0–14.4	14.2 ± 0.18	0.019	0.009
NED	2.4–3.4	2.9 ± 0.36	3.0–3.9	3.4 ± 0.36	2.7–3.0	2.8 ± 0.11	0.060	0.618
NSD	3.5–4.3	3.8 ± 0.29	3.7–4.6	4.2 ± 0.34	3.4–4.1	3.8 ± 0.27	0.101	0.683
IND	5.7–7.5	6.7 ± 0.62	6.8–7.7	7.2 ± 0.34	5.8–6.3	6.0 ± 0.18	0.150	0.056
IOD	3.7–5.3	4.5 ± 0.59	4.7–5.8	5.1 ± 0.45	4.2–5.3	4.9 ± 0.44	0.117	0.257
ED	5.4–6.9	6.3 ± 0.58	6.1–7.4	6.7 ± 0.51	5.1–6.0	5.6 ± 0.34	0.280	0.041
UEW	5.1–6.2	5.6 ± 0.43	5.1–6.1	5.7 ± 0.42	4.5–6.1	5.0 ± 0.65	0.484	0.126
LAL	20.4–25.4	24.0 ± 1.84	26.2–28.2	26.9 ± 0.78	24.0–25.1	24.3 ± 0.44	0.014	0.654
LW	5.7–7.4	6.6 ± 0.55	6.1–6.7	6.4 ± 0.24	5.5–7.4	6.3 ± 0.72	0.394	0.364
HLL	76.9–93.7	87.8 ± 6.07	97.3–105.0	100.3 ± 2.84	85.7–99.0	91.8 ± 5.27	0.003	0.280
THL	24.1–28.4	26.6 ± 1.82	27.9–31.6	29.6 ± 1.59	26.1–29.8	27.6 ± 1.38	0.019	0.343
TL	25.0–32.4	29.2 ± 2.63	31.6–32.6	32.2 ± 0.42	28.9–30.4	29.6 ± 0.63	0.038	0.713
TW	7.0–8.7	8.0 ± 0.58	7.3–8.1	7.7 ± 0.32	6.0–8.0	7.0 ± 0.91	0.404	0.053
TFL	34.5–44.0	40.4 ± 3.58	42.9–46.1	44.2 ± 1.32	39.2–43.1	40.9 ± 1.55	0.062	0.761
FL	24.5–29.4	27.5 ± 1.95	26.7–29.9	28.9 ± 1.28	26.4–29.6	28.1 ± 1.16	0.201	0.531

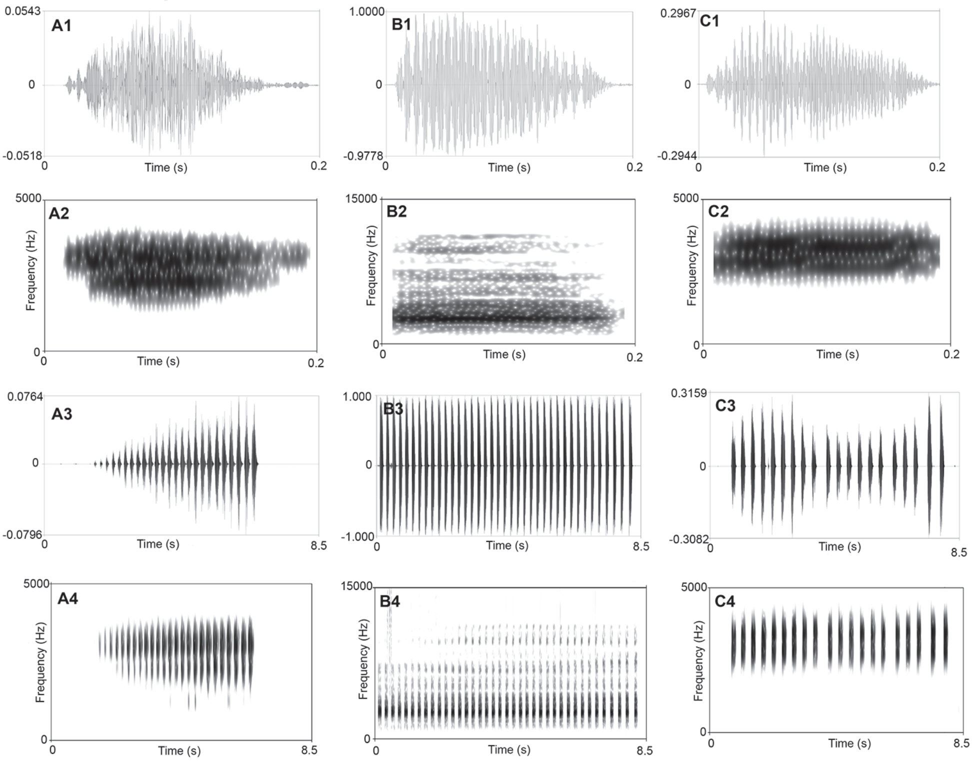

Figure 4. Visualization of advertisement calls of *Megophrys qianbeiensis* sp. nov., *M. sangzhiensis*, and *M. spinata* **A1** waveform showing one note of *Megophrys qianbeiensis* sp. nov. **A2** sonogram showing one note of *Megophrys qianbeiensis* sp. nov. **A3** waveform showing 25 notes of one call of *Megophrys qianbeiensis* sp. nov. **A4** sonogram showing 25 notes of one call of *Megophrys qianbeiensis* sp. nov. **B1** waveform showing one note of *M. sangzhiensis* **B2** sonogram showing one note of *M. sangzhiensis* **B3** waveform showing 38 notes of one call of *M. sangzhiensis*. **B4** sonogram showing 38 notes of one call of *M. sangzhiensis* **C1** waveform showing one note of *M. spinata* **C2** sonogram showing one note of *M. spinata* **C3** waveform showing 20 notes of one call of *M. spinata* **C4** sonogram showing 20 notes of one call of *M. spinata*.

Table 5. Comparisons of characteristics of advertisement calls of *Megophrys qianbeiensis* sp. nov., *M. sangzhiensis*, and *M. spinata*.

Call character	***Megophrys qianbeiensis* sp. nov.**		***M. sangzhiensis***		***M. spinata***	
	Range	**Mean ± SD**	**Range**	**Mean ± SD**	**Range**	**Mean ± SD**
Number of notes in a call	14–26	22.5 ± 4.4	38	/	7–28	17 ± 7.92
Call duration (ms)	2832–5621	4413 ± 972	8152	/	1500–6623	3905 ± 2010
Call interval (ms)	6812–14387	10878 ± 2701	/	/	592–5770	2708 ± 1863.33
Note duration (ms)	129– 211	167 ± 0.02	107–155	120.3 ± 8.73	107–123	114 ± 3.79
Note interval (ms)	34–94	57 ± 0.01	72–132	95.6 ± 13.89	113–232	147 ± 33.12
Dominant frequency (Hz)	2250–3000	2469 ± 197.47	10380–13200	11795 ± 670.58	4260–4589	4416 ± 130.04
Temperature (°C)	20.5		18.5		19.0	

increasing to the maximum by approximately one-four note and then decreasing to the mid note then increasing to the second highest energy pulses and then decreasing towards the end of note.

Taxonomic accounts

***Megophrys qianbeiensis* sp. nov.**

http://zoobank.org/C6C89A51-8178-4C7B-A100-80C0D2D42AD3
Figures 4A1–C1, 5, 6A1–A6, 7; Tables 1, 2, 4, 5, Suppl. material 2: Table S2

Type material. *Holotype.* CIBTZ20190608017 (Figs 5, 6), adult male, from Huanglian Nature Reserve, Tongzi County, Guizhou Province, China (28.498056°N, 107.046944°E, ca. 1500 m a.s.l.), collected by Shi-Ze Li 8 June 2019.

Paratype. Four adult males from the same place as holotype, and one from Kuankuoshui National Nature Reserve (28.21835°N, 107.166388°E, ca.1520 m a.s.l.) collected by Shi-Ze Li. CIBKKS20180722001 collected 22 July 2018 from Kuankuoshui National Nature Reserve and CIBTZ20160715003 collected 15 July 2016, CIBTZ20190608015, CIBTZ20190608016 and CIBTZ20190608018 collected 8 June 2019 from Kuankuoshui National Nature Reserve.

Diagnosis. *Megophrys qianbeiensis* sp. nov. is assigned to the genus *Megophrys* based on molecular phylogenetic analyses and the following generic diagnostic characters: snout shield-like; projecting beyond the lower jaw; canthus rostralis distinct; chest glands small and round, closer to the axilla than to midventral line; femoral glands on rear part of thigh; vertical pupils.

Megophrys qianbeiensis sp. nov. could be distinguished from its congeners by a combination of the following morphological characters: body size moderate (SVL 49.3–58.2 mm in males); vomerine ridges present distinctly, vomerine teeth present; tongue feebly notched behind; tympanum distinctly visible, oval; two metacarpal tubercles in hand; toes with one-third webbing and wide lateral fringes; heels overlapped when thighs are positioned at right angles to the body; tibiotarsal articulation reaching the level between tympanum and eye when leg stretched forward; an internal single subgular vocal sac present in male; in breeding male, the nuptial pads with large and sparse black nuptial spines present on the dorsal bases of the first two fingers.

Description of holotype. (Figs 5, 6). SVL 56.3 mm; head width larger than head length (HDW/HDL ratio ca. 1.3); snout obtusely pointed, protruding well beyond the margin of the lower jaw in ventral view; loreal region vertical and concave; canthus rostralis well-developed; top of head flat in dorsal view; eye large, eye diameter 44.5 % of head length; pupils vertical; nostril orientated laterally, closer to snout than eye; tympanum distinct, TYP/EYE ratio 0.49; vomerine ridges present distinctly as V-shape, vomerine teeth present; margin of tongue smooth, feebly notched behind.

Forelimbs slender, the length of lower arm and hand 42.6 % of SVL; fingers burly, relative finger lengths: II < I < V < III; tips of digits globular, without lateral fringes; subarticular tubercle distinct at the base of each finger; two metacarpal tubercles, prominent, oval-shaped, the inner one bigger than the outer one.

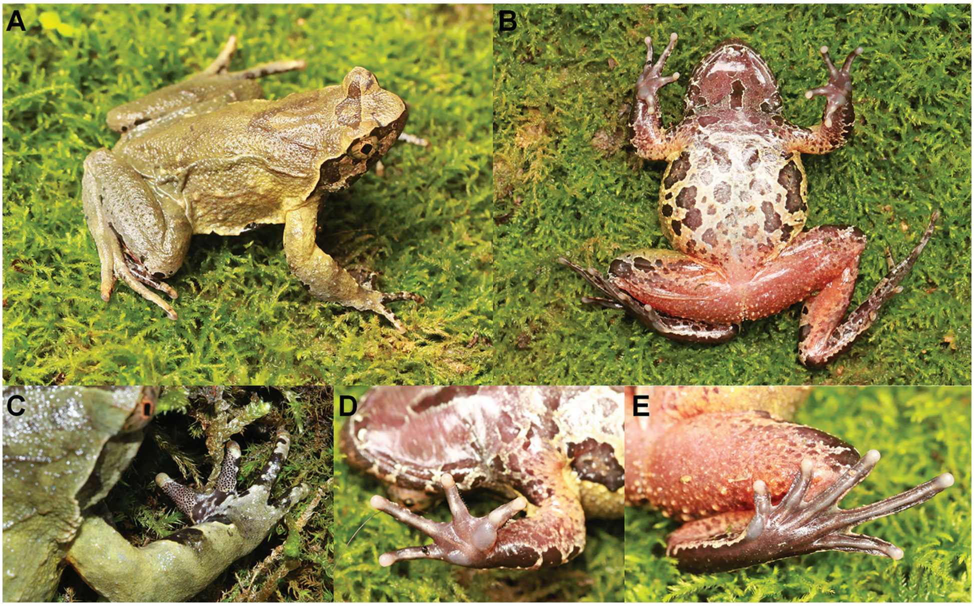

Figure 5. Photos of the holotype CIBTZ20190608017 of *Megophrys qianbeiensis* sp. nov. in life **A** dorsal view **B** ventral view **C** dorsal view of hand **D** ventral view of hand **E** ventral view of foot.

Hindlimbs slender, 1.54 times of SVL; heels overlapping when thighs are positioned at right angles to the body, tibiotarsal articulation reaching tympanum to eye when leg stretched forward; tibia length longer than thigh length; relative toe lengths I < II < V < III < IV; tips of toes round, slightly dilated; subarticular tubercles present on the base of each toes ; toes with one-third webbing and relative wide lateral fringe; inner metatarsal tubercle oval-shaped; outer metatarsal tubercle absent.

Dorsal skin rough, with numerous granules with black spins; several large warts scattered on flanks; tubercles on the dorsum forming a weak V-shaped ridge; two discontinuous dorsolateral parallel ridges on either side of the V-shaped ridges; an inverted triangular brown speckle between two upper eyelids; several tubercles on the flanks and dorsal surface of thighs and tibias; supratympanic fold distinct.

Ventral surface smooth with numerous white granules; glands on chest indistinct; femoral glands on rear of thighs, numerous white granules on outer thighs; posterior end of the body distinctly protruding and forming an arc-shaped swelling above the anal region.

Coloration of holotype in life (Fig. 5). An inverted triangular brown speckle between the eyes; V-shaped ridges on the dorsum with brown speckle, on transverse bands on the dorsal surface of the thigh and shank; several dark brown and white vertical bars on the lower and upper lip; belly whitish grey with dark brown marbling; ventral surface of posterior limb orange with numerous granules; palms, soles and tip of digits uniform purple grey; femoral glands white.

Coloration of holotype in preservation (Fig. 6). Color of dorsal surface fades to brownness; the inverted triangular brown speckle between the eyes and V-shaped ridges on dorsum indistinct; ventral surface greyish white; creamy-white substitutes

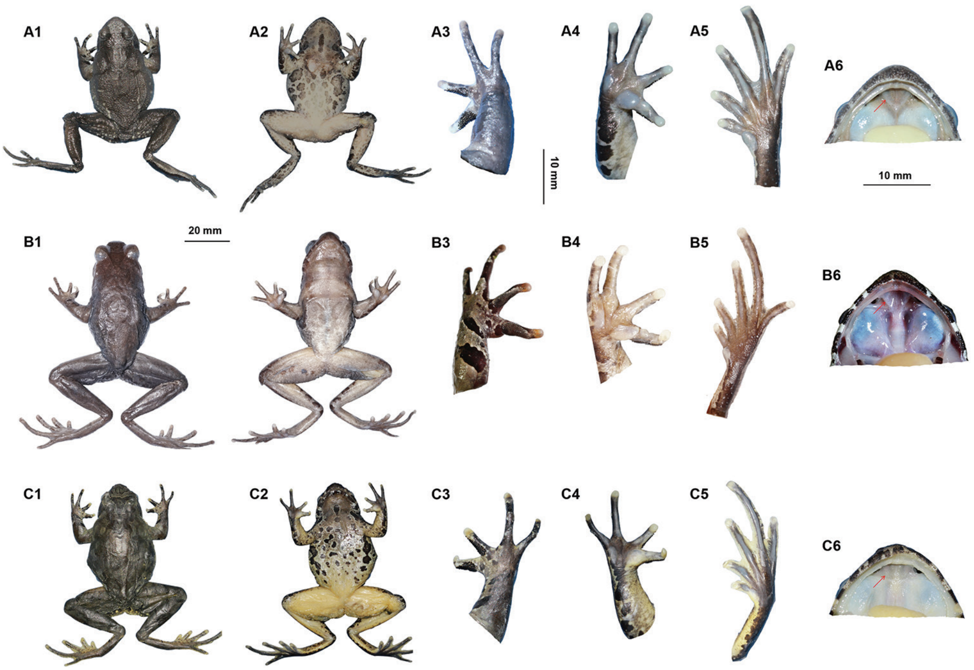

Figure 6. Photos of specimens of *Megophrys qianbeiensis* sp. nov., *M. sangzhiensis* and *M. spinata* **A1–A6** dorsal view, ventral view, dorsal view of hand, ventral view of hand, ventral view of foot and view of oral cavity of the holotype specimen CIBTZ20190608017 of *Megophrys qianbeiensis* sp. nov. **B1–B6** dorsal view, ventral view, dorsal view of hand, ventral view of hand, ventral view of foot and view of oral cavity of CIBSZ2012062005 of *M. sangzhiensis* **C1–C6** dorsal view, ventral view, dorsal view of hand, ventral view of hand, ventral view of foot and view of oral cavity of CIBLS20190801001 of *M. spinata*. Arrow point to vomerine ridge.

the purple grey on tip of digits; the posterior of ventral surface of body, inner of thigh and upper of tibia fades to creamy-white.

Variation. In CIBTZ20160715003 the dorsolateral parallel ridges are short, just a little bit above the shoulder (Fig. 7A); in CIBTZ20190608015 the X-shaped marking on back of trunk consists of a ridge with brown spots (Fig. 7B) and the posterior belly are orange with black spots on the flank belly (Fig. 7C); in CIBKKS20180722001 the belly is grey brown with some white spots (Fig. 7D).

Advertisement call. The call description is based on recordings of the holotype CIBTZ20190608017 (Fig. 4) from the shrub leaf near the streamlet, and the ambient air temperature was 20.5 °C. Each call consists of 14–26 (mean 22.5 ± 4.4, $N = 6$) notes. Call duration was 2832–5621 ms (mean 4413 ± 972, $N = 6$). Call interval was 6812–14387 ms (mean 10878 ± 2701, $N = 5$). Each note had a duration of 129–211 ms (mean 167 ± 0.02, $N = 135$) and the intervals between notes 34–94 ms (mean 57 ± 0.01, $N = 128$). Amplitude modulation within note was apparent, beginning with moderately high energy pulses, increasing slightly to a maximum by approximately mid note, and then decreasing towards the end of each note. The average dominant frequency was 2469 ± 197.47 (2250–3000 Hz, $N = 6$).

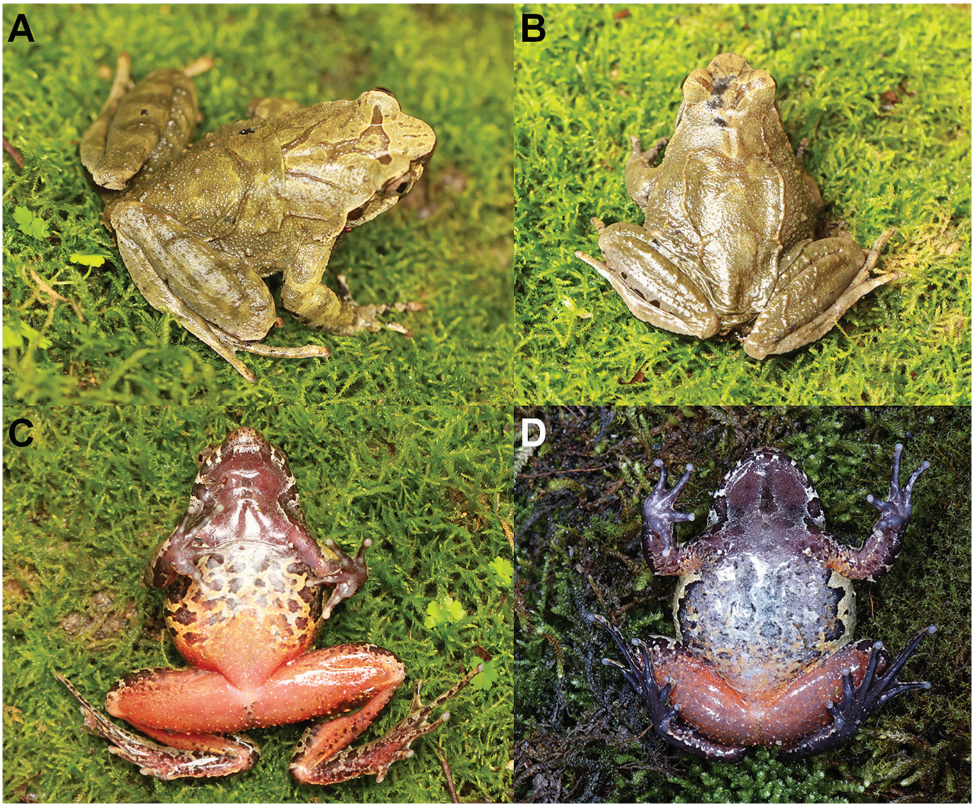

Figure 7. Color variation in *Megophrys qianbeiensis* sp. nov. **A** dorsolateral view of the specimen CIBTZ20160715003 **B** dorsolateral view of the specimen CIBTZ20190608015 **C** ventral view of the male specimen CIBTZ20190608015 **D** ventral view of the specimen CIBKKS20180722001.

Secondary sexual characters. Adult males have a single subgular vocal sac. In breeding males, brownish red nuptial pads are present on the dorsal bases of the first two fingers with big and sparse black nuptial spines (Fig. 5A).

Comparisons. By having moderate body size (minimum SVL > 49.8 mm in males), *Megophrys qianbeiensis* sp. nov. differs from *M. aceras*, *M. acuta*, *M. angka*, *M. ancrae*, *M. baluensis*, *M. baolongensis*, *M. binchuanensis*, *M. binlingensis*, *M. boettgeri*, *M. brachykolos*, *M. caobangensis*, *M. cheni*, *M. daweimontis*, *M. dongguanensis*, *M. dringi*, *M. edwardinae*, *M. elfina*, *M. fansipanensis*, *M. feii*, *M. gerti*, *M. hansi*, *M. hoanglienensis*, *M. huangshanensis*, *M. insularis*, *M. jiangi*, *M. jinggangensis*, *M. jiulianensis*, *M. kuatunensis*, *M. lancip*, *M. leishanensis*, *M. lini*, *M. lishuiensis*, *M. longipes*, *M. major*, *M. microstoma*, *M. minor*, *M. monticola*, *M. mufumontana*, *M. nankunensis*, *M. nanlingensis*, M. *obesa*, *M. ombrophila*, *M. oropedion*, *M. pachyproctus*, *M. palpebralespinosa*, *M. parallela*, *M. parva*, *M. rubrimera*, *M. serchhipii*, *M. shimentaina*, *M. shunhuangensis*, *M. tuberogranulata*, *M. vegrandis*, *M. wawuensis*, *M. wugongensis*, *M. wuliangshanensis*, *M. wushanensis*, *M. xianjuensis*, *M. zhangi*, *M. zunhebotoensis*, *M. xiangnanensis*, and *M. yangmingensis* (vs. minimum SVL < 48.0 mm).

By having moderate body size (minimum SVL < 59.0 mm in males), *Megophrys qianbeiensis* sp. nov. differs from *M. auralensis*, *M. carinense*, *M. caudoprocta*, *M. caudoprocta*, *M. chuannanensis*, *M. feae*, *M. gigantica*, *M. glandulosa*, *M. himalayana*, *M. kalimantanensis*, *M. kobayashii*, *M. ligayae*, *M. mangshanensis*, *M. orientalis*, *M. periosa*, *M. platyparietus*, *M. popei*, *M. shapingensis*, and *M. shuichengensis* (vs. minimum SVL > 60.0 mm).

By having vomerine teeth, *Megophrys qianbeiensis* sp. nov. differs from *M. aceras*, *M. acuta*, *M. angka*, *M. auralensis*, *M. baolongensis*, *M. binchuanensis*, *M. binlingensis*, *M. boettgeri*, *M. brachykolos*, *M. caobangensis*, *M. cheni*, *M. chishuiensis*, *M. dringi*, *M. jiangi* , *M. leishanensis*, *M. lini* , *M. lishuiensis*, *M. major* , *M. microstoma*, *M. minor*,. *M. mirabilis*, *M. mufumontana*, *M. nankiangensis*, *M. obesa*, *M. ombrophila*, *M. shapingensis*, *M. shuichengensis*, *M. shunhuangensis*, *M. tuberogranulata*, *M. vegrandis*, *M. wawuensis*, *M. wugongensis*, *M. wuliangshanensis*, *M. wushanensis*, *M. xianjuensis*, *M. xiangnanensis*, and *M. yangmingensis* (vs. absent).

By the absence of horn-like tubercle at the edge of each upper eyelid, *Megophrys qianbeiensis* sp. nov. differs from *M. aceras*, *M. acuta*, *M. angka*, *M. ancrae*, *M. auralensis*, *M. baluensis*, *M. baolongensis*, *M. boettgeri*, *M. brachykolos*, *M. caobangensis*, *M. carinense*, *M. caudoprocta*, *M. cheni*, *M. chishuiensis*, *M. chuannanensis*, *M. daweimontis*, *M. dongguanensis*, *M. dringi*, *M. edwardinae*, *M. elfina*, *M. fansipanensis*, *M. feae*, *M. feii*, *M. flavipunctata*, *M. gerti*, *M. glandulosa*, *M. hansi*, *M. himalayana*, *M. hoanglienensis*, *M. huangshanensis*, *M. insularis*, *M. intermedia*, *M. jiangi*, *M. jingdongensis*, *M. jinggangensis*, *M. jiulianensis*, *M. kalimantanensis*, *M. koui*, *M. kuatunensis*, *M. lancip*, *M. leishanensis*, *M. lekaguli*, *M. liboensis*, *M. ligayae*, *M. lini*, *M. lishuiensis*, *M. longipes*, *M. mangshanensis*, *M. medogensis*, *M. microstoma*, *M. mirabilis*, *M. montana*, *M. mufumontana*, *M. nankunensis*, *M. nanlingensis*, *M. nasuta*, *M. obesa*, *M. ombrophila*, *M. omeimontis*, *M. oreocrypta*, *M. orientalis*, *M. palpebralespinosa*, *M. parallela*, *M. parva*, *M. periosa*, *M. platyparietus*, *M. popei*, *M. rubrimera*, *M. shimentaina*, *M. shuichengensis*, *M. shunhuangensis*, *M. stejnegeri*, *M. synoria*, *M. vegrandis*, *M. wugongensis*, *M. xianjuensis*, *M. xiangnanensis*, and *M. yangmingensis* (vs. present).

With the tongue feebly notched behind, *Megophrys qianbeiensis* sp. nov. differs from *M. aceras*, *M. acuta*, *M. angka*, *M. auralensis*, *M. brachykolos*, *M. caobangensis*, *M. caudoprocta*, *M. dongguanensis*, *M. elfina*, *M. hansi*, *M. jiangi*, *M. jinggangensis*, *M. lancip*, *M. leishanensis*, *M. lekaguli*, *M. lini*, *M. lishuiensis*, *M. megacephala*, *M. mufumontana*, *M. nankunensis*, *M. obesa*, *M. ombrophila*, *M. orientalis*, *M. palpebralespinosa*, *M. parallela*, *M. parva*, *M. shunhuangensis*, *M. takensis*, *M. wushanensis*, and *M. xianjuensis* (vs. tongue not notched behind in the latter), and differs from *M. cheni*, *M. damrei*, *M. dringi*, *M. flavipunctata*, *M. gigantica*, and *M. popei* (vs. tongue notched behind).

By having lateral wide fringes on toes, *Megophrys qianbeiensis* sp. nov. differs from *M. angka*, *M. baolongensis*, *M. brachykolos*, *M. caobangensis*, *M. damrei*, *M. daweimontis*, *M. dongguanensis*, *M. fansipanensis*, *M. feae*, *M. himalayana*, *M. hoanglienensis*, *M. huangshanensis*, *M. insularis*, *M. jiangi*, *M. jiulianensis*, *M. kalimantanensis*, *M. koui*, *M. leishanensis*, *M. lekaguli*, *M. lishuiensis*, *M. major*, *M. mangshanensis*, *M. medogensis*, *M. megacephala*, *M. microstoma*, *M. minor*, *M. nankunensis*, *M. obesa*, *M. ombrophila*, *M. oreocrypta*, *M. oropedion*, *M. pachyproctus*, *M. parva*, *M. periosa*, *M. shunhuangensis*, *M. takensis*, *M. tuberogranulata*, *M. wawuensis*, *M. wugongensis*, *M. wuliangshanensis*, and *M. xianjuensis* (vs. lacking lateral fringes on toes).

By toes with one-third webs, *Megophrys qianbeiensis* sp. nov. differs from *M. aceras*, *M. acuta*, *M. angka*, *M. auralensis*, *M. baluensis*, *M. baolongensis*, *M. binchuanensis*, *M. binlingensis*, *M. boettgeri*, *M. brachykolos*, *M. caobangensis*, *M. caudoprocta*, *M. cheni*, *M. chuannanensis*, *M. damrei*, *M. daweimontis*, *M. dongguanensis*, *M. dringi*, *M. elfina*, *M. fansipanensis*, *M. feae*, *M. feii*, *M. flavipunctata*, *M. gerti*, *M. gigantica*, *M. glandulosa*, *M. hansi*, *M. hoanglienensis*, *M. huangshanensis*, *M. insularis*, *M. jiangi*, *M. jinggangensis*, *M. jiulianensis*, *M. kalimantanensis*, *M. koui*, *M. kuatunensis*, *M. lancip*, *M. leishanensis*, *M. lekaguli*, *M. liboensis*, *M. lini*, *M. lishuiensis*, *M. longipes*, *M. major*, *M. mangshanensis*, *M. medogensis*, *M. medogensis*, *M. megacephala*, *M. microstoma*, *M. minor*, *M. mufumontana*, *M. nankiangensis*, *M. nankunensis*, *M. nanlingensis*, *M. obesa*, *M. ombrophila*, *M. omeimontis*, *M. oropedion*, *M. pachyproctus*, *M. parva*, *M. periosa*, *M. robusta*, *M. rubrimera*, *M. serchhipii*, *M. shunhuangensis*, *M. takensis*, *M. tuberogranulata*, *M. vegrandis*, *M. wawuensis*, *M. wugongensis*, *M. wuliangshanensis*, *M. wushanensis*, *M. xianjuensis*, and *M. zhangi* (vs. with rudimentary or without webs).

By heels overlapping when thighs are positioned at right angles to the body, *Megophrys qianbeiensis* sp. nov. differs from *M. acuta*, *M. brachykolos*, *M. dongguanensis*, *M. huangshanensis*, *M. kuatunensis*, *M. nankunensis*, *M. obesa*, *M. ombrophila*, and *M. wugongensis* (vs. not meeting).

By the tibiotarsal articulation reaching to the level between tympanum and eye when leg stretched forward, *Megophrys qianbeiensis* sp. nov. differs from *M. daweimontis*, *M. glandulosa*, *M. lini*, *M. major*, *M. medogensis*, and *M. obesa* (vs. reaching the anterior corner of the eye or beyond eye or nostril and tip of snout).

By having an internal single subgular vocal sac in male, *Megophrys qianbeiensis* sp. nov. differs from *M. caudoprocta*, *M. shapingensis*, and *M. shuichengensis* (vs. vocal sac absent).

The congeners *M. carinense* and *M. jiangi* have sympatric distribution with *Megophrys qianbeiensis* sp. nov. (Fei et al. 2012). The new species can be distinguished from these species by a series of morphological characters as follows. The new species differs from *M. carinense* in the smaller body size in the new species (adult males with 49.3–58.2 mm vs. adult males with 92–123 mm in the latter), a horn-like tubercle at the edge of each upper eyelid absent (vs. prominent in the latter), the tongue feebly notched behind (vs. notched behind in the latter). The new species differs from *M. jiangi* by a larger body size (49.3–58.2 mm in males in the new species vs. 34.4–39.2 mm in the latter), a horn-like tubercle at the edge of each upper eyelid absent (vs. present in the latter), the tongue feebly notched behind (vs. notched behind in the latter), presence of wide lateral fringes on the toes (vs. lacking in the latter), and toes with one-third webbing (vs. rudimentary webbing in the latter).

Megophrys qianbeiensis sp. nov. is phylogenetically closest to *M. sangzhiensis* and *M. spinata*. The new species differs from *M. sangzhiensis* by the following characters: horn-like tubercle absent at the edge of each upper eyelid (vs. present in the latter), toes with one-third webs (vs. with rudimentary webbing in the latter), vomerine ridges present distinctly as V-shape and vomerine teeth present (vs. vomerine ridges separated and weak, vomerine teeth absent in the latter), tibiotarsal articulation reaching to the level between tympanum and eye when leg stretched forward (vs. reaching the anterior corner of eye in the latter), spines on nuptial pads on the first two fingers larger and sparser (vs. finer and thicker in the latter), and having significantly higher ratios of HDL, LAL, HLL, TL, and IAE to SVL. On bioacoustics, the new species differs from *M. sangzhiensis* in the following characters: lower dominant frequency (2250–3000 Hz in the new species vs. 10380 – 13200 Hz in the latter), the amplitude beginning with moderately high energy pulses, increasing slightly to a maximum by approximately mid note, and then decreasing towards the end of each note (vs. beginning with maximum energy pulses and then decreasing towards the end of note in the latter).

The new species differs from *M. spinata* by the following characters: tibiotarsal articulation reaching the level between tympanum to eye when leg stretched forward (vs. reaching the anterior corner of eye in the latter), present distinctly as V-shape and vomerine teeth present (vs. vomerine ridges separated and weak, vomerine teeth absent in the latter), spines on nuptial pads on the first two fingers little weaker (vs. spines larger in the latter), and having significantly higher ratios of HDW, ED, LAL, TYD and IAE to SVL. On bioacoustics, the new species differs from *M. spinata* in the following characters: lower dominant frequency (2250–3000 Hz in the new species vs. 4260–4589 Hz in the latter), the amplitude beginning with moderately high energy pulses, increasing slightly to a maximum by approximately mid note, and then decreasing towards the end of each note (vs. beginning with lower energy pulses, then increasing to the maximum by approximately one-four note and then decreasing to the mid note then increasing to the second highest energy pulses and then decreasing towards the end of note in the latter).

Distribution and habitats. *Megophrys qianbeiensis* sp. nov. is known from Huanglian Nature Reserve, Tongzi County and Kuankuoshui National Nature Reserve, Suiyang County, Guizhou Province, China at elevations between 1400–1600 m. The individuals of the new species were frequently found on stone in the streams surrounded by evergreen broadleaved forests (Fig. 8), and three sympatric amphibian species were found, i.e., *Megophrys jiangi*, *Odorrana margaratae* (Liu, 1950), and *Zhangixalus omeimontis* (Stejneger, 1924).

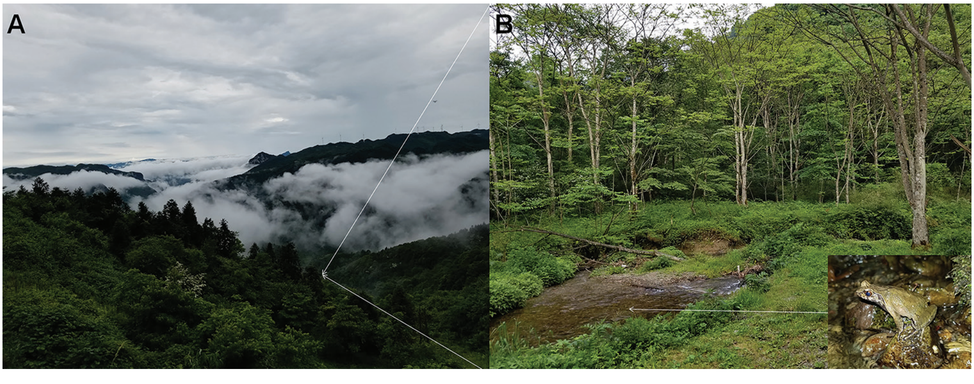

Figure 8. Habitats of *Megophrys qianbeiensis* sp. nov. in the type locality, Huanglian Nature Reserve, Tongzi County, Guizhou Province, China **A** landscape of montane forests in the type locality **B** a mountain stream where toads of the new species live (*insert* the holotype CIBTZ20190608017standing on the stone).

Etymology. The specific epithet *qianbeiensis* refers to northern part of Guizhou, also called "黔", the province where the type locality of the species belongs to. We propose the common English name "Qianbei horned toad" and Chinese name "Qian Bei Jiao Chan (黔北角蟾)".

Discussion

The new species *Megophrys qianbeiensis* sp. nov. resembles *M. spinata* and *M. sangzhiensis*, and detailed comparisons with different data are important for recognizing them. Our molecular phylogenetic data on mitochondrial DNA and morphological comparisons both separated the new species from the two closely related species. *Megophrys spinata* were reported to be distributed widely through the provinces of Sichuan, Guizhou, Hunan, Chongqing, Yunnan, and Guangxi (Fei et al. 2012), but detailed investigations with multiple data suggested that several populations of the species should contain cryptic species (including *Megophrys qianbeiensis* sp. nov. and *M. sangzhiensis*). In recent years, many new species of the genus *Megophrys* have been gradually described, of which a large part of number was found in China (Frost 2020). To date, among the 106 species of *Megophrys*, 56 species were discovered in China. Even so, many cryptic species still need to be described just in southern China (Chen et al. 2017; Liu et al. 2018).

South-western China has long been proposed as biodiversity hotspot (Myers et al. 2000). Guizhou Province is an important part of southwest China, especially with the particular environments of karst rocky desertifcation, and knowledge of biodiversity levels and/or patterns are still seriously lacking. Recently, a series of new amphibian species were described from this province (Zhang et al. 2017; Li et al. 2018a, b, 2019a, b; Lyu et al. 2019; Wang et al. 2019c; Luo et al. 2020; Liu et al. 2020; Wei et al. 2020; Xu et al. 2020), indicating that species diversity of amphibians in this region is highly underestimated. It is urgent for herpetologists to conduct comprehensive and in-depth surveys to explore the level of amphibian species diversity in this region under accelerating climate changes. Obviously, more work should be conducted on detecting the differentiation of the populations and further describe the cryptic species in this region.

Acknowledgements

We are grateful to the editors and reviewers for their working on the manuscript. This work was supported by National Natural Sciences Foundation of China (NSFC31960099), Key project for bio-diversity conservation, Ministry of Ecology and Environment of People's Republic of China. (Code: 2018-02-06-M2019-49/50), Basic research project of science and technology department of Guizhou Province (Nos. [2020] 1Y083), Science and technology support project of science and technology department of Guizhou Provincial (No. [2020] 4Y029) and Guizhou Provincial Department of Education Youth Science and Technology Talents Growth Project (Nos. KY[2018]455 and KY[2018]468).

References

Boulenger GA (1886) Description of a new frog of the genus *Megalophrys*. Proceedings of the Zoological Society of London1885: 1–850.

Boulenger GA (1887) Description of a new frog of the genus *Megalophrys*. Annali del Museo Civico di Storia Naturale di Genova Serie 2, 4: 512–513.

Boulenger GA (1889) Description of a new batrachian of the genus *Leptobrachium*, obtain by M. L. Burma. Annali del Museo Civico di Storia Naturale di Genova. Serie 2, 7: 748–750.

Boulenger GA (1893) Descriptions of three new batrachians from Tonkin. Annals and Magazine of Natural History, Series 7 12: 186–188. https://doi.org/10.1080/00222930308678835

Boulenger GA (1899a) Descriptions of three new reptiles and a new batrachian from Mount Kina Balu, North Borneo. Annals and Magazine of Natural History, Series 7(4):1–453. https://doi.org/10.1080/00222939908678228

Boulenger GA (1899b) On a collection of reptiles and batrachians made by Mr. J. D. La Touche in N.W. Fokien, China. Proceedings of the Zoological Society of London 1899: 159–172.

Boulenger GA (1903) Report on the batrachians and reptiles. In: Annandale N, Robinson HC (Eds) Fasciculi Malayenses. Anthropological and Zoological Results of an Expedition to Perak and the Siamese Malay States 1901–1903 undertaken by Nelson Annandale and Herbert C. Robinson under the auspices of the University of Edinburgh and the University of Liverpool (Vol. 2), Zoology, Part 1: 131–176.

Boulenger GA (1908) A revision of the oriental pelobatid batrachians (genus *Megophrys*). Proceedings of the Zoological Society of London 78(2): 407–430. https://doi.org/10.1111/j.1096-3642.1908.tb01852.x

Bourret R (1937) Notes herpétologiques sur l'Indochine française. XIV. Les batraciens de la collection du Laboratoire des Sciences Naturelles de l'Université. Descriptions de quinze especes ou variétés nouvelles. Annexe au Bulletin Général de l'Instruction Publique Hanoi, 1937: 5–56.

Che J, Chen HM, Yang JX, Jin JQ, Jiang K, Yuan ZY, Murphy RW, Zhang YP (2012) Universal COI primers for DNA barcoding amphibians. Molecular Ecology Resource 12: 247–258. https://doi.org/10.1111/j.1755-0998.2011.03090.x

Chen JM, Zhou WW, Nikolay A, Poyarkov Jr, Stuart BL, Brown RM, Lathrop A, Wang YY, Yuan ZL, Jiang K, Hou M, Chen HM, Suwannapoom C, Nguyen SN, Duong TV, Papenfuss TJ, Murphy RW, Zhang YP, Che J (2017) A novel multilocus phylogenetic estimation reveals unrecognized diversity in Asia toads, genus *Megophrys* sensu lato (Anura: Megophryidae). Molecular Phylogenetics and Evolution 106: 28–43. https://doi.org/10.1016/j.ympev.2016.09.004

Delorme M, Dubois A, Grosjean S, Ohler A (2006) Une nouvelle ergotaxinomie des Megophryidae (Amphibia, Anura). Alytes 24: 6–21.

Deuti K, Grosjean S, Nicolas V, Vasudevan K, Ohler A (2017) Nomenclatural puzzle in early *Megophrys nomina* (Anura, Megophryidae) solved with description of two new species from India (Darjeeling hills and Sikkim). Alytes 34: 20–48.

Dubois A (1987) Miscellanea taxinomica batrachologica (I). Alytes 1987[1986]: 7–95.

Fei L, Hu SQ, Ye CY, Huang YZ (2009) Fauna Sinica. Amphibia (Vol. 2). Anura. Science Press, Beijing, 328–481. [In Chinese]

Fei L, Ye CY, Huang YZ (1983) Two new subspecies of *Megophrys omeimontis* Liu from China (Amphibia, Pelobatidae). Acta Herpetologica Sinica. New Series, Chengdu 2(2): 49–52. [In Chinese with English abstract]

Fei L, Ye CY, Huang YZ (1990) Key to Chinese Amphibians. Publishing House for Scientific and Technological, Chongqing, 108–110. [In Chinese]

Fei L, Ye CY, Huang YZ (2001) Colour Handbook Amph. Sichuan, Science Press, Beijing, 138–139. [In Chinese]

Fei L, Ye CY (2005) Two new species of Megophryidae from China. In: Fei et al. (Ed.) The Key and Illustration of Chinese. Sichuan Publishing House of Science and Technology, Chongqing, 253–255. [In Chinese]

Fei L, Ye CY, Jiang JP (2012) Colored atlas of Chinese Amphibians and their distributions. Sichuan Publishing House of Science and Technology, Chengdu, 135–247. [In Chinese]

Fei L, Ye CY (2016) Genus *Liuophrys* Fei, Ye and Jiang, new genus; Subgenus *Atympanophrys* (*Borealophrys*) Fei, Ye and Jiang, new subgenus; Subgenus *Atympanophrys* (*Gigantophrys*) Fei, Ye and Jiang, new subgenus; Genus *Boulenophrys* Fei, Ye and Jiang, 2016, new genus; Subgenus *Xenophrys* (*Tianophrys*) Fei, Ye and Jiang, new subgenus. In: Fei L, Ye CY (Eds) Amphibians of China (Vol. (I)). Science Press, Beijing, 611–735.

Frost DR (2020) Amphibian Species of the World: an Online Reference. Version 6.0. Electronic Database. American Museum of Natural History, New York, USA. http://research.amnh.org/herpetology/amphibia/index.html [Accessed on 20 Apr 2020]

Günther ACLG (1864) The reptiles of British India. Ray Society, London, 414–415.

Guindon S, Dufayard JF, Lefort V, Anisimova M, Hordijk W, Gascuel O (2010) New algorithms and methods to estimate maximum-likelihood phylogenies: assessing the performance of PhyML 3.0. Systematic Biology 59(3): 07–321. https://doi.org/10.1093/sysbio/syq010

Hall TA (1999) BIOEDIT: a user-friendly biological sequence alignment editor and analysis program for Windows 95/98/NT. Nucleic Acids Symposium Series 41(41): 95–98.

Hu SX, Zhao EM, Liu CZ (1966) A herpetological survey of the Tsinling and Ta-pa shan region. Acta Zoologica Sinica 18(1): 57–89.

Hu SX, Zhao EM, Liu CZ (1973) A survey of amphibians and reptiles in Kweichow province, including a herpetofauna analysis. Acta Zoologica Sinica 19(2): 149–171.

Huang YZ, Fei L (1981) Two new species of amphibians from Xizang. Acta Zootaxonomica Sinica 6: 211–215.

Inger RF (1989) Four new species of frogs from Borneo. Malayan Nature Journal. Kuala Lumpur 42: 229–243.

Inger RF, Romer JD (1961) A new pelobatid frog of the genus *Megophrys* from Hong Kong. Fieldiana. Zoology 39(46): 533–538. https://doi.org/10.5962/bhl.title.3373

Inger RF, Stuebing RB, Lian TF (1995) New species and new records of Anurans from Boreno. Raffles Bulletin of Zoology, Singapore 43(1): 115–131.

Inger RF, Iskandar DT (2005) A collection of amphibians from west Sumatra, with description of a new species of *Megophrys* (Amphibia: Anura). Raffles Bulletin of Zoology, Singapore 133–142.

Jiang JP, Yuan FR, Xie F, Zheng ZH (2003) Phylogenetic relationships of some species and genera in megophryids inferred from partial sequences of mitochondrial 12S and 16S rRNA genes. Zoological Research 24: 241–248. [In Chinese with English abstract]

Jiang JP, Ye CY, Fei L (2008) A New Horn Toad *Megophrys sangzhiensis* from Hunan, China (Amphibia, Anura). Zoological Research 29(2): 219–222. [In Chinese with English abstract] https://doi.org/10.3724/SP.J.1141.2008.00219

Kuhl H, Van Hasselt JC (1822) Uittreksels uit breieven van de Heeren Kuhl en van Hasselt, aan de Heeren C. J. Temminck, Th. van Swinderen en W. de Haan. Algemeene Konst-en Letter-Bode 7: 99–104.

Lathrop A (1997) Taxonomic review of the megophryid frogs (Anura: Pelobatoidea). Asian Herpetological Research 7: 68–79. https://doi.org/10.5962/bhl.part.18857

Lemmon AR, Moriarty EC (2004) The importance of proper model assumption in Bayesian phylogenetics. Systematic Biology 53(2): 265–277. https://doi.org/10.1080/10635150490423520

Li YL, Jin MJ, Zhao J, Liu ZY, Wang YY, Pang H (2014) Description of two new species of the genus *Megophrys* (Amphibia: Anura: Megophryidae) from Heishiding Natural Reserve, Fengkai, Guangdong, China, based on molecular and morphological data. Zootaxa 3795(4): 449–471. https://doi.org/10.11646/zootaxa.3795.4.5

Li SZ, Xu N, Lv JC, Jiang JP, Wei G, Wang B (2018a) A new species of the odorous frog genus *Odorrana* (Amphibia, Anura, Ranidae) from southwestern China. PeerJ 6(e5695): 1–28. https://doi.org/10.7717/peerj.5695

Li SZ, Xu N, Liu J, Jiang JP, Wei G, Wang B (2018b) A New Species of the Asian Toad Genus *Megophrys sensu lato* (Amphibia: Anura: Megophryidae) from Guizhou Province, China. Asian Herpetological Research 9(4): 224–239. https://doi.org/10.16373/j.cnki.ahr.180072

Li SZ, Wei G, Xu N, Cui JG, Fei L, Jiang JP, Liu J, Wang B (2019a) A new species of the Asian music frog genus *Nidirana* (Amphibia, Anura, Ranidae) from Southwestern China. PeerJ 7: e7157. https://doi.org/10.7717/peerj.5695

Li SZ, Zhang MH, Xu N, Lv JC, Jiang JP, Liu J, Wei G, Wang B (2019b) A new species of the genus *Microhyla* (Amphibia: Anura: Microhylidae) from Guizhou Province, China. Zootaxa 4624: 551–575. https://doi.org/10.11646/zootaxa.4624.4.7

Li Y, Zhang DD, Lyu ZT, Wang J, Li YL, Liu ZY, Chen HH, Rao DQ, Jin ZF, Zhang CY, Wang YY (2020) Review of the genus *Brachytarsophrys* (Anura: Megophryidae), with revalidation of *Brachytarsophrys platyparietus* and description of a new species from China. Zoological Research 41(2): 105–122. https://doi.org/10.24272/j.issn.2095-8137.2020.033

Liu CZ (1950) Amphibians of Western China. Fieldiana. Zoology Memoires 2: 1–400. https://doi.org/10.5962/bhl.part.4737

Liu CZ, Hu SQ, Yang HH (1960). Amphibian of Yunnan collected in 1958. Acat Zoological Sinica 12(2): 149–174.

Liu ZY, Zhu TQ, Zeng ZC, Lyu ZT, Wang J, Messenger K, Greenberg A J, Gou ZX, Yang ZH, Shi SH, Wang YY (2018) Prevalence of cryptic species in morphologically uniform taxa-Fast speciation and evolutionary radiation in Asian frogs. Molecular Phylogenetics and Evolution 127: 723–731. https://doi.org/10.1016/j.ympev.2018.06.020

Liu J, Li SZ, Wei G, Xu N, Cheng YL, Wang B, Wu J (2020) A new species of the Asian toad genus *Megophrys sensu lato* (Anura: Megophryidae) from Guizhou Province, China. Asian Herpetological Research 11(1): 1–18. https://doi.org/10.16373/j.cnki.ahr.190041

Lyu ZT, Zeng ZC, Wan H, Yang JH, Li YL, Pang H, Wang YY (2019b) A new species of *Amolops* (Anura: Ranidae) from China, with taxonomic comments on *A. liangshanensis* and Chinese populations of *A. marmoratus*. Zootaxa 4609: 247–268. https://doi.org/10.11646/zootaxa.4609.2.3

Lyu ZT, Li YQ, Zeng ZC, Zhao J, Liu ZL, Guo GX, Wang YY (2020) Four new species of Asian horned toads (Anura, Megophryidae, *Megophrys*) from southern China. ZooKeys 942: 105–140. https://doi.org/10.3897/zookeys.942.47983

Luo T, Xiao N, Gao K, Zhou J (2020) A new species of *Leptobrachella* (Anura, Megophryidae) from Guizhou Province, China. ZooKeys 923: 115–140. https://doi.org/10.3897/zookeys.923.47172

Mahony S (2011) Two new species of *Megophrys* Kuhl & van Hasselt (Amphibia: Megophryidae), from western Thailand and southern Cambodia. Zootaxa 2734: 23–39. https://doi.org/10.11646/zootaxa.2734.1.2

Mahony S, Sengupta S, Kamei RG, Biju S D (2011) A new low altitude species of *Megophrys* Kuhl and van Hasselt (Amphibia: Megophryidae), from Assam, Northeast India. Zootaxa 3059: 36–46. https://doi.org/10.11646/zootaxa.3059.1.2

Mahony S, Teeling EC, Biju SD (2013) Three new species of horned frogs, *Megophrys* (Amphibia: Megophryidae), from northeast India, with a resolution to the identity of *Megophrys boettgeri* populations reported from the region. Zootaxa 3722(2): 143–169. https://doi.org/10.11646/zootaxa.3722.2.2

Mahony S, Nicole MF, Biju SD, Teeling EC (2017) Evolutionary history of the Asian Horned Frogs (Megophryinae): integrative approaches to time tree dating in the absence of a fossil record. Molecular Phylogenetics and Evolution 34(3): 744–771. https://doi.org/10.1093/molbev/msw267

Mahony S, Kamei RG, Teeling EC, Biju SD (2018) Cryptic diversity within the *Megophrys major* species group (Amphibia: Megophryidae) of the Asian Horned Frogs: Phylogenetic perspectives and a taxonomic revision of South Asian taxa, with descriptions of four new species. Zootaxa 4523: 1–96. https://doi.org/10.11646/zootaxa.4523.1.1

Malkmus R, Matsui M (1997) *Megophrys kobayashii*, ein neuer pelobatider Frosch vom Mount Kinabalu. Sauria, Berlin 19: 31–37.

Mathew R, Sen N (2007) Description of two new species of *Megophrys* (Amphibia: Anura: Megophryidae) from North-east India. Cobra 1: 18–28.

McGuire JA, Witt CC, Altshuler DL, Remsen JV (2007) Phylogenetic systematics and biogeography of hummingbirds: Bayesian and maximum likelihood analyses of partitioned data and selection of an appropriate partitioning strategy. Systematic Biology 56(5): 837–856. https://doi.org/10.1080/10635150701656360

Messenger KR, Dahn HA, Liang YR, Xie P, Wang Y, Lu CH (2019) A new species of the genus *Megophrys* Gunther, 1864 (Amphibia: Anura: Megophryidae) from Mount Wuyi, China. Zootaxa 4554(2): 561–583. https://doi.org/10.11646/zootaxa.4554.2.9

Mo XY, Shen YH, Li HH, Wu MS (2010) A new species of *Megophrys* (Amphibia: Anura: Megophryidae) from the northwestern Hunan Province, China. Current Zoology 56(4): 432–436. https://doi.org/10.1093/czoolo/56.4.432

Munir M, Hamidy A, Farajallah A, Smith EN (2018) A new *Megophrys* Kuhl and Van Hasselt (Amphibia: Megophryidae) from southwestern Sumatra, Indonesia. Zootaxa 4442: 389–412. https://doi.org/10.11646/zootaxa.4442.3.3

Munir M, Hamidy A, Matsui M, Iskandar DT, Sidik I, Shimada T (2019) A new species of *Megophrys* Kuhl & Van Hasselt (Amphibia: Megophryidae) from Borneo allied to *M. nasuta*. Zootaxa 4679: 1–24. https://doi.org/10.11646/zootaxa.4679.1.1

Myers N, Mittermeier RA, Mittermeier CG, Da Fonseca GAB, Kent J (2000) Biodiversity hotspots for conservation priorities. Nature 403: 853–858. https://doi.org/10.1038/35002501

Nguyen TQ, Pham CT, Nguyen TT, Luong AM, Ziegler T (2020) A new species of *Megophrys* (Amphibia: Anura: Megophryidae) from Vietnam. Zootaxa 4722: 401–422. https://doi.org/10.11646/zootaxa.4722.5.1

Ohler A, Swan SR, Daltry JC (2002) A recent survey of the amphibian fauna of the Cardamom Mountains, Southwest Cambodia with descriptions of three new species. Raffles Bulletin of Zoology, Singapore 50(2): 465–481.

Ohler A (2003) Revision of the genus *Ophryophryne* Boulenger, 1903 (Megophryidae) with description of two new species. Alytes 21(1): 23–44.

Pope CH (1929) Four new frogs from Fukien Province, China. American Museum Novitates 352: 1–5.

Poyarkov NA, Duong Jr TV, Orlov NL, Gogoleva SI, Vassilieva AB, Nguyen LT, Nguyen VDH, Nguyen SN, Che J, Mahony S (2017) Molecular, morphological and acoustic assessment of the genus *Ophryophryne* (Anura, Megophryidae) from Langbian Plateau, southern Vietnam, with description of a new species. ZooKeys 672: 49–120. https://doi.org/10.3897/zookeys.672.10624

R Development Core Team (2008) R: a language and environment for statistical computing. Vienna: R Foundation for Statistical Computing. http://www.Rproject.org

Rao DQ, Yang DT (1997) The karyotypes of Megophryinae (Pelobatidae) with a discussion on their classification and phylogenetic relationships. Asian Herpetological Research 7: 93–102. https://doi.org/10.5962/bhl.part.18858

Robert L, Brett C, Simon YWH, Stephane G (2012) PartitionFinder: Combined Selection of Partitioning Schemes and Substitution Models for Phylogenetic Analyses. Molecular Phylogenetics and Evolution 29(6): 1695–1701. https://doi.org/10.1093/molbev/mss020

Ronquist FR, Huelsenbeck JP (2003) MrBayes3: Bayesian phylogenetic inference under mixed models. Bioinformatics 19(12): 1572–1574. https://doi.org/10.1093/bioinformatics/btg180

Sambrook J, Fritsch EF, Maniatis T (1989) Molecular Cloning: A Laboratory Manual. Cold Spring Harbor Laboratory Press, New York, 1659 pp.

Schlegel H (1858) Handleiding tot de Beoefening der Dierkunde (Vol. 2). Koninklijke Militaire Akademie, Breda, 57 pp. https://doi.org/10.5962/bhl.title.11648

Shen Y H (1994) A new pelobatid toad of the genus *Megophrys* from China (Anura: Pelobatidae). Zoological Society of China Editor. The 60th Anniversary of the Foundation of the Zoological Society of China, Nanking (China), September 1994. China Science and Technology Publishing House, Nanjing, 603–606.

Simon C, Frati F, Beckenbach A, Crespi B, Liu H, Flook P (1994) Evolution, weighting and phylogenetic utility of mitochondrial gene sequences and a compilation of conserved polymerase chain reaction primers. Annals of the Entomological Society of America 87(6): 651–701. https://doi.org/10.1093/aesa/87.6.651

Sjöander K, Beskow J (2000) Wavesurfer (Anura: Pelobatidae). Acoustical society of China Editor. The International Conference on Spoken Language Processing, Beijing (China), October 2000. Military Yiwen Publishing House, Beijing, 464–467.

Smith MA (1921) New or little-known reptiles and batrachians from southern Annam (Indo-China). Proceedings of the Zoological Society of London 1921: 423–440. https://doi.org/10.1111/j.1096-3642.1921.tb03271.x

Stejneger L (1926) Two new tailless amphibians from western China. Proceedings of the Biological Society of Washington 39: 53–54.

Stuart BL, Chuaynkern Y, Chan-ard T, Inger RF (2006) Three new species of frogs and a new tadpole from eastern Thailand. Fieldiana Zoology, New Series 1543: 1–10. https://doi.org/10.3158/0015-0754(2006)187[1:TNSOFA]2.0.CO;2

Tamura K, Stecher G, Peterson D, Fiipski A, Kumar S (2013). MEGA6: molecular evolutionary genetics analysis, version 6.0. Molecular Biology and Evolution 30: 2725–2729. https://doi.org/10.1093/molbev/mst197

Tapley B, Cutajar T, Mahony S, Nguyen CT, Dau VQ, Nguyen TT, Luong HV, Rowley JJL (2017) The Vietnamese population of *Megophrys kuatunensis* (Amphibia: Megophryidae) represents a new species of Asian horned frog from Vietnam and southern China. Zootaxa 4344(3): 465–492. https://doi.org/10.11646/zootaxa.4344.3.3

Tapley B, Cutajar TP, Mahony S, Nguyen CT, Dau VQ, Luong AM, Le DT, Nguyen TT, Nguyen TQ, Portway C, Luong HV, Rowley JJL (2018) Two new and potentially highly threatened *Megophrys* Horned frogs (Amphibia: Megophryidae) from Indochina's highest mountains. Zootaxa 4508: 301–333. https://doi.org/10.11646/zootaxa.4508.3.1

Taylor EH (1920) Philippine Amphibia. Philippine Journal of Science 16: 213–359. https://doi.org/10.5962/bhl.part.4751

Taylor EH (1962) The amphibian fauna of Thailand. University of Kansas Science Bulletin 43: 265–599. https://doi.org/10.5962/bhl.part.13347

Tian YZ, Sun A (1995) A new species of *Megophrys* from China (Amphibia: Pelobatidae). Journal of Liupanshui Teachers College 52(3): 11–15. [In Chinese].

Tian WS, Hu QX (1983) Taxonomic study on genus *Megophrys*, with descriptions of two genera. Acta Herpetologica Sinica 2: 41–48.

Wang J, Liu ZY, Lyu ZT, Wang YY (2017a) A new species of the genus *Megophrys* (Amphibia: Anura: Megophryidae) from an offshore island in Guangdong Province, southeastern China. Zootaxa 4324(3): 541–556. https://doi.org/10.11646/zootaxa.4324.3.8

Wang YE, Liu BQ, Jiang K, Jin W, Xu JN, Wu CH (2017b) A new species of the Horn Toad of the genus *Xenophrys* from Zhejiang, China (Amphibia: Megophryidae). Chinese Journal of Zoology 52: 19–29. [in Chinese with English abstract]

Wang YY, Zhang TD, Zhao J, Sung YH, Yang JH, Pang H, Zhang Z (2012) Description of a new species of the genus *Megophrys* Günther, 1864 (Amphibia: Anura: Megophryidae) from Mount Jinggang, China, based on molecular and morphological data. Zootaxa 3546: 53–67. https://doi.org/10.11646/zootaxa.3546.1.4

Wang YY, Zhao J, Yang JH, Zhou ZM, Chen GL, Liu Y (2014) Morphology, molecular genetics, and bioacoustics support two new sympatric *Megophrys* (Amphibia: Anura Megophryidae) species in Southeast China. PLoS ONE 9(4): e93075. https://doi.org/10.1371/journal.pone.0093075

Wang L, Deng XJ, Liu Y, Wu QQ, Liu Z (2019a) A new species of the genus *Megophrys* (Amphibia: Anura: Megophryidae) from Hunan, China. Zootaxa 4695(4): 301–330. https://doi.org/10.11646/zootaxa.4695.4.1

Wang J, Lyu ZT, Liu ZY, Liao CK, Zeng ZC, Li YL, Wang YY (2019b) Description of six new species of the subgenus *Panophrys* within the genus *Megophrys* (Anura, Megophryidae) from southeastern China based on molecular and morphological data. ZooKeys 851: 113–164. https://doi.org/10.3897/zookeys.851.29107

Wang J, Li YL, Li Y, Chen H-H, Zeng YJ, Shen JM, Wang Y-Y (2019c) Morphology, molecular genetics, and acoustics reveal two new species of the genus *Leptobrachella* from northwestern Guizhou Province, China (Anura, Megophryidae). ZooKeys 848: 119–154. https://doi.org/10.3897/zookeys.848.29181

Wang B, Wu YQ, Peng JW, Shi SC, Lu NN, Wu J (2020) A new *Megophrys* Kuhl and Van Hasselt (Amphibia: Megophryidae) from southeastern China. ZooKeys 851: 113–164. https://doi.org/10.3897/zookeys.904.47354

Wei G, Li SZ, Liu J, Cheng YL, Xu N, Wang B (2020) A new species of the Music frog *Nidirana* (Anura, Ranidae) from Guizhou Province, China. ZooKeys 904: 63–87. https://doi.org/10.3897/zookeys.904.39161

Wu YH, Suwannapoom C, Jr. Poyarkov NA, Chen JM, Pawangkhanant P, Xu K, Jin JQ, Murphy RW, Che J (2019) A new species of the genus *Xenophrys* (Anura: Megophryidae) from northern Thailand. Zoological Research 40: 564–574. https://doi.org/10.24272/j.issn.2095-8137.2019.032

Xu N, Li SZ, Liu J, Wei G, Wang B (2020) A new species of the horned toad *Megophrys* Kuhl & Van Hasselt, 1822 (Anura, Megophryidae) from southwest China. ZooKeys 943: 119–144. https://doi.org/10.3897/zookeys.943.50343

Yang JH, Wang J, Wang YY (2018) A new species of the genus *Megophrys* (Anura: Megophryidae) from Yunnan Province, China. Zootaxa 4413: 325–338. https://doi.org/10.11646/zootaxa.4413.2.5

Ye CY, Fei L (1992) A new Pelobatid toda of the genus *Megophrys* from Xizang, China. Acta Herpetologica Sinica 1–2: 50–52. [In Chinese]

Ye CY, Fei L (1995) Taxonomic studies on the small type *Megophrys* in China including descriptions of the new species (subspecies) (Pelobatidae: genus *Megophrys*). Herpetologica Sinica 4–5: 72–81. [In Chinese]

Ye CY, Fei L, Xie F (2007) A new species of Megophryidae *Megophrys baolongensis* from China (Amphibia, Anura). Herpetologica Sinica 11: 38–41. [In Chinese]

Zhang Y, Li G, Xiao N, Li J, Pan T, Wang H, Zhang B, Zhou J (2017) A new species of the genus *Xenophrys* (Amphibia: Anura: Megophryicae) from Libo County, Guizhou, China. Asian Herpetological Research 8: 75–85. https://doi.org/10.16373/j.cnki.ahr.160041

Zhao J, Yang JH, Chen GL, Chen CQ, Wang YY (2014) Description of a new species of the genus *Brachytarsophrys* Tian and Hu, 1983 (Amphibia: Anura: Megophryidae) from Southern China based on molecular and morphological data. Asian Herpetological Research 5(3): 150–160. https://doi.org/10.3724/SP.J.1245.2014.00150

Supplementary material 1

Table S1. Uncorrected p-distances between the *Megophrys* species based on COI gene sequences

Authors: Haijun Su, Shengchao Shi, Yanqing Wu, Guangrong Li, Xiaogang Yao, Bin Wang, Shize Li

Data type: molecular data

Link: https://doi.org/10.3897/zookeys.974.56070.suppl1

Supplementary material 2

Table S2. Diagnostic characters separating the new species described in this study from other species of *Megophrys*

Authors: Bin Wang

Data type: morphological data

Link: https://doi.org/10.3897/zookeys.974.56070.suppl2